Reactive Coupling for Biodiesel Production with Integrated Glycerol Valorisation

By

Ibrahim Aris Mohammed

Supervised by Prof. A. Harvey and Dr J. Lee

Process Intensification Group

School of Engineering

Newcastle University

United Kingdom

January 2021

ABSTRACT

The increasing production of biodiesel globally over the last 20 years has increased the supply of “crude” glycerol. Initially, glycerol was a valuable by-product but is now low value or a waste product, due to mismatch between supply and demand. Valorisation of glycerol is an obvious route to improving the process economics. In this work, we investigated glycerols *in situ* valorisation by conversion to various oligomers (used in the pharmaceutical, food, and cosmetics industries) and glycerol ethers (used as oxygenated compounds to improve fuel combustion in Diesel engines). This is an example of "reactive coupling", a technique in which the by-product of one reaction is simultaneously converted to an added value product in a second reaction (in a single "pot"), thereby reducing the number of process steps.

The main objective for this work is to produce glycerol free biodiesel with reduced methanol usage and fast triglyceride conversion using reactive coupling as a novel technique. This work will for the first time demonstrate the production of biodiesel and glycerol ethers in a single pot. This aimed to reduce glycerol byproduct and methanol recycling. First, the study the convert glycerol in a stainless steel reactor. Reactive coupling was then performed to convert triglyceride with simultaneous conversion of the glycerol to added value products. Sulfuric acid was used as catalyst for the reaction, as it is compatible with all the desired reactions. It is also cheap and can tolerate triglyceride with high FFA levels during biodiesel production. High temperature in transesterification results in fast conversion of triglyceride. The catalyst and temperatures used are suitable for both biodiesel reaction and glycerol etherification.

Highest conversion of glycerol achieved was 68%, with over 90% selectivity to diglycerol in 5h. To avoid producing undesired by-products (such as acrolein) and higher oligomers (such as pentaglycerol), the recommended conditions are 3 wt% catalyst concentration, and a temperature of less than 150 ^{o}C. Furthermore, a kinetic model was fitted to the experimental data with activation energy of 112 kJmol^{-1} and pre-exponential factor of 2.18x10^{11} L.mol^{-1}s^{-1}. The thermodynamic analysis showed the reaction to be endothermic, less disordered, and non-spontaneous with an enthalpy (ΔH) 109 kJmol^{-1}, entropy (ΔS) – 38.1 Jmol^{-1}K^{-1}, and Gibbs free energy (G) 125 kJmol^{-1} respectively.

Reactive coupling achieved complete conversion of triglycerides and 100% FAME yield in 1h. About 60% of the glycerol was converted in parallel, with approximately 90% selectivity to glycerol ether and 10% to diglycerol. A temperature of not more than 150 ^{o}C is sufficient for this process with 3 wt% catalyst concentration and molar ratio 4:1 – 6:1. Some of the benefits of the reactively coupled process vs conventional processing are the rapid separation of the biodiesel phase from the glycerol phase, low alcohol to oil ratios, and the production of value-added products from the crude glycerol. The model should make scale-up of this process more predictable and robust.

Combined reactive extraction and reactive coupling were also studied, i.e., reactive coupling on the oilseeds, rather than the oil. Over 90% of biodiesel production was achieved and complete conversion of the glycerol to glycerol ether and polyglycerol. However, a substantially higher molar ratio of methanol to oil (400:1) was required, likely to be uneconomic. There were various non-triglyceride products in the extract, which would probably necessitate extra downstream processing.

In summary, for the first time, this work demonstrates reactive coupling to produce biodiesel, polyglycerol, and glycerol ether production using sulfuric acid as catalyst. The main advantages of this technique were:

i. Reduced glycerol by-product by up to 60%.
ii. Reduced methanol usage, from 20:1 to 4:1 – 6:1. This will remove/reduce downstream processing.
iii. Rapid conversion of triglyceride.
iv. Easy/fast separation of glycerol phase from FAME phase.

Furthermore, this study demonstrated proof-of-concept for combined reactive extraction and reactive coupling. Hence, oil in seeds can be converted *directly* to biodiesel, glycerol, and added-value products. This study's success shows that the glycerol by-product can be converted to a useful product directly during biodiesel production. Potentially, this will reduce waste generation and diversify the market of biodiesel producers.

DEDICATION

This study is dedicated to my loving family for their prayers, support, encouragement, and love.

ACKNOWLEDGEMENTS

I want to give all praise to the Almighty for His infinite blessings, strength, perseverance, knowledge, and wisdom to complete this work. The guidance, support, invaluable knowledge contribution, and constructive criticism of my supervisory team: Prof. Adam Harvey and Dr Jonathan Lee are immensely appreciated. Your contributions individually and collectively brought this work to the limelight. I would also like to acknowledge the support and assistance from friends too numerous to mention. Also, the encouragement from all members of the Process Intensification Group is worth acknowledging.

I acknowledged the technical support I enjoyed from the CEAM technical staff to re-construct the reaction rig and helped whenever it breaks down. I also appreciate your help with some of the analytical tools. I will forever be grateful. The CEAM administrative staff were also wonderful, answering my mails and making sure my work was hitch-free. The IT team were always there to resolve my software and hardware computer problem. I say thank you all.

My profound appreciation goes to all member of my family, especially my loving parent and siblings. This acknowledgement is incomplete without appreciating my wife and son for their love, support, prayer, encouragement and above all patient throughout the period of this work. You always keep me going with your smiles even after having a difficult time in school.

Finally, I express profound gratitude to my sponsor Petroleum Technology Development Fund (PTDF), Nigeria, for providing funds for this programme. I also acknowledged the support of Federal University of Technology, Minna Nigeria, for the fellowship to complete this programme and the staff of the Chemical Engineering Department for their advice and support. To Newcastle University, my appreciation goes to you for providing an enabling environment and experienced human resources for world-class research.

TABLE OF CONTENTS

NOMENCLATURE

A	pre-exponential factor	$L.mol^{-1}s^{-1}$
A_{DG}	peak area of diglycerols from the GC	
A_G	peak area of glycerol from the GC	
A_I	area of the internal standard from the GC	
A_{MDP}	peak area of 3-methoxyl 1,2-propanediol from the GC	
A_{TG}	peak area of triglycerols from the GC	
A_{TTG}	peak area of tetraglycerols from the GC	
B	Titration volume of the blank	mL
C	concentration of species	mol/L
C_B	concentration of FAME	M
C_C	concentration of catalyst	M
C_{DGE}	concentration of diglyceride	M
C_{FFA}	concentration of free fatty acid	M
C_G	concentration of glycerol	M
C_{G0}	initial concentration of glycerol	M
C_I	concentration of the internal standard	mg/mL
C_L	concentration of the lipid	g/mL
C_M	concentration of methanol	M
C_{MGE}	concentration of monoglyceride	M
C_{TGE}	concentration of triglyceride	M
C_W	concentration of water	M
E	activation energy	kJ/mol
G_{DG}	slope of calibration for diglycerols	
G_G	slope of calibration for glycerol	
G_{MDP}	slope of calibration for 3-methoxyl 1,2-propanediol	
G_{TG}	slope of calibration for triglycerols	
G_{TTG}	slope of calibration for tetraglycerols	
k	rate constant	
k_F	rate constant of forward reaction	
k_{obs}	observed rate constant	
k_F	rate constant of reverse reaction	
^{m}	order of reaction with respect to the catalyst	
m_a	mass of density bottle	mg
m_E	mass of the empty tube	g
m_F	mass of the FAME	mg
m_{FT}	total mass of the upper layer after separation	mg
m_{Ft}	theoretical mass of FAME	mg
m_G	mass of the glycerol after reactive coupling	g
m_{G1}	theoretical mass of glycerol base on the conversion of triglyceride	g
m_i	mass different species	g
m_L	mass of the sample after drying	g
m_s	mass FAME analyzed in the GC	mg
m_{sd}	mass of sample and density bottle	g
m_T	total mass of glycerol phase after separation	g
m_w	mass of water and density bottle	g
^{n}	order of reaction with respect to the glycerol	

N	concentration of sodium hydroxide	g/mL
P_{DG}	percentage content of diglycerols	%wt/wt
P_F	percentage FAME content	%wt/wt
P_G	percentage content of glycerol	%wt/wt
P_i	percentage content of different species	%wt/wt
P_{MPD}	percentage content of 3-methoxyl 1,2-propanediol	%wt/wt
P_{TG}	percentage content of triglycerols	%wt/wt
P_{TTG}	percentage content of tetraglycerols	%wt/wt
r	rate of reaction	$molL^{-1}s^{-1}$
r_F	rate of forward reaction	$molL^{-1}s^{-1}$
r_R	rate of reverse reaction	$molL^{-1}s^{-1}$
S_i	selectivity of different species	%
V	Titration volume of the sample	mL
V_I	Volume of the internal standard	mL
V_S	Volume of sample	mL
V_w	Volume of water	mL
W_f	final weight of the seed	g
W_s	initial weight of the seed	g
W_o	weight of the oil extracted	g
X_G	conversion of glycerol	%
Y_i	yield of reactive coupled species	%
$\sum A_P$	summation of the peak area from the GC	
ρ_s	density of the sample	g/mL
ρ_w	density of the water	g/mL

ABBREVIATIONS

AOCS	American Oil Chemist Society
ASTM	American society for testing and materials
ATR	Attenuated total reflection
AV	Acid value
BSTFA	N, O-Bis (trimethylsilyl) trifluoroacetamide
CAGR	Compound annual growth rate
DG	Diglycerols
DMC	Dimethyl carbonate
DMF	2,5-dimethylfuran
EN	European standard
FAME	Fatty acid methyl ester
FFA	Free fatty acid
FID	Flame ionization detector
FSD	Full – scale deflection
FTIR	Fourier transform infrared spectroscopy
G	Glycerol
GC	Gas chromatography
GLC	Glycerol carbonate
HPLC	High performance liquid chromatography
NMR	Nuclear magnetic resonance spectroscopy

OBR	Oscillatory baffled reactor
PDA	Photodiode array detector
PEG	Polyethylene glycolate
PG	Polyglycerols
PTFE	polytetrafluoroethylene
PVDF	Polyvinylidene fluoride
PVF	Polyvinyl fluoride
RI	Refractive index detector
RPM	Revolution per minute
SEM	Scanning electron microscopy
TCD	Thermal conductivity detector
TG	Triglycerols
TTG	Tetraglycerols

LIST OF FIGURES

LIST OF TABLES

Chapter 1. INTRODUCTION

The Earth population is increasing rapidly, and so are the consequences of the ever-increasing demand for energy. Hence, one of the key challenges worldwide is the future provision of energy. Generally, the production and utilisation of energy can measure the rate at which a nation is developing (Karthikeyan et al., 2014, Yang et al., 2012). Therefore, these have triggered the use of sustainable energy by must nations and their availability for the future. For centuries, fossil fuels have been the major sources of energy for industrial and domestic purposes (Shah et al., 2014). However, these energy sources have significant disadvantages, such as depleting reserves and rising demand leading to increasing cost, and environmental impact, mainly in the form of global warming through the emission of greenhouse gases (Chee Loong and Idris, 2017, Endalew et al., 2011).

These challenges necessitate research into alternative or renewable energy sources. These renewable energy sources include solar, wind, tidal, geothermal, hydro, and biofuel energy sources. They are associated with benefits such as energy security, increased job opportunities, and reduced emissions (Karmakar et al., 2012). According to the BP statistical review of global energy 2020, renewable energy consumption has increased with over 40% in primary energy in 2019. To meet up with the current target of "net-zero by 2050" the use of renewable energy becomes more essential. However, developing renewable energy for transport poses a range of problems such as:

I. Intermittency: Weather or geographical location can disrupt the continuous supply of solar or wind energy sources.
II. Storage capabilities: Though batteries are developed to store energy from solar or wind, they come with extra cost and environmental concern during disposal.
III. Space: Large farm spaces are required to harvest solar or wind energy sources.

Ideally, these sources should be renewable, degradable, available, efficient, accessible, relatively cost-effective, reliable, and environmentally friendly. Biofuels have been developed that have must of these qualities. They are energy sources produced from biomass that are renewable and environmentally friendly and can be used in place of fossil fuels (Zhang et al., 2003). Some of the biofuels other key benefits are improving

energy security for certain fossil fuel-poor nations, its economic value, and direct benefit to the local populations domestic livelihood (Demirbas, 2008).

Biofuels include biogas, bioethanol, and biodiesel (Demirbas, 2011, Nigam and Singh, 2011). They can be classified into the first, second, third, and fourth generation, as shown in ***Figure 1-1*** below. The classification is based on the feedstock used for production. The first-generation biofuels are sourced from edible feedstocks (rich in sugar and starch). These biofuels compete with food, especially for feedstocks that are produced in low quantities. The idea of using biomass waste such as lignocellulosic and non-edible crops (e.g., wood, straw, or grass) dominate the second-generation. Third-generation fuels are usually algae. This was due to its availability in large and small water bodies and also non-edible. In the fourth-generation, genetically modified crops are used due to the high yield. Most of these crops are mainly produced for biofuels production.

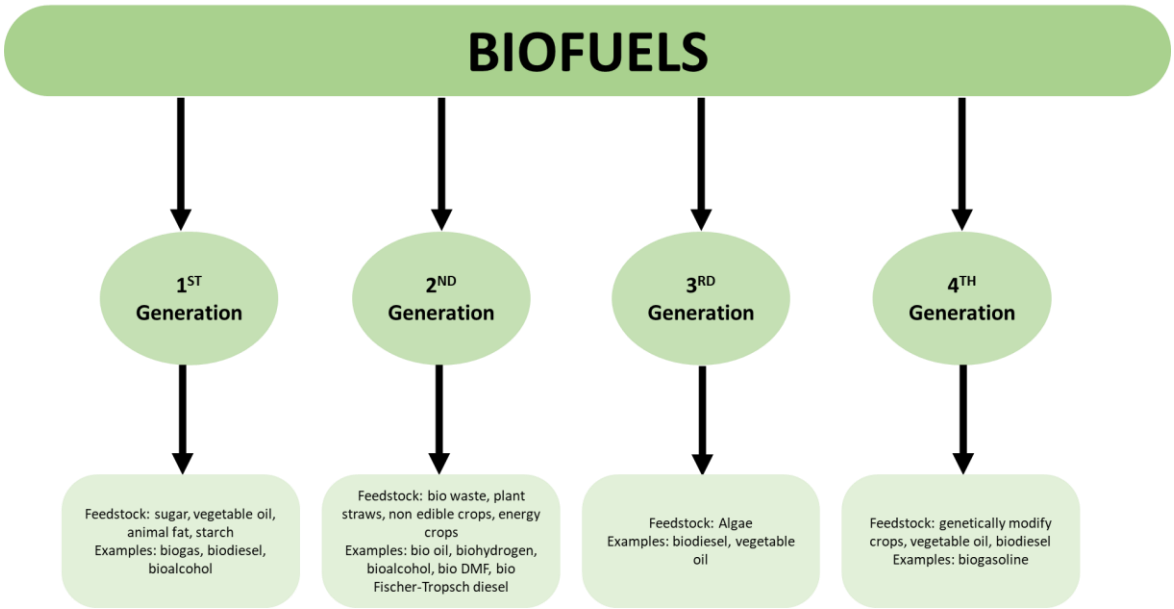

Figure 1-1: Classification of biofuels.

Bioethanol and biodiesel are the two main biofuels produced worldwide. The world bioenergy association (WBA) in its 2019 statistics report, reported global bioethanol production of 85.1 billion litres for 2017. This accounts for 62% of global biofuels production. The global biodiesel production for the same year was 36.1 billion litres,

equivalent to 26% of the world biofuels production. Both bioethanol and biodiesel accounted for 88% of the global biofuel production in 2017. According to the BP statistical review of world energy, 2020, biodiesel production grew strongly to 37% in 2019. Although biodiesel production is less than bioethanol, biodiesel yields 93% more energy on a lifecycle analysis than the energy used for its production. This is far greater than 25% recorded for bioethanol (Hill et al., 2006). This is because, in bioethanol production, fermentation is slow and requires lots of energy during distillation. In contrast, biodiesel is a fast reaction and can be separated by gravity. Also, less air pollution is produced by biodiesel compared to bioethanol. With the increasing demand for biodiesel, coupled with the aforementioned advantages, biodiesel production will continue for the foreseeable future.

1.1 Biodiesel

Biodiesel is a monoalkyl ester that contains long-chain fatty acids obtained from vegetable oil or animal fat (Demirbas, 2008). It is a renewable fuel for Diesel engines, produced by reducing the size of triglyceride molecules (oils or fats) to flow and atomise properly in a Diesel engine (Van Gerpen, 2005).

Biodiesel is usually produced through “transesterification”, a reaction between vegetable oils or animal fats and alcohols (**Figure 1-2** and **Figure 1-3**). This reduces the molecule size by removing the glycerol "backbone" of the molecule, rendering it more like Diesel fuels, particularly by reducing the high viscosity of feedstock (Demirbas, 2005). The conversion takes place in three consecutive reversible reactions: vegetable oil (triglyceride) to diglyceride, diglyceride to monoglyceride, and finally monoglyceride to fatty alkyl ester and glycerol (Galadima and Muraza, 2016, Demirbas, 2011), as shown below (**Figure 1-2**):

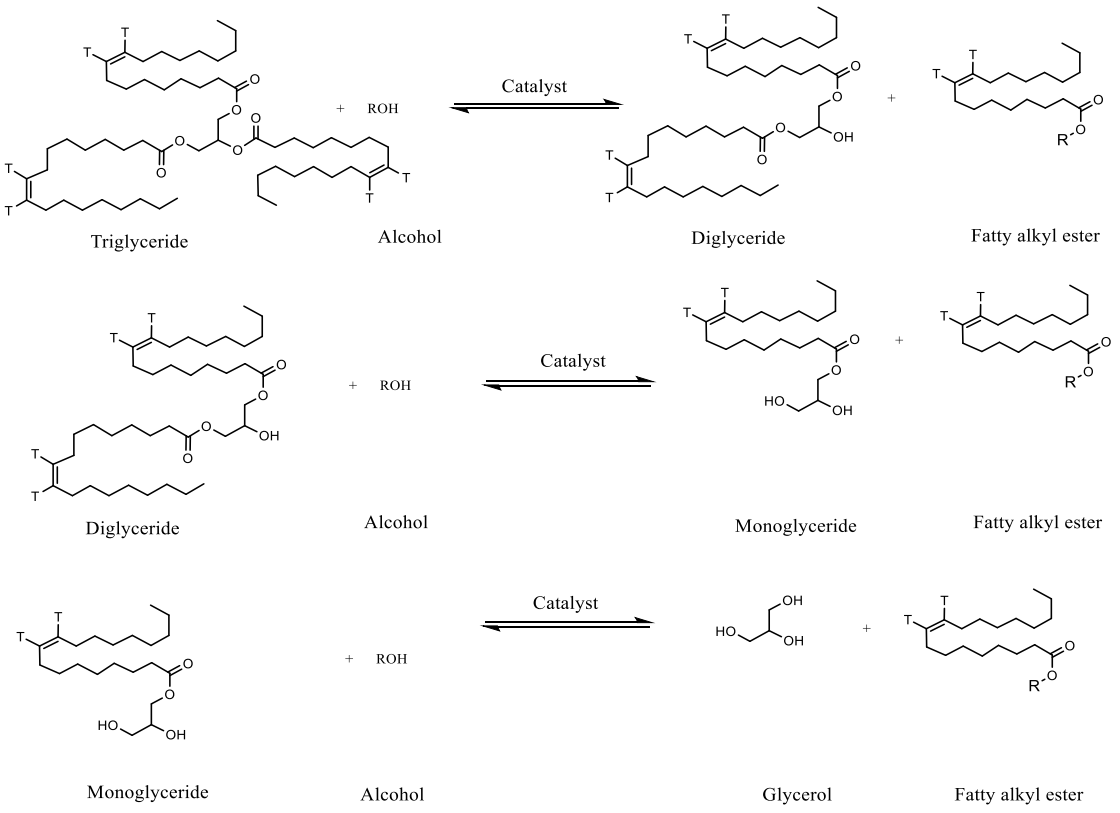

Figure 1-2: Consecutive conversion from Triglyceride to Fatty Alkyl Ester.

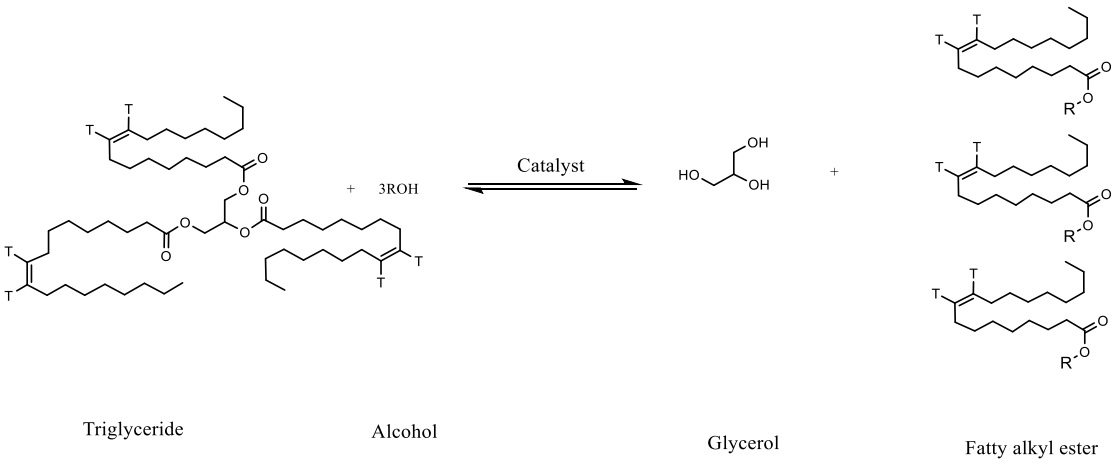

Figure 1-3: Transesterification reaction of Triglyceride with an alcohol.

Figure 1-3 shows the overall transesterification reaction. The reaction occurs in the presence of a catalyst, usually sodium hydroxide (NaOH) or potassium hydroxide (KOH).

The product is then purified downstream, such that it combusts easily in a Diesel engine in its pure form or can be blended with petroleum diesel (Anastopoulos et al., 2009).

In this study, biodiesel is produced using rapeseed oil. This is due to it availability and less cost in UK compared to the other triglycerides available. This will motivate farmers in this region to grow more. The technique used in this study produced biodiesel with reduced alcohol usage. These techniques were considered to intensify the biodiesel process. Example of such intensification technique is reactive extraction in which a reaction (such as transesterification) is performed simultaneously with an extraction, usually with both processes benefits. Here, biodiesel is produced *in situ* from the oil-bearing seeds. Oil is simultaneously extracted from the oilseed and converted to alkyl ester in a single reactor. On the other hand, reactive coupling in this system is an intensification process in which the co-product of biodiesel (glycerol) is simultaneously converted to an added value product. Combining the two techniques (combined reactive extraction/reactive coupling) would extract the oils from the oil-bearing feedstock, transesterify, and convert the glycerol by-products to added-value products in one step.

There has been rapid growth in biodiesel production worldwide over the last 20 years. Naylor and Higgins (2018) reported an over 700% increase in production between 2005 and 2015. "Crude" glycerol is the major co-product (**Figure 1-3**). It accounts for 10 to 18 wt% of the total product. It typically contains catalyst, alcohol, and unreacted feedstock, depending on the production conditions (Shah et al., 2014, Santibáñez et al., 2011). Pure glycerol is non-toxic, renewable, and environmentally friendly. It can be used in food, cosmetics, or pharmaceutical industries (Algoufi et al., 2017, da Silva et al., 2009, Bookong et al., 2015). However, the high cost of purifying crude glycerol obtained from biodiesel production (using different methods in combination depending in the level of purity required which includes distillation, filtration, adsorption using activated carbon, ion-exchange using resin, extraction, decantation, and crystallisation) is usually too high due to the high capital cost of the equipment, especially for small-scale biodiesel producers. The market for crude glycerol is poor due to oversupply. Furthermore, disposal of crude glycerol has adverse environmental effects due to impurities such as alcohol, catalyst (acid or base), salts (organic and inorganic), water, and soap (Anitha et al., 2016, Tan et al., 2013).

As the crude glycerol is potentially an inexpensive feedstock, this has encouraged research into alternative ways of converting the crude glycerol into the value-added products. This includes processes such as gasification to syngas, dehydration to acrolein, etherification to fuel-oxygenate, fermentation to alcohol, digestion to biogas, liquefaction to bio-oil, pyrolysis to biochar, steam reforming to hydrogen, and polymerisation to polyglycerol (He et al., 2017, Tan et al., 2013). The use of such processes could make the "biodiesel industry" into a more profitable "biorefining industry" (García-Sancho et al., 2011, Frusteri et al., 2009). ***Figure 1-4*** shows various products that can be produced from glycerol using different methods.

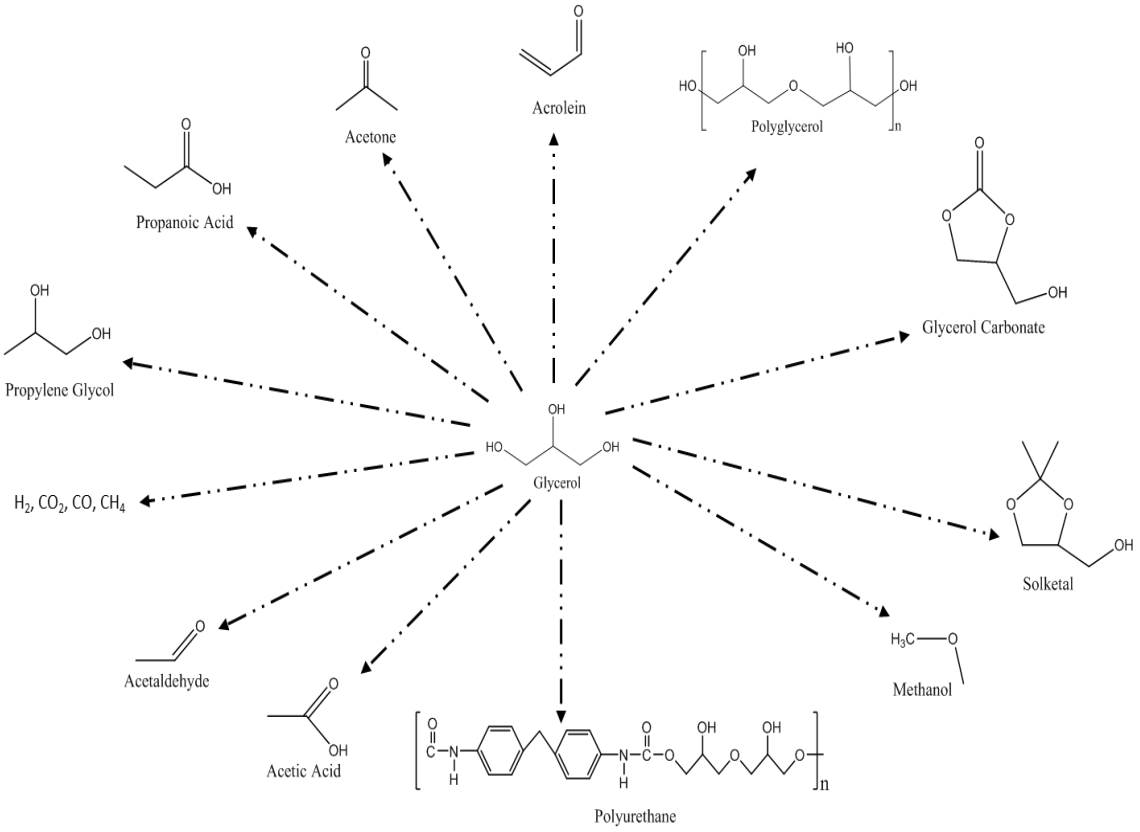

Figure 1-4: Possible reaction pathways to added-value products from glycerol.

Table 1-1: Comparison of market size for glycerol and glycerol derivatives.

Product	Market value size ($ billion)	Reference
Glycerol	3.0 (2020)	https://www.grandviewresearch.com/industry-analysis/glycerol-market
Acrolein	1.5 (2020)	https://www.marketwatch.com/press-release/acrolein-market-2021-revenue-growth-rate-market-size-restraints-forecast-analysis-by-2026-with-top-countries-data-2021-03-18
Propanoic acid	0.7 (2020)	https://www.marketwatch.com/press-release/global-propionic-acid-market-2021-industry-analysis-by-future-scope-business-size-revenue-growth-development-leading-players-regional-analysis-with-top-countries-forecast-to-2027-2021-03-09
Propylene glycol	4.5 (2020)	https://www.wicz.com/story/43076566/propylene-glycol-market-size-rising-at-cagr-of-78-during-2020-2026-global-industry-brief-analysis-of-top-countries-data-trends-and-drivers-with-top
Hydrogen	120 (2020)	https://www.grandviewresearch.com/industry-analysis/hydrogen-generation-market
Acetaldehyde	1.6 (2020)	https://www.marketwatch.com/press-release/acetaldehyde-market-2021-analytical-overview-key-players-growth-factors-demand-market-size-trends-and-forecast-to-2026-with-top-countries-data-2021-03-01
Acetic acid	9.3 (2020)	https://www.grandviewresearch.com/industry-analysis/acetic-acid-market
Polyurethane	70.7 (2020)	https://www.grandviewresearch.com/industry-analysis/polyurethane-pu-market
Methanol	31.8 (2018)	https://www.grandviewresearch.com/industry-analysis/methanol-market
Solketal	0.019 (2020)	https://www.marketwatch.com/press-release/solketal-market-share-analysis-with-demand-status-2021-latest-technological-advancement-industry-trends-competitive-landscape-explosive-factors-of-revenue-by-key-vendors-size-forecast-analysis-2027-2021-03-05
Polyglycerol	1.9 (2017)	https://www.grandviewresearch.com/industry-analysis/polyglycerol-market

The market size for polyglycerol is higher than some of the glycerol derivatives (as shown in *Table **1**-**1***). The polymerisation of glycerol by etherification to produce polyglycerol has recently been a topic of interest due to its significant applications in food, pharmaceutical, cosmetics, polymers, biomedical and drug industries, among others. One of the common applications is in producing polyglycerol esters, which are used as emulsifying agents in the food industry. Gholami et al. (2014) reported that in 2012, two-thirds of the total emulsifiers were polyglycerol ester and polyglycerol polyricinoleate. It has been projected that the food emulsifier market will increase with an annual growth rate of 5.2% from 2013 to 2018. The demand for polyglycerol is clear: the polyglycerol market was estimated at $1.91 billion in 2017 (see *Table **1**-**1***). With the increasing demand in most sectors, a compound annual growth rate (CAGR) of 9% was projected (Grand View Research, 2020).

The polymer is produced by the condensation of two or more glycerols in the presence of a catalyst to form diglycerol, triglycerol, tetraglycerol, or any of the higher polyglycerols (as shown in **Figure 1-5** below), depending on the reaction conditions, with water as the by-product (Sivaiah et al., 2012).

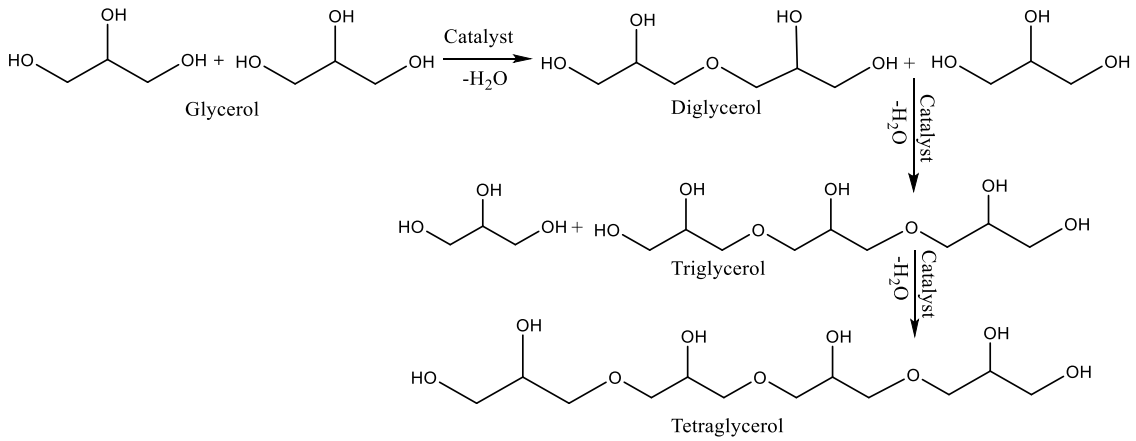

Figure 1-5: Polymerisation of Glycerol.

The reactions to produce the higher polymers (triglycerols, tetraglycerols) take place in series, as the "chain" grows (see **Figure 1-5**).

The polymerisation of crude or pure glycerol through etherification has been successfully documented by various researchers using various catalysts (acid or alkaline

and homogeneous or heterogeneous) for different applications. There is currently no report on studies of the kinetics of polyglycerol production from pure or crude glycerol. In principle, *in situ* conversion of glycerol to polyglycerol is possible but has not been reported. The reaction would combine transesterification and etherification in a single process. Furthermore, this process could reduce the methanol-to-oil molar ratio below that (6:1) used in the conventional method, significantly changing biodiesel production economics.

1.2 Aim and Objectives

The principal aim of this research is to develop and understand the new intensified conversion process by converting the glycerol produced when producing biodiesel into value-added products *in situ* via *reactive coupling*, and in so doing, reduce the excess methanol requirement.

This aim shall be achieved through the following objectives:

1. To understand the effect of process variables on the production of polyglycerol from pure glycerol. The effect of acid (H_2SO_4) catalyst concentration (0 – 6 wt%), temperature (130 – 160 ^oC), and reaction time shall be study in a pressurised vessel.
2. Data shall be collected from the glycerol polymerisation process to develop the kinetic rate expressions. The model shall be simulated using MATLAB to fit the experimental result.
3. Process variables in co-production of biodiesel and added value products from extracted vegetable oil using reactive coupling shall be study in a modify reaction rig. Low molar ratio of methanol to triglyceride, suitable temperature, and catalyst concentration shall be used with reaction time of up to one hour.
4. To develop and validate a kinetic model for the reactive coupling, it should help establish insight into the reaction and determine optimal conditions. The model shall be simulated to fit the experimental data using MATLAB.
5. Parametric study of combined reactive extraction and reactive coupling for biodiesel and added value products shall be studied using rapeseed. The modified

reaction rig shall be use for the study with similar reaction temperature but higher molar ratio (150:1 – 450:1).

1.3 Scope

This study will be limited to glycerol conversion to polyglycerol and simultaneously biodiesel production from the seed using a novel method (combined reactive extraction and reactive coupling). The conversion rate of the crude glycerol shall also be examined together with the degree of polymerisation. The study will also monitor the extent of methanol consumption, emphasising reducing short-chain alcohol during transesterification.

Different authors have studied the production and characterisation of polyglycerol from pure and crude glycerol and their works documented (Kumar et al., 1984, Gholami et al., 2014, Ardila-Suárez et al., 2015, Anuar et al., 2013, García-Sancho et al., 2011, Gholami et al., 2013a, Guerrero-Urbaneja et al., 2014, Bookong et al., 2015, Ayoub et al., 2014, Garti et al., 1981, Soi et al., 2014, Salehpour and Dubé, 2012, Sivaiah et al., 2012). However, the detailed reaction kinetics of the process are not apparent in the literature. Also, the interaction of the process variables should be studied. The production of polyglycerol and other value-added products in a single pot has never been considered, nor has the rate at which the polymers are produced during the process. The kinetic model should predict the production of polyglycerol at a given condition of the reaction and aid process design.

The biodiesel and polyglycerol simultaneous production will add value to the crude glycerol in a single step. In conventional processes, biodiesel is produced separately, and the crude glycerol is converted to the polymer, making the process time-consuming, thereby adding to the cost of the biorefinery. This method will also reduce the consumption of methanol. Since excess alcohol is required for the efficient production of fatty alkyl esters, the removal of glycerol by conversion into other value-added products can reduce the excess alcohol use. This can be achieved through Le-Chatelier's principle by continuous removal/conversion of one of the co-products. This is based on the second law of thermodynamics in which the entropy (S) predicts if the reaction is

reversible ($S_{final} = S_{initial}$) or irreversible ($S_{final} > S_{initial}$). The entropy can be related to Gibbs free energy and enthalpy as shown in the equation below.

$$\Delta G = \Delta H - T\Delta S \quad 1.1$$

At equilibrium, ΔG is zero (0) hence the reaction stops. However, when ΔG is not zero, the reaction occurs either favouring the forward or backward reaction until equilibrium is achieve. With the process intensification such as reactive coupling, the equilibrium constant is altered thereby changing the Gibbs free energy.

Similar process occurs with reactive extraction and has been studied for biodiesel production. The combination of reactive extraction and reactive coupling will decrease production cost with the simultaneous production of biodiesel and polyglycerol. The study of the process variables for the production will help determine the best conditions and the extent of the excess methanol used.

1.4 Summary of Chapter One

The increasing population of the world increased the demand for energy with fossil fuel in fore front of the energy source. Due to its environmental effect, increasing economy, employment opportunities, and government policies, renewable energies were researched and utilised to consolidate the fossil fuel. Biodiesel as example of such renewable energy have been produced commercially by reacting triglyceride with an alcohol in the presence of a selected catalyst. Glycerol is the by-product of the reaction, which requires series of steps for purification. The use of reactive coupling technique was introduced as a novelty to convert glycerol by-product to added value products in a single-pot during biodiesel production. The major achievements expected from this research is the reduction in the use of the molar ratio of vegetable oil to alcohol, fast triglyceride conversion to biodiesel using acid catalyst, and reduction/free glycerol by-products in biodiesel production.

1.5 Outline of the Thesis

This thesis is presented in a sequence of five chapters. The results from this report were obtained from experimental work performed.

Chapter 1. Introduction. The introduction explains the background and motivation for this research.

Chapter 2. Literature Review. The review includes a brief history of the biodiesel process and the techniques (conventional and intensification processes) of biodiesel production. It also includes the effect of the process variable and the kinetics of the process. The chapter also reviewed the various process for the valorisation of glycerol. The various product reviewed includes polyglycerol, acetins, acetals, alkyl tert-butyl ether, ethyl ether, acrolein, hydrogen, and acrylic acid.

Chapter 3. Materials and Methods. The procedure for glycerol conversion to polyglycerols was reported. Then, the steps involved in reactive coupling for biodiesel and glycerol valorisation was explicitly reported. It was then followed by the steps for the combined reactive extraction and reactive coupling method. The analytical tools and conditions are also reported. A kinetic model for glycerol to polyglycerol is developed and then extended to reactive coupling.

Chapter 4. Results and Discussion. This chapter covers:

i. The production of polyglycerol from pure glycerol. The yield and selectivity of the different oligomers formed during the reaction were examined and compared to previous authors. Other side-products were investigated. Development of a kinetic model, iteration, and comparison to the result.
ii. Full reactive coupling experiments, as a function of various variables with comparison to related literature.
iii. The kinetics for the biodiesel production was studied and combined with the kinetics for the etherification. The model obtained was simulated with MATLAB and compared with the experimental result.
iv. Combined reactive extraction for biodiesel production and reactive coupling of glycerol valorisation.

Chapter 5. Conclusions and Further Work. This chapter is a summary of the whole work reported in the previous chapters.

Chapter 2. LITERATURE REVIEW

2.1 Biodiesel and Biodiesel Production

Biodiesel is an alkyl ester produced mainly through the transesterification of vegetable oil, animal fat, grease, or waste vegetable oil with short-chain alcohol (usually methanol or ethanol) (Wang et al., 2005). The reaction proceeds in the presence of a suitable catalyst, which can be homogeneous, heterogeneous or enzymatic (Ma et al., 2017). In most of the processes, inexpensive homogeneous alkaline catalysts such as NaOH or KOH is used.

The biodiesel can be used in a Diesel engine directly or as a blend of fossil diesel fuel without necessarily changing the engine specification (Galadima and Muraza, 2016, Sanli and Canakci, 2008). The use of biodiesel can also raise the social well-being of developed and developing nations, via creating job opportunities and increase the economic status of nations through enhanced energy security, particularly for fossil fuel-poor nations, with substantial arable land (Liu et al., 2017, Saifuddin et al., 2015).

The use of biodiesel considerably increased Worldwide over the last 20 years. This has been mainly driven by government policies aimed at increasing the use of renewable, environmentally friendly fuels, and reducing fossil fuel dependence (Muthukumaran et al., 2017b, Galadima and Muraza, 2016, IEA, 2019). World energy demand is predicted to increase by 1.3 % yearly to 2040 (IEA, 2019). The production and utilisation of alternative energy sources, such as biodiesel, have been encouraged to meet this demand. The industrial and domestic use of renewable energy sources can reduce greenhouse emission compared to fossil fuel. These led to no increase in CO_2 emission between 2018 and 2019 with 33 gigatonnes (Gt) of CO_2 equivalent (IEA, 2019).

2.2 History of Biodiesel Production

The conventional biodiesel production method is via the transesterification reaction with extracted vegetable oil or animal fat as feedstock (Fan et al., 2011, Tremblay et al., 2008). The fuel can also be produced by an *in situ* (Reactive extraction) method using the oilseed directly as feedstock (Shuit et al., 2009, Kasim and Harvey, 2011). The method used and the feedstock account for the high percentage cost of production. This

implies that research into various feedstocks and methods to intensify the process is necessary (Lim and Lee, 2013, Alptekin and Canakci, 2011).

Biodiesel production and utilization started in the 1890s by applying pure vegetable oil as fuel in the Diesel engine by Dr Rudolph Diesel (Pahl, 2008). The main idea behind the invention was to increase efficiency over existing steam engines and provide an engine more suited for agricultural purposes (Demirbas, 2008). Dr Diesel patented the compression ignition engine in 1893. The application of peanut oil (vegetable oil) on the Diesel engine was first used in 1900 at the World's Fair in Paris (Demirbas, 2008, Demirbas, 2005). With the growth in crude oil and its products during the 1900s, Diesel engines were changed to be suitable for the petrol Diesel (Pahl, 2008). As the energy demand increased, and problems in obtaining fossil fuel during World War II were confronted, vegetable oil was again investigated. However, problems were encountered in making vegetable oil work with the new Diesel engines due to its high viscosity (Abdalla and Oshaik, 2013).

Pyrolysis, blending with different solvents, and emulsifying with water or alcohol were some of the methods investigated to reduce the vegetable oil's viscosity. These methods present significant technical issues that need to be overcome for large-scale applications to fuel production (Pahl, 2008). E. Duff and J. Patrick in 1853 were the first to work on the transesterification of vegetable oil. However, no application of the product as a source of fuel was mentioned (Abdalla and Oshaik, 2013, Demirbas, 2008). In 1937 G. Chavanne, a Belgian inventor developed transesterification for reducing the viscosity of vegetable oil to be used in a Diesel engine without the requirement for significant adjustments to the engine (Krahl et al., 2010). Chavanne used ethanol as the short-chain alcohol for the reaction granted a patent for converting vegetable oil to useful fuels. This was the start of biodiesel production, though it was not named biodiesel until 1984. Since then, there have been numerous investigations into the production of biodiesel (Knothe et al., 2005, Demirbas, 2008). However, methanol is nowadays used due to it higher reactivity and absorb less water than ethanol (Musa, 2016).

The first commercial biodiesel plant was constructed in Austria in 1987. By 1992, commercial production was established across Europe and in the United States. In 2004, the number of biodiesel plants in the United States had increased to 25. Data shows

global production in 2005 to be over 1 billion gallons and increased to 1.3 billion gallons in 2006 as reported by the United States Environmental Protection Agency (EPA) Moderated Transaction System (EMTS). In 2013 biodiesel production in the United States alone exceeded 1.3 billion gallons. Strong growth in the production of over 1.7 billion gallons was produced in 2019 (see *Figure **2**-**1***). Massive increase was also observed in United Kingdom from 175 million liters in 2010 to 573 million liters (see *Figure **2**-**2***).

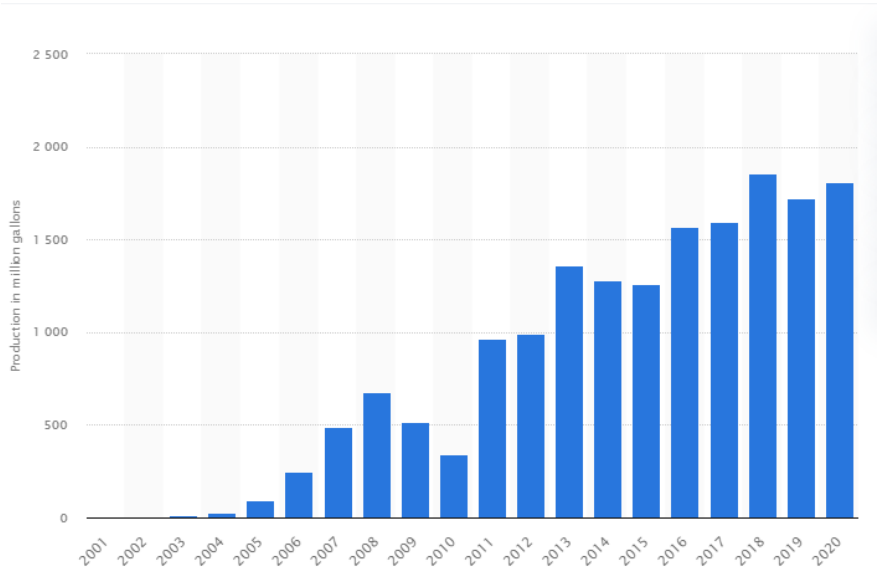

Figure 2-1: US biodiesel production from 2001 to 2020. Source: https://www.statista.com/statistics/509875/production-volume-of-biodiesel-in-the-us/

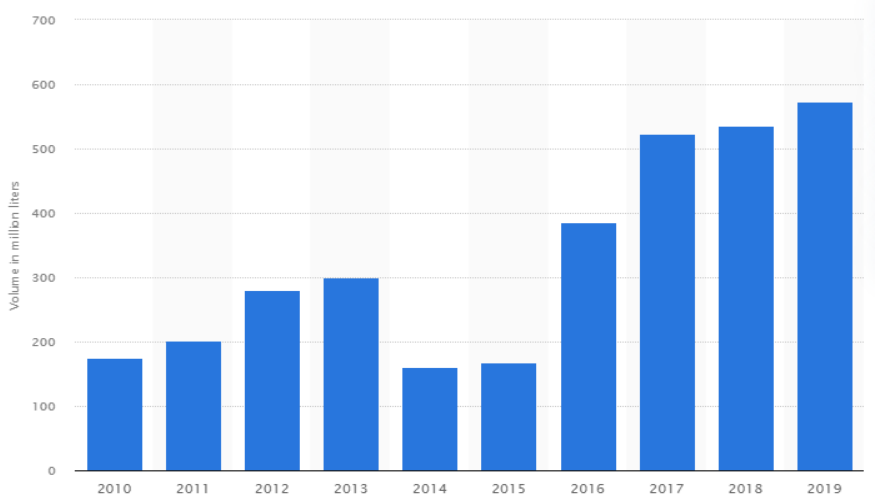

Figure 2-2: Biodiesel production in UK from 2010 to 2019 in million liters. Source: https://www.statista.com/statistics/791692/biodiesel-production-united-kingdom-uk/.

2.3 Methods of Biodiesel Production

There are different methods for biodiesel production. Among the most reported in the literature is the conventional and reactive extraction (*in situ*) methods. Others include microemulsion, supercritical fluid, ultrasound-assisted, membrane technology, microwave-assisted, and microreactor.

2.3.1 Microemulsion

Microemulsions reduce vegetable oil viscosity by isotropic mixing of the vegetable oil to solvent (usually methanol, ethanol, or 1-butanol) and surfactant (Bora et al., 2016). The surfactant (amphiphilic molecules either ionic or non-ionic) lowers the surface tension and improves the vegetable oil and solvent miscibility. Unlike conventional methods that require catalysts, microemulsions do not require any catalyst. However, surfactants are necessary, which in some cases are effectively more expensive than the catalyst used for the conventional method. Some surfactant and co-surfactants used in previous work are shown in *Table **2**-**1***.

Table 2-1: Review of biodiesel production using microemulsion method

Feedstock	Solvent	Surfactant	Reference
Soybean oil	Methanol	lipase	Tan et al. (2014)
Waste cooking oil	Ethanol	1-butanol	Bora et al. (2016)
Canola oil	Ethanol	Carboxylate-base	Attaphong et al. (2012)
Jatropha curcas oil	Ethanol	Ethylene oxide	Sankumgon et al. (2018)
Canola oil	Ethanol	Carboxylate-base, Ethoxylate, Sorbitan monolaurate, Sorbitan monooleate, Sorbitan trioleate, Oleyl alcohol	Attaphong and Sabatini (2013)

Algae, Canola, Palm oil	Ethanol	Oleyl alcohol, Oleyl amine, 2 Ethylhexanol, 2 Ethylhexylnitrate, n-Octanol, Ethylene glycol butyl ether	Do et al. (2011)
Peanut oil		Rhamnolipid, Sophorolipid, Lecithin, Sodium bis(2-ethyl) dihexyl sulfosuccinate, Oleyl alcohol	Nguyen et al. (2010)

Another drawback of this method is the deposition of carbon and incomplete combustion in the Diesel engine (Ma and Hanna, 1999). Most of the previous work (as shown in *Table **2**-**1***) used ethanol for the formulation. This result to lower miscibility with diesel. The formulation with vegetable oil is also less stable than formulation with diesel (Attaphong et al., 2012). Another drawback from this method is the selection of suitable surfactant and co-surfactant. Due to the environmental friendliness, surfactant and co-surfactant that do not contained nitrogen and sulfur are encouraged (Bora et al., 2016).

2.3.2 Process Intensification Methods for Biodiesel Production

According to Reay et al. (2013), process intensification is "*Any chemical engineering development that leads to a substantially smaller, cleaner, safer and more energy efficient technology*". For a process to be intensified, it is expected that one or more of the following point is achieved;

I. Capital investment is appreciably reduced
II. Reduce operating cost
III. Reduced energy usage
IV. Increase quality
V. Increased process flexibility and inventory reduction
VI. Process safety
VII. Better environment
VIII. Size reduction
IX. Increase speed of the process
X. Reduced waste

(Reay et al., 2013, Kiss, 2014, Klemeš and Varbanov, 2013)

Process intensification in biodiesel production is necessary due to wastewater generated, high energy requirement, thermodynamic equilibrium, limited mass transfer, and multiple downstream processing (Shuit et al., 2012). Various techniques has been applied for the intensification of biodiesel production process. These methods are used to either reduced reaction time, increase quality of the product, reduced size of the reaction process, or decrease both capital and operating cost. Some of these methods include membrane technology, microwave irradiation, supercritical, ultrasound, oscillatory baffle reactors (OBR), and micro reactors.

2.3.2.1 Membrane Technology

Membrane technology also refer to as membrane-based reactive separator combines transesterification and separation technology. The membrane act as a barrier and regulate the flow of substances with different mass transfer rates. The mass transfer is controlled by the permeability of the membrane. The process simultaneously reacts and separates the glycerol from the product stream or retain the unreacted triglycerides from the FAME produced, as shown in *Figure 2-3*.

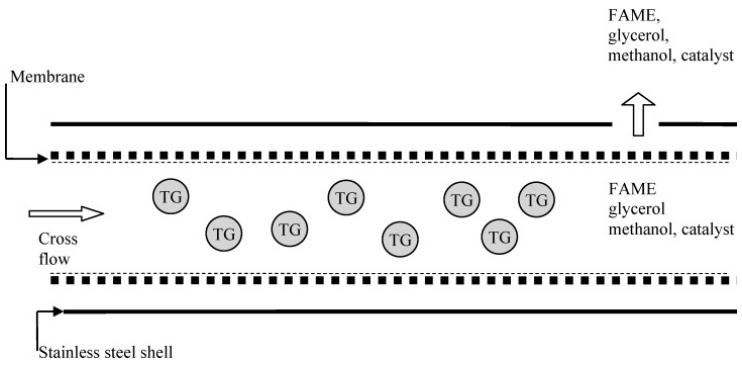

Figure 2-3: Membrane technology for biodiesel production (Cao et al., 2007).

This method has an added advantage of separating the unreacted triglyceride from FAME, reducing the side reaction, and recycling needs (Baroutian et al., 2011). Membrane technology has been applied in biodiesel production and *Table **2-2*** below shows some previous studies.

Table 2-2: Review of biodiesel production using membrane technology.

Feed	Catalyst	Membrane pore size (μm)	Reaction conditions	Conversion (%)	Reference
Canola oil	H_2SO_4, NaOH	0.05	60 – 70 ^{O}C, 6 h, 0.5 – 6 wt%, 138 kPa	96	Dubé et al. (2007)
Canola, Soybean, Palm, Yellow grease	NaOH	0.02	65 ^{o}C, 1 h, 37 – 43 kPa		Cao et al. (2008a)
Canola oil	NaOH	0.02	65 ^{o}C, 8 h, 173 kPa	> 90	Cao et al. (2008b)
Waste cooking oil	PSSA/PVA		8 h, 64 ^{o}C	92	Zhu et al. (2010)
Canola oil	NaOH		20 – 60 ^{o}C, 2 h, 0.05 – 0.5 wt%	100	Cheng et al. (2010)
Palm oil	KOH/palm shell activated carbon	0.05	50 – 70 ^{o}C	> 90	Baroutian et al. (2011)
Canola oil	NaOH	0.05 – 1.4	55 ^{o}C, 0.5 wt%, 550 kPa, 2.5 h	99	Cao et al. (2007)
Canola, Corn, Sunflower, Soy, Waste cooking oil	H_2SO_4	0.03	90 kPa, 65 ^{o}C, 6 h, 0.5 – 1.4 wt%		Falahati and Tremblay (2012)

The method is expensive for a targeted application and poor separation (Atadashi et al., 2011). The technique also support leaching when reaction is perform with solid catalyst, limited to the shape of the material to be filtered and pore size of the membrane (Atadashi et al., 2011, Atadashi et al., 2013).

2.3.2.2 Supercritical Fluid

This method produced biodiesel at the supercritical condition. The biodiesel is produced in the absence of a catalyst with a short reaction time. Feedstock such as grease, animal fat, or high free fatty feedstock is more suitable for biodiesel production than conventional transesterification. Some drawbacks of the method include the need for

high temperatures (above 250 ^{o}C), high pressures (above 10 MPa), and high alcohol (usually methanol or ethanol)-to-oil molar ratio (Marulanda et al., 2010b, Velez et al., 2012). These conditions make the method uneconomic even on a large-scale, hence may have fewer industrial competitors. Some of the documented works are reviewed in the *Table **2**-**3*** below.

Table 2-3: Review of biodiesel production using supercritical method.

Feed	Methodology				Yield (%)	Reference
	Supercritical	Molar ratio	Temp (^{o}C)	Pressure (bar)		
Lamb fat	CO_2	5:1 – 20:1	45 – 50	200	53.5	Al-Zuhair et al. (2012)
Palm oil	Ethyl acetate	30:1	380	160	90.9	Komintarachat et al. (2015)
Waste cooking oil	Methanol	37:1	253.5	198.5	91	Aboelazayem et al. (2018a)
Jatropha oil	Methyl acetate	20:1 – 60:1	330 – 420	47	68	Niza et al. (2013)
Sunflower oil	Ethanol	40:1	300 – 345	165 – 200	91	Velez et al. (2012)
Waste canola oil	Methanol	1:1 – 2:1	240 – 270	100	102	Lee et al. (2012)
Chicken fat	Methanol	3:1 – 6:1	300 – 400	411	88	Marulanda et al. (2010b)
Waste cooking oil	Methanol	20:1 – 40:1	240 – 280	85 – 185	98.8	Aboelazayem et al. (2018b)

From *Table **2**-**3***, it is clear that high yield is achieved with supercritical method. However, high molar ratio, temperature, and pressure is required which makes the method economically not viable.

2.3.2.3 Ultrasound-Assisted

The ultrasound-assisted method is frequently used on low-cost feedstocks with a high free fatty acid such as animal fat. It is performed in ultrasound condition with low frequencies between 20 – 40 kHz and without a mechanical stirrer (Veljković et al., 2012). When compared to the conventional method, the ultrasound-assisted method produces biodiesel faster. The method is also known for the high yield of biodiesel production and less energy requirement (Tan et al., 2019). *Table **2-4*** shows review of previous literatures using different catalyst type.

Table 2-4: Review of biodiesel production using ultrasound-assisted method.

Feedstock	Frequency (kHz)	Power (W)	Catalyst type	Operation conditions	Yield (%)	Reference
Blend of non-edible oil (WCO 30%, crude palm oil 30%, rubber 25%, jatropha 15%	35	35	*Thermomyces lanuginosus*	Methanol, 4:1-10:1, 1-5 wt%, 25-45 ^{o}C, 120 min	94	Malani et al. (2019)
Sunflower oil	24	200	NaOH	Methanol, 7:1, 1-2 wt%, 60 ^{o}C, 5-60 min	95	Georgogianni et al. (2008)
Orechromis niloticus oil	40	60	H_2SO_4	Methanol, 3:1-9:1, 30 ^{o}C, 0.5-2 wt%, 90 min	98	Santos et al. (2010)
Coconut oil	40	132	Novozym 435	Ethanol, 40-70 ^{o}C, 5-20 wt%, 3:1-10:1, 360 min	80	Michelin et al. (2015)
Canola oil	20	60	CaO, calcined dolomite, calcium diglyceroxide	Methanol, 4:1-12:1, 45-60 ^{o}C, 75-135 min	99	Korkut and Bayramoglu (2018)
Palm fatty acid distillate	25	1000	H_2SO_4	Isopropyl, 3:1-9:1, 30-60 ^{o}C, 5 wt%, 360 min	80	Deshmane et al. (2009)

Solid food waste oil	40 – 70		H_2SO_4,	Methanol, 4.5:1-6.5:1, 0.8-2 wt%, 40-65 °C, 120 mins	94	Carmona-Cabello et al. (2019)
Canola oil	20	20-50	Calcined dolomite, CaO	Methanol, 4:1-15:1, 3-7 wt%, 25-60 °C, 60-120 min	97	Korkut and Bayramoglu (2016)
Neat vegetable oil	28 – 40	400	NaOH	Methanol, 6:1, 0.5-1.5 wt%, 25 °C, 10-40 min	98	Stavarache et al. (2003)

High yield is produced using ultrasound-assisted method. However, the method requires high catalyst concentration which increases the waste generation and cost of production.

2.3.2.4 Microwave-Assisted

This method uses electromagnetic waves within the frequencies of 0.3 – 300 GHz and wavelengths from 0.01 – 0.1 m (Motasemi and Ani, 2012). It has an advantage of short reaction time, and higher yield when compared to conventional transesterification (Khedri et al., 2019). Microwave-assisted method of biodiesel production do not improved mixing, rather utilized irradiation to directly transfer energy to the mixture. This makes the method faster than the conventional method used (Qiu et al., 2010, Shuit et al., 2012). Microwave-assisted transesterification is suitable for low-cost feedstocks with high free fatty acid (Nayak and Vyas, 2019, Jaliliannosrati et al., 2013). This is because of its effective heat transfer. *Table **2-5*** below is the review of some previous studies performed using microwave-assisted technique.

Table 2-5: Review of biodiesel production using microwave-assisted method.

Feedstock	Power (W)	Catalyst type	Operation conditions	Yield (%)	Reference
Papaya oil	700	NaOH	Methanol, 3:1-15:1, 0.5-1.5 wt%, 50-70 °C, 0.5-10.5 min	99	Nayak and Vyas (2019)
Waste cotton seed cooking oil	900	KOH, CaO	Methanol, 6:1-12:1, 0.3-2 w/w%, 6-12 min, 50 °C	96	Sharma et al. (2019)

Waste cooking oil	100-400	H_2SO_4	Methanol, 1:0.1, 0.17-1 min, 1 wt%		Supraja et al. (2020)
Wet microalgal	700	Ionic liquid (1-ethyl-3-methylimmidazolium methyl sulphate)	Methanol, 4:1-12:1, 65-95 ^oC, 5-25 min, methanol to ionic liquid 1:0.5-1:1	40.9	Wahidin et al. (2018)
Waste cooking oil	10 – 55	Novozym 435	Dimethyl carbonate, 2:1-9:1, 5-15 w/w%, 300 min, 50-80 ^oC	94	Panadare and Rathod (2016)
Rapeseed oil	1000	KSF montmorillonite	Methanol, 9:1-18:1, 170 ^oC, 10-60 min, 10 %w/w	56	Mazzocchia et al. (2004)
Palm Oil	900	KOH	Methanol, 2-10 min	97	Jimmy (2015)
Palm oil	450-900	CaO from eggshell	Methanol, 12:1-24:1, 5-15 wt%, 1-4 min	97	Khemthong et al. (2012)
Coconut oil, rice bran oil, Waste cooking oil	800	NaOH	Ethanol, 9:1, 0.5-1 min, 1 %	100	Lertsathapornsuk et al. (2005)
Jatropha curcas	110	H_2SO_4/KOH	Ethanol to seed 10.5 %(v/w), 7.5 wt%, 35 min	90	Jaliliannosrati et al. (2013)

Generally, the method produced biodiesel with high yield and short reaction time. However, the method still has fewer industrial competitors due to the high capital cost.

2.3.2.5 Micro-reactor

Micro-reactor is an emerging technique with a reduced internal dimension of between 1000 – 10 µm for the continuous reaction. Transesterification with a micro-reactor has fast conversion, reduced mass, and energy transfer limitation. This is due to the high surface area to volume ratio created in the channel (Pontes et al., 2017). Due to the high heat transfer rate with micro-reactors, it has the tendency to consumed less energy when compared to stirrer tank reactor (Shuit et al., 2012). Review of some previous studies on biodiesel production using micro-reactor are shown in *Table **2-6*** below.

Table 2-6: Review of biodiesel production using micro-reactor method.

Feedstock	Reactor	Catalyst	Operation conditions				Yield (%)	Reference
			Cat. (wt%)	Temp (°C)	Residence time (min)	Molar ratio		
Palm oil	i.d = 1.6-0.58 mm l = 1000 mm T-shape	KOH	0.5-5	60	1-3	21:1	98.8	Azam et al. (2016)
Soybean oil	l= 1.07 m d_h = 0.24 – 0.9 zigzag	NaOH	0.55-1.5	40-75	0.3-0.47	4:1-17:1	99.5	Wen et al. (2009)
Rapeseed Cottonseed	i.d= 0.25 mm l= 30 m	KOH	1	60	6	6:1	99	Sun et al. (2008)
Microalgal	i.d= 0.25 mm l= 20 m Y-shape	H_2SO_4	2	80-100	10-35			Liu et al. (2018)
Vegetable oils		NaOH	1	60	25	6:1	100	Fatoni et al. (2018)
Soybean oil	d_p= 1-10 mm w= 2 mm l= 15.24 cm T-shape	NaOH		55-65	15	6:1	100	Kalu et al. (2011)
Microalgae	i.d= 0.5 mm l= 500 mm T-shape	DBSA	1-15	30-140	5-30	5:1-50:1	99	Jazie et al. (2020)
Sunflower oil	i.d= 0.076 mm l= 5 m	NaOH		60	4	6:1	99	López-Guajardo et al. (2011)
Castor oil	l= 1 m d_h= 0.5 mm T-Shape	NaOH	1	50	10	12:1	93.5	Martinez Arias et al. (2012)

High yield and short residence time is obtained using micro-reactor. As shown in *Table **2**-**6***, micro-reactor technique requires high molar ratio. Another drawback of this method is the industrial scaling and volumetric production.

2.3.2.6 Oscillatory Baffled Reactor (OBR)

Oscillatory baffle reactor has been referred to as a plug flow reactor in a continuous state. The reactor contains equally spaced orifice plate baffles combined with oscillatory flow. This increase mixing by the production of vortices thereby increase mass and heat transfer (Shuit et al., 2012, Phan et al., 2011, Qiu et al., 2010). Also, the technique has advantage of an improved residence time distribution and multi-phase suspension. *Figure **2**-**4*** below shows different configurations of oscillatory baffled reactors.

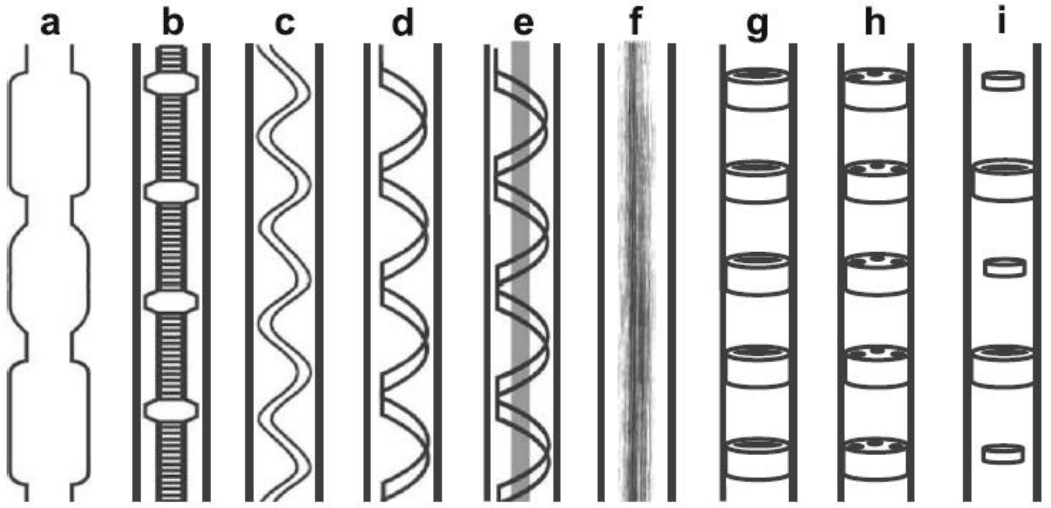

Figure 2-4: Oscillatory baffled reactors with different configurations (Bianchi et al., 2020).

According to Qiu et al. (2010), the techniques has low capital cost, reduced cost of pumping, and easy to control due to the smaller length to diameter ratio. *Table **2**-**7*** below show previous studies on biodiesel production using oscillatory baffled reactors.

Table 2-7: Review of biodiesel production using oscillatory flow reactor method.

Feedstock	Reactor	Catalyst	Operation conditions				Yield (%)	Reference
			Cat. (wt%)	Temp (°C)	Residence time (min)	Molar ratio		
Waste cooking oil	i.d= 14.4 cm, o.d= 17.4 cm, h= 110 cm, 0.33-0.67 Hz 6 baffles, 15.3 cm space, Disc d= 5 cm	NaOH	1	60	20-30	6:1-10:1	78.8	García-Martín et al. (2018)

Rapeseed oil	d= 5 mm, l= 340 mm, baffles (central sharp-edge and helical-[round cross-section wire and sharp-edge helical])	KOH		60	10-40	4:1 – 12:1	>90	Phan et al. (2011)
Rapeseed oil	l= 340 mm, v= 20 mL, baffles (integrally baffled, wire wool, and sharp-edge helical)	KOH CH_3ONa	0.35-1.5	60	5-15		>95	Phan et al. (2012)
Rapeseed oil	i.d= 25 mm, l= 1.5 m, i.v= 1.56 dm^3	NaOH		20-70	10-30			Harvey et al. (2003)
Waste cooking oil	l= 70 cm, i.d = 15 mm, spaced = 26 mm, 0.4 – 1.4 Hz	NaOH H_2SO_4		44	6		92	Mazubert et al. (2014)
Hexanoic acid	i.d = 5 mm, l= 340 mm, d_f = 2.5 mm, spaced =7.5 mm	$PrSO_3H$-SBA-15	5	60	30-60	6:1		Eze et al. (2013)
Waste cooking oil	d= 0.06m, h= 0.55 m, 2.4 – 4.9 Hz, spaced = 0-05 – 0.09 m	KOH	1	40-60	5	6:1	81.9	Soufi et al. (2017)
Waste cooking oil	V= 300 mL, l= 448.5 cm, i.d= 6 mm, spaced= 14.5 mm, 0-8 Hz	KOH H_2SO_4	2.5-3.5	65	0.6-1	9:1-15:1	98	Santikunaporn et al. (2020)
Vegetable oil	i.d= 5 mm, l= 20 cm, meso tube (d= 5 mm, λ = 15.2 mm, δ = 6.4 mm), 6-15 Hz	NaOH	4.2	60	30-40	6:1	>98	Zheng et al. (2007)

High yield of biodiesel and short residence time is possible for the production of biodiesel using oscillatory flow reactors. However, the drawback from this technique is

the complicated design of the reactors and difficulty with a viscous fluid. The method is currently not use for commercial biodiesel production.

2.3.3 The "Conventional Method"

The conventional biodiesel production method transesterified the oil/fat/grease feedstock with short-chain alcohol. Transesterification is currently by far the most widely used commercial method of biodiesel production across the globe. Typically, in this process, following pretreatment steps such as drying and grinding (Salimon et al., 2010), oil is extracted from the oilseeds using a solvent (Islam et al., 2015, Bhuiya et al., 2016) and mechanical press (Subroto et al., 2015, Ahmad et al., 2016) or (more usually) a combination of the two methods (Tan et al., 2017) for optimal extraction. The extracted oil contains impurities such as sterols, odour, water, and free fatty acids, which in most cases are removed before use (Ma and Hanna, 1999). **Error! Reference source not found.** is a flow diagram showing the biodiesel production process. After extraction, the oil is esterified (if the FFA exceeds 0.5 wt%) to remove free fatty acids (Lotero et al., 2005) by reaction with short-chain alcohol in the presence of an acid catalyst, usually sulphuric acid. The esterification reaction conditions mainly depend on the feedstock FFA and water content (Lotero et al., 2005). During this step, the free fatty acid in the vegetable oil is converted into esters (Lotero et al., 2005, Lotero et al., 2006, Tesser et al., 2010). The esterified sample is then dried. The next step is transesterification of the triglycerides to their alkyl ester, biodiesel. The reaction rate of this step is much higher with a base catalyst than an acid. However, the base catalyst can only be used if the feedstock's free fatty acid is reduced to < 1 %. Otherwise, saponification will occur simultaneously as the biodiesel reaction, converting at least some of the triglyceride into soap rather than biodiesel (Fadhil et al., 2017, Ong et al., 2013a). It can also consume the catalyst since FFA can react directly with the catalyst.

Figure 2-5: Process flow diagram for conventional biodiesel production.

The two phases resulting from the transesterification reaction, the GRP (glycerol-rich phase) and the BRP (biodiesel-rich phase) are separated by gravity. The BRP is purified by neutralising the catalyst used, wet-washing with warm water repeatedly, centrifuging, and drying (*Figure **2-5***). The alcohol and glycerol purification is performed using the various technique (neutralisation, distillation, adsorption, ion-exchange, crystallisation, decantation, filtration). For high purification, some of the techniques are used in combination. This increases the cost of production. One benefit this current work wishes to achieve is eliminating the "alcohol recovery and glycerol purification" section.

The conventional method varies with the catalyst type. This includes homogeneous alkaline and acidic, heterogeneous alkaline and acidic or enzyme-catalysed methods as reported by various authors (Atadashi et al., 2013, Saifuddin et al., 2015, Manique et al., 2017, Lotero et al., 2005, Demirbas, 2009).

2.3.3.1 Homogeneous base-catalysed transesterification

Base-catalysed transesterification is favoured due to its fast rate compared to acid-catalysed transesterification. It is not corrosive and does not produce water. Complete triglyceride conversion can be achieved within 30 – 60 minutes. However, for quality biodiesel production, the feedstock must have it FFA less than 0.5 wt%, else the reaction produced soap. This means the feedstock (if FFA is greater than 0.5 wt%) must be purified or pretreated (with an acid catalyst) before transesterification with alkaline. Also, after transesterification, the waste must be adequately managed. Some examples of these catalysts include sodium hydroxide (NaOH), potassium hydroxide (KOH), sodium methoxide (CH_3ONa), and potassium methoxide (CH_3OK). *Table 2-8* below includes previous work using the alkaline catalyst for biodiesel production.

Table 2-8: Review of biodiesel production using base catalyse

Feedstock	Process variables					Result		Reference
	Catalyst	Temp (°C)	Ratio	Conc. (wt%)	Time (mins)	Conv (%)	Yield (%)	
Silybum marianum	KOH	60	6:1	0.9	100	95		Fadhil et al. (2017)
Chicken fat	NaOH KOH CH_3ONa CH_3OK	25 – 60	6:1	1	60 – 360		>90	Alptekin and Canakci (2011)
Sunflower oil	NaOH KOH CH_3ONa CH_3OK	65	6:1	1			85.9 91.7 99.3 98.5	Vicente et al. (2004)
Cottonseed oil	NaOH	53	7.9:1	1	45		97	Fan et al. (2011)
Sunflower oil	NaOH KOH CH_3ONa CH_3OK	30 – 60	6:1	0.5 – 1	120	94 – 99	97.1	Rashid et al. (2008)
Waste cooking oil	CH_3ONa	60	6:1 – 18:1	0.6 – 3	0.5 – 60		98	Eze et al. (2018)

From *Table 2-8*, it can be concluded that high biodiesel yield is produced with a base catalyst within 60 minutes. However, the process still required additional process to recover the excess alcohol and purify the glycerol.

2.3.3.2 Homogeneous acid-catalysed transesterification

The yield of biodiesel with an acid catalyst is high, although the reaction is (4000 times) slower and requires a high molar ratio (Lotero et al., 2005). These make it a less favourable technique for commercial purposes. It is corrosive and produces water. However, it is suitable for feedstock with high FFA. Examples of this catalyst include

hydrochloric acid (HCl), sulfuric acid (H_2SO_4), sulfonic acid (H_2SO_3), and ferric sulfate ($Fe_2(SO_4)_3$).

Table 2-9: Review of biodiesel production using acid catalyse.

Feedstock	Process variables					Result		Reference
	Catalyst	Temp (°C)	Ratio	Conc. (wt%)	Time (mins)	Conv (%)	Yield (%)	
Used frying oil	H_2SO_4	65	3.6:1	0.1	2400		64 – 79	Nye et al. (1983)
Trap grease	H_2SO_4	95	35:1	11.27	275	~ 90		Wang et al. (2008)
Soybean oil	H_2SO_4	25 – 60	30:1	1 – 5	2880 – 5760		98.4	Canakci and Van Gerpen (1999)
Waste tallow	H_2SO_4	50 – 60	30:1	1.25 – 5	1440	93 – 99		Bhatti et al. (2008)
Waste frying oil	H_2SO_4	70 – 80	174:1 – 245:1		240	99		Zheng et al. (2006)

Table 2-9 shows the review of transesterification with an acid catalyst. It can be concluded that high biodiesel yield or conversion is achieved using feedstocks with high FFA. However, the process required long reaction time and a high molar ratio. It also requires recovery of the excess alcohol and purification of both biodiesel and glycerol by-product.

2.3.3.3 Heterogeneous base-catalysed transesterification

The advantages of homogeneous base catalysts were fast reaction and high yield. Apart from the waste generated after neutralisation with an acid, the catalyst cannot be recovered. It is also not suitable when used in feedstocks with high FFA and water content. On the other hand, a solid base catalyst is reusable and can be used in a continuous fixed bed reactor. It also has high activity and achieved good yield with a

moderate condition. However, the reaction rate is also slow, and the catalyst is leached during transesterification. Some of these catalysts have complicated preparation steps and expensive. Examples of this catalyst include CaO, ZnO, $Ca(OH)_2$, and MgO.

Table 2-10: Review of biodiesel production using solid base catalyse.

Feedstock	Process variables					Result		Reference
	Catalyst	Temp (°C)	Ratio	Conc. (wt%)	Time (mins)	Conv (%)	Yield (%)	
Soybean oil	Zeolite/ CaO	65	9:1	30	180		95	Wu et al. (2013)
Jatropha oil	Wood ash/ K_2CO_3 and $CaCO_3$	65	12:1		180	97 – 99		Sharma et al. (2012)
Sunflower	CaO	60	13:1	1	90		60 – 90	Granados et al. (2007)
Fried vegetable oil	CaO SrO K_3PO_4	65	6:1	5	180		92 86 78	Viola et al. (2012)
Olive oil	SrO/SiO_2	45 – 65	6:1	5	10 – 60	95		Chen et al. (2012)
Palm kernel	Limestone Dolomite	60	30:1	6	180		49 98	Ngamcharussrivichai et al. (2007)

Although the technique achieved high triglyceride conversion and biodiesel yield (*Table 2-10*), it depends on the catalyst activeness. It also takes a long reaction time and a high molar ratio.

2.3.3.4 Heterogeneous acid-catalysed transesterification

Homogeneous acid catalysts are more effective than heterogeneous acid catalysts. However, it has a contamination problem and makes separation difficult, which translates to a high production cost. To increase the process economic viability, the solid acid catalyst is used in a continuous process to reduce waste generation. Solid acid

catalyst has a low reaction rate due to low catalytic activity. This might be due to mass transfer limitation during mixing (Semwal et al., 2011).

Table 2-11: Review of biodiesel production using solid acid catalyse.

Feedstock	Process variables					Result		Reference
	Catalyst	Temp (^oC)	Ratio	Conc. (wt%)	Time (mins)	Conv (%)	Yield (%)	
Castor Jatropha	Si-MMT-Ph-SO_3H	60 110	12:1 6:1	5	300 150	90 98		Negm et al. (2017)
Rubber seed oil	Fe/C	50 – 60	9:1 – 15:1	4.5 – 5.5	60		97	Dhawane et al. (2017)
Soybean oil	WO_3/ZrO_2 SO_4/SnO_2 SO_4/ZrO_2	200 – 300	40:1		1200 – 6000	>90		Furuta et al. (2004)
Palm kernel oil Coconut oil	SO_4/ZrO_2	200	6:1	1 – 3	240	>90		Jitputti et al. (2006)
Eruca sativa	$Cs_{2.5}H_{0.5}PW_{12}O_{40}$	60	5.3:1		60	98		Chai et al. (2007)

The catalyst can be used in feedstocks with high FFA, although it requires long reaction time and high temperature (*Table 2-11*). Also, preparing some of these catalysts is complicated and expensive, which makes it economically not viable.

2.3.3.5 Enzyme-catalysed transesterification

Enzyme-catalysed transesterification is used on feedstocks with high FFA. Hence, it can be used for both transesterification and esterification. This technique produced a high yield and is environmentally friendly. Also, previous works have reported it to have high purity and to be easily separable. However, its cost makes it uneconomic. Some examples of such catalysts includes *Candida sp, Pseudomonas cepacian, and Pseudomonas fluorescens*.

Table 2-12: Review of biodiesel production using enzymes as catalyse.

Feedstock	Process variables				Result	Reference
	Catalyst	Temp (°C)	Ratio	Time (mins)	Yield (%)	
Jatropha oil	*Candida rugosa* *Chromobacterium viscosum*	40	4:1	480	71	Shah et al. (2004)
Soybean oil	*Pseudomonas cepacia*	35	7.5:1	60	67	Noureddini et al. (2005)
Cottonseed oil	*Candida antarctica*	50		1440	95	Royon et al. (2007)
Jatropha oil	*Pseudomonas cepacia*	50	4:1	480	98	Shah and Gupta (2007)
Soybean oil	*Thermomyces lanuginose*	30 – 50	3:1 – 5:1	180 – 720	92	Du et al. (2003)
Canola oil	*Thermomyces lanuginose*	50	6:1	1440	97	Dizge et al. (2009)
Pomace oil	*Thermomyces lanuginose*	25	6:1	1440	93	Yücel (2011)

The catalyst is used at relatively low temperatures in a feedstock with high FFA or water content. The technique also can easily separate the biodiesel rich phase from the glycerol rich phase. However, the cost of the catalyst makes it economically not viable. All the catalysts used have their merit and demerit. This can be summarised in *Table 2-13*.

Table 2-13: Various catalyst effects.

Catalyst Type	Example	Advantage	Disadvantage
Homogeneous acid catalyst	HCl, H_2SO_4, H_2SO_3	Used in esterification and transesterification, no soap formation, used in feedstock with high FFA	Corrosive, waste generated, low reaction rate, high energy consumption, not recyclable
Homogeneous base catalyst	NaOH, KOH, CH_3ONa, CH_3OK	High reaction rate, less corrosive, moderate reaction condition	Used on pretreated or feedstock with low FFA, high purification cost, soap formation, high waste generated
Heterogeneous acid catalyst	WO_3/ZrO_2, SO_4/SnO_2, SO_4/ZrO_2	Less waste generated, environmentally friendly, recyclable, easy separation, high glycerol purity	Leaching, expensive than homogeneous, complicated preparation steps, slow rate
Heterogeneous base catalyst	CaO, MgO, ZnO	Less waste generated, environmentally friendly, recyclable, easy separation, high glycerol purity	Leaching, expensive than homogeneous, complicated preparation steps, slow rate
Enzymatic catalyst	*Pseudomonas cepacia, Thermomyces lanuginose, Candida antarctica*	environmentally friendly, high purity of the product, easy separation	High cost

In summary, the conventional method for biodiesel production combines three processes (extraction, esterification, and transesterification, as shown in *Figure **2**-**5***) to achieve the desired product. However, the methods can be improved for process intensification. One method used to do this was reactive extraction; hence, no

purification of the vegetable oil (degumming, neutralisation, dewaxing, dephosphorisation, dehydration) is required.

2.3.4 Reactive Extraction Methods

Reactive extraction combines extraction and transesterification in a single step, making the production process faster with fewer process operations and equipment. The difference between the two methods is the direct contact of the raw seed feedstock with alcohol, in the presence of a catalyst. This makes it possible for simultaneous extraction and transesterification to occur. The alcohol is the extraction solvent and esterification or transesterification reagent (Shuit et al., 2009). Reactive extraction is an intensified process of the conventional method, as shown in *Figure **2-6***.

Figure 2-6: Process flow diagram of the reactive extraction method of biodiesel production.

Many studies on reactive extraction have been reported in the literature using various feedstocks and catalyst types. Feedstocks with low FFA (free fatty acid) contents are treated using an alkaline catalyst, while acid catalysts are used for feedstocks with high FFA (Liu et al., 2017) or water content. There are also reports of the use of enzymes in the reactive extraction method (Su et al., 2009). However, the high cost of the enzymes and their denaturing due to reaction with short-chain alcohols are significant disadvantages, due to which they have not been used commercially (Atadashi et al., 2013). Few of the documented works on reactive extraction are reviewed in *Table **2-14*** below.

Table 2-14: Review of reactive extraction with various feedstock and reaction condition.

Feed	Variables				Yield (%)	Reference
	Catalyst	Mole ratio	Temp. (°C)	Time (min)		
Jatropha curcas	H_2SO_4	7.5mL/g	60	1440	99.8	Shuit et al. (2009)
Jatropha curcas	Supercritical	5.0mL/g	300	30	100	Lim and Lee (2014)
Jatropha curcas	Supercritical	10mL/g	200 – 300	45 – 80	103	Lim et al. (2010)
Cottonseed	$S_2O_8^{2-}ZrO_2$–TiO_2–Fe_3O_4	5 – 21mL/g	35 – 55	60 – 1380	98.5	Wu et al. (2014)
Rapeseed	NaOH	170:1 – 550:1	60	120 – 240	80.6	Koutsouki et al. (2016)
Solid coconut waste	KOH	10mL/g	55 – 65	60 – 420	88.5	Sulaiman et al. (2013)
Crude palm oil	KOH	147:1 – 225:1	60	480 – 660	97.3	Jairurob et al. (2013)
Jatropha curcas	H_2SO_4	5 – 20 mL/g	30 – 60	60 – 1440	98.1	Shuit et al. (2010)
Rapeseed	NaOH	300:1 – 900:1	60	350	> 85	Zakaria and Harvey (2012)

From *Table* ***2-14*** reactive extraction was successful using various feedstock, catalyst, techniques, and reaction time. However, high alcohol and reaction are required for higher yield. Also, similar to the conventional method, reactive extraction requires purification of the products and recycling of short-chain alcohol. Purifying crude glycerol increases the cost of the process (Tan et al., 2013). This encourage research on utilising crude glycerol to produce value-added chemicals such as acrolein, acetic acid, methane, hydrogen, or polyglycerol. Using reactive coupling as an intensification process, the downstream can be reduced, as shown in *Figure* ***2-6***.

2.4 Glycerol and Glycerol Properties

Stoichiometrically, transesterification reaction requires 3 moles of short-chain alcohol per mole of triglyceride, to produce 3 moles of biodiesel and a glycerol mole (***Figure 2-7***). However, conventional biodiesel production uses excess alcohol to increase the rate of reaction and equilibrium conversion. This increases the cost of biodiesel production due to the costs of excess alcohol recovery and recycling. This recovery process is a significant part of economics, especially for small and medium biodiesel producers, as it requires distillation.

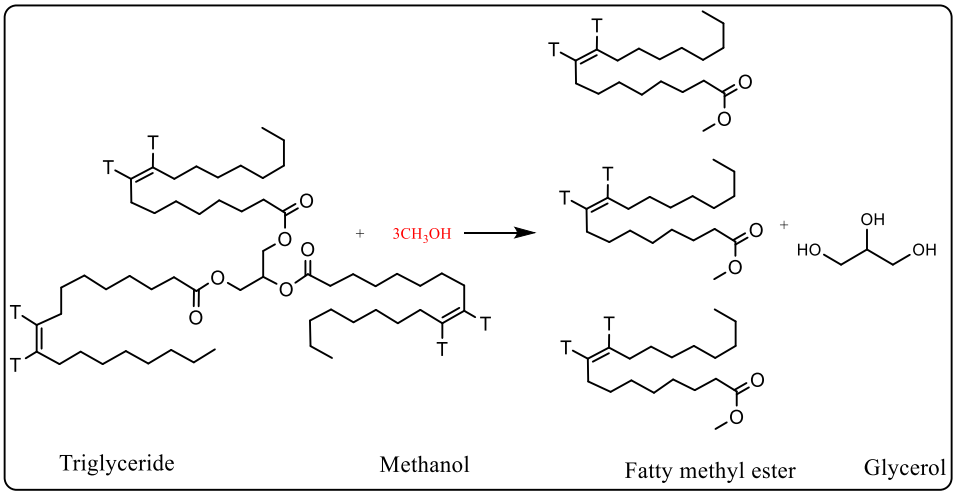

Figure 2-7: Transesterification based on stoichiometric.

One of the key issues in biodiesel process economics is the fate of the crude glycerol by-product. Glycerol is an odourless and colourless viscous liquid, which is also known as 1,2,3-propanetriol (Krahl et al., 2010). It has been known since 2800 BCE as a by-product

in soap formation from reactions of ash and fat (Quispe et al., 2013). Glycerol is hygroscopic and very soluble in water, because of the hydroxyl groups in its structure. As such, it is a useful molecule. However, supply has outstripped demand for the last 20 years due to the biodiesel industry, so prices have fallen to historic lows.

Crude glycerol constitutes ~10 wt.% of the products of biodiesel production and has low quality and market value. It is projected that global crude glycerol output will increase significantly over the next 5 years (see Figure 2-8 (Ciriminna et al., 2014)). Currently, crude glycerol from biodiesel production has a market value of about 0.44 $/kg, approximately half the price (1 $/kg) for refined glycerol after purification (Corma et al., 2008).

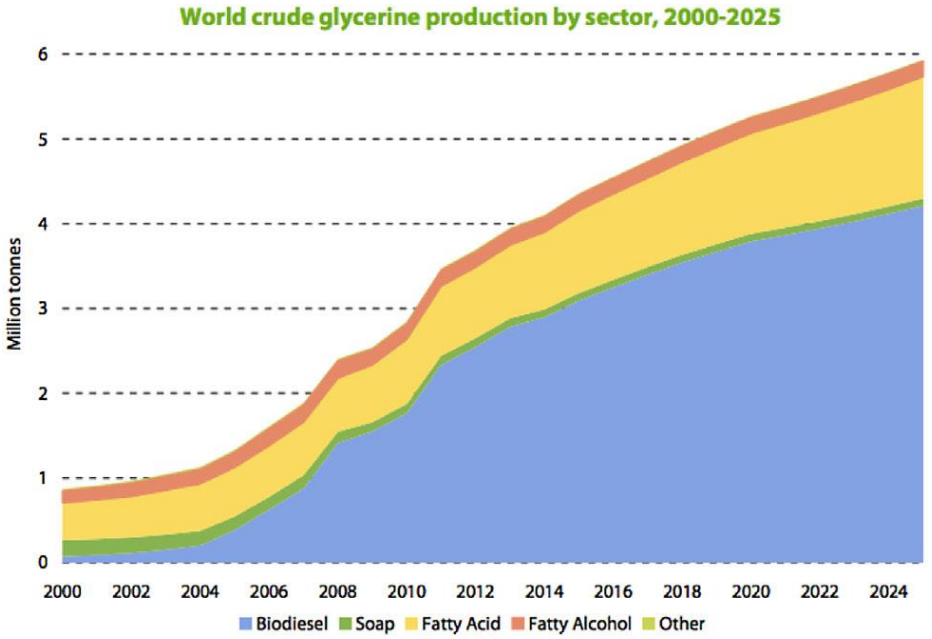

Figure 2-8: Prediction amount crude glycerol around the world (Ciriminna et al., 2014).

2.5 Glycerol Valorisation from Conventional Biodiesel Processes

The enormous amount of glycerol worldwide makes it important to find an economical way to upgrade into various valuable products. Many alternatives have been suggested, including the production of animal feed, drugs, cosmetics, tobacco, fuel additives, waste treatment, and production of various chemicals (Leoneti et al., 2012, Mu et al., 2006, Papanikolaou et al., 2002, Ashby et al., 2004, Krahl et al., 2010, Yang et al., 2012). These glycerol valorisation processes, and more, are shown in *Figure 2-9*.

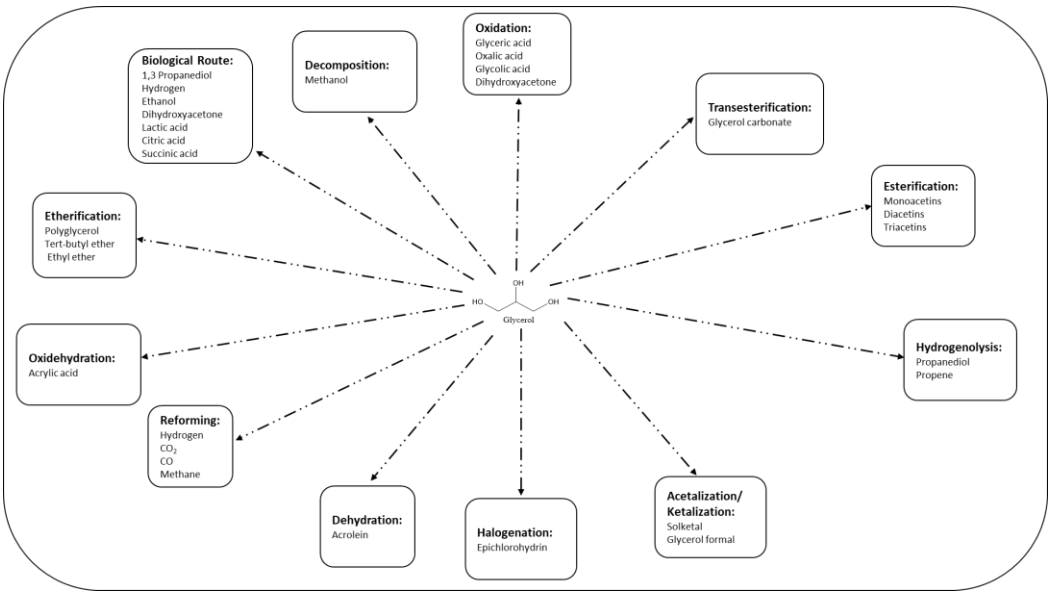

Figure 2-9: Possible reaction processes for glycerol valorisation.

There is a wide range of processes by which crude glycerol can be valorised. However, to be usable in the reactive coupling, the reactions "operating windows" must overlap with either transesterification or esterification. There must be no other unwanted side reactions, with the other reagents introduced (the triglyceride, methanol, and acid or base catalyst).

2.6 The Concept of Reactive Coupling in the Biodiesel Process

Reactive coupling is when two or more reactions take place simultaneously and convert co-products of the initial reaction to the higher added value products in the subsequent reaction. Some examples of the coupled reactions (which will be discussed later) are shown in *Figure 2-10*. It is a form of a process reducing the overall number of process steps, e.g., reducing the need to recycle methanol, in biodiesel production (see *Figure **2**-**5*** and *Figure **2**-**6***). This should reduce the capital cost of the plant, following the original drivers of process intensification.

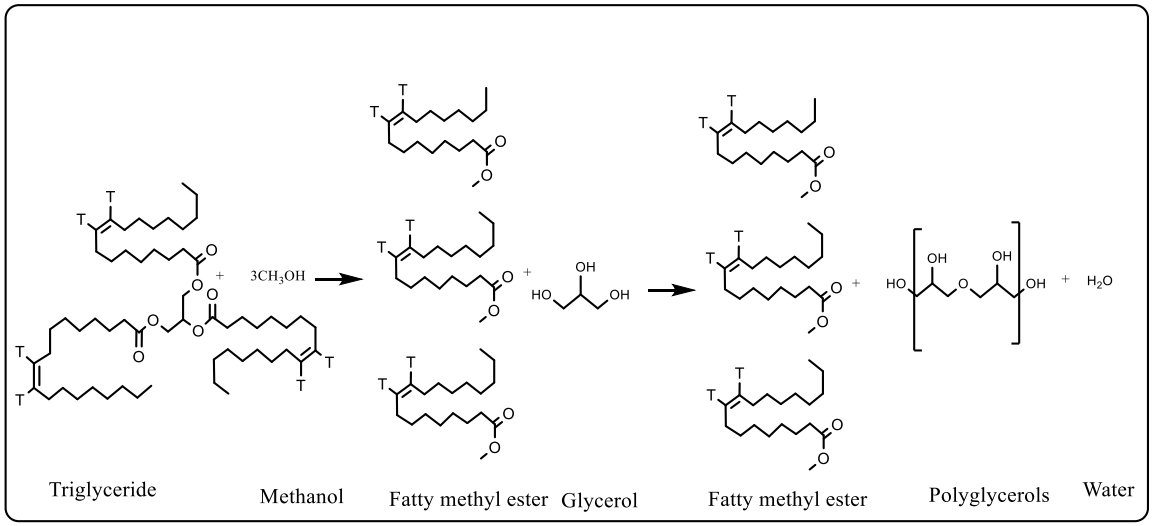

a: The concept of reactive coupling for biodiesel and polyglycerol production

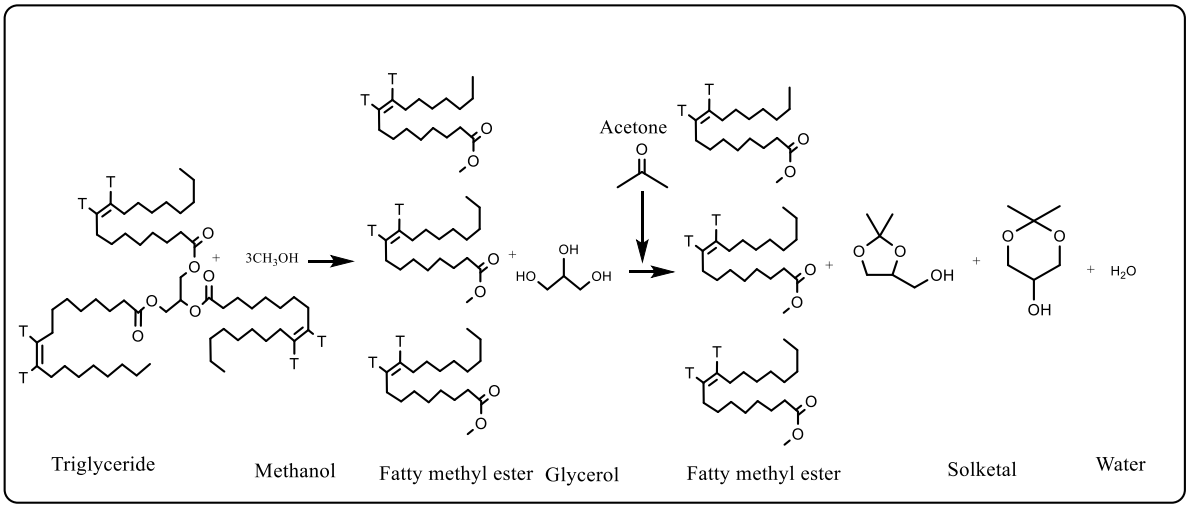

b: The concept of reactive coupling for biodiesel and solketal production

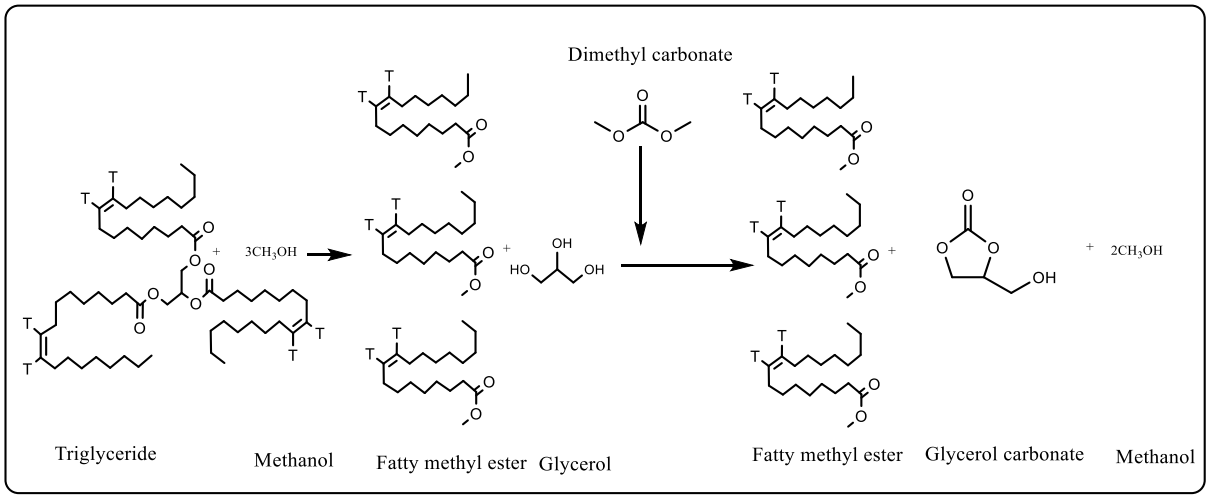

c: The concept of reactive coupling for biodiesel and glycerol carbonate production

Figure 2-10: Reactive coupling processes for biodiesel productions and in situ glycerol valorisation.

Biodiesel production via reactive coupling typically involves continuous removal of one of the products (i.e., glycerol) from the reaction mixture, which shifts the equilibrium to the right, favouring biodiesel formation in this case. This should reduce alcohol usage in biodiesel production and increase the revenue generated from the valorised glycerol. Examples of such reactions are shown below.

2.6.1 Acetins

Glycerol can be valorised through esterification with acetic acid or acetic anhydride to produce monoacetins, diacetins, and triacetins. Acetins can also be produced through transesterification using methyl acetate with methanol as the by-product. The products have applications in polymers and cryogenics (Kale et al., 2013, Bedogni et al., 2014). Triacetins are used as anti-knocking agents in gasoline, diesel, and biodiesel, and as octane boosters in gasoline to replace alkyl ethers such as mono-tert-butyl ether (MTBE) di-tert-butyl ether (DTBE) or, tri-tert-butyl ether (TTBE) (Veluturla et al., 2017, Smirnov et al., 2018). Triacetin also has applications in cosmetics, explosives, plasticisers, and pharmaceutical industries (Veluturla et al., 2017, Smirnov et al., 2018). Glycerol esterification proceeds, as shown in *Figure **2**-**11*** to produce esters and water. The reaction rate and conversion depend on the ratio of glycerol to acetic acid or acetic anhydrides. In industry, excess acetic acid/acetic anhydrides increase the conversion by favouring the forward reaction. Removing the reactively formed water also improves the production of the triacetin. This is because the reaction is reversible and removing the water will favour the forward reaction.

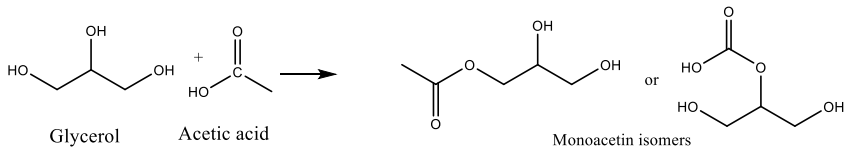

(a) Glycerol conversion to monoacetin isomers

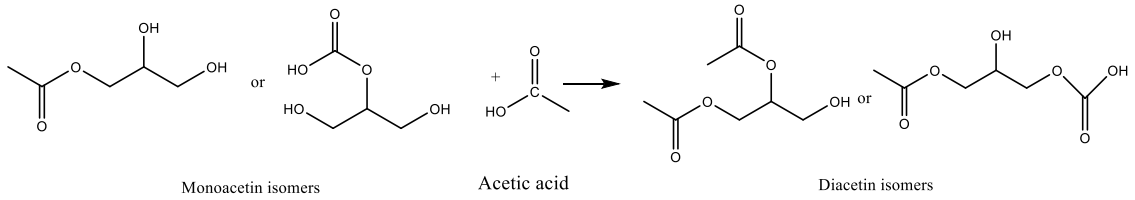

(b) Monoacetin conversion to diacetin isomers

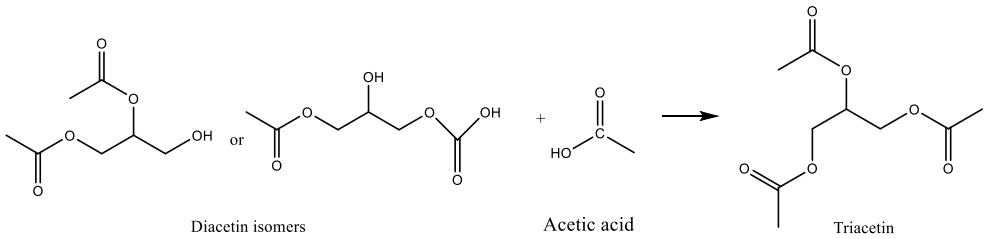

(c) Diacetin conversion to triacetin

Figure 2-11: Glycerol esterification with acetic acid.

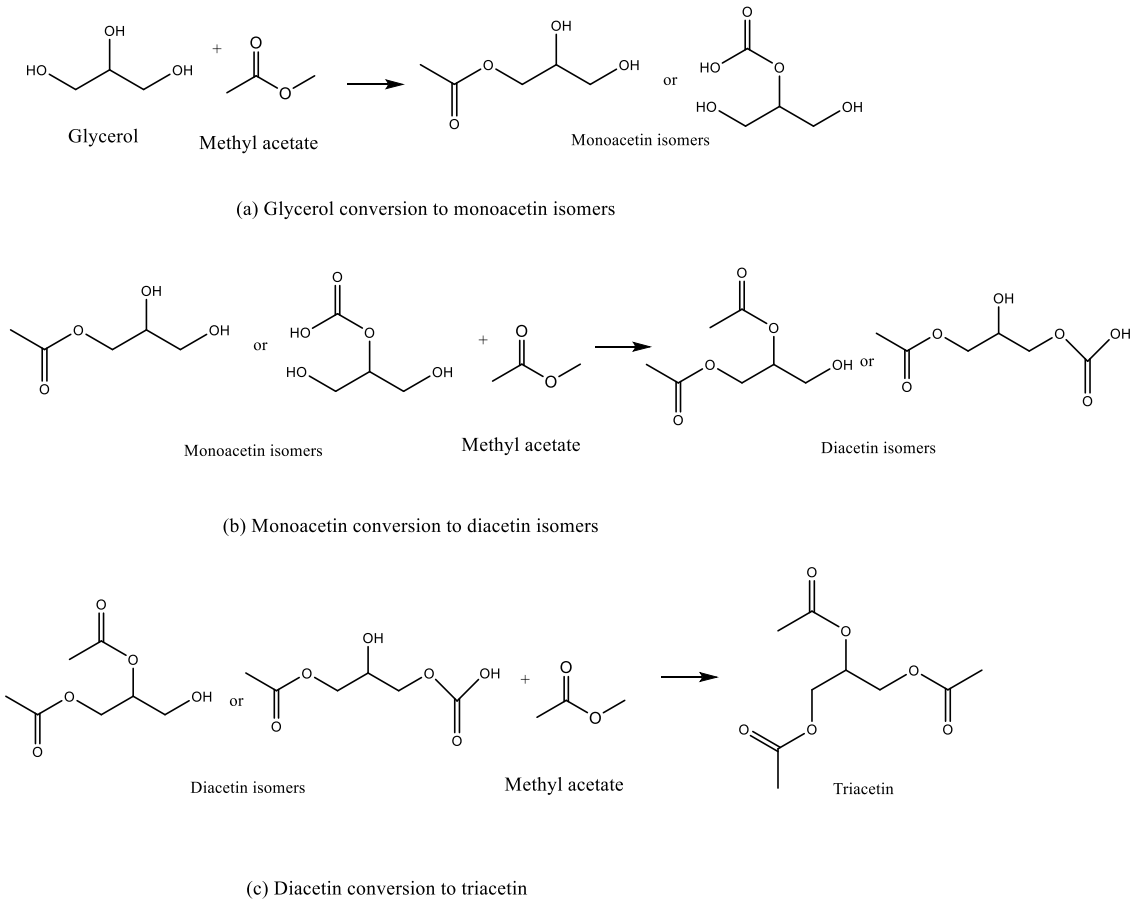

Figure 2-12: Glycerol transesterification with methyl acetate.

In the production of acetins, various homogeneous and heterogeneous acidic catalysts have been investigated (Bedogni et al., 2014). Homogeneous catalysts have been reported to be more active in the acetylations, but they have disadvantages including corrosion, poor separation of the catalyst after the reaction, and lack of recyclability. Heterogeneous catalysts can be reused, although the cost of production and activeness of these catalyst type still requires improvement.

Veluturla et al. (2017) reported a kinetic study of acetin production using a solid catalyst. The authors reported the effects of temperature, catalyst loading, and a molar ratio of acetic acid to glycerol. The maximum conversion achieved was 98% at 5% catalyst concentration, 110 ^{o}C, and 9:1 molar ratio of acetic acid to glycerol. In another study, Kale et al. (2015) used toluene as an entrainer in an acidic ion-exchange catalyst for glycerol acetylation. The authors reported that the toluene was able to constantly remove the water by-product produced during acetylation, thereby favouring the

production of triacetins. Complete glycerol conversion was reported with over 95% selectivity to triacetins, while the 5% consists of monoacetins and diacetins. Kim et al. (2014) compared the acetylation of glycerol with various solid acid catalysts at low temperatures. The authors reported the rate of the acetylation with the different catalyst to follow the order: $PrSO_3H$-SBA-15 > Amberlyst-15 > HPMo/Nb_2O_5 ≥ HPMo/SBA-15 > HUSY > SCZ > SiO_2–Al_2O_3. The complete conversion was reported with amberlyst-15, $PrSO_3H$-SBA 15, SO_3H-SBA 15, and SO_3H-Cell and total selectivity of DAG and TAG was 79%, 84%, 89%, and 68%, respectively.

Bedogni et al. (2014), reported the esterification of glycerol with acetic acid using Amberlyst 36 as the catalyst. The optimum condition used was 6:1 molar of acetic acid to glycerol, 140 ^oC, 5 wt% catalyst concentration, and 800 rpm agitation. The reaction was performed for 4 h exhibited a maximum glycerol conversion of 93%. Liu et al. (2011), studied the "esterification of glycerol with acetic acid using double SO_3H-functionalized ionic liquids as a recoverable catalyst". The reaction was conducted batch-wise in a 50 mL round bottom flask at 100 ^oC for 1 h. The highest glycerol conversion achieved was 96% with about 40% selectivity to the monoacetin, while the diacetin was over 50%. The authors concluded that the nature of the ionic liquid determined the performance of the catalyst.

The table below shows some of the reported literature in the production of acetins from glycerol. All the work used glycerol as feed rather than in situ from triglyceride.

Table 2-15: Glycerol acetylation with different catalyst.

Catalyst	Conditions			Result				Reference
	Temp ^oC	Time h	Molar ratio	Conversion %	Selectivity %			
					MAG	DAG	TAG	
Bu_2SnCl_2, Me_2SnCl_2, $BuSnCl_3$, Bu_2SnLau_2, BuSnO(OH), Bu_2SnO	40-120	3	3:1-5:1	100	25.7	43.5	30.8	da Silva et al. (2020)
Synthesized catalyst from palm kernel shell	120	1 – 5	6:1	>97	5.8	32.2	58.9	Nda-Umar et al. (2020)

Purolite CT-275	70 – 110	5.8	4 – 9	100				Banu et al. (2020)
ZSM-5	110	5	9:1	99				Almas et al. (2019)
H-ZSM-5, H-Beta, Pr-SO_3H-SBA-15	120	4.5	6:1	96	13	55	32	Dalla Costa et al. (2017)
SBA-15	150	4	9:1	94	11	51	38	Trejda et al. (2012)
Amberlyst 15	80-110		3:1-9:1	>97		46	43	Zhou et al. (2012)
Zeolite Beta K-10 Montmorillonite Amberlyst 15 Niobium phosphate	60-120	0.33-1.33	4:1	100			100	Silva et al. (2010)
$Fe_4(SiW_{12}O_{40})_3$	60	2	3:1-12:1	99.9				Da Silva et al. (2016)
Zeolite Mesoporous sulfonated carbon	120		1:1-5:1	100		41-0	59-100	Konwar et al. (2015)
Dodecatungsto phosphoric acid	60–120	7	6:1-16:1	99	24	70		Ferreira et al. (2009)
Sulfated activated carbon	60–135		5:1-10:1	91		28	34	Khayoon and Hameed (2011)
Sulphated zirconia	55			62		98.3		Dosuna-Rodríguez et al. (2011)

Table 2-15 shows that higher conversion of glycerol to acetins can be achieved with a solid catalyst. These may also be efficacious for coupled reactions since the catalyst could also take part in transesterification. However, the drawback of this method in

reactive coupling is the addition of acetic acid and heterogeneous catalysts, which increase the cost of production.

The concept of reactive coupling for the simultaneous production of biodiesel and acetins is possible. There is literature that reports the simultaneous production of biodiesel and acetins. This could be carried out by esterification of acetic acid with methanol to produce methyl acetate and water. The methyl acetate can then further react with triglyceride to produce biodiesel and acetins. This method might be accompanied by low biodiesel yield due to the water content during the esterification. To avoid this, transesterification of triglyceride with methyl acetate and methanol without the esterification is used. It is possible to have all reactants in a single pot or use two steps, as shown in *Figure 2-13*.

The advantage of using methyl acetate is to produce methanol as a by-product, which will be used for the biodiesel step, unlike the esterification of acetic acid that produces water as a by-product and deactivates the catalyst. However, this will require recovery or purification of the methanol before recycling. The transesterification is initiated by the addition of methyl acetate, methanol, and catalyst. The glycerol then reacts with the methyl acetate to produce the acetins and methanol by-product (*Figure 2-13***).** With this reaction, it is possible to produce biodiesel with even less methanol than required from the stoichiometric. A suitable catalyst is chosen for both triglyceride transesterification and glycerol esterification.

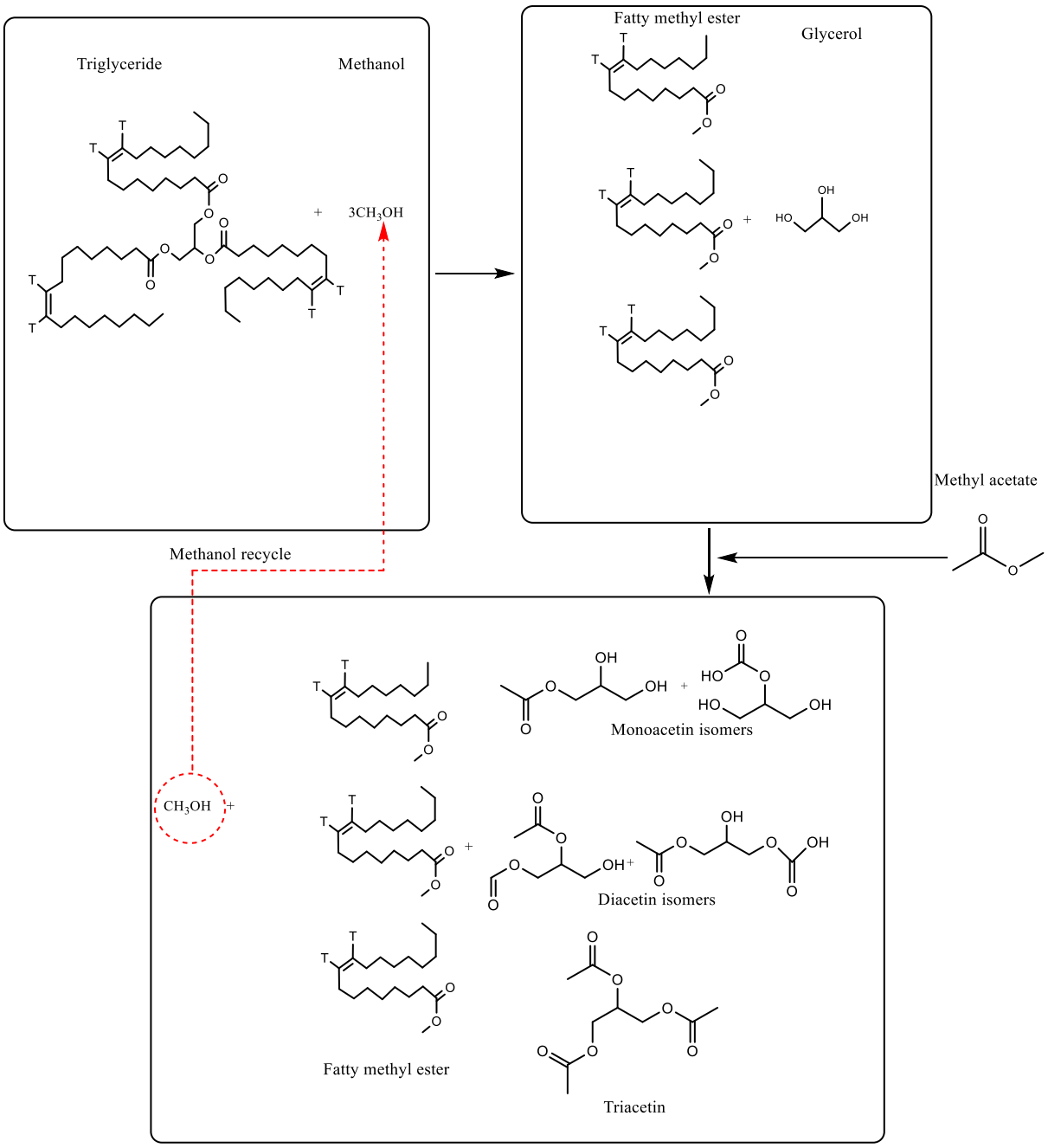

Figure 2-13: Transesterification reaction for the acetins production.

Some of the reviews for the simultaneous biodiesel and triacetin production are reported in *Table 2-16* below. The authors directly reacted alkyl acetate to triglycerides to produce fatty alkyl esters and acetins. This method is also referred to as interesterification.

Table 2-16: Reactive coupling for biodiesel and triacetin.

Operating conditions				Yield %	References
Catalyst	Temp. °C	Mole ratio	Time h		
CH_3OK	30 – 50	1:8 – 1:24	0.5	98	Medeiros et al. (2018)
γ-Al_2O_3	225 – 300	1:10 – 1:40	1	82	Ribeiro et al. (2018)
Ferric sulfate	120	1:10 – 1:30	3 - 24	83	Tian et al. (2018)
CH_3OK	50	1:12 – 1:48		77	Casas et al. (2013)
KOH, CH_3OK, and PEG	50			77	Casas et al. (2011)
Supercritical method	350	1:42	0.25 – 0.75	98	Goembira et al. (2012)
Supercritical method	340 – 420	1:20 – 1:60	0.25 – 1.25	99	Tan et al. (2011)

Homogeneous alkaline catalyst has proven to be attractive for this process with the high conversion and less reaction temperature than the heterogeneous catalyst. Although supercritical is non-catalytic and has higher conversion, the process is not economically viable due to the high temperature and high pressure. However, the process generally required the use of excess methyl acetate.

2.6.2 Acetals

Conversion of glycerol into acetals such as solketal and glycerol formal via reactions with ketones or aldehydes in the presence of an acid catalyst as shown in *Figure **2**-**14*** is one of the most economical and promising ways of utilising crude glycerol (Mota et al., 2010). The oxygenated compound produced by glycerol reaction with a ketone such as acetone (to produce solketal) or aldehyde such as formaldehyde (to produce glycerol formal) can be used as an additive to improve fuel properties. They also have applications in pharmaceutical cosmetics and polymer industry (Nanda et al., 2014, Chen et al., 2018, Smirnov et al., 2018).

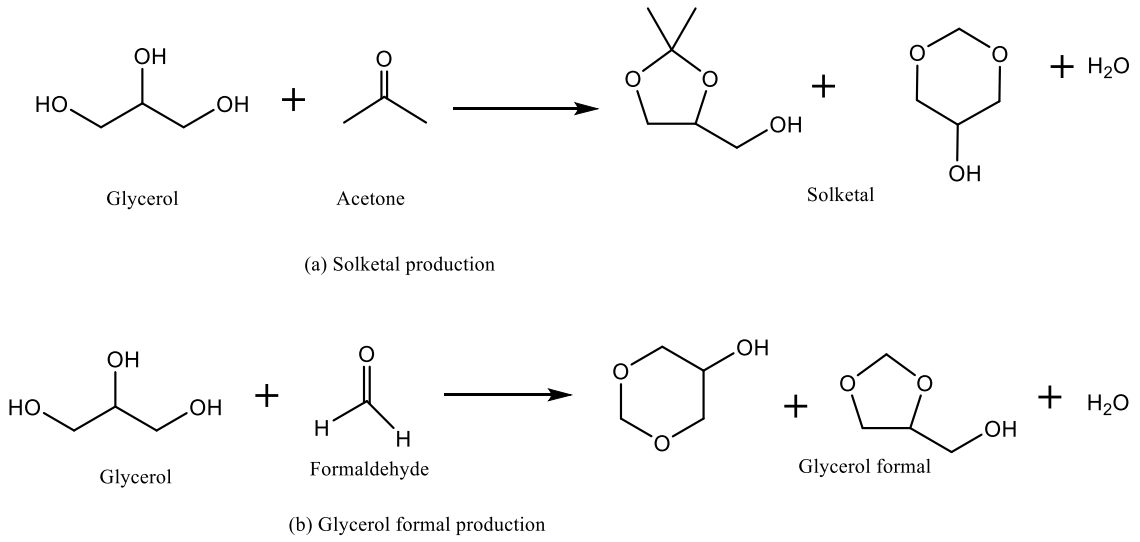

Figure 2-14: Producing solketal and glycerol formal from glycerol.

The glycerol by-product from biodiesel production has been converted to various oxygenated compounds. Chen et al. (2016) studied the production of oxygenated compounds by acetalisation of glycerol with formaldehyde using solid acidic catalysts such as mesoporous organosilicas, ZSM-5, heteropoly compounds, and Amberlyst 15, due to their water tolerance to reduce deactivation. The highest glycerol conversion achieved was over 70%. This might not be suitable for reactive coupling due to the long reaction time required when using an acid catalyst in biodiesel production. Umbarkar et al. (2009) react benzaldehyde with glycerol in the presence of a solid acid catalyst for solketal production. The maximum conversion obtained was 72% at 100 ^{o}C after 8 h. The conversion is low and long reaction time to be economically viable. However, Nanda et al. (2014) used a continuous flow reactor to produce solketal, with the highest yield of 94±2% at 25 ^{o}C and 4:1 molar ratio of acetone to glycerol. They also observed that both water and salt (which can be present in the crude glycerol from biodiesel) in the reaction reduces the yield. The water can create a thermodynamic barrier, thereby limiting solketal production. It was also reported that the salt (NaCl) might deactivate the acid resin (Amberlyst 36) used as a catalyst. Based on their economic analysis, the authors concluded that methanol as a co-solvent would make the process economically feasible due to the high conversion and cost of the solvent. This would, of course, complement reactive coupling since methanol is used in the biodiesel process. Feliczak-Guzik and Nowak (2019) used solid catalysts to acetalise glycerol at 50 – 100 ^{o}C for 24 h to achieve

approximately 65% conversion. The work was repeated in a microwave reactor at 30 ^{o}C for 20 to 40 min to achieve about 90% conversion. The author concluded that the synthesised catalyst was both reusable and water-tolerant during the reaction.

Ammaji et al. (2018) modified SBA-15 as catalysts to produce solketal. Niobium-doped SBA-15 exhibited a higher conversion compared to the other metals used. The author reported a 95% conversion of the glycerol and 100% solketal selectivity at 3:1 molar ratio and 100 mg catalyst loading for 1 h. Narkhede and Patel (2014) produced solketal at room temperature, using benzaldehyde silicotungstates attached to MCM as a catalyst. About 91% glycerol conversion was reported when the catalyst was increased from 10 to 30% silicotungstate loading.

The concept of reactive coupling for simultaneous biodiesel production and *in situ* acetalisations of glycerol to produce solketal was established for the first time by Al-Saadi et al. (2019) and Eze and Harvey (2018).

The reactive coupling for the simultaneous production of biodiesel and solketal can either be a single or two-step process. In the single step, all reactants are charged into the reactor simultaneously, as shown in *Figure 2-15*. One of the advantages of the single step is that acetone increases triglyceride miscibility with methanol during transesterification (Luu et al., 2014). A two-step process can be adopted to ensure high triglyceride conversion before ketone additions (acetone) (*Figure 2-16*).

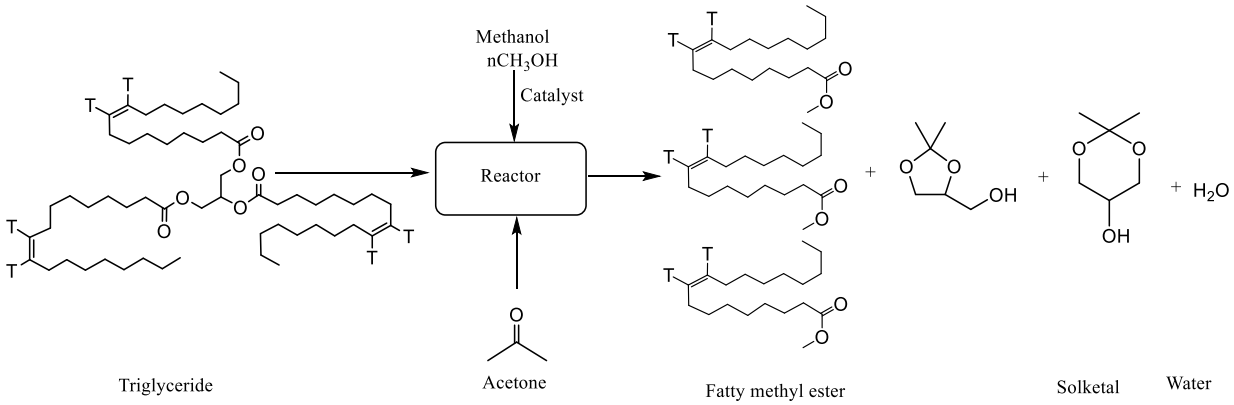

Figure 2-15: Single-step reactive coupling for biodiesel and solketal production. Source: Eze and Harvey (2018).

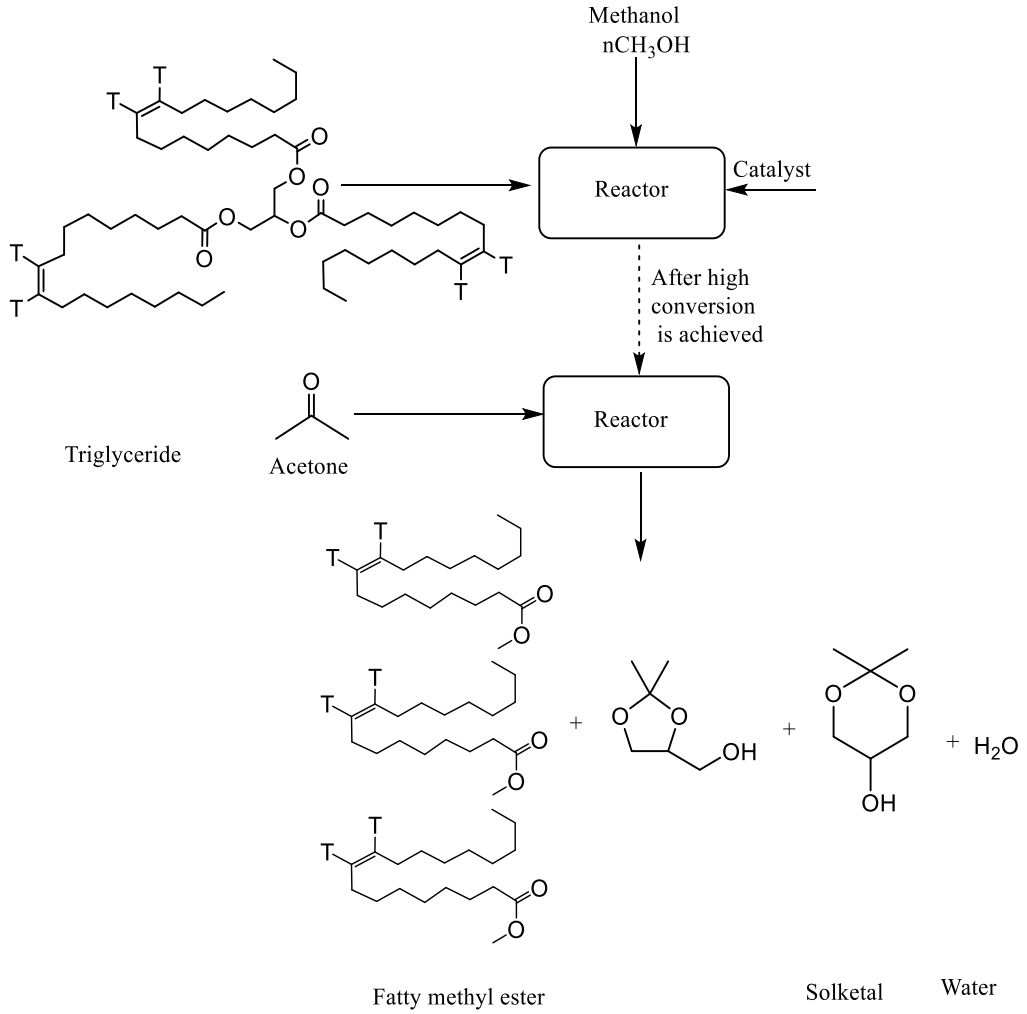

Figure 2-16: Two steps reactive coupling for biodiesel and solketal production. Source: Eze and Harvey (2018).

Al-Saadi et al. (2019) in a recent study performed reactive coupling of biodiesel and solketal in the presence of surfactant acid catalyst, 4- Dodecylbenzenesulfonic acid (DBSA). It was observed that at operating conditions of 7:10:1 molar ratio of acetone to methanol to rapeseed oil, up to 82 % of the crude glycerol was converted to solketal in two-steps compared to about 39% from a single step. However, 98% of the FAME yield was achieved with each method. A previous study has also shown that glycerol produced from the reaction of triacetin with methanol in a continuous process can be *in situ* converted to solketal (Eze and Harvey, 2018). The study was conducted with mesoscale oscillatory baffled reactors (meso-OBRs) in the presence of Amberlyst 70-SO_3H resin with acetone. About 99% triacetin conversions to methyl acetate were reported with 48.5 ± 2.7 % solketal yield achieved in the single-step process, as compared to 76.5%

yield in the two-stage process after 35 minutes. A high yield of the oxygenated compound was produced from the reactive coupling. The addition of acetone will increase the purification of the downstream.

2.6.3 Alkyl tert-butyl ether

Glycerol can be etherified with olefins (such as isobutene), alcohol (such as ethanol), or self-reaction to produce glycerol tert butyl ether, glycerol ethyl ether, or polyglycerol, respectively. The production of glycerol tert butyl ether involves glycerol reacts to olefins, alcohol, or another ether such as methyl tert butyl ether. When glycerol is reacted with isobutene (as shown in Figure **2-17**), mono, di, and tri-tert butyl ether are produced. It is an excellent additive to the diesel and biodiesel fuel. Di and tri-tert-butyl ether are desired due to their excellent mixture with the fuel. They have low water solubility, density, and viscosity compared to mono-tert-butyl ether (Bozkurt et al., 2019). These additives improve engine performance and reduce the unwanted emission of carbon monoxide, particulate matter, and hydrocarbons (Da Silva et al., 2019).

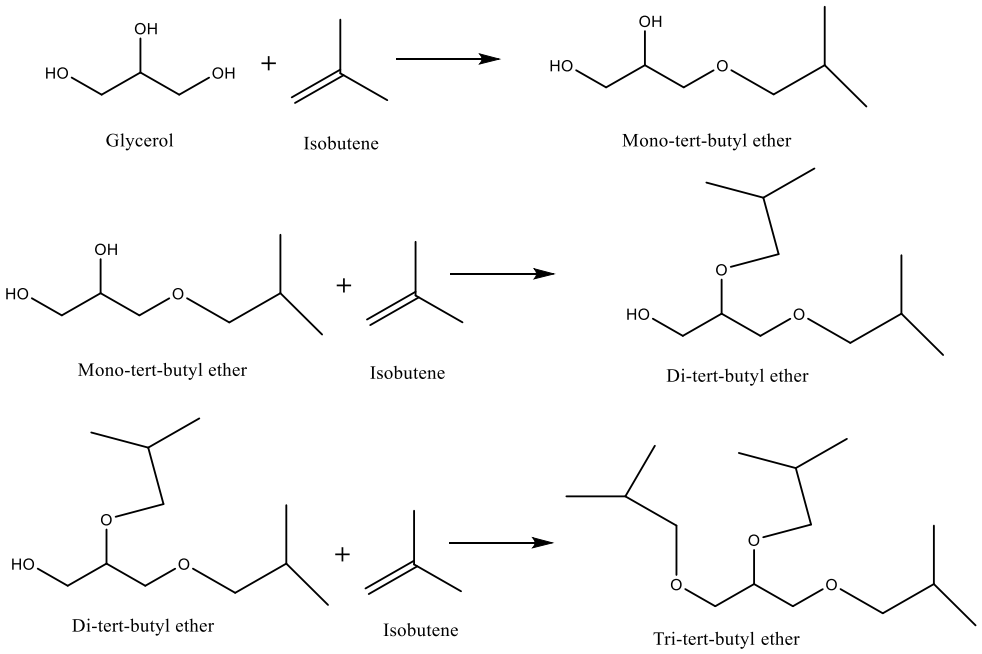

Figure 2-17: Production of glycerol tert butyl ether.

Bozkurt et al. (2019) studied the blend of tert-butyl ethers in gasoline. The authors used di and tri tert-butyl glycerol which they prepared in various concentrations with the

reference gasoline. A slight increase in the octane number after blending and good emission properties were reported. This makes glycerol tert-butyl ether an excellent replacement for the methyl tert-butyl ether due to its environmental challenge. Various acid catalysts have been used for production. *Table 2-17* below shows the conditions, catalysts, and results obtained from literature in glycerol tert-butyl ether production.

Table 2-17: Glycerol tert-butyl ether production.

Catalyst	**Operating conditions**				**Conversion (%)**	**Reference**
	Temp ^{o}C	Stirring RPM	Cat. %	Time h		
Sulfonated graphene	90	1200	7.5	10	80	Miranda et al. (2019)
Amberlyst 15 Zeolite beta	75	1200	7.5	6		Bozkurt et al. (2019)
Tin (II) phosphotunstate heteropolyacid salt	90		10	4	95	Da Silva et al. (2019)
Amberlyst 15, silica, alumina, silica-alumina, FAU, MOR, BEA and MFI	90	1200		10	64	Miranda et al. (2018)
Sulfonated hybrid silicas and Amberlyst 15	70 -85		2.5-7.5	17	74	Estevez et al. (2016)
Nanostructured MFI zeolites	120		5	12	78 – 83	Simone et al. (2016)

Conversion to glycerol tert butyl using solid acid catalysts is accompanied by long reaction times and high stirring rates. This will reduce its economic viability. The concept of reactive coupling for productions of biodiesel and glycerol tert-butyl ether has been

reported. Farobie et al. (2014) used a single step (*Figure 2-18*), by reacting canola oil with methyl tert-butyl ether in supercritical conditions to produce biodiesel glycerol tert-butyl ether. The authors reported a first-order kinetics rate with an ester yield of 94% after 12 mins reaction at 400 ^{o}C and 40:1 molar ratio of MTBE to canola oil at 10 MPa. The authors also confirmed the complete conversion of glycerol in the reaction. However, the supercritical method is not viable for biodiesel production economically. This is due to the high energy requirement of the method which translate to high capital expenditure of the technique. It also requires a high ratio of the solvent, which increased the production cost.

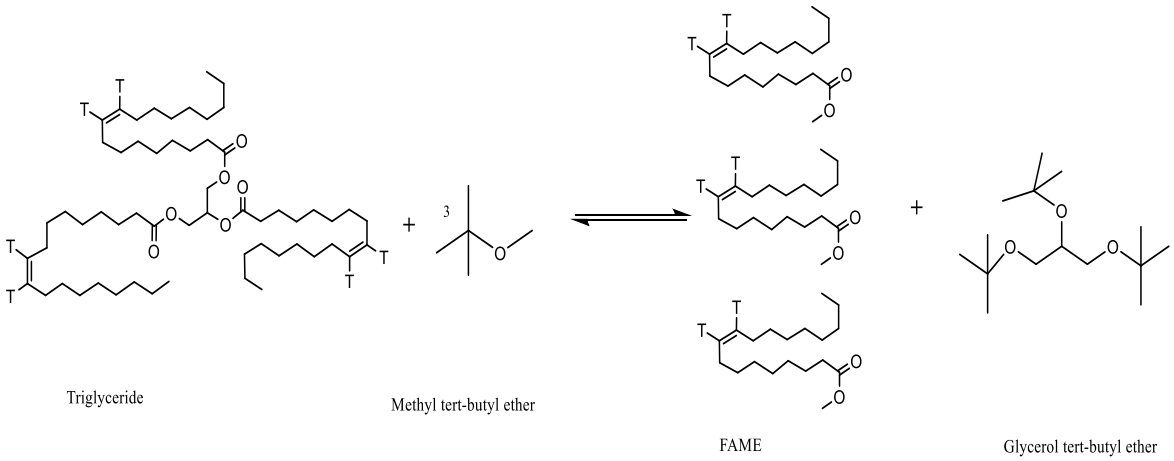

Figure 2-18: Reactive coupling for biodiesel and glycerol tert-butyl production.

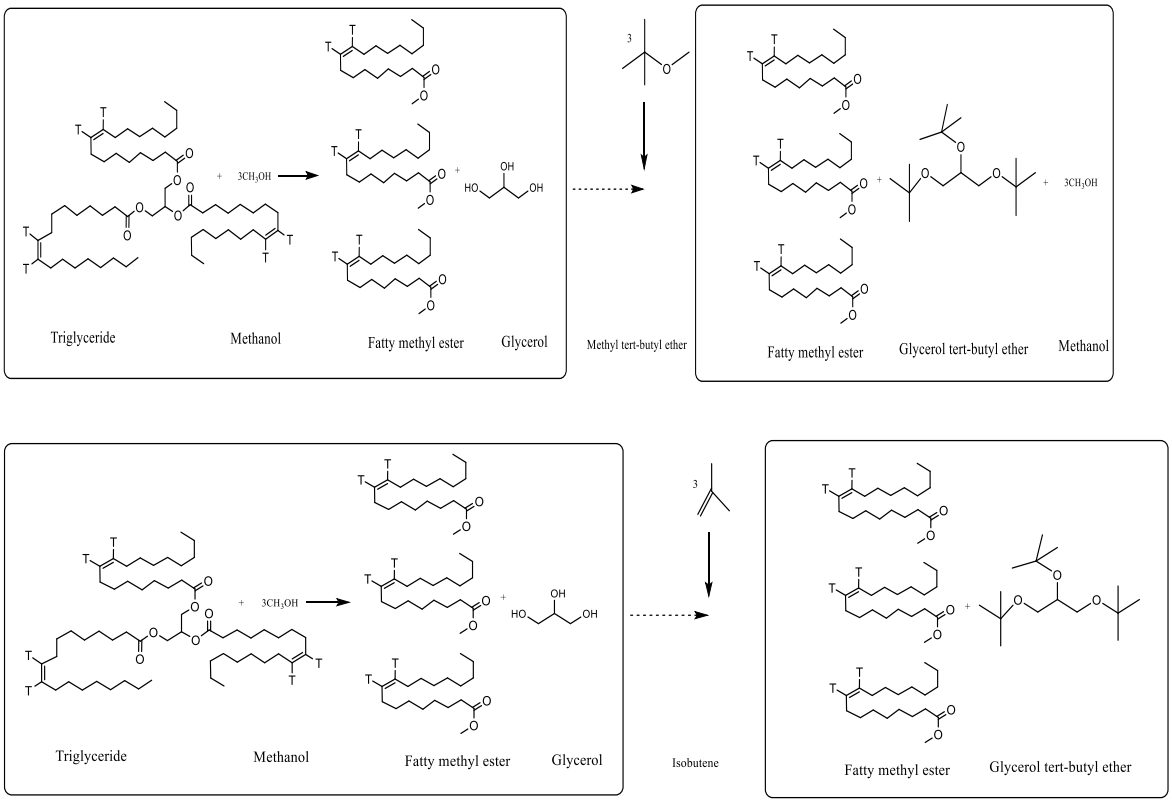

Figure 2-19: Two steps reactive coupling for biodiesel and glycerol tert-butyl ether production.

The reaction is also possible in two steps (*Figure 2-19*) by reacting the triglyceride with methanol and adding tert-butyl alcohol to couple the glycerol. The two-step reaction with tert-butyl alcohol (such as methyl tert-butyl alcohol) will produce alcohol as a by-product. In contrast, only biodiesel and glycerol tert-butyl ether will be produced when isobutene is used. However, there is currently no reactive coupling report for the simultaneous biodiesel and glycerol ethyl ether using two steps.

2.6.4 Glycerol carbonate

Another promising way to valorised crude glycerol is by transesterification to produce glycerol carbonate (GLC). This reaction is mainly performed with dialkyl carbonates, such as dimethyl carbonate (DMC), to produce GLC as a main product and methanol as a side product (Esteban et al., 2015, Ishak et al., 2016). DMC is a mutual solvent for triglyceride and methanol, leading to an increased rate of reaction (Zhang et al., 2010, Luu et al., 2014). It is also a methanol source and can replace methanol in biodiesel reaction (Zhang et al., 2010, Dawodu et al., 2014).

The reactive coupling process for producing glycerol-free biodiesel via triglyceride reactions with dimethyl carbonate (DMC) to form FAME alongside glycerol carbonate (GLC) has been established, as shown in *Figure 2-20*. This reaction occurs in base catalysts, producing biodiesel as a main product and GLC as a by-product. Except when the supercritical method is used which does not require a catalyst.

Rathore et al. (2014) obtained up to 97 % FAME yield and 93.2 % glycerol carbonate selectivity in 45 min under supercritical conditions. The authors used 40:1 of DMC to non-edible oil (jatropha and pongamia oil) with 325 ℃ at 150 bar. The supercritical process was fast, but energy-intensive due to operations at high temperatures and pressure. Also, a high molar ratio of the DMC to oil was required. Seong et al. (2011), used Novozym 435 as a catalyst at 60 ℃ and 6:1 of DMC-to-soybean oil molar ratio. About 84.9% yield of biodiesel was achieved and 92 % glycerol carbonate. The biodiesel yield was observed to improve when tert-butanol was used as a solvent by Lee et al. (2017). The authors obtained up to 95 % biodiesel yield and 99 % glycerol carbonate production with the enzymatic catalyst at 9.27:1 DMC to soybean oil and 52.56 ℃. However, the high cost of the enzymatic catalysis is one of the major disadvantages in these works.

Zhang et al. (2010) showed that operating at the dimethyl carbonate boiling point (90 ℃) can achieve more than 96 % FAME with 9:1 DMC to palm oil, 8.5 wt% KOH, and 8 h. Fan et al. (2017) used 110 ℃ in a high-pressure reactor with 5:1 of DMC to rapeseed oil molar ratio, 25wt% of 1-propyl sulfonate-3-methylimidazolium hydrogen sulphate as a catalyst and 5 h to achieved 95% biodiesel yield. Even though moderate reaction conditions were required to attain high biodiesel yields, these reactions required long residence times (≥ 5 h) (Zhang et al., 2010) and a high concentration of catalysts, making it economically not viable increase the purification in downstream.

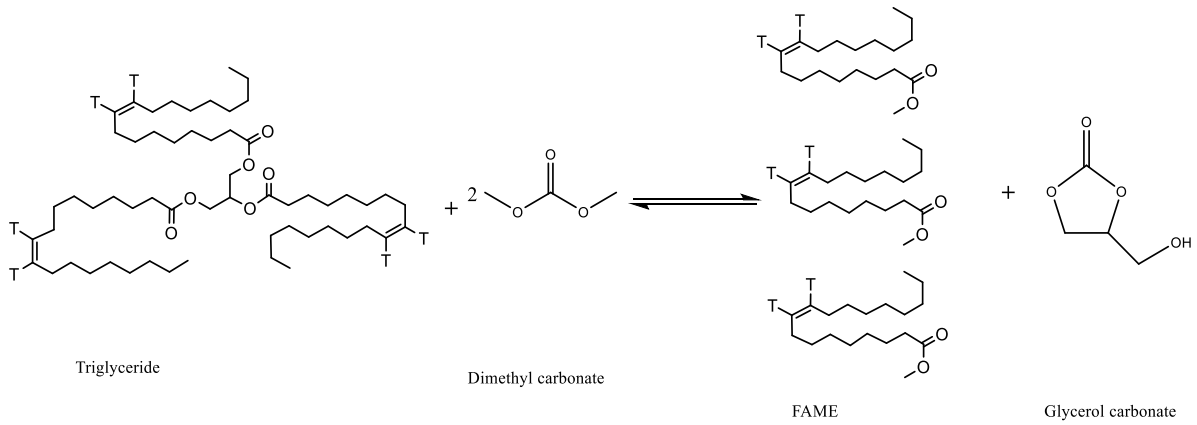

Figure 2-20: Reactive coupling for biodiesel and glycerol carbonate production. Source: Al-Saadi et al. (2018)

The addition of methanol as a co-solvent can result in high biodiesel yield in a short time. A recent study showed that at 1:90:30 of methanol to DMC to soybean oil molar ratio and 150 ℃ takes 3 hours to achieve 97.3 % biodiesel yield and 93.2 % glycerol carbonate selectivity (Dhawan and Yadav, 2018). In this study, the time required for getting equilibrium triglyceride yield was reduced, but large amounts of methanol and DMC were used. Al-Saadi et al. (2018) used 2:1 methanol to rapeseed oil molar ratio and was found to be a very effective route, with about 90% of crude glycerol converted to glycerol carbonate and 98% of FAME yield at 3:1 of DMC: RSO and 60 ℃.

2.6.5 Acrolein

The dehydration of glycerol to acrolein is another chemical route for utilising the surplus crude glycerol from biodiesel production. Acrolein has various applications in agricultural and chemical industries as an intermediate, such as acrylic acid, fragrance, dyes, and herbicide (Alhanash et al., 2010). Its production from glycerol will reduce the use of propene from fossil derivative. The conventional oxidation of the propene is as shown in *Figure 2-21* below:

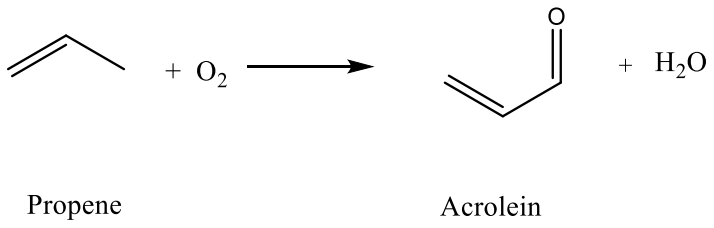

Figure 2-21: Oxidation of propene for acrolein production.

The dehydration of glycerol for acrolein production has been recorded since the early nineteenth century (Corma et al., 2008). The reaction removes two molecules of water from glycerol. The reaction pathway indicates the possible production of other products such as 3-hydroxypropanal (or 3-hydroxypropionaldehyde) and hydroxyacetone (or acetol) (see *Figure **2**-**22***). The conversion occurs in either liquid or gas phase. Higher yields of the acrolein were reported in the gaseous phase than the liquid phase. However, a higher temperature is required in the gaseous phase than the liquid. Aqueous solutions of glycerol were used as feed during the dehydration for high yield of the acrolein. Increasing the percentage glycerol in the solution lowered the yield of the acrolein during dehydration. Corma et al. (2008) reported that high glycerol concentrations in the aqueous solution favoured condensation reactions, acetol production, and the formation of other larger molecules oxygenates. Low concentrations of glycerol in the solution, favoured cracking, and formation of acetaldehyde.

Various authors have reported various catalysts (homogeneous or heterogeneous) on the dehydration of glycerol. Must of the literature uses a solid acid catalyst in a fixed-bed reactor. Corma et al. (2008) reported the possibility of coke formation in the event of using glycerol from biodiesel production due to the presence of basic impurity.

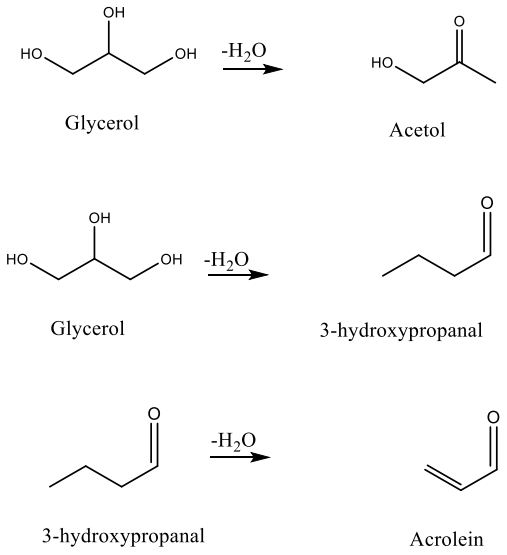

Figure 2-22: Dehydration of glycerol for acrolein production.

Table 2-18 is based on a review of the literature concerning acrolein production from glycerol. The effect of temperature, the concentration of glycerol (molar ratio of glycerol to water), and time are some of the conditions that affect its production.

Table 2-18: Acrolein production from glycerol.

Catalyst	Reactor	Phase	Reaction condition			Result		Reference
			Glycerol wt%	Temp °C	Time h	Conversion %	Selectivity %	
Zr-supported catalyst	Fixed bed		36.2	315			71	Chai et al. (2009)
Cs 12/HPW	Fixed bed	gas		275 - 350	1 - 6	100	98	Alhanash et al. (2010)
W/HA Ca/P/HA	Fixed bed	gas	30	350	1.5	100	33 51	Stošić et al. (2012)
HPW/TiO_2	Fluidise bed	Gas		280	0.5 - 3		48	Dalil et al. (2016)
HZSM-5, HBeta, HMordenite and HY	Fixed bed		10 - 50	275 - 400	7	100	81	Witsuthammakul and Sooknoi (2012)
W, Mo, Mo/V and W/V oxides	Fixed bed	Gas	20	250 – 350			50.3	Shen et al. (2014a)
V_2O_5/MFI	Fixed bed	Gas	10	300 – 350		97		Possato et al. (2015)
WO_3/ZrSBA	Fixed bed		10	325	2 – 8	97	41	Cecilia et al. (2016)
HPW/Cs-SBA	Fixed bed		20	300	60		85	Liu et al. (2016a)

HSiW/ZrO_2 and HSiW/ Al_2O_3	Fixed bed	Gas	10	280 – 320		97	88.5	Talebian-Kiakalaieh et al. (2016)
Heteropolyacid catalyst (ZR24)	Fixed bed		21 – 34	270 – 310	8		60 – 75	Martinuzzi et al. (2015)
Silica-supported nickel sulfate catalyst	Fixed bed	Gas	20	340		90	70	Gu et al. (2013)
VPO	Fixed bed		20 – 50	290 – 340	50	100	70.1	Feng et al. (2015)
Various brønsted acidic ionic liquids	Semi batch	liquid		250 – 270	0 – 4.6		50	Shen et al. (2014b)
H-ZSM5 treated with alkaline medium (NaOH)	Fixed bed		20		1 – 5		80	Decolatti et al. (2015)
Montmorillonite clay activated by sulfuric acid	Fixed bed		10	240 – 380		54.2	44.9	Zhao et al. (2013)
W/Zr	Fixed bed	Gas	20	280 – 320		100		Ginjupalli et al. (2014)
Various mixed oxides	Fixed bed		40	280	5 – 40		80 – 90	Deleplanque et al. (2010)
Zr/SiW	Fixed bed		10	300	3	92	63.75	Talebian-Kiakalaieh and Amin (2015)

From the literature reviewed, solid catalysts are used in a fixed bed reactor. This results in the application of high temperatures (>240 ^{o}C), leaching, and longer reaction times. Some of the catalysts have complexed preparation and used precious metals that can add to the cost of production. Another problem with this reaction is the decrease in the selectivity due to the deactivation of catalyst from cokes formation. However, excess acid sites in the catalyst might make the complete conversion steady within the reaction period. For high acrolein production, excess water is required to make the aqueous solution of glycerol. Hence, the idea of reactive coupling to produce acrolein during biodiesel production can be hindered due to biodiesel hydrolysis in the presence of excess water.

2.6.6 Hydrogen

Hydrogen has been identified as a "clean" form of energy due to its combustion without the production of CO_2. It can be produced from biomass, making it renewable and environmentally friendly (Zhang et al., 2007, Adhikari et al., 2007). The crude glycerol by-product from biodiesel production is currently used as feedstock for hydrogen production due to its availability (Yurdakul et al., 2016).

The technologies for hydrogen production include steam reforming, partial oxidation, and auto thermal reforming. These technologies can be applied to the glycerol feedstock, as shown in *Figure 2-23***.** The impurities in glycerol after biodiesel production can also serve as catalyst or reactant in the hydrogen production.

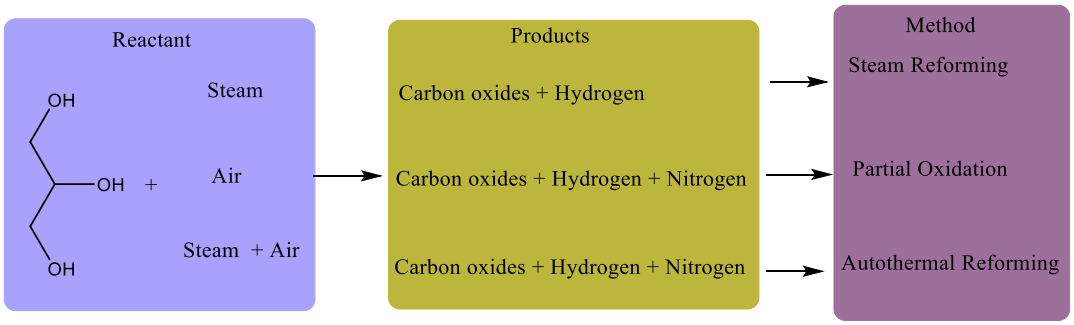

Figure 2-23: Different technology for hydrogen production.

There is various work on the production of hydrogen. The reaction mostly requires high temperature (above the boiling point of the feed) and pressure. Just as in acrolein, the feedstock (glycerol) is made to an aqueous solution.

Table 2-19: Glycerol reforming for hydrogen production.

Catalyst	Method	Feed wt%	Temp °C	Pressure MPa	Result		Reference
					Conversion %	Selectivity %	
Pt/Al_2O_3, Rh/ Al_2O_3	Autothermal steam reforming	Methanol Ethylene glycol Glycerol	90 230 300		100 100 100	89 92 79	Dauenhauer et al. (2006)
Ru/Al_2O_3	Supercritical water	40	700-800	24.1	100	70	Byrd et al. (2008)
Pt	Aqueous phase reforming	5 -10	180-220	1.14-2.5		95	Luo et al. (2008)
Ni/ CeO_2 and Ni/ Al_2O_3	Steam reforming	10	500-600	0.4	100		Iriondo et al. (2010)
Ni–Cu–Al	Steam reforming	Glycerol: Water (1:9)	500-600		72	78.6	Dou et al. (2014)
NiAlLa	Aqueous phase reforming	10 – 50	200-240	3.8-5.0	100	55%	Remón et al. (2016)
$NiO/NiAl_2O_4$	Steam reforming		425-700			96.5	Dou et al. (2016)

As shown in *Table 2-19*, the hydrogen production process required catalyst that some includes precious metal. This can increase the cost of production. The process might have the difficulty of reactive coupling. A similar problem as in the case of acrolein will affect its coupling. This is because of the high water requirement in the reaction, especially during the water-gas shift reaction. This might compromise the yield of biodiesel production. Also, the reaction conditions for biodiesel and hydrogen production differs. Again, the possibility of coke or other solid carbon residue production is possible, especially when the water content in the reaction is low.

2.6.7 Acrylic acid

Acrylic acid is mainly used in the production acrylate esters as an intermediate during the production of adhesives, textile, plastics, paints, diapers, resins, and coatings (Sun et al., 2017). The high demand for acrylic acid in the chemical industries has inevitably made it a subject of interest for research. The acrylic acid has been produced from propylene (source from fossil fuels) by converting to acrolein and finally acrylic acid, as shown in *Figure 2-24***.** Various catalysts (such as Bi-Mo oxide or Bi-V oxide) have been used for production (Kim and Lee, 2017).

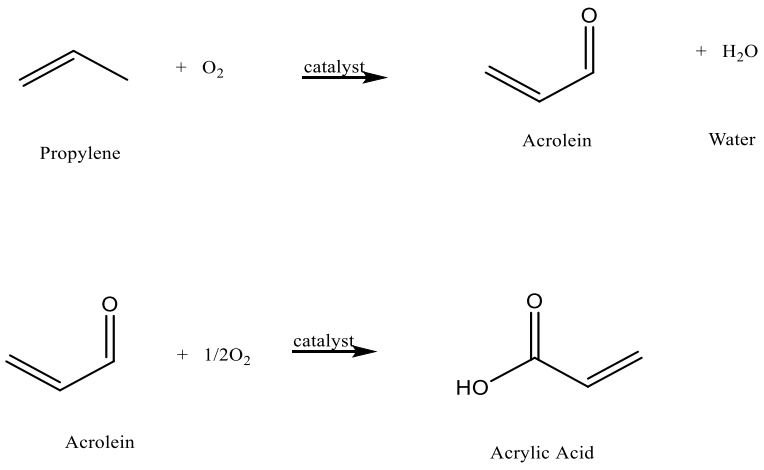

Figure 2-24: Acrylic acid production from fossil fuel source propylene.

Crude glycerol from biodiesel production has been used as feedstock to replace propylene from fossil, due to its availability, cheap, and sustainability. Converting glycerol to acrylic acid has environmental and economic advantages, considering its marketability and numerous applications (Paula et al., 2016). The reaction pathway can

be via dehydration to form acrolein as an intermediate, followed by oxidation to form acrylic acid. Another method is to directly convert glycerol in one pot to acrylic acid by oxidative dehydration. It can also be produced through the deoxydehydration method with allyl alcohol as an intermediate (see *Figure 2-25*). Kim and Lee (2017) reported producing acrylic acid through an intermediate such as allyl alcohol or acrolein rather than one step conversion was to increase the yield of the product.

Acrylic acid has another pathway with propylene as an intermediate. It involves hydrogenolysis of the glycerol to propylene then oxidation of the propylene to acrylic acid. A method using lactic acid as an intermediate is also possible. The pathway requires converting the glycerol to lactic acid by oxidation, then followed by dehydration to acrylic acid.

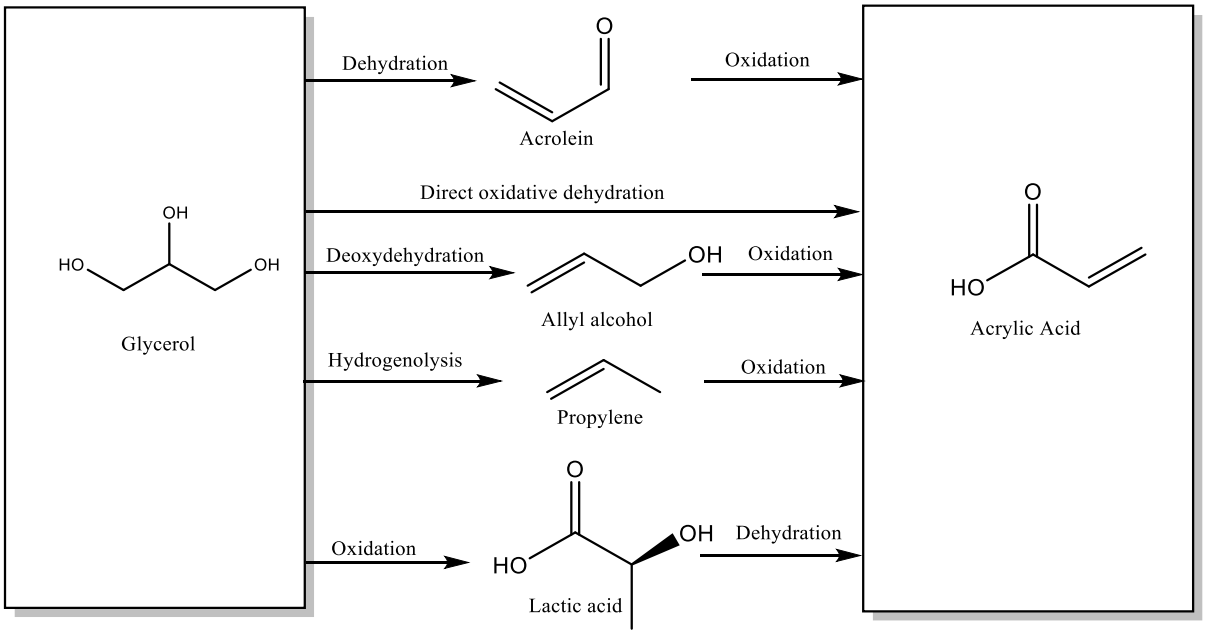

Figure 2-25: Various pathways to acrylic acid production from glycerol.

Table 2-20: Acrylic acid production using a different method.

Method	Catalyst	Temp. °C	Flow mL/h	Conc. Wt%	Conv. %	Sel. %	Reference
Oxidative dehydration	Fe-MCM-22	320	2.2		97	24.8	dos Santos et al. (2019)
Oxidative dehydration	Mo-V mixed oxides	290-350	3	10	100	33.5	Rasteiro et al. (2017)
Deoxydehydration-Oxidation	Au/CeO_2	210				87	Kim and Lee (2017)
Oxidative dehydration	Vanadosilicates	320	3		93.6	85.4	Paula et al. (2016)
Oxidative dehydration	Fe-BEA zeolites	275	0.6		90	23	Diallo et al. (2016)
Oxidative dehydration	POM/Al_2O_3	90		20	84	25	Thanasilp et al. (2013)
Oxidative dehydration	V_2O_5/MFI	300-350	3	10	97	17	Possato et al. (2015)
Oxidative dehydration	Mo_3VO_x/ $H_4SiW_{12}O_{40}$/ Al_2O_3	300	1.5	20	100	46.2	Liu et al. (2015)
Oxidative dehydration	Nb/Oxides	355			100	81.8	Omata et al. (2016)
Oxidative dehydration	V_2O_5/ZSM-5	300	3	10	100		Possato et al. (2017)
Oxidative dehydration	Co, Fe, V / $AlPO_4$	220-280		36	90		Lopez-Pedrajas et al. (2018)
Oxidative dehydration	Mo/V and W/V	250-350	6	20		25.7	Shen et al. (2014a)
Oxidative dehydration	Zeolites and V-Mo oxides	275-400		10 – 50	100	40	Witsuthammakul and Sooknoi (2012)

From *Table 2-20*, the selectivity for acrylic is generally low, due to the production of acrolein as an intermediate. Hence, reactive coupling with this technique will as well produce low yield. Again, the requirement of excess water in the intermediates production will hinder the production of fatty acid alkyl ester, which is the main reason for the reaction.

2.6.8 Glycerol etherification

Glycerol can undergo self-etherification to polyglycerol or react with alcohols such as methanol or ethanol to produce glycerol ether. The reactions occur at suitable conditions favourable for biodiesel production.

2.6.8.1 Glycerol ethyl ether

Etherification of glycerol with ethanol produces glycerol ethyl ether and water (*Figure 2-26*). The reaction requires an acid catalyst such as sulphuric acid, phosphoric acid, or a solid acid catalyst. Glycerol ethyl ether is an oxygenated compound capable of improving fuel properties (Pinto et al., 2016). Like the properties of glycerol-tert-butyl ether, glycerol ethyl ether can reduce the emission of particulate matter, hydrocarbon, and carbon monoxide, and also improve the cold flow properties of the fuel (Yadav et al., 2017).

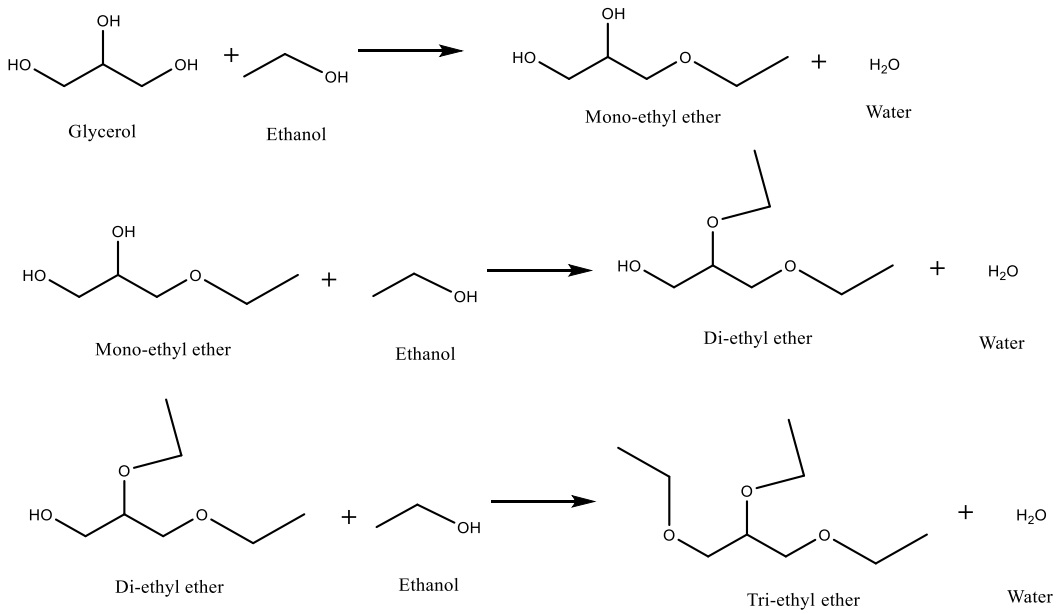

Figure 2-26: Glycerol ethyl ether production.

Various authors have reported the production of glycerol ethyl ether. Pinto et al. (2016) studied the effect of various solid catalysts (K-10 Montmorillonite, Amberlyst-15, Zeolite H-ZSM-5, and Zeolite H-Beta) for the etherification of glycerol and ethanol. The authors reported that Amberlyst 15 gave the highest conversion of glycerol (96%) and selectivity to ethyl ether (80%) at 180 ^{o}C and 3:1 molar ratio of ethanol glycerol after 4 h of reaction. The authors confirmed the reduction of the pour and cloud point after blending glycerol ethyl ether with biodiesel. Similarly, Veiga et al. (2017) used USY, H-ZSM-5, and H-Beta zeolite to etherify glycerol with tert-butyl and ethyl alcohols. Five different ether isomers (3-ethoxy-1,2,-propanediol, 2-ethoxy-1,3-propanediol, 1,3,-diethoxy-2-propanol, 2,3-diethoxy-1-propanol and 1,2,3-triethoxy-propane) were produced. The highest conversion was 81% with ethyl alcohol and 74% with tert-butyl alcohol. However, the downside of this catalyst was leaching, which was directly proportional to the glycerol conversion.

Mravec et al. (2017) also produced glycerol ethyl ether using solid catalysts (BEA, MOR, FAU, H-Beta, and Amberlyst 35). The reaction was performed in an autoclave with 1000 rpm stirring speed, constant catalyst loading, and temperature of 180 – 220 ^{o}C. The highest conversion was 51.7% with H-Beta. The selectivity of the catalysts was towards the mono ethyl ether. Lemos et al. (2018) used analysis of variance (ANOVA) to study the effect of temperature (180 – 250 ^{o}C), ethanol to glycerol molar ratio (4:1 – 20:1), and catalyst loading (0 – 0.8 g) with conversion and yield as responses. The reaction was performed in a fixed bed reactor in the presence of Amberlyst-15 as a solid catalyst. The authors reported an optimum condition of the yield at 238 ^{o}C, 16:1 molar ratio, and 0.61 g catalyst loading. The optimum was achieved with excess ethanol (16:1), which would increase production costs, mainly due to the energy costs of separation for recycling and increased downstream washing. Sulfonic acid modified catalysts were used by Melero et al. (2012) for the etherification of glycerol with anhydrous ethanol. The highest conversion (74%) was reported at 200 ^{o}C with a 15:1 molar ratio of ethanol to glycerol and 19 wt% catalyst concentration after 4 hours of reaction. An oxygenated compound was produced with the etherification of glycerol and ethanol. But the downsides of the process were high temperature, molar ratio, and reaction time.

The method is suitable for reactive coupling, as excess alcohol can be used for biodiesel production. However, the high ratio of alcohol will still require recovery and purification steps in the downstream.

2.6.8.2 Polyglycerol

Production of polyglycerols has become more common in recent years due to the availability of the glycerol feedstock in bulk from the biodiesel processing (Mohammed et al., 2019). This polymer is attractive due to its potential applications in pharmaceuticals, food, and cosmetics (Clacens et al., 2002, Sivaiah et al., 2012). The polymerisation takes place with the production of water, as hydroxyl groups of the glycerol are lost during the reaction, being replaced by the ether groups *Figure **2-27***.

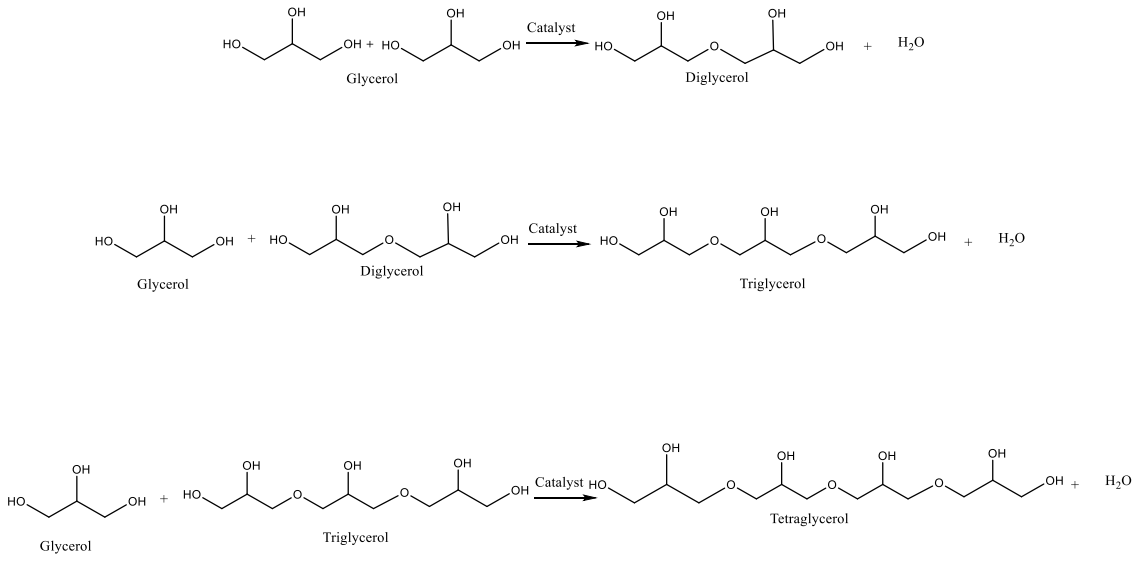

Figure 2-27: Reaction path for polyglycerol production.

It has been reported (Gholami et al., 2013a, Ardila-Suárez et al., 2015, Anuar et al., 2013, Salehpour and Dubé, 2012) that polyglycerol can be produced at temperatures between 100˚C and 270 ºC and atmospheric pressure, in the presence of selected catalysts. Though polyglycerols can be produced in the absence of the catalyst, the conversion will be slow, and the yield relatively low (Soi et al., 2014). Either homogeneous or heterogeneous catalyst, in acidic or alkaline, can be used for polyglycerol production as shown in *Table **2-21*** below.

Table 2-21: Glycerol etherification for polyglycerol production.

Catalyst type	Temp (°C)	Time (h)	Conv (%)	Reference
KOH	150 – 240	2	-	Shikhaliev et al. (2016)
LiOH	230 – 260	1 – 12	35.7	Nosal et al. (2015)
Na_2CO_3	220 – 270	0.5 – 3	93	Bookong et al. (2015)
$Ca(OH)_2$, $CaCO_3$, H_2SO_4, and PTSA	140	4	72	Salehpour and Dubé (2011)
H_2SO_4	140		42	Salehpour and Dubé (2012)
H_2SO_4	280	2	90	Medeiros *et al.* (2009)
$CsHCO_3$	260	0 - 24	100	Richter *et al.* (2008)
NaOH	220 – 280	0.5 – 5		Garti *et al.* (1981)
MgAl and CaAl – LDH	235	24	98	Pérez-Barrado et al. (2015)
Zeolite Y/LiOH	240 – 260	8	99	Ayoub et al. (2014)
Li/MK-10	240	12	98	Ayoub and Abdullah (2013b)
Mg-Fe/ oxides	220	24	41	Guerrero-Urbaneja et al. (2014)
$Ca_{1+x}Al_{1-x}La_xO_3$	200 – 260	8	91	Gholami et al. (2013a)
$Ca_{1.6}Al_{0.6}La_{0.4}O_3$	200 – 260	8	96	Gholami et al. (2013b)
Mg-Al/ oxides	220	24	50.7	García-Sancho et al. (2011)
BaO, SrO, CaO, and MgO	220	20	80	Ruppert et al. (2008)
Na_2CO_3	260	0 – 24	94	Clacens et al. (2002)

Similar catalyst types have proven to be successful for glycerol etherification and biodiesel production (compare *Table 2-21* to *Table 2-8* - *Table 2-11*) which makes them suitable for reactive coupling. However, higher conversions are achieved for

polyglycerol production when homogenous acid catalysts are used (see ***Table 2-21***). Although the catalyst type from previous works shows lower selectivity for the short-chain polyglycerol and favour side reaction such as acrolein production (Garti et al., 1981, Salehpour and Dubé, 2011). On the other hand, heterogeneous catalysts achieve higher selectivity to produce short-chain polyglycerols, especially with mixed oxides. Their drawback is low glycerol conversion, high temperature and longer reaction time required, which are less economically viable. Since heterogeneous and alkali homogeneous catalyst produced lower glycerol conversion, required higher temperature and longer reaction time than homogenous acid catalyst, this makes homogeneous acid catalyst an excellent choice for reactive coupling.

2.6.8.3 Glycerol methyl ether

The methylation of glycerol produces glycerol ether, an oxygenated product that can be used as a fuel additive (Chang et al., 2012). Oxygenated compounds are added to enhance the combustion of the fuel and reduce harmful emissions. It also has medical applications (as a cryoprotectant for the preservation of tissues, bone marrow, and blood cell), biological (such as antifungal, antibacterial, anti-inflammatory, and anti-tumour), polymer, cosmetics, lubricant, solvent, and ink (Bruniaux et al., 2019, Gu et al., 2008, Cucciniello et al., 2016).

Both homogeneous and heterogeneous catalysts have been used to produce methyl ethers. The first hydroxyl group of glycerol reacts to methanol. It produces 2 – methoxy – 1,3 – propanediol and 3 – methoxy – 1,2 – propanediol (as shown in *Figure **2-28***). It is also known as mono-alkyl glyceryl ethers (MAGE) or alkyl propanediol.

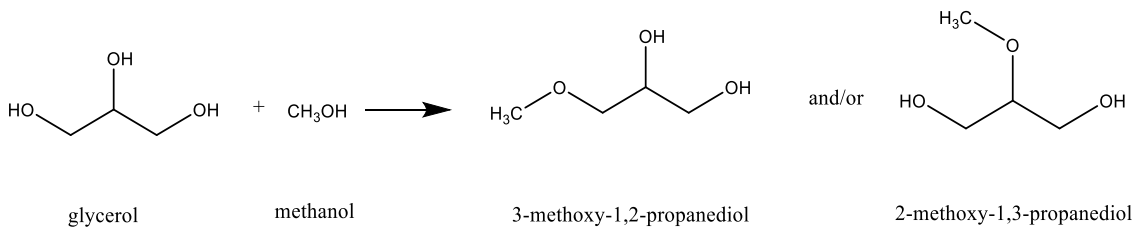

Figure 2-28: Methylation of glycerol to methoxy propanediol.

When glycerol reacts with two methanol molecules, methoxy propanol is produced, as shown in *Figure **2-29***. When 3 – methoxy 1,2 – propanediol reacted, either 1,3 – dimethoxy – 2 – propanol or 2,3 – dimethoxy – 1 – propanol is produced. But when 2 – methoxy 1,3 – propanediol reacted, only 2,3 – dimethoxy – 1 – propanol is produced. They are also called dialkyl glyceryl ethers (DAGE) or dialkyl propanol.

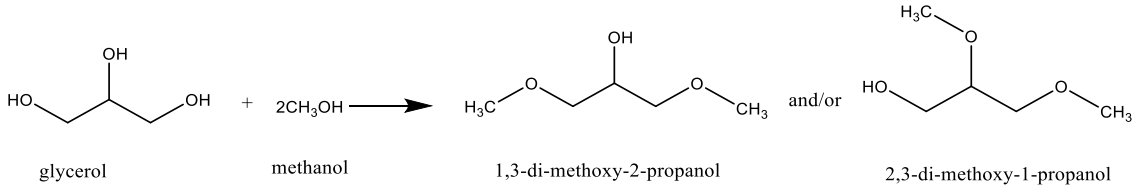

Figure 2-29: Glycerol methylation to produce methoxy propanol.

Finally, when glycerol reacts with three methanol molecules, all the hydroxyl groups will be replaced with the methoxy group to produce 1,2,3 – tri – methoxy propane, as shown in *Figure **2-30***. Either of the methoxy propanols will react to methanol to produce the methoxy propane. However, previous authors limitations were side reactions such as dehydration, self-etherification, and poly-etherification of glycerol and alcohol (Cucciniello et al., 2016, Liu et al., 2013).

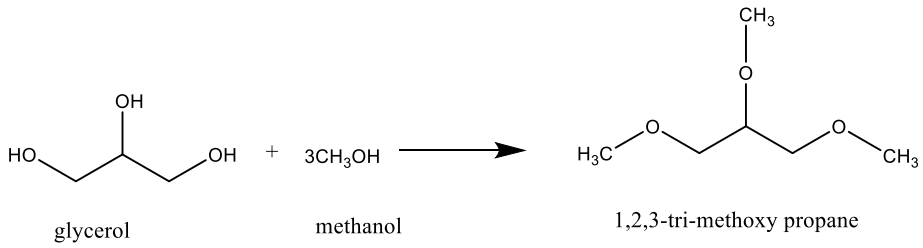

Figure 2-30: Glycerol methylation to produce 1,2,3 trimethoxy propane.

There are documented works on the production of glycerol ethers. Bruniaux et al. (2019) produce 3 – methoxy 1,2 – propanediol in subcritical methanol. The reaction was performed in an autoclave by mixing glycerol and methanol at 180 – 260 ^{o}C in the presence of a various base catalyst for 15 h. The highest yield produce was 40%, which is low compared to the long reaction time and higher temperature. It might also be due to the alkaline catalyst used just as in the case of polyglycerol. Gu et al. (2008) used

various solid acid catalyst at 80 ^{o}C for 7.5 h. A higher yield (96%) of the methoxy propanediol (also known as mono-ether glyceryl ether) were produced. Waggoner and Hatcher (2016) used two different continuous flow reactors. The authors mixed glycerol with methanol containing 25% tetramethylammonium hydroxide at 330 ^{o}C. Approximately 90% conversion was achieved with higher selectivity towards dimethoxy propanol. Although the process is continuous and high conversion achieved, the addition of tetramethylammonium hydroxide might increase the downstream processing.

Chang et al. (2012) reacted glycerol with dimethyl sulfate in the presence of sodium hydroxide. The reaction was performed in a stirred tank with a temperature of 70 ^{o}C for 48 h. About 93.5% conversion was achieved as the best conversion after 24 h with a combined yield of dimethoxy propanol and trimethoxy propane of 71%. Cucciniello et al. (2016) achieved 100% conversion and 99% selectivity of methoxy propanediol at 25 – 100 ^{o}C for 1 h with various metal salt as catalyst. The authors used various alcohol and glycidol (which can be produced from glycerol) as feedstock through the catalytic ring-opening method. This method achieved high conversion and selectivity. However, to produce glycidol from glycerol before converting to glycerol ether will be an additional step and resource. It will also be complicated for reactive coupling because more than a single catalyst might be needed, introducing more side reactions. Also, Yadav et al. (2017) reported the production of glycerol ether using glycerol and ethanol in an autoclave at 120 – 150 ^{o}C in the presence of various solid catalysts under the nitrogen environment. The highest glycerol conversion achieved was about 15% with H-Beta zeolite as a catalyst.

Liu et al. (2013) mentioned that the acid-catalysed etherification of glycerol with alcohol is desirable. This is because transition metals are avoided in the reaction. However, acid catalysts have less selectivity towards the target products. The authors reacted glycerol with butanol in various metal salt as the catalyst at 150 ^{o}C for 24 h. 30% was the highest glycerol conversion that was achieved with about 70% selectivity of alkyl-propanediol. Ricciardi et al. (2018) used various heterogeneous catalysts for the production by reacting glycidol with alcohol at 80 ^{o}C for 3 h. The authors recommend Nafion as the best catalyst due to its reusability and higher selectivity (94%). However, the conversion with Nafion (56%) is lower compare to Amberlyst (91%), though low selectivity (33%)

towards the glycerol ether. Pariente et al. (2009) also used various acidic heterogeneous catalyst at 100 – 200 ^{o}C for 0.5 – 10 h in a stainless-steel reactor with a mechanical stirrer. The highest glycerol conversion achieved was 68% with 100% combined selectivity of alkyl-propanediol and di-alkyl-propanol.

This process is promising for reactive coupling, considering excess alcohol is used for transesterification. The excess alcohol can, however, take part simultaneously in glycerol etherification. The reaction might occur together with self-etherification and poly-etherification. Hence a catalyst with high selectivity will be required.

From the previous literature on self-etherification of glycerol (to polyglycerol) and glycerol etherification, the reactions occurred at a temperature between 80 – 280 ^{o}C using either acid or alkaline catalyst, with homogeneous or heterogeneous catalyst but at relatively longer reaction time.

Reactive coupling for biodiesel, polyglycerols, and glycerol ethers productions are possible and will be reported as a proof-of-concept in this work. The triglyceride will be reacted with various alcohol (methanol) to oil ratio in the presence of sulphuric acid as a catalyst at 130 – 160 ^{o}C. The triglyceride conversion is expected to be very high (approximately 100%) after an hour of reaction. The production of the polyglycerol might be low, while glycerol ether is high. This is because glycerol etherification can occur at a much lower temperature than 80 ^{o}C. The reactive coupling reaction is shown in *Figure **2-31*** below.

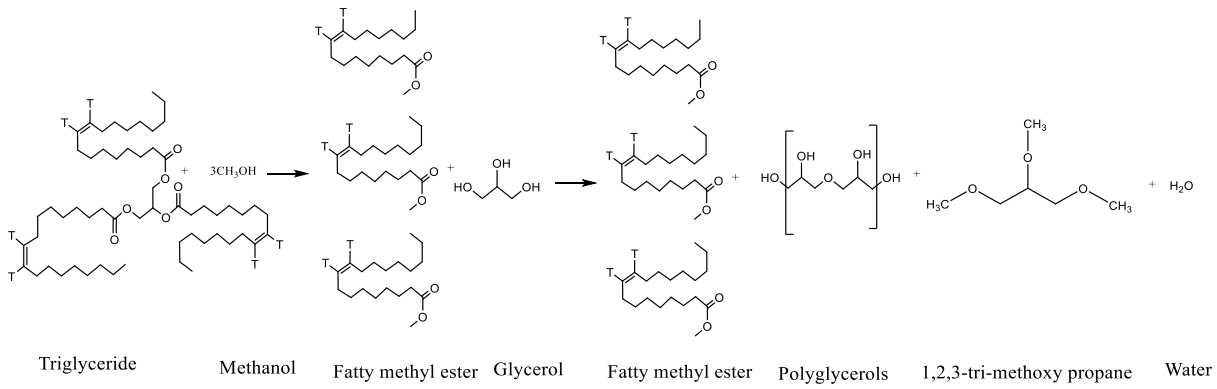

Figure 2-31: Reactive coupling for biodiesel and polyglycerol production.

2.7 Kinetics of Biodiesel Production

The kinetics depends on the reaction steps and mechanism of the reaction. Biodiesel is produce based on the reaction sequence as shown in *Figure **2**-**32***.

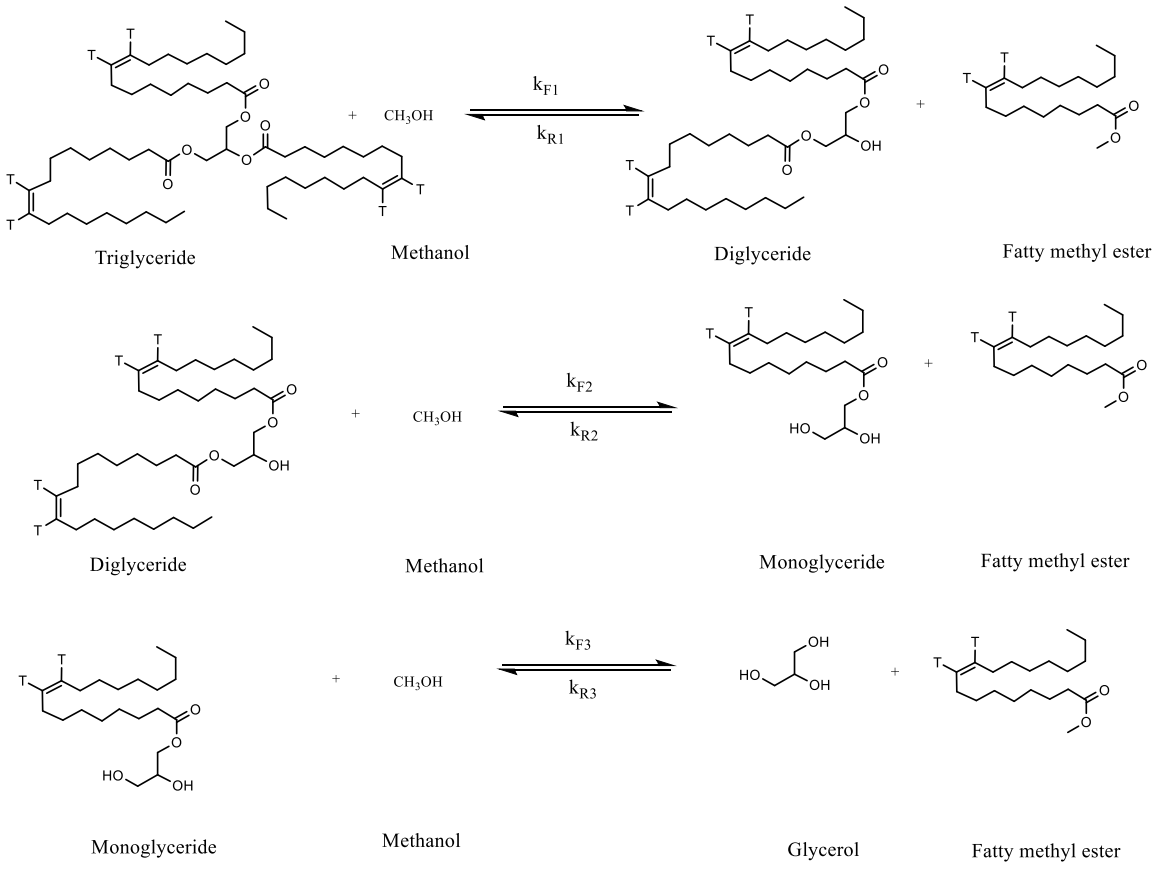

Figure 2-32: Reaction sequence for biodiesel production.

Depending on the catalyst type (acid or base) the reaction in *Figure **2**-**32*** above proceed with different activities due to the mechanism of the reaction (Lotero et al., 2005, Lotero et al., 2006, Darnoko and Cheryan, 2000, Freedman et al., 1986, Noureddini and Zhu, 1997). The reaction mechanism with a base catalyst produced an alkoxide (methoxide) ion which is a strong nucleophile (*Figure **2**-**33***(a)). It attack the carbonyl moiety in triglyceride molecules (*Figure **2**-**33***(b)) to produce alkyl ester (*Figure **2**-**33***(c)). The procedure continue with diglyceride and monoglyceride to produce more esters.

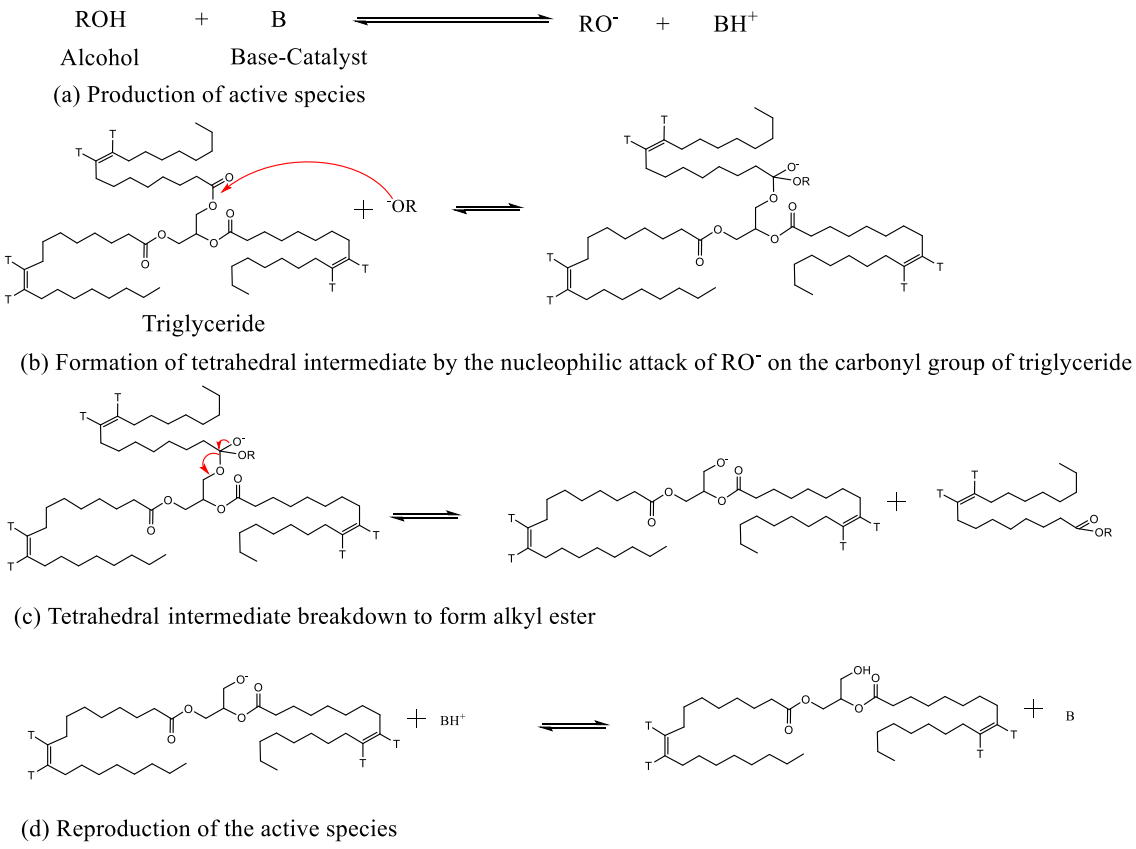

Figure 2-33: Homogenous base-catalysed reaction mechanism for alkyl esters production (Lotero et al., 2005).

With acid-catalysed reaction of the triglyceride, protonation of the carbonyl oxygen is the important step. This increases the electrophilicity of the carbon, which makes it more vulnerable to nucleophilic attack. See *Figure **2-34*** below.

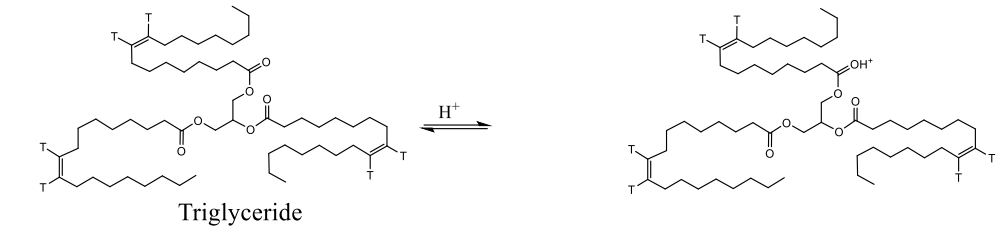

(a) Protonation of the carbonyl group by the acid catalyst

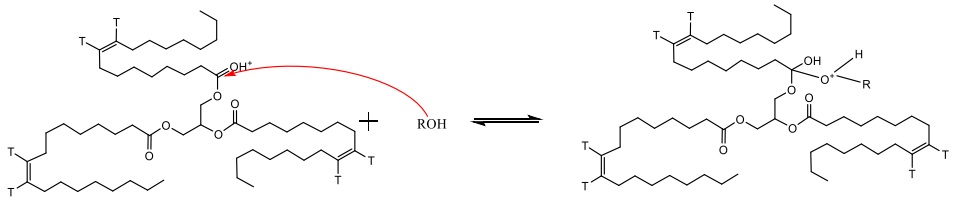

(b) Formation of tetrahedral intermediate by the nucleophilic attack of alcohol on the carbonyl group of triglyceride

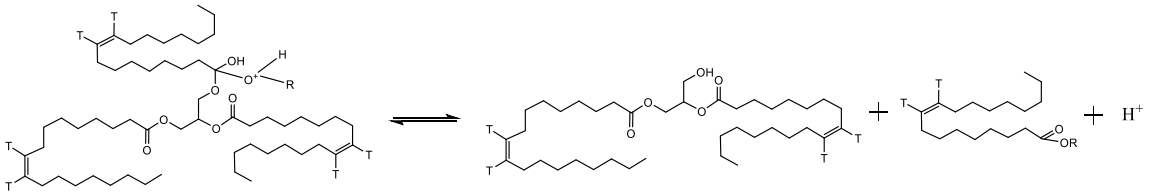

(c) Proton migration and tetrahedral intermediate breakdown to form alkyl ester

Figure 2-34: Homogenous acid-catalysed reaction mechanism for alkyl esters production (Lotero et al., 2005).

The difference in the activity of the reaction mechanisms observed can influence the kinetics of the reaction. This is due to the formation of strong nucleophile with base catalyst and more electrophile with acid catalyst (Lotero et al., 2005). The kinetics of the biodiesel production has been reported by several authors depending on the feedstock, catalyst type, alcohol used, conditions for the reaction or transesterification method. These kinetics studies provide data that help understand the reaction condition and the extent of conversion of the reaction (Darnoko and Cheryan, 2000). The data also help during designs and optimisation of the process. Some of the reported literature are reviewed below.

Sahani and Sharma (2018) determined the kinetics and thermodynamics of biodiesel production using *Madhuca indica* oil and methanol as feedstock. The oil was esterified with 2 wt% sulphuric acids, 1:12 oil to methanol ratio, 75 minutes at 60 ^{o}C and a stirring speed of 500 rpm. The process was followed with transesterification at 60 ^{o}C with

various synthesised solid catalysts and 97.5% conversion achieved. The kinetic model was developed by assuming the process to be elementary (hence the intermediates formed (diglyceride and monoglyceride) were not considered) and pseudo-first-order due to excess used of the methanol (this is because the concentration of the methanol is approximately constant during the reaction). The rate constant of 0.0052, 0.0073 and 0.011 min^{-1} as the temperature varies from 45, 55 and 65 ^oC, respectively, were obtained. The activation energy (E_a) was determined using the Arrhenius equation as 34.44 $kJmol^{-1}$ and pre-exponential factor (A) as 7.94 min^{-1}.

A similar kinetic method was used by Ma et al. (2017) for waste cooking oil with $FeCl_3$ – modified resin as heterogeneous catalyst. Methanol to oil ratio (10:1), reaction time (2 h) and catalyst loading (8%) at 90 ^oC was applied for the experiment with 92% conversion. The authors developed a model which fitted the experimental values with rate constant of 0.0073, 0.0093, 0.0135 and 0.0210 min^{-1} at 60, 70, 80 and 90 ^oC, respectively. And obtained activation energy of 35.51 $kJ{\cdot}mol^{-1}$ and pre-exponential factor of 2.55×10^3. Wu et al. (2017) used a novel mesoporous catalyst at 50 – 70 ^oC and molar ratio 6:1 – 15:1 for 24 h. They also varied the catalyst concentration (1 – 2.5 wt%) and obtained the highest biodiesel yield of 91.9%. The authors assumed a pseudo-first-order reaction due to the excess use of the methanol. The authors reported an agreement between the model and the experimental data. The rate constant for the forward reaction increase (k_1 = 0.082 – 0.139 $L{\cdot}mol^{-1}{\cdot}min^{-1}{\cdot}g^{-1}$) while the backward reaction decrease (k_{-1} = 0.062 – 0.010 $L{\cdot}mol^{-1}{\cdot}min^{-1}{\cdot}g^{-1}$) with an increase in temperature, mole ratio and catalyst loading.

Muthukumaran et al. (2017a) used various catalyst for the reaction and methanol as the short-chain alcohol. Approximately 92% yield was obtained as the highest. The power-law method was used for the kinetic, assuming that the reaction is not reversible due to the excess methanol and that the order of the reaction is first order. The model fits well to the experimental result with a rate constant of 0.011, 0.014, 0.014 and 0.014 min^{-1} at 40, 50, 60 and 70 ^oC, respectively. The activation energy (E_a) was 22.306 $kJ{\cdot}mol^{-1}$ and pre-exponential factor of 60.51 min^{-1}. Zeng et al. (2017) study the kinetics of biodiesel production with supercritical methanol. They reported maximum biodiesel yield of 97.42% at 20 minutes using 250 ^oC with 23:1 methanol to oil ratio and 1 wt% catalyst concentration (sodium methoxide). The authors reported 1.4 as the order of reaction

and 0.0387 as the rate constant. Also, activation energy was 27.06 kJ·mol^{-1} and 102.71 as the pre-exponential factor.

Berrios et al. (2007) esterified triglyceride from sunflower oil with methanol using sulphuric acid as the catalyst. The reaction was performed for 2 h, and varied mole ratio from 10:1 to 80:1 assumed pseudo-first-order. The authors reported an increase in the rate constant for the forward reaction, increasing the mole and catalyst concentration. In contrast, the rate constant for the reverse reaction is negligible.

The kinetics model for biodiesel production can be developed using the reaction as shown in *Figure **2**-**32***. Where $r_{1,2,3}$ is the rate, $k_{F1,2,3}$ is the rate constant for the forward reaction, $k_{R1,2,3}$ is the rate constant for reversed reaction $C_{TG,DG,MG,M,B}$ is the concentration of triglyceride, diglyceride, monoglyceride, methanol and biodiesel respectively. Hence, using power rate law as

$$r_1 = -\frac{dC_{TG}}{dt} = k_{F1}C_{TG}C_M - k_{R1}C_BC_{DG}$$

$$r_2 = -\frac{dC_{DG}}{dt} = k_{F2}C_{DG}C_M - k_{R2}C_BC_{MG}$$

$$r_3 = -\frac{dC_{MG}}{dt} = k_{F3}C_{MG}C_M - k_{R3}C_BC_G$$

Some assumed the reaction is elementary and not reversible and used the equation

$$r = -\frac{dC_{TG}}{dt} = k_F C_{TG}{C_M}^3 - k_R {C_{BD}}^3 C_G$$

Arrhenius equation is applied to determine the rate constant

$$k = Aexp^{\left(-\frac{E}{RT}\right)}$$

Some of the reported activation energy (E) and pre-exponential factor (A) reported in literatures are shown in *Table 2-22*.

Table 2-22: Kinetics parameters for biodiesel production.

Catalyst	A_1	A_{-1}	A_2	A_{-2}	A_3	A_{-3}	A_{FFA}	A_{-FFA}	E_1	E_{-1}	E_2	E_{-2}	E_3	E_{-3}	E_{FFA}	E_{-FFA}	Reference
H_2SO_4	1.59	0.33	3.194	5.97	1.01×10^{11}	4.03×10^{-4}	9.5	1.67×10^{-5}	38.7	38.7	38.7	38.7	107.11	38.74	37.99	12.76	Marchetti et al. (2010)
	$L \cdot (mol \cdot s)^{-1}$								$kJ \cdot mol^{-1}$								
$H_3PW_{12}O_{40}$	0.0087	0.6971	7.211	0.0022	2.113	0.0022			31.3	35.2	46.1	10.5	44.1	14.7			Yuan et al. (2013)
	$m^3 \cdot (g_{cat.} s)^{-1}$								$kJ \cdot mol^{-1}$								
Al/Sr	3.38×10^{7}								72.86								Feyzi and Shahbazi (2017)
	s^{-1}								$kJ \cdot mol^{-1}$								
Zr/W	1.5×10^{10}								51.9								Zubir and Chin (2010)
	$L^2 \cdot (mol \cdot g \cdot min)^{-1}$								$kJ \cdot mol^{-1}$								
NaOH	3.7×10^{7}	9.4×10^{5}	5.82×10^{12}	1.06×10^{10}	5.33×10^{3}	9.16×10^{3}			13.14	9.93	19.86	14.64	6.42	9.59			Bashiri and Pourbeiram (2016)
	$L \cdot (mol \cdot min)^{-1}$								$kcal \cdot mol^{-1}$								
Base	1176.67								36.01								Ong et al. (2013b)
Acid	1372.9	2.11							28.38	5.66							
	min^{-1}								$kJ \cdot mol^{-1}$								

NaOH	0.110	0.482[a]	0.171	0.482[a]	0.076	0.482[a]	3.1[b]	0.062[c]	48.7	57.9[a]	49.3	57.9[a]	53.9	57.9[a]		57.9[c]	Reyero et al. (2015)
	$L^2 \cdot (mol^2.s)^{-1}$ / $(L \cdot (mol \cdot s)^{-1})$ [a,b,c]								$kJ \cdot mol^{-1}$								
H_2SO_4	2.92×10^9			3.84×10^13					79.24			119.76					Yingying et al. (2012)
	Forward (h^{-1})			Reverse $L \cdot (mol \cdot h)^{-1}$					$kJ \cdot mol^{-1}$								
H_2SO_4	702.7		1926 2.2	3.57× 10^{27}	1028.6	20685.7			47.4		55.8	264.5	46	58.1			Liu et al. (2016b)
	$L \cdot (mol \cdot min)^{-1}$								$kJ \cdot mol^{-1}$								
F^+-SO_4^{--}/ MWCNT	1.88			1.90					32.73			32.61					Shu et al. (2019)
	$L \cdot (mol \cdot h)^{-1}$								$kJ \cdot mol^{-1}$								
NaOH									13.1	9.9	19.9	14.6	6.4	9.6	300 rpm		Noureddini and Zhu (1997)
30 – 70 °C									13.6	9.8	18.8	11.2	5.2	9.9	600 rpm		
									$kcal \cdot mol^{-1}$								
NaOH									14.0	10.7	16.0	13.9	7.2	11.0			Bambase et al. (2007)
25 – 60 °C									$kcal \cdot mol^{-1}$								
KOH									14.7		14.2		6.4				Darnoko and Cheryan (2000)
50 – 65 °C									$kcal \cdot mol^{-1}$								

[a] is the TG, DG and MG to soap [b] ethoxide and hydroxide reaction [c] biodiesel to soap

As shown in *Table 2-22* the activation energy (E) for the reaction are within the same range (less than 100kJ·mol^{-1}). This shows the kinetics and reaction mechanism compared well and follows similar trend. However, from all the many documented literature on kinetics of biodiesel production, no literature has been reported on the kinetics of reactive coupling for biodiesel, polyglycerol, and glycerol ether production. The data obtained from the kinetics of reactive coupling will give better understanding of the reaction conditions, design process, optimizing and scaling up of the process.

2.8 Summary of Chapter Two

Various techniques have been applied for biodiesel production with selected catalyst. Higher molar ratio of methanol to triglyceride were used, leading to increase in cost for the purification of both biodiesel and glycerol by-product. The glycerol (if purified) are converted to various products, to increase the revenue for biodiesel industries. For the purpose of this research, the novelty is to reduce the molar ratio of alcohol to triglyceride by converting the glycerol by-products to added value products in a single pot using reactive coupling technique. The effect of process variables for the technique shall be determined and the kinetic model of the process developed.

Chapter 3. MATERIALS AND METHODS

This chapter reports the materials, equipment, and methods used in this research. All chemicals were purchased from vendors and used without further treatment. The first part of this chapter concerns glycerol valorisation using commercial glycerol as feedstock. The second part contains reactive coupling procedures for the simultaneous production of biodiesel and valorisation of glycerol. The third part is the methodology used for combined reactive extraction and reactive coupling. This includes extraction of rapeseed oil using Soxhlet extraction, reactive extraction, and combined reactive extraction and reactive coupling. The fourth part describes the model developed for the production of polyglycerol from commercial glycerol and reactive coupling.

3.1 Materials

Table 3-1: List of materials, supplier, and the purity.

Name	Supplier	Purity
Glycerol	Sigma-Aldrich	99.5 wt%
Sulfuric acid	Sigma-Aldrich	99.999%
Acetonitrile	Fisher Scientific	HPLC Grade
Distilled Water	Fisher Scientific	HPLC Grade
Diglycerol	Inovyn	90.6%
Polyglycerol – 3	Inovyn	49%
Polyglycerol – 4	Inovyn	28.5
Anhydrous Methanol	Sigma-Aldrich	>99.5%
Anhydrous Pyridine	Sigma-Aldrich	99.8%
N, O-Bis (trimethylsilyl) trifluoroacetamide	Sigma-Aldrich	>98.5%
Methyl Heptadecanoate (Analytical Standard)	Sigma-Aldrich	>99%
3-methoxyl 1,2-propanediol (Analytical Standard)	Sigma-Aldrich	
Propan-1-ol	Acros Organics	99.5%
Toluene	Sigma-Aldrich	

Hexane with mixed Isomers	Alfa Aesar	98.5+%
Rapeseed Oil	Tesco vegetable oil	
Rapeseed	Newcastle farm	

3.2 Polyglycerols Production from Commercial Glycerol

This section explains the procedures to produce polyglycerols from commercial glycerol. The reaction was conducted in a pressurised vessel at low temperature, compared to the previous works (Salehpour and Dubé, 2011, Ardila-Suárez et al., 2015, Gholami et al., 2013a, Bookong et al., 2015) that used a distillation flask equipped with the Deans – Stark apparatus.

3.2.1 Experimental Apparatus for Polyglycerol Production

The experimental rig is shown in *Figure **3**-**1*** below. The reactor was made of stainless steel (T316 Parr instrument 4760) with a volume of 300 mL and was pressure-rated to 200 bar. The vessel was 101.63 mm in height and had an inner diameter of 63.30 mm. It was equipped with a pressure relief valve set at 20 bar. The vessel was also equipped with a 7 bar pressure gauge to measure the pressure, a thermocouple, catalyst line, liquid sampling line, and gaseous sampling line. Wet gas from the reactor is dried using packed ice and the dried gas collected through the gas sampling point. The polymerised sample was collected through the liquid sampling point. The experimental rig was set to accommodate the reaction conditions for both polyglycerol and biodiesel production.

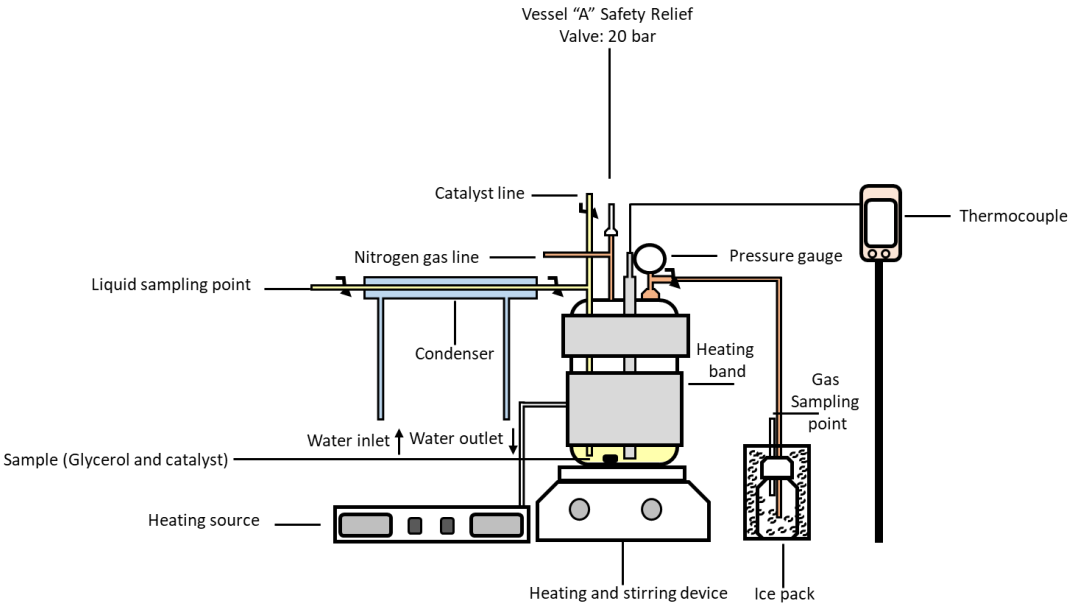

Figure 3-1: Pressurised vessel equipped with thermocouple and pressure gauge.

3.2.2 Reaction Procedure for Polyglycerol Production

100 g of glycerol was poured into the reaction vessel and heated to the desired temperature. Then 1 wt% sulfuric acid was added through the catalyst line, initiating the reaction. The reactor was nitrogen blanketed (filled and closed). Both gas and liquid samples were collected at intervals (0 – 5 hours). The composition of gas samples was determined using a GC. Liquid samples were analysed with FTIR and HPLC for the functional groups and compositions, respectively. The experiment was repeated with various temperature (130 – 160 ^{o}C) and catalyst concentration (1 – 6 wt%).

The conversion of glycerol, the selectivity of the individual oligomers, the total oligomers, and the percentage yield were calculated using the equations below:

$$Glycerol\ conversion\ (\%) = \frac{initial\ concentration - final\ concentration}{initial\ concentration} \times 100 \qquad 3.1$$

$$Selectivity\ of\ DG = \frac{final\ concentration\ of\ DG}{initial\ concentration - final\ concentration} \times 100 \qquad 3.2$$

$$Selectivity\ of\ PG = \frac{sum\ of\ final\ concentration\ of\ PG}{initial\ concentration - final\ concentration} \times 100 \qquad 3.3$$

$$Yield\ (\%) = \frac{glycerol\ conversion \times sum\ of\ selectivity}{100} \qquad 3.4$$

3.2.3 Sample Preparation and Characterization

Both gas and liquid samples were collected at the interval. The gas sample was characterised using the GC while HPLC, FTIR, and refractive index were used to characterise the liquid samples. The GC and HPLC were used to determine the concentration of samples while the refractive index is for easy monitoring of the reaction progress.

3.2.3.1 Gas Chromatography (GC) Analysis of Gas Sample

The gas sample was collected into a 1-litre PVF film gas sampling bag with polypropylene fittings. The dry gas was carefully collected by connecting the fittings of the gas bag to the sampling point. A syringe was then used to collect the gas from the sampling bag and injected it directly into GC.

The GC used was Varian/Agilent technology (Varian 450 – GC). It was equipped with a thermal conductivity detector (TCD) to measure the permanent gases and flame ionisation detector (FID) to determine hydrocarbons and alcohols. It consists of 2 ovens; the first has three (3) columns (Haye Sep T 1.64 ft (0.5 m) long by 0.125 inch outer diameter UltiMetal, Haye Sep Q 1.64 ft (0.5 m) long by 0.125 inch outer diameter UltiMetal and Molsieve 13 by 1.5 m by 0.125 inch UltiMetal for permanent gases). The second contains two (2) columns (CP – SIL 5 CB FS 25 m long by 0.25 mm inner diameter for hydrocarbons and CP – WAX 52 CB FS 25m long by 0.32 mm inner diameter for alcohols).

The GC was connected to four gas cylinders: nitrogen, as the make-up gas; hydrogen and compressed air combusting gases, and argon as the carrier gas. Both front and middle injector set points were at 250 ^{o}C. The initial and final oven temperatures were 40 and 120 ^{o}C, respectively, with a ramp of 10 ^{o}C·min^{-1} and end time of 13.25 min. The flow rate at the column pneumatics for both the front and middle column was 1.0 mL·min^{-1} with the front TCD set point of 175 ^{o}C, and filament temperature of 275 ^{o}C and positive polarity while the middle FID is at 255 ^{o}C set point.

3.2.3.2 High Performance Liquid Chromatography (HPLC) Analysis of Samples

The sample was prepared by diluting a known amount of the product with 5 mL HPLC-grade water. The mixture was then shaken to homogeneity. It was then filtered into 2 mL vials using a 4 mm syringe filter of 0.45 µm PVDF (polyvinylidene fluoride) material. The vials were then sealed with a PTFE (polytetrafluoroethylene)/ silicone septa screw cap (11 mm) from Restek.

The liquid samples were analysed with the Perkin Elmer "Flexar" HPLC. A hypersil GOLD Amino column ((from Restek) with 250 mm by 4.6 mm diameter by 5 µm particle size) was used at a flow rate of 1.5 $mL \cdot min^{-1}$ and temperature of 40 ^{o}C. The eluate was a mixture of acetonitrile and water (70:30). The HPLC was equipped with a photodiode array (PDA) detector and a refractive index (RI) detector. The LCs were analysed using "Chromera" software. The samples were arranged in the autosampler tray according to the sequence number. The method was loaded, and the sequence was run. The method used was based on the work of previous authors (Wan et al., 2015, Soi et al., 2014, Kumar et al., 1984, Din et al., 2013).

3.2.3.3 Fourier Transform Infrared Spectroscopy (FTIR)

The analysis was performed using an Agilent Technologies Cary 630 FTIR spectrometer, with a spectral range of 4000 to 650 cm^{-1}. Salehpour and Dubé (2012) used a similar system.

The sample holder and the diamond ATR (attenuated total reflection) cell were cleaned with 2-propanol. The sample was added dropwise to cover the diamond ATR using a transfer pipette for liquid samples. In solid samples, tweezers or spatulas are required to drop the sample to cover the diamond ATR. Before spectrum capture for the solid samples, the cap was then screwed down to lock the sample to the diamond ATR.

3.2.3.4 Refractive Index

The refractive index was measured using a refractometer (Mettler Toledo Refracto 30PX). The refractive index of the tool ranges between 1.32 – 1.5. Using a transfer pipette, the sample was taken and carefully dropped onto the illuminated surface, which holds the sample.

3.3 Reactive Coupling for Biodiesel and Glycerol Valorisation

Commercial (Tesco) rapeseed oil was used as biodiesel feedstock. It was purchased from a local store in Newcastle. The same experimental set-up as in the polymerisation of glycerol (**3.2.1**) was used with modification.

3.3.1 Reaction Rig for Reactive Coupling

The apparatus for this experiment (see *Figure **3**-**2*** below) is like the experimental set-up for polyglycerol production with the addition of a pressurised vessel. This is because alcohol is required and is used at a higher temperature than its ambient pressure boiling point. The additional pressurised vessel was connected through the catalyst line so that the alcohol could be added at pressure. The additional vessel also had a dedicated relief valve.

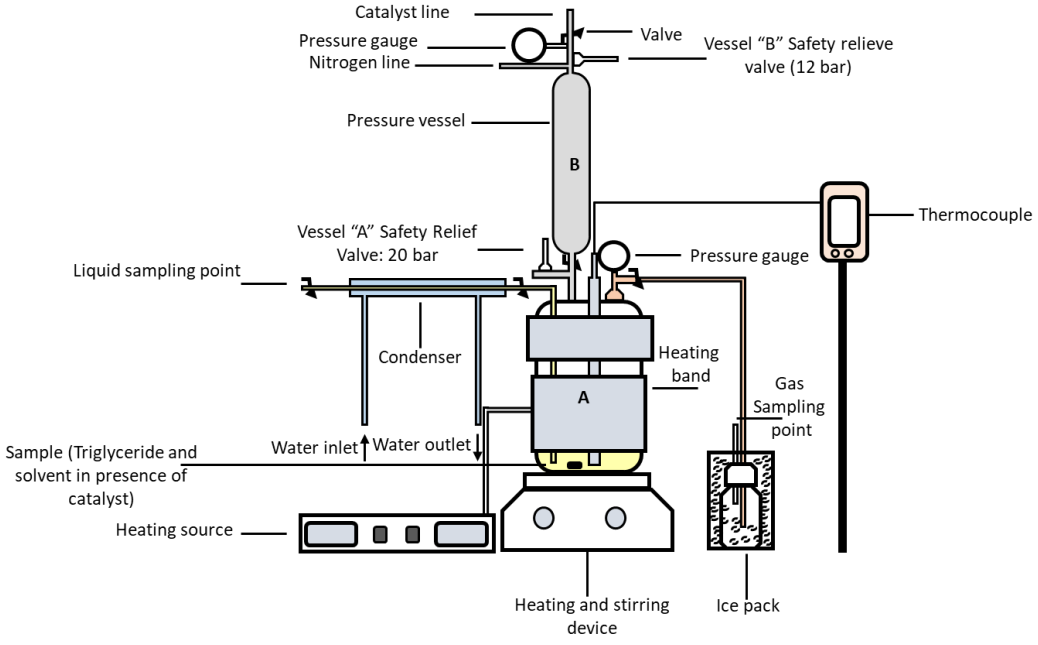

Figure 3-2: Experimental set-up for reactive coupling.

3.3.2 Procedure for the Reactive Coupling

100 ml of triglyceride were poured into the reaction vessel (A) and heated to the desired temperature. The required methanol (4:1, 5:1, 6:1, and 8:1) and sulfuric acid (1%, 2%, 3%, and 5%) were measured into the pressure vessel (B). Nitrogen gas was then allowed into the vessel (B), which pushes the mixture of the methanol and catalyst into the main

reactor (vessel A), initiating the reaction. The reaction was conducted in a nitrogen environment to minimise dehydration of glycerol into acrolein and acetol. Liquid samples were collected at the end of the experiment to determine the percentage of FAME content.

3.3.3 Preparation and Characterization of Reactive Coupling Sample

The gas sample was characterised as reported in 3.2.3.1. Also, the FTIR and refractive index were performed as reported in section 3.2.3.3 and 3.2.3.4, respectively. The liquid phase, which consists of the FAME rich phase and the heavy glycerol rich phase separate almost immediately after the reaction using gravity, were characterised for density, viscosity, and compositions.

3.3.3.1 GC Analysis of FAME

1000 mg of methyl heptadecanoate was measured into a 100 mL volumetric flask. It was dissolved in propan-1-ol and made up to 100 mL. The mixture was used as the internal standard for the GC analysis of the FAME percentage content. About 50 mg of the FAME sample was measured into a 2 ml vial, and using a pipette, 1 ml of the methyl heptadecanoate standard solution was added.

The FAME content was analysed following the report by Al-Saadi et al. (2018). The GC (HP6890 series) with a fused silica capillary column of 30 m by 0.32 mm by 0.25 µm was used. The oven was ramped at 15 $^{o}C{\cdot}min^{-1}$ from 120 to 260 ^{o}C after an initial time of 5 mins. The final temperature was held for another 15 mins. The injector was set at 250 ^{o}C while the flame ionisation detector (FID) was set to 260 ^{o}C. The prepared sample was injected using an autosampler. The FAME content was then calculated using the equation below.

$$P_F = \frac{(\sum A_P - A_I)}{A_I} \times \frac{(C_I \times V_I)}{m_S} \times 100 \quad 3.5$$

$$m_F = \frac{P_F \times m_{FT}}{100} \quad 3.6$$

$$Yield\ of\ FAME\ \left(\%\frac{w}{w}\right) = \frac{m_F}{m_{Ft}} \times 100 \quad 3.7$$

P_F is percentage FAME content, $\sum A_P$ is the summation of the peak area from the GC, A_I is the internal standard area, and C_I is the internal standard concentration. The internal standard volume is represented as V_I while the mass of the sample analysed is m_s. Also, m_F is the mass of FAME, m_{FT} is the total mass of the upper layer after separation and m_{Ft} is the theoretical mass of FAME.

3.3.3.2 GC Analysis of Polyglycerol

Derivatisation of the polyglycerol was necessary to have good separation from the GC or MS by enhancing the sample volatility and detectability. Derivatisation of analytical samples for GC is often applied to compounds that contain active hydrogen atoms in their functional groups. These groups (hydroxyl (-OH), amine (-NH), carboxylic acid (-COOH), and thiol (-SH)) are either thermally unstable, not sufficiently volatile, or too strongly bound to the stationary phase of the GC column (Knapp, 1979). Must derivatisation for GC are acylations, alkylations, esterifications, or silylations. Silylation is used for polyglycerols to modify the –OH groups, as they interact with the stationary phase too strongly. Typically, silylation increases the volatility and decrease the surface adsorption by displacing the active hydrogen of hydroxyl (-OH), amine (-NH), or thiol (-SH) groups (Moldoveanu and David, 2019). The silylation mechanism comprises a nucleophilic attack by the silicon, which removes the low basicity leaving group. The leaving groups low basicity stabilises the negative charge in the transition state (Knapp, 1979).

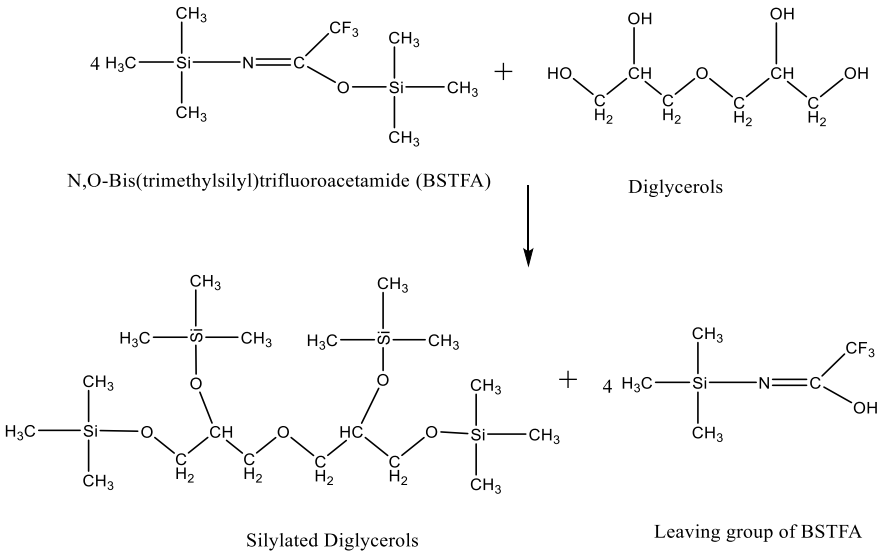

Figure 3-3: Silylation of polyglycerol with BSTFA as the silylating agent.

Here, the polyglycerol analysis produced in the GC was performed after silylation, following Guerrero-Urbaneja et al. (2014). About 50 mg of the heavy phase was measured and dissolved in 0.5 mL of dried pyridine as bought. Using a micropipette, 0.04 mL of the dissolved sample was taken into a 2 mL vial. A 25 mg·mL^{-1} concentration of the standard (butan-1, 2, 4-triol) was prepared with the dried pyridine, and 0.04 mL was added to the sample in the vial. The mixture was then added 0.06 mL of N, O-Bis (trimethylsilyl) trifluoroacetamide (BSTFA), and the vial sealed. The mixture was then allowed to age for an hour in an oven at 60 ^{o}C before analysis with the GC.

A Hewlett Packard 5890 series II was used, equipped with Elite-5MS column (30 m by 0.32 mm by 0.25 µm) and FID. The injector temperature was operated at 250 ^{o}C, and FID was set at 280 ^{o}C. The tool was operated with the initial temperature set at 150 ^{o}C and an initial time of 2 minutes. It was ramp at the rate of 10 ^{o}C·min^{-1} to the final temperature of 300 ^{o}C. The final temperature was held for 15 minutes. 1 µL of the silylated sample was injected manually.

The equations below were used to calculate the contents, yield, and selectivity of the compositions of the sample.

$$P_G = \frac{A_G}{A_I} \times \frac{(C_I \times V_I)}{m_S} \times \frac{1}{G_G} \times 100 \qquad 3.8$$

$$P_{DG} = \frac{A_{DG}}{A_I} \times \frac{(C_I \times V_I)}{m_S} \times \frac{1}{G_{DG}} \times 100 \quad 3.9$$

$$P_{TG} = \frac{A_{TG}}{A_I} \times \frac{(C_I \times V_I)}{m_S} \times \frac{1}{G_{TG}} \times 100 \quad 3.10$$

$$P_{TTG} = \frac{A_{TTG}}{A_I} \times \frac{(C_I \times V_I)}{m_S} \times \frac{1}{G_{TTG}} \times 100 \quad 3.11$$

$$P_{MPD} = \frac{A_{MPD}}{A_I} \times \frac{(C_I \times V_I)}{m_S} \times \frac{1}{G_{MPD}} \times 100 \quad 3.12$$

$$m_i = \frac{P_i \times m_T}{100} \quad 3.13$$

$$S_i = \frac{m_i}{m_{G1} - m_G} \times 100 \quad 3.14$$

$$X_G = \frac{m_{TG} - m_G}{m_{TG}} \times 100 \quad 3.15$$

$$Y_i = \frac{X_G \times S_i}{100} \quad 3.16$$

Where $P_{G, DG, TG, TTG, MPD}$ are the percentage content by weight of glycerol, diglycerols, triglycerols, tetraglycerols and 3-methoxyl 1,2-propanediol. $A_{G, DG, TG, TTG, MPD}$ are the area and $G_{G, DG, TG, TTG, MPD}$ are the slopes of calibration for glycerol, diglycerols, triglycerols, tetraglycerols and 3-methoxyl 1,2-propanediol, respectively. A_I, C_I and V_I are the peak area of the internal standard from the GC, concentration of internal standard and volume of the internal standard. Mass of the various species was represented as m_i, total mass of the glycerol heavy phase after separation m_T and percentage content of the different species C_i. The selectivity of the specie is S_i, while m_{G1} and m_G are the theoretical mass of glycerol base on the conversion of triglyceride and mass of the glycerol after reactive coupling. The yield of the coupled species are Y_i and the conversion of glycerol is X_G.

3.3.3.3 Density of FAME

The density of the sample was measured using Mettler Toledo Densito 30PX. The portable meter can be set to analyse the liquid sample for density or specific gravity. The meter has an accuracy of ± 0.001 g·cm^{-3} and a temperature range of 5 – 35 ^{o}C. Distilled water is used to clean the measuring cell before the analysis of the sample.

3.3.3.4 Viscosity of FAME

The viscosity of the FAME was measured using Haake viscotester 2 plus. The device has a rotor speed of 62.5 rpm with a maximum temperature of 150 ^{o}C. The rotor was connected to the device and clamp to the support stand. The sample was then carefully poured into the measuring cup. The rotor was gently immersed into the measuring cup with the sample. The device was then switched on, and the viscosity was measured.

3.4 Combined Reactive Extraction and Reactive Coupling

The extraction of the rapeseed, reactive extraction and Soxhlet reactive extraction using the Soxhlet apparatus is explained in this section. It also includes the procedure for the combined reactive extraction and reactive coupling.

3.4.1 Soxhlet Extraction

The seed was grounded using a manual grain crusher (Eschenfelder). A known amount of the ground seed was taken into a thimble and carefully inserted into the Soxhlet apparatus extractor. 60 mL of hexanes with mixed isomers was poured into the three-neck distillation flask, equipped with a thermocouple. The extraction was performed at 70 ^{o}C (above the boiling point of the solvent). The effect of time was observed by extracting from 10 – 60 mins. The experimental set-up is, as shown in *Figure 3-4*.

The percentage of oil yield in the seed was determined using the equation below.

$$Oil\ Yield\ \% = \frac{W_o}{W_s} \times 100\% \qquad 3.17$$

Where W_o = weight of the oil extracted (g)

W_s = initial weight of the seed (g)

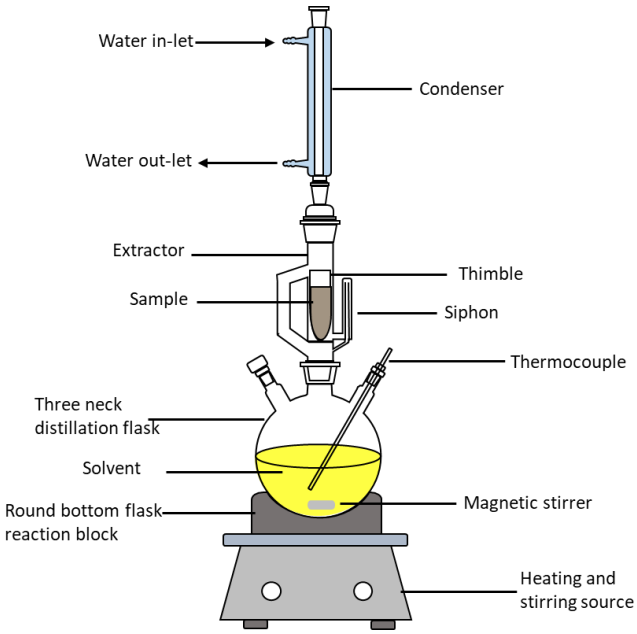

Figure 3-4: Soxhlet extraction apparatus for rapeseed oil extraction.

Methanol was also used as a solvent for the extraction. The mixture of the extracted oil and solvents was separated by evaporating the solvent at room temperature in an open flask inside the fume cupboard for 24 h. Samples were analysed for density, viscosity, refractive index, free fatty acid, and FTIR. The cake was also analysed for the morphology using SEM/EDX.

3.4.2 Reactive Extraction for Biodiesel Production

A known amount of the grounded rapeseed was measured and poured into the three-neck round bottom flask. The flask was equipped with a thermocouple, condenser, and a magnetic stirrer, as shown in *Figure 3-5*. The distillation flask was heated and stirred with the aid of the combined hot and stirring plate. A known amount of methanol (200:1, 300:1, 400:1, and 480:1) was preheated to the desired temperature (65 ^{o}C) before introducing the three-neck distillation flask. The reaction was initiated with the addition of 1 wt% sulfuric acid. Samples were withdrawn at intervals. The experiment was performed with a stirring speed of 200 rpm.

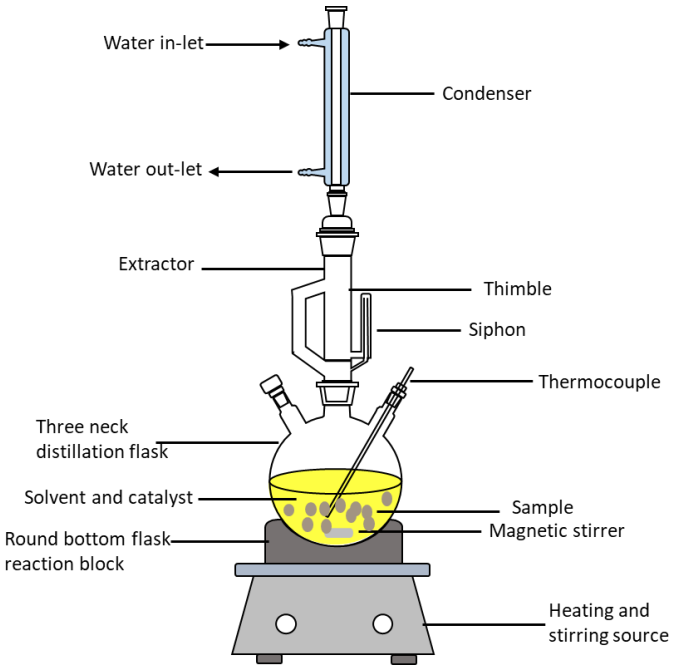

Figure 3-5: Set up for the reactive extraction.

Samples were analysed with the GC for the FAME content after separation. Selected samples of the seed residue were also characterised for the FTIR and SEM.

3.4.3 Soxhlet Extraction with Parallel Reaction for Biodiesel Production

The concept of Soxhlet extraction and reactive extraction were combined in this method. Unlike reactive extraction that the ground seed is mixed and stirred with the solvent, Soxhlet extraction with parallel reaction has its sample in a thimble and placed into the Soxhlet apparatus extractor, as shown in *Figure 3-6*.

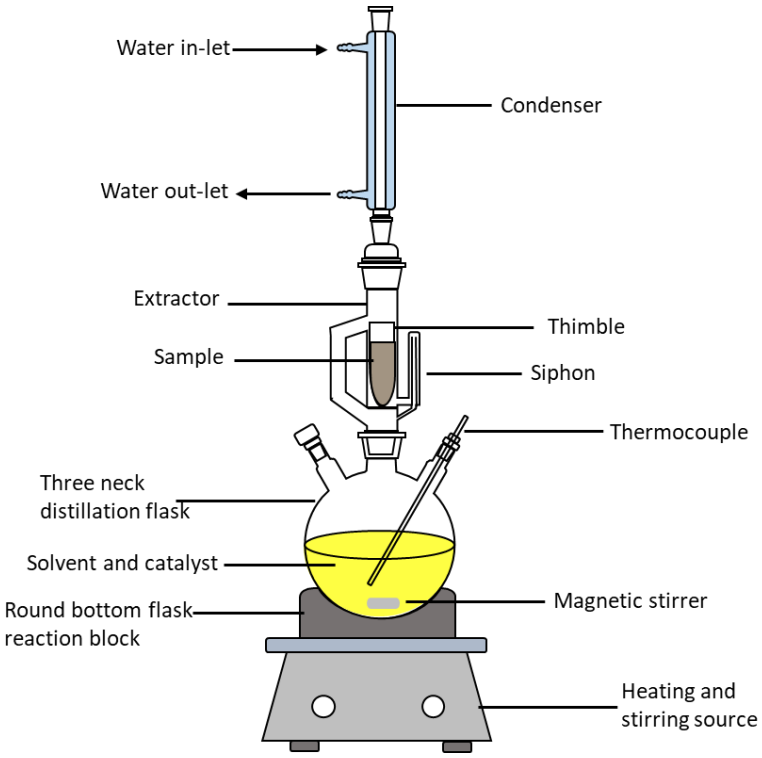

Figure 3-6: Soxhlet reactive extraction.

A known amount of the grounded sample was poured into a thimble and placed into the extractor. Methanol was mixed with 1 wt% of a catalyst (sulfuric acid) and stirred at 200 rpm at 65 ^{o}C. The condensed solvent overflow through the siphon, which contains the extracted triglyceride, will mix with the catalyst in the three-neck distillation flask to initiate the reaction. The experiment was repeated with various molar ratios (200:1, 300:1, 400:1, and 480:1). The GC characterised the samples for composition.

3.4.4 Combined Reactive Extraction and Reactive Coupling

The same experimental set-up as in section **3.3.1** was used, as shown in **Figure 3-7**.

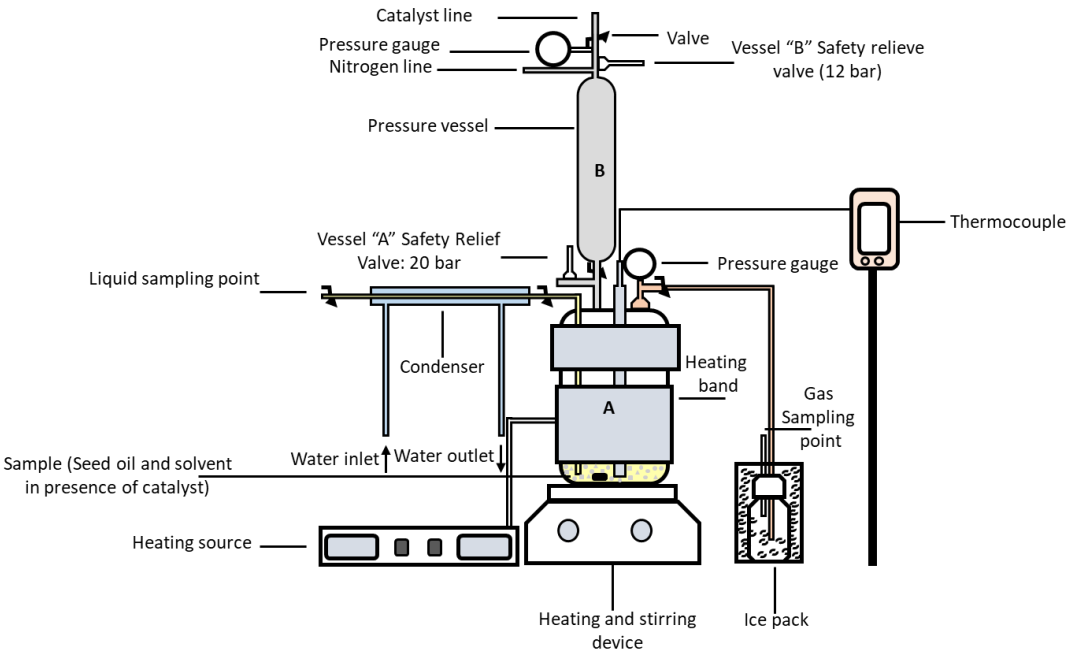

Figure 3-7: Combined reactive extraction and reactive coupling.

The grounded rapeseed was poured into the reaction vessel (A). A measured amount of methanol was taking and divided into two-part. The first part was added into the vessel (A) to mix with the grounded rapeseed. The mixture was then heated until the required temperature was attained. The second part of the methanol was then poured into the pressure vessel (B) and 1 wt% sulfuric acid. Nitrogen gas was used to push down the mixture (vessel B) into the main reactor (vessel A) as the temperature required was attained. At the end of the reaction time, samples were analysed for each phase as in section **3.3.3**. The reaction was repeated with various molar ratio (150:1, 200:1, 250:1, 300:1, 400:1 and 450:1), temperature (130, 140, 150 and 160 ^{o}C) and catalyst concentration (0.5, 1, 2, 3 and 5 %).

3.4.5 Sample Characterizations

Gas chromatography was used to analyse the liquid samples composition in the combined reactive extraction and reactive coupling as in section 3.3.3.1 and 3.3.3.2. A similar procedure was used for reactive extraction and pseudo reactive extraction method. Samples from Soxhlet extraction, reactive extraction, Soxhlet extraction with parallel reaction, and combined reactive extraction and reactive coupling were also characterised for density (see section 3.3.3.3), viscosity (see section 3.3.3.4), refractive

index (see section 3.2.3.4), FTIR (see section 3.2.3.3), free fatty acid, and acid value. The rapeseed water content was determined before grounding, and the SEM of the residue before and after the various experiment.

3.4.5.1 Water Content in the Rapeseed Sample

Rapeseed used for this work was obtained from Cockle Park farm (Newcastle University farm) and was stored airtight. The experiment to determine the water content was performed following the work of Zakaria (2010), which was based on the American Oil Chemist Society (AOCS) Ca-2d-25 method. A known amount of the ungrounded sample was weighed and oven-dried at 100 ^{o}C until a constant weight was achieved. The percentage of water content was calculated using the equation below.

$$Water\ Content\ \% = \frac{W_s - W_f}{W_s} \times 100\% \qquad 3.18$$

Where W_f = final weight of the seed (g) W_s = initial weight of the seed (g)

3.4.5.2 Free Fatty Acid and Acid Value

The American oil chemist society method (AOCS) Ca 5a-40 for the determination of free fatty acid (FFA), and acid value (AV) was used as reported by (Zakaria, 2010). A known amount (in gram) of the extracted oil was poured into a conical flask and mixed with 75 mL ethanol preheated to 40 ^{o}C. The mixture was gently swirled before adding 2 mL of phenolphthalein indicator. The mixture was then titrated over sodium hydroxide solution with constant stirring using a magnetic stirrer. The percentage of free fatty acid and acid number were then calculated using the equations below:

$$\%\ FFA\ (as\ oleic\ acid) = \frac{(V-B)\times N\times 28.2}{m_s} \qquad 3.19$$

$$AV = FFA \times 2 \qquad 3.20$$

Where V = titration value of the sample, B = titration value of the blank, N = concentration of sodium hydroxide

3.5 Kinetics

The conditions used for the glycerol etherification in this work produce polyglycerol and traces of by-product such as acrolein and hydrogen. The assumed reaction pathway is, as shown in *Figure **3-8***.

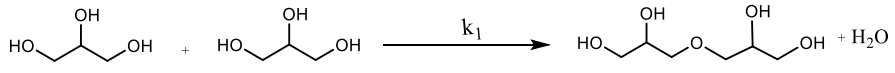

(ai) Etherification of glycerol to diglycerol

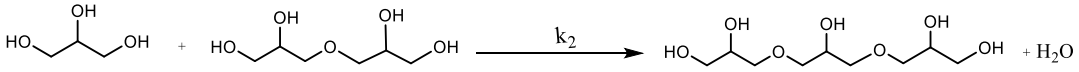

(aii) Etherification for triglycerol production

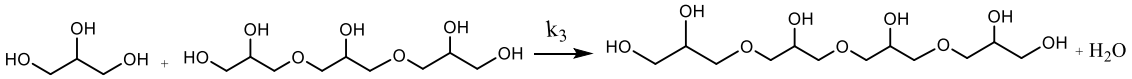

(aiii) Etherification for tetraglycerol production

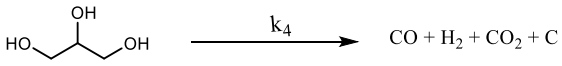

(b) Glycerol decomposition as a side product

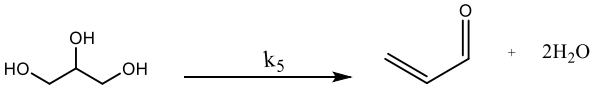

(ci) Glycerol dehydration to produce acrolein

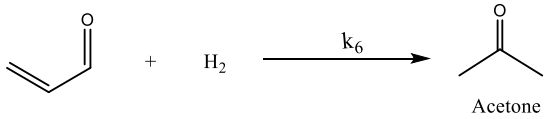

(cii) Acrolein hyrogenation to produce acetone

Figure 3-8: Possible reaction pathway for (a) polyglycerol production (b) glycerol decomposition (c) glycerol dehydration.

This shows that glycerol can undergo a parallel reaction of etherification, dehydration, and decomposition due to the three-hydroxyl group. However, the reaction favours the etherification reaction. This was because it was performed in a nitrogen environment, and dehydration is favoured in an air environment. Also, the temperature was limited

to 160 °C to reduce the decomposition of glycerol. The following assumptions were made for this kinetics study:

i. **All polyglycerols are diglycerol and triglycerol.** Early proof of concept studies has demonstrated that diglycerols are the main form of the polyglycerol product, accounting for approximately 90% of the polyglycerols. Triglycerols and tetraglycerols production (through the pathway of k_2 and k_3) are only significant at higher temperatures, catalyst concentrations or/and times. However, triglycerols are produced within the first hour, while tetraglycerols are not. Hence tetraglycerol is assumed negligible for this scheme.

ii. **Higher polyglycerols are produced in parallel to the glycerol feed.** Since there is not enough data for the higher polyglycerol, the trial and error method was used to develop the model. The model was developed based on the selectivity of the diglycerol.

iii. **Acrolein formation is minimal.** The formation of the acrolein is minimised here by using an atmosphere of inert gas. Hence, k_5 and k_6 can be assumed to be negligible.

iv. **Hydrogen production is minimal.** In proof-of-concept experiments, hydrogen was detected. However, the yield was negligible (about 4% maximum, see *Figure **4-3*** to *Figure **4-6***) compared to the amount of polyglycerol (over 60%, see *Figure **4-7***) produced. Hence, k_4 can also be assumed negligible.

Error! Reference source not found. can then be reduced to *Figure 3-9* after removing the pathway for k_2, k_3, k_4, k_5, and k_6.

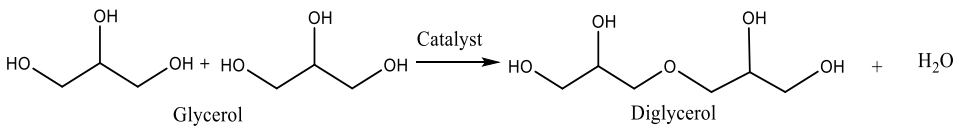

Figure 3-9: Reaction for diglycerols production.

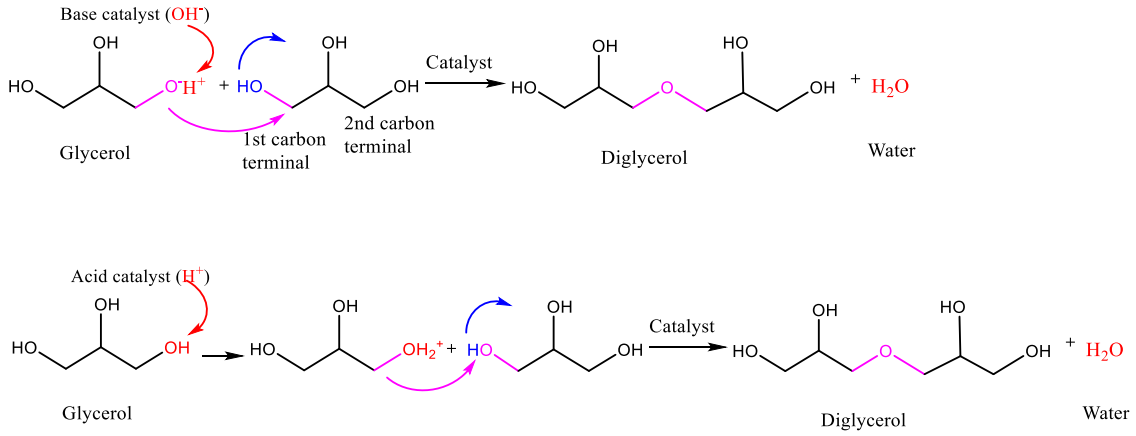

Figure 3-10: Reaction path for alkaline and acid catalyst for glycerol oligomerisation

The reaction mechanism with either base or acid catalyst can proceed in accordance with nucleophilic chemical substitution S_N2 type (Krisnandi et al., 2008, Salehpour and Dubé, 2011). The base catalyst will deprotonate one of the OH group of the glycerol feed. This aid to increase the nucleophilic strength of the oxygen to enhance attack on the carbon terminals of another glycerol molecule. This will now give out water in the process and form the much needed oligomer. Similarly, the process occurs with an acid catalyst by the protonation of one of the OH group of the glycerol to produce a good leaving group. The production of this good leaving group makes the acid catalyst process faster than the base catalyst due to it low activation barriers.

The overall kinetic equation for the consumption of glycerol is used.

$$R = kC_{GL}{}^{n}C_{C}{}^{m} \qquad 3.21$$

At constant catalyst concentration,

$$R = k_{obs}C_{GL}{}^{n} \qquad 3.22$$

Where $k_{obs} = kC_{C}{}^{m}$ 3.23

C_{GL} = glycerol concentration, C_C = catalyst concentration, n = order of reaction with respect to the glycerol, m = order of reaction with respect to the catalyst, and k = rate constant.

Using the second order kinetics, n in equation 3.22 was substituted to give

$$R = \frac{dGL}{dt} = k_{obs} {C_{GL}}^2 \quad 3.24$$

$$\frac{1}{C_{GL}} = \frac{1}{C_{GL0}} + k_{obs}t \quad 3.25$$

$$plot\ \frac{1}{C_{GL}}\ vs\ t. The\ intercept\ is\ \frac{1}{C_{GL0}}\ and\ the\ slope\ is\ k_{obs}$$

$$Note\ that\ k_{obs} = k{C_C}^m$$

$$lnk_{obs} = lnk + mlnC_C \quad 3.26$$

The plot of Lnk_{obs} against LnC_C will give a slope of m (order of the catalyst) and intercept Lnk (rate constant).

$$From\ Arrhenius\ equation, k = Ae^{-\frac{E}{RT}} \quad 3.27$$

$$lnk = lnA - \left(\frac{E}{R}\right)\left(\frac{1}{T}\right)$$

$$Plot\ lnk\ vs \frac{1}{T}.\ Intercept\ is\ lnA\ and\ slope\ is -\frac{E}{R}$$

The reactive coupling model was developed by adopting the conventional kinetics model of biodiesel using an acid catalyst as reported by previous authors (Marchetti et al., 2010, Qing et al., 2011). It was combined with the model developed for the polyglycerol

production from this work and glycerol ether using trial and error method. The reaction pathway is as shown in *Figure **3-11***

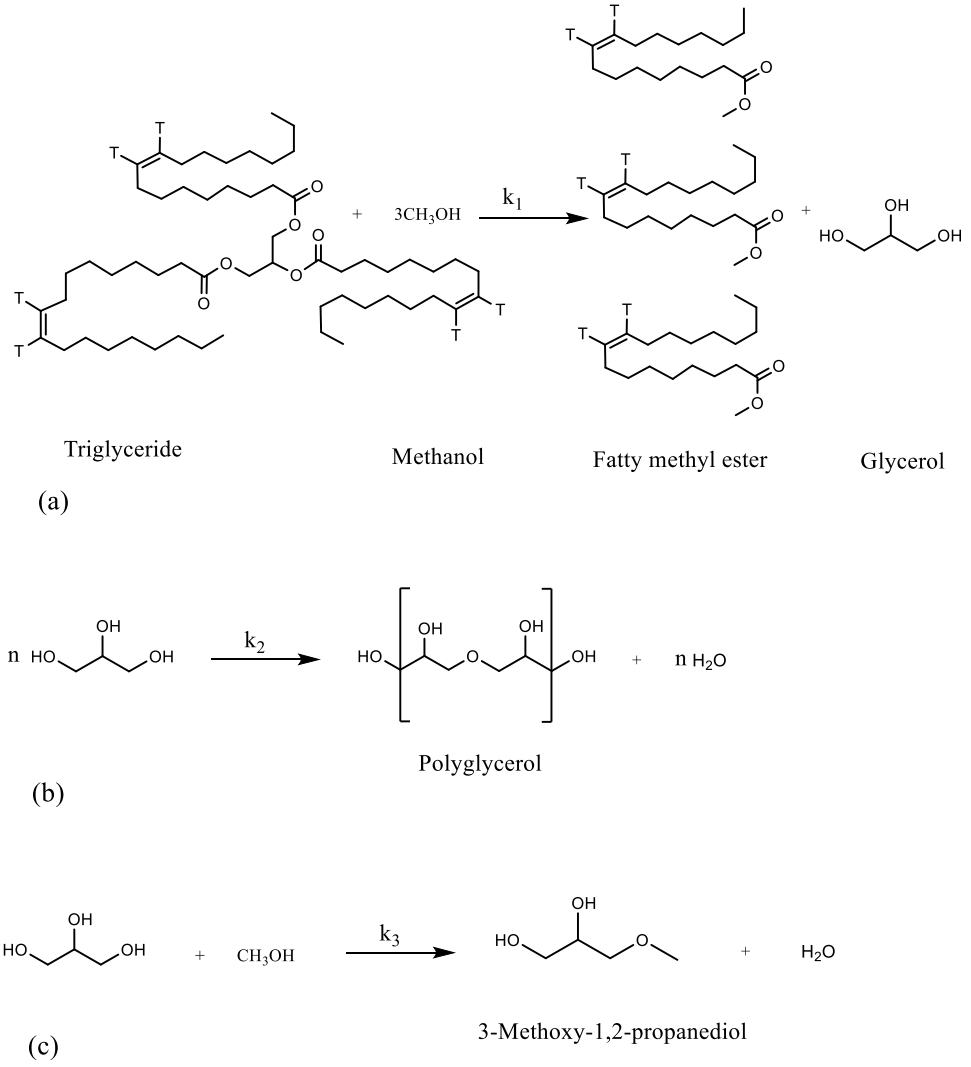

Figure 3-11: Reaction pathway for the reactive coupling showing (a) Biodiesel production (b) Polyglycerol production (c) Glycerol etherification with the excess methanol of transesterification.

The conversion of triglyceride to biodiesel and glycerol occurs with an intermediate (diglyceride and monoglyceride) production in a three-consecutive reaction. Both reactions were reported to be reversible, as shown in **Figure 3-12** below.

The rate of both the forward and reverse reaction of the FAME production with respect to the intermediate can be represented in the equations below.

$$r_{F1} = k_{F1} C_{TGE} C_M \quad 3.28$$

$$r_{R1} = k_{R1} C_{DGE} C_B \quad 3.29$$

$$r_{F2} = k_{F2} C_{DGE} C_M \quad 3.30$$

$$r_{R2} = k_{R2} C_{MGE} C_B \quad 3.31$$

$$r_{F3} = k_{F3} C_{MGE} C_M \quad 3.32$$

$$r_{R3} = k_{R3} C_G C_B \quad 3.33$$

The rate of each of the intermediate can be determined as shown in equation 3.34 – 3.36.

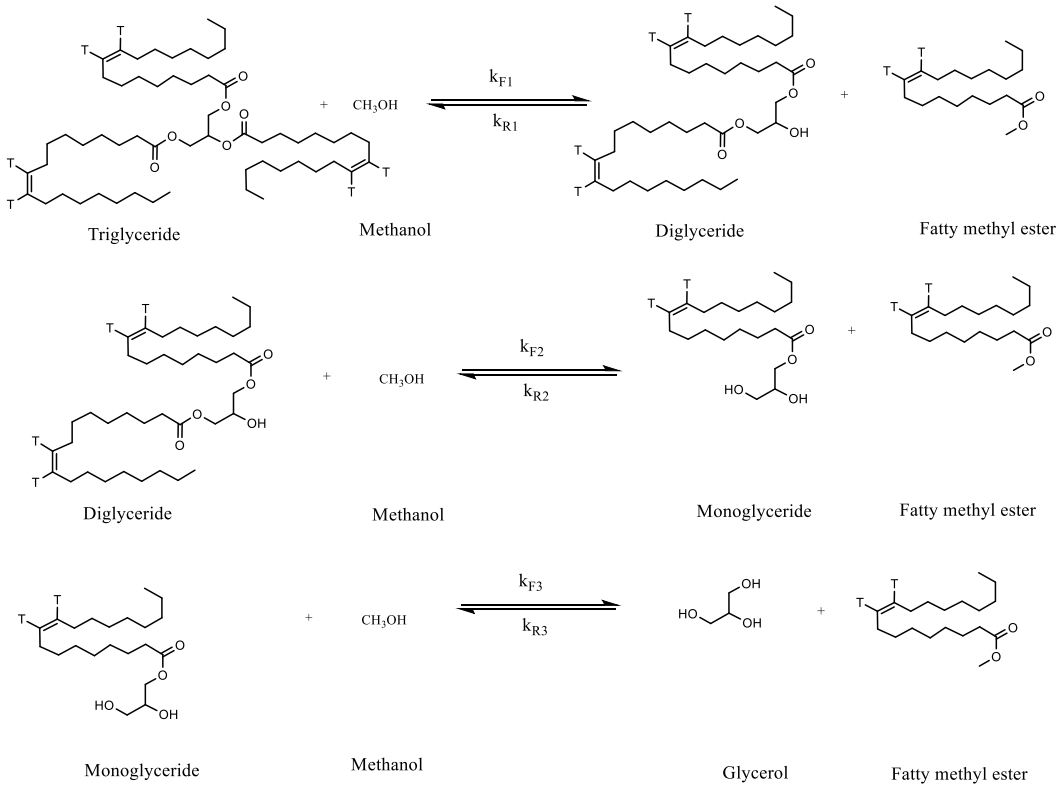

Figure 3-12: Consecutive reaction of triglyceride to biodiesel.

$$r_1 = r_{F1} - r_{R1} = k_{F1} C_{TGE} C_M - k_{R1} C_{DGE} C_B \quad 3.34$$

$$r_2 = r_{F2} - r_{R2} = k_{F2} C_{DGE} C_M - k_{R2} C_{MGE} C_B \quad 3.35$$

$$r_3 = r_{F3} - r_{R3} = k_{F3} C_{MGE} C_M - k_{R3} C_G C_B \quad 3.36$$

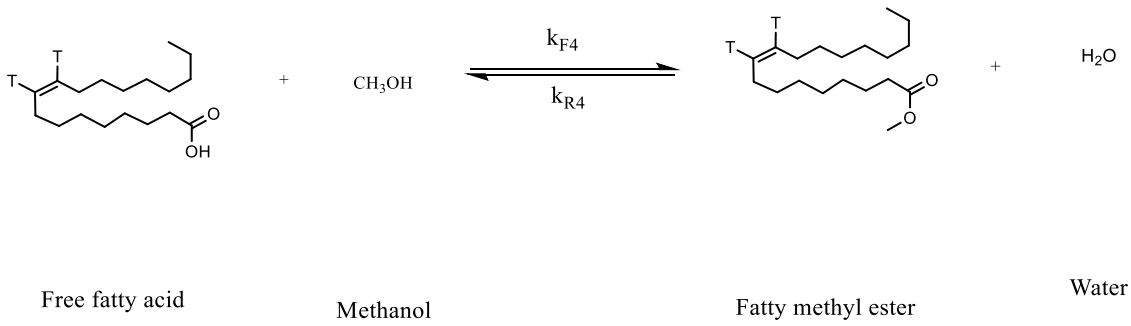

Figure 3-13: Reaction of the free fatty acid to produce biodiesel.

Since the FFA can also be converted to biodiesel as shown in *Figure 3-13*, the equation for the FFA was derived as shown in equation 3.37 – 3.39.

$$r_{F4} = k_{F4} C_{FFA} C_M \quad 3.37$$

$$r_{R4} = k_{R4} C_W C_B \quad 3.38$$

$$r_4 = r_{F4} - r_{R4} = k_{F4} C_{FFA} C_M - k_{R4} C_W C_B \quad 3.39$$

The overall rate for each component is shown in the equations below.

$$\frac{dC_{TGE}}{dt} = -r_1 \quad 3.40$$

$$\frac{dC_{DGE}}{dt} = r_1 - r_2 \quad 3.41$$

$$\frac{dC_{MGE}}{dt} = r_2 - r_3 \quad 3.42$$

$$\frac{dC_G}{dt} = r_3 \quad 3.43$$

$$\frac{dC_{FFA}}{dt} = -r_4 \quad 3.44$$

$$\frac{dC_B}{dt} = r_1 + r_2 + r_3 + r_4 \quad 3.45$$

Equation 3.21 for the polyglycerol production was adapted into the kinetics of reactive coupling. The model for glycerol ether was obtained using “trial and error” method. The trial and error from this work is an equation adopted from a similar process to glycerol ether. This is due to insufficient data for the glycerol ether to develop model or kinetics

model from previous literature. Both self-glycerol polymerisation and glycerol ethers are etherification process, hence, the adapting of the model from polyglycerol production. The model developed for the polyglycerol was used as the starting point and tested with various order of reaction. Also, the percentage selectivity were tested with the model to test the fitness to the experimental data.

3.6 Summary of Chapter Three

Polyglycerol was produced using a stainless steel vessel in presence of acid catalyst, with concentration varied from 1 – 6 wt%. The reaction was performed at 130 – 160 ^{o}C for up to 5 hours and the samples were analysed using HPLC and GC. The rig was modified to be suitable for reactive coupling because of methanol that will be introduced. With reactive coupling, triglyceride was converted to biodiesel in presence of acid catalyst with concentration 1 – 5 wt%, temperature 130 – 160 ^{o}C, and molar ratio 4:1 – 8:1. Same modified rig was used for combined reactive extraction and reactive coupling as a proof-of-concept. Samples produced from the process were analysed using GC. Kinetic model for glycerol etherification and reactive coupling were developed. It will be simulated using MATLAB to fit the experimental data obtained from this work.

Chapter 4. RESULT AND DISCUSSIONS

The first part of this chapter shows the results for the glycerol valorisation using commercial glycerol as feedstock. It also discusses the effect of the process variables and the kinetics of the process. The second section results from the reactive coupling for the simultaneous production of biodiesel and glycerol valorisation. Also, the kinetics of reactive coupling are discussed in this section. The last part of this chapter results from the combined reactive extraction/reactive coupling process, including the extraction of rapeseed oil using both hexane and methanol. It also explains the result of conventional reactive extraction and Soxhlet extraction in parallel with reaction, then the combined reactive extraction and reactive coupling findings.

4.1 Glycerol Valorisation

As mentioned in chapter two (section 2.5), glycerol can be valorised into various products or intermediates. This section concerns the conversion of glycerol to polyglycerol through the etherification process.

4.1.1 Properties of the Glycerol Feed

The glycerol and polyglycerols (diglycerol, triglycerol, and tetraglycerol) used as analytical standards in this research were characterised for the density, refractive index, and viscosity. These physical properties can be used in determining the changes in a polymer. The results were compared to the polyglycerol samples produced at various temperature (130 – 160 ^{o}C) and 6 wt% catalyst concentration. The result is shown in*Table **4-1***.

Table 4-1: Properties of glycerol and polyglycerol.

	Density (g·cm^{-3})	Refractive index	Viscosity (Pa·s)
Glycerol	1.25	1.473	0.961
Diglycerol	1.28	1.487	1.270
Triglycerol	1.29	1. 491	-
Tetraglycerol	1.28	1.497	-

Polyglycerol sample at 130 °C	1.26	1.480	1.040
Polyglycerol sample at 140 °C	1.27	1.484	1.170
Polyglycerol sample at 150 °C	1.27	1.485	1.210
Polyglycerol sample at 160 °C	1.28	1.487	1.230
Glycerol	1.261	-	1.500

One of the main reasons triglycerides are not used directly in combustion engines is their high viscosity, resulting in incomplete combustion in the Diesel engine. This high viscosity can be reduced by removing the glycerol, leaving the alkyl ester. Clearly, polymerising the glycerol increases the density and viscosity. Viscosity increases from 1.04 to 1.23 Pa·s as the reaction temperature increased from 130 – 160 °C. This leads to the production of higher degree polymer as the temperature increased to 160 °C. The density of polyglycerols (1.29 g·cm^{-3}) is very similar to glycerol (1.25 g·cm^{-3}). This might be due to the incomplete conversion and presence of impurity such as acrolein.

The refractive index of the polyglycerol samples obtained were higher than 1.473 obtained for glycerol. However, the results were lower than 1.491 and 1.497 recorded for triglycerol and tetraglycerol, respectively, used as a standard sample. The values of the polyglycerol samples are within 1.487 obtained for diglycerol. This might be an indication of the higher composition of diglycerol than other oligomers are produced.

4.1.2 Total glycerol conversion

The conversion of glycerol to polyglycerols, and other by-products, was studied as a function of catalyst concentration (1 – 6 wt%) and temperature (130 – 160 °C). This was to understand the reaction before incorporating to biodiesel. Using H_2SO_4 as catalyst, the kinetics was determined to understand the rate of the reaction. The products were characterised using HPLC. Some typical chromatograms are shown in *Figure **4-1***:

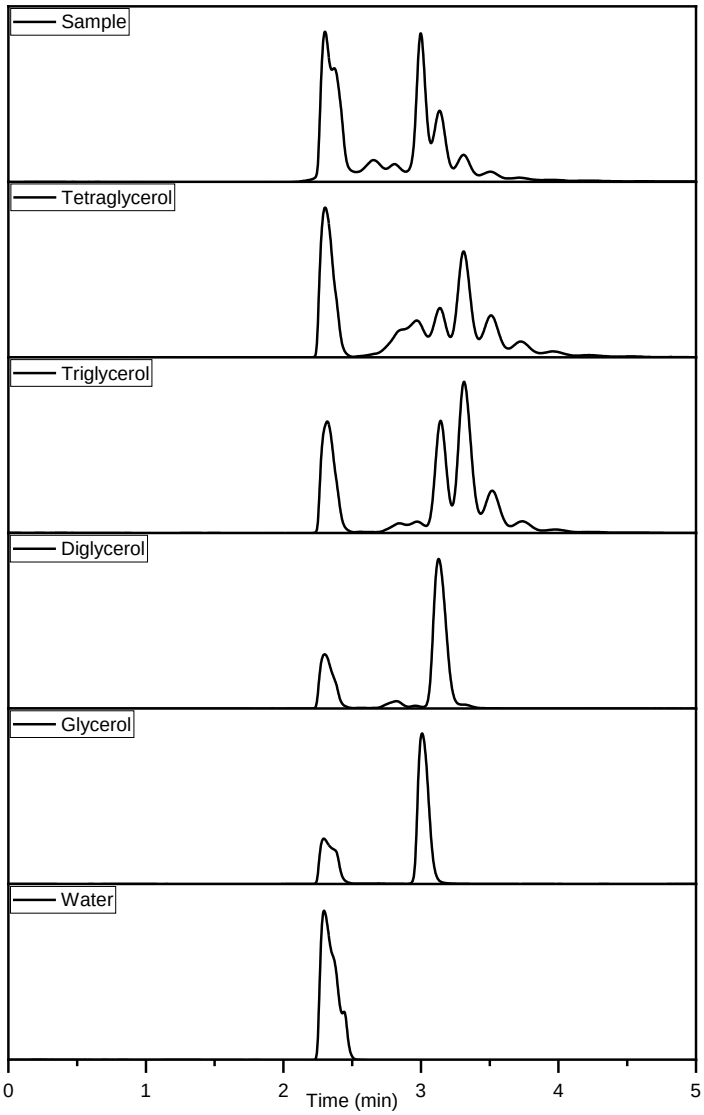

Figure 4-1: HPLC of spectrum of standard samples and polymerised sample.

Distilled water, glycerol and polyglycerols used as standards were analysed with HPLC using the method described in section 3.2.3.2. The experimental polyglycerol samples were analysed using the same method. The water appears at 2.3 min while glycerol has a retention time of 3.0 min. Diglycerol, triglycerol, and tetraglycerol appear at 3.1, 3.3 and 3.5 min, respectively. Calibration curves for the glycerol, diglycerol, triglycerol, and tetraglycerol were plotted as shown in *Figure A-* ***1*** to *Figure A-* ***4*** of appendix A. Areas from the peaks were determined and matched to the calibration curve to obtain the concentration. Conversion and selectivity were determined as shown in equation 3.1 – 3.4.

Figure ***4-2*** below shows the conversion of glycerol, as a function of catalyst concentration (1, 2, 3 and 6 wt% H_2SO_4), time (up to 5 h) and temperature (130, 140, 150, and 160 °C).

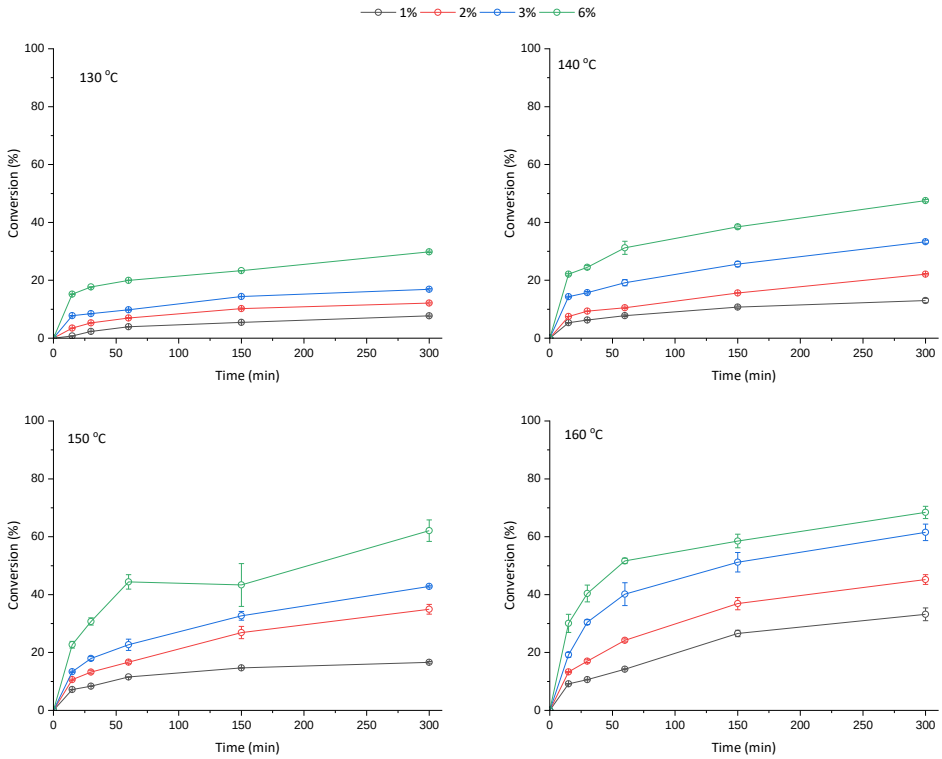

Figure 4-2: Glycerol conversion at (a) 130 °C (b) 140 °C (c) 150 °C and (d) 160 °C at various catalyst concentration.

Clearly, conversion increases monotonically with time, temperature, and catalyst concentration, as might be expected. At the lowest reaction temperature used (130 °C), between 7 and 30% glycerol conversion was achieved. Increasing the temperature to 140 °C, the conversion increased (13 – 47%). When the reaction was set at 150 and 160 °C, the conversions increased from 16 – 62% and 33 – 68%, respectively. The highest glycerol conversion within this parameter space (68%) was obtained at 160 °C, 6 wt% catalyst concentration, and 5 h. This is slightly lower than the 72% conversion reported by Salehpour and Dubé (2011) at 140 °C for 4 h with 4.8 wt% catalyst concentration, but this is due to their constant removal of the product water using Dean-Stark apparatus. The result is also lower than 79% reported by Sayoud et al. (2015) at 150 °C and 5 h. However, they used various triflate homogenous acid catalysts, which are also referred to as superacid.

4.1.3 By-products

The decomposition and dehydration side reactions, which produce hydrogen/CO and acrolein, respectively, at must account for about 2.4% of the total yield and broadly increase with time, temperature, and catalysts concentration (see *Figure **4-3*** to *Figure **4-6***), as expected. This side-products might explain why the samples are dark brown in colour. Hasenhuettl (2019) reports that the side-products are favoured over the etherification of glycerol at higher temperatures. Garti et al. (1981) reported that side products such as acrolein and other condensation products are produced by oxidation when there is a trace of acid or oxygen in the reaction. Both sources (Hasenhuettl, 2019, Garti et al., 1981) state that side-products caused the final products dark colour.

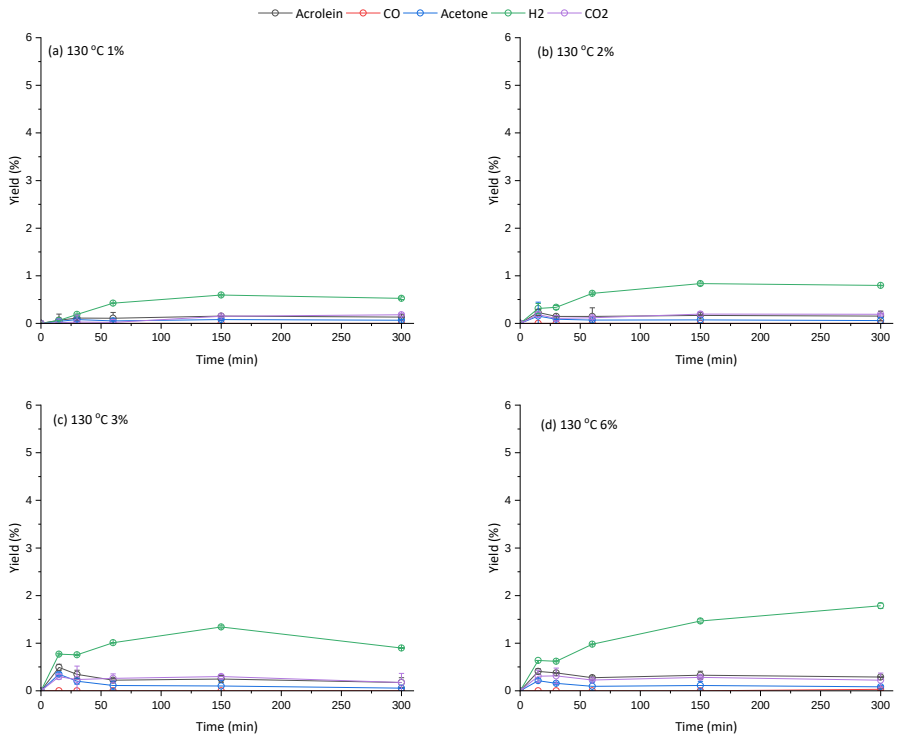

Figure 4-3: Yield of various by-products produced at 130 °C with (a) 1 wt% (b) 2 wt% (c) 3 wt% and (d) 6 wt% catalyst concentration.

*Figure **4-3*** shows the by-products yield at 130 °C with various catalyst concentration (1, 2, 3, and 6 wt%) for up to 5 h. At the lowest temperature (130 °C) used, the by-product of the reaction was hydrogen, carbon dioxide, acrolein, and acetone. The yield of hydrogen produced increased from 0.5% with 1 wt% to 1.7% when the concentration was increased to 6 wt%. Acrolein also increased from 0.2% to 0.3% as the catalyst

concentration increased from 1 to 6 wt%. Carbon dioxide was within the same range within acrolein, while the only trace of the carbon monoxide was obtained at this temperature. The yield of by-product at these conditions was clearly observed to be low. However, it increases with an increase in catalyst concentration and time as expected.

The reaction temperature was increased to 140 °C at various catalyst concentration (1 – 6 wt%). The yield obtained for the by-product is shown in *Figure **4**-**4***.

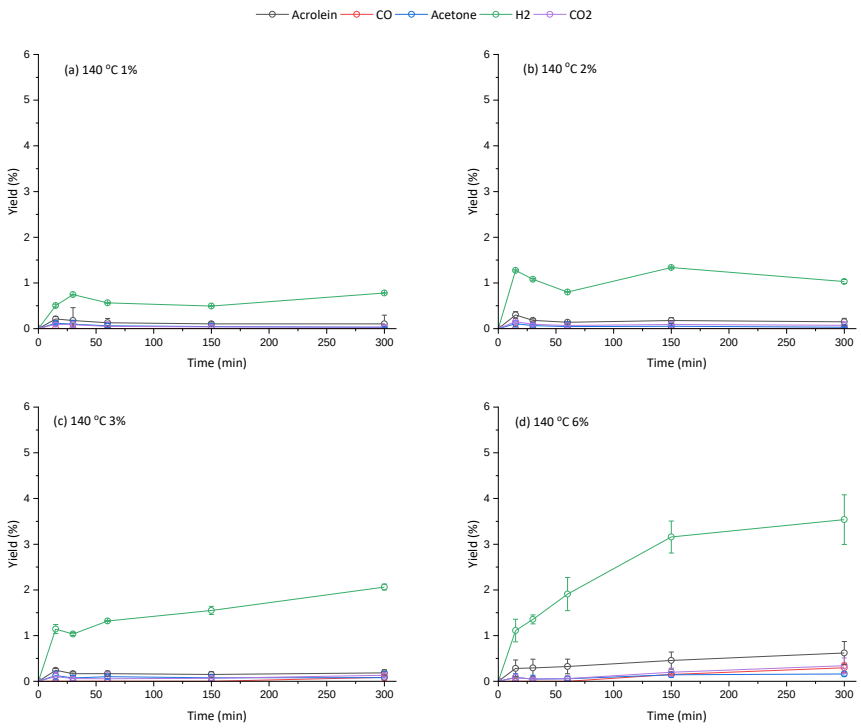

Figure 4-4: Yield of various by-products produced at 140 °C with (a) 1 wt% (b) 2 wt% (c) 3 wt% and (d) 6 wt% catalyst concentration.

The yield of hydrogen increased from 0.8 to 3.5% as the catalyst concentration was increased from 1 to 6 wt%, respectively. This is higher than the yield of hydrogen obtained at 130 °C. Acrolein is the next highest by-product produced after hydrogen. The highest yield of acrolein obtained with 140 °C was 0.6%, which is higher than 0.3% obtained at 130 °C. On the other hand, the yield of carbon dioxide at 140 °C was approximately 0.3%, similar to the yield obtained at 130 °C. Although a trace amount of carbon monoxide was recorded at 130 °C, the yield increased to 0.3% at 140 °C. All the by-product increases with an increase in both time and catalyst concentration.

As the reaction temperature was increased to 150 °C at various catalyst concentrations (1 – 6 wt%), the by-product yields were also affected. *Figure **4-5*** shows the yield of the by-products at 150 °C.

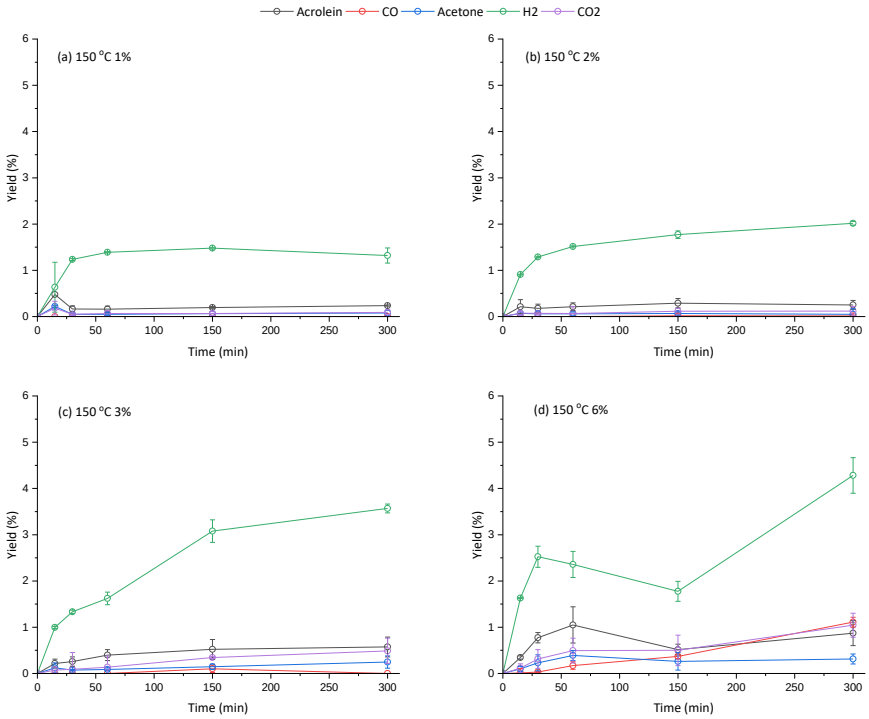

Figure 4-5: Yield of various by-products produced at 150 °C with (a) 1 wt% (b) 2 wt% (c) 3 wt% and (d) 6 wt% catalyst concentration.

As expected, the same by-products produced at 130 and 140 °C were produced at 150 °C. Hydrogen recorded the highest yield of 4.3% with 6 wt% catalyst concentration. This is the highest yield of hydrogen with all the temperatures considered in this research. The highest yield of acrolein (0.9%) obtained at 150 °C is obtained with 6 wt% catalyst concentration. This is slightly higher than 0.6% obtained with 140 °C. Just as hydrogen, the highest yield of acrolein in this research was obtained with 150 °C. This shows that the highest acrolein as a by-product that can be produced from this reaction is less than 1% due to the nitrogen environment the reaction was subjected. The yields of both carbon oxides (CO_2 and CO) are the same as when the reaction was conducted at 140 °C. However, there is an increase from 0.3% at 140 °C to 1% at 150 °C. Another by-product produced is acetone. However, the yields with 130 and 140 °C were in trace quantity. At 150 °C, the highest yield of 0.3% was obtained. This indicates that the by-

products in this reaction are favoured must with a temperature of 150 °C while catalyst concentration and time are varied.

The temperature was increased to 160 °C using catalyst concentrations of 1, 2,3, and 6 wt% with a reaction time of up to 5h. The yields of the by-product are shown in *Figure **4-6***.

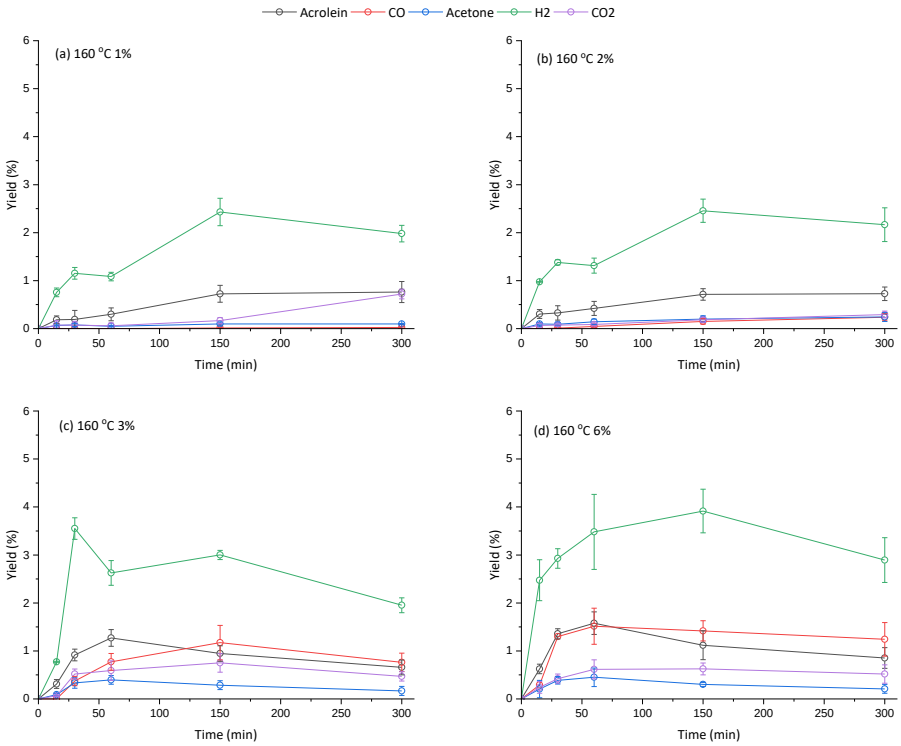

Figure 4-6: Yield of various by-products produced at 160 °C with (a) 1 wt% (b) 2 wt% (c) 3 wt% and (d) 6 wt% catalyst concentration.

A decrease in hydrogen yield was observed at 160 °C. The highest yield of hydrogen produced at 160 °C was 3.9% after 2.5h. A decrease to 2.9% was observed when the reaction was allowed for 5h. Similarly, the yield of carbon dioxide, acrolein, and acetone decrease to 0.5%, 0.8% and 0.2% respectively, as the highest with 160 °C. Carbon monoxide was the only by-product that slightly increased in yield to 1.2% at 160 °C, compared to 1% at 150 °C. Generally, this indicates that the by-products yield decreases at a temperature beyond 150 °C after 5h. This is because, at a higher temperature, the conversion of the feedstock is towards polyglycerols production. The concentrations of acrolein were low. It is not the desired product for this reaction. Hence, the reaction was blanketed using nitrogen gas to minimise the condensation reaction that produces acrolein.

4.1.4 Effect of Process Variables

The variables considered were the catalyst concentration (1, 2, 3, and 6 wt%), temperature (130, 140, 150 and 160 ^{o}C), and time (up to 5 h). The catalyst (sulfuric acid) concentration used was from 1 – 6 wt% of the glycerol feed. The range chosen was within that used by other investigators. The reaction temperature for this work was 130 – 160 ^{o}C. This value is low compared to the previous literature (Anuar et al. (2013) – 240 ^{o}C; Ardila-Suárez et al. (2015) – 130 to 170 ^{o}C; Ayoub and Abdullah (2013a) – 240 ^{o}C; Barros et al. (2017) – 200 to 245 ^{o}C) which generally used temperatures around 240 ^{o}C, especially when the alkaline or heterogeneous catalyst was used (Ayoub et al. (2014) – LiOH and Li-ZeY; Nguyen et al. (2017) – K_2CO_3; Bookong et al. (2015) – Na_2CO_3). Since this research was to incorporate transesterification later, the reaction was limited to 5h. This is because longer reaction time will not be economically viable for biodiesel production. However, Nosal et al. (2015) reported that low catalyst concentration and short reaction time would favour the production of diglycerol and triglycerol.

4.1.4.1 Catalyst Concentration

*Figure **4-7*** below shows the effect of catalyst concentrations (1, 2, 3, and 6 wt%) on polyglycerol oligomers production.

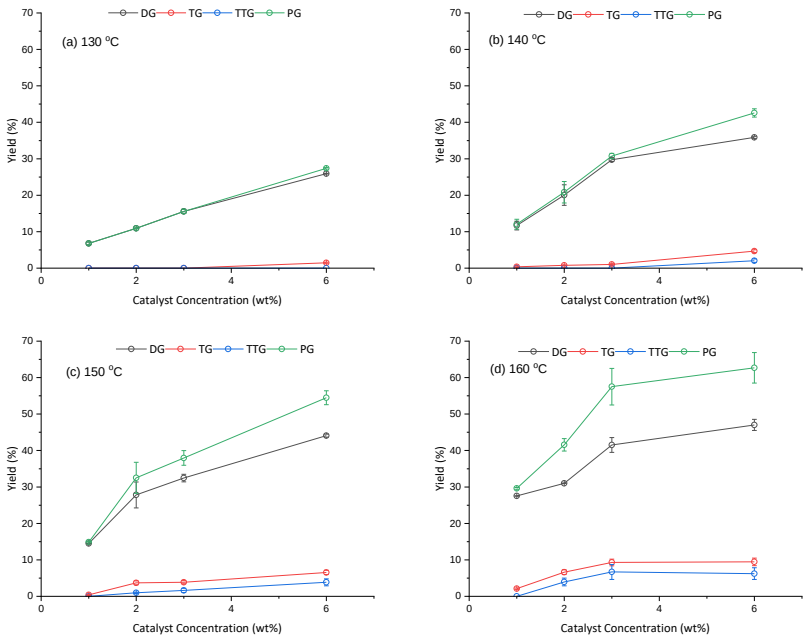

Figure 4-7: Yield of polyglycerol produced after 5 h with (a) 130 ^{o}C (b) 140 ^{o}C (c) 150 ^{o}C and (d) 160 ^{o}C and various catalyst concentration (1, 2, 3, and 6 wt%).

The yield of polyglycerol increased with increasing catalyst concentration (*Figure **4**-**7***). The highest polyglycerol yield obtained here was 62.7%, achieved at 6 wt% catalyst concentration, at 160 °C after 5 h (*Figure **4**-**7***). The product was 47% diglycerol, 9.4% triglycerol, and 6.2% tetraglycerol. At 3 wt%, the total polyglycerol yield was 58%, 42% of which was diglycerol, 9% triglycerol and 7% tetraglycerol. Using 2 wt% catalyst concentration, the total polyglycerol yield was 42%. The oligomers include 31% diglycerol, 7% triglycerol, and 4% tetraglycerol. As expected, the increase in polyglycerol yield as catalyst concentration increases is due to the fast conversion of the glycerol feed to the desired product.

One of the advantages of using sulphuric acid as the catalyst for glycerol etherification is that it can be used at relatively low temperatures (130 – 170 °C). On the other hand, base catalysts require temperatures of 220 – 270 °C (Galy et al., 2017, Shikhaliev et al., 2016, Nosal et al., 2015, Bookong et al., 2015). However, acid catalysts also promote dehydration; hence, the acrolein yield increases with increasing catalyst concentration and turns the final product dark.

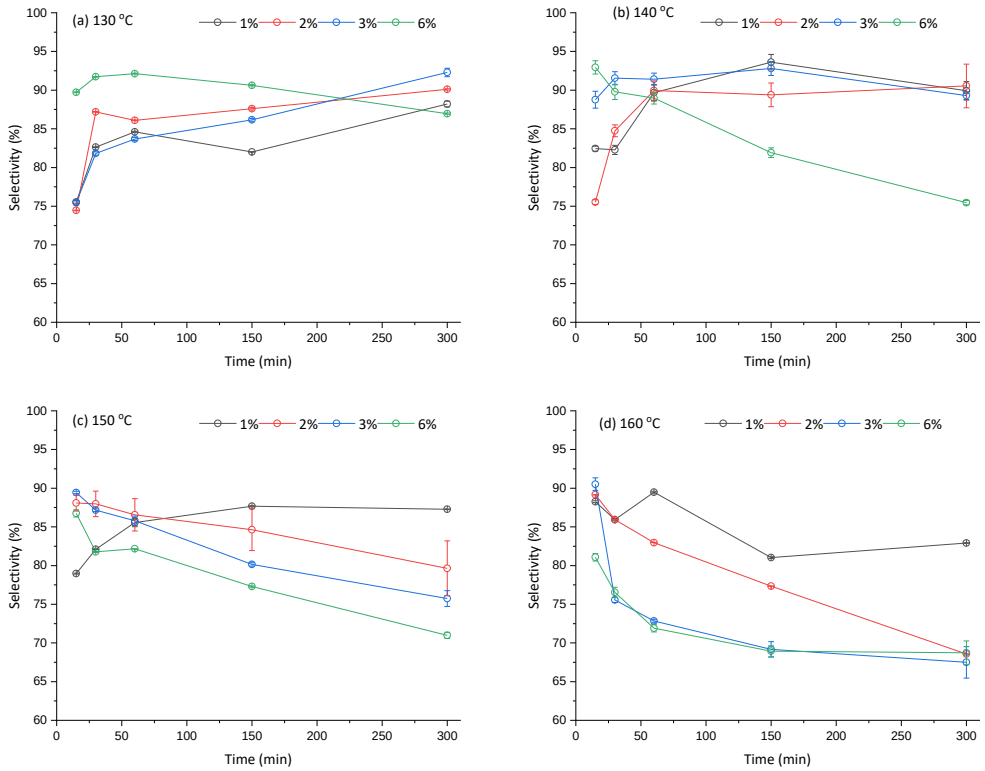

Figure 4-8: Selectivity for diglycerol (a) 130 °C (b) 140 °C (c) 150 °C and (d) 160 °C at 1, 2, 3, and 6 wt% H_2SO_4.

The selectivity to diglycerol formation was generally approximately 90% (*Figure **4**-**8***). A 20% decrease in the selectivity to diglycerol was observed when the catalyst concentration increased due to the conversion of the diglycerol to higher polyglycerols and the direct conversion of glycerol to other side products. Hence, the minimum selectivity to diglycerol was approximately 70%. The yield of higher oligomers increased as the catalyst concentration increased. Catalyst concentrations above 3% produce higher polymers and other, undesirable side products. This may be why previous researchers (Barros et al., 2017, Ayoub and Abdullah, 2013a, Anuar et al., 2013) used 2 wt% catalyst concentrations. However, none of the previous authors reported hydrogen produced among the by-products. They constantly condense the vapour and remove the water produced using a Dean-Stark apparatus from the reaction.

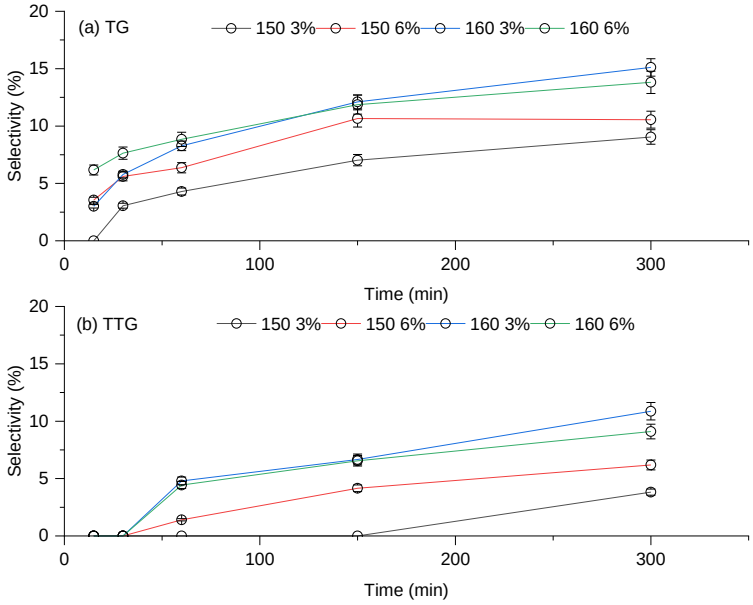

Figure 4-9: Selectivity at various temperature and catalyst concentration for (a) TG and (b) TTG.

The selectivity to higher polyglycerol production (triglycerol and tetraglycerol) is ~10% at 150 and 160 ^{o}C (see *Figure **4**-**9***). The other by-products totalled ~12%.

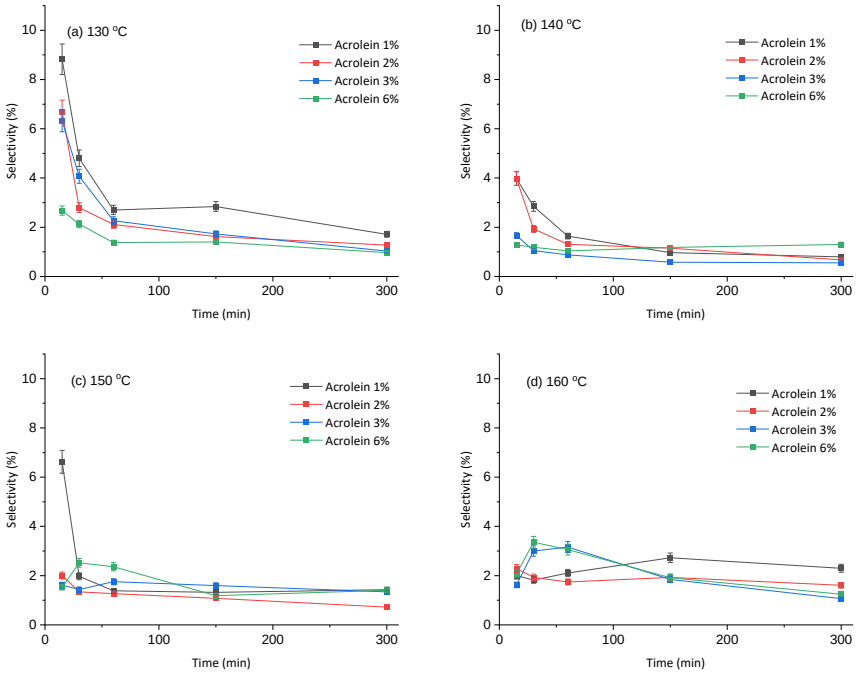

Figure 4-10: Selectivity of acrolein with various catalyst concentration for (a) 130 °C (b) 140 °C (c) 150 °C (d) 160 °C.

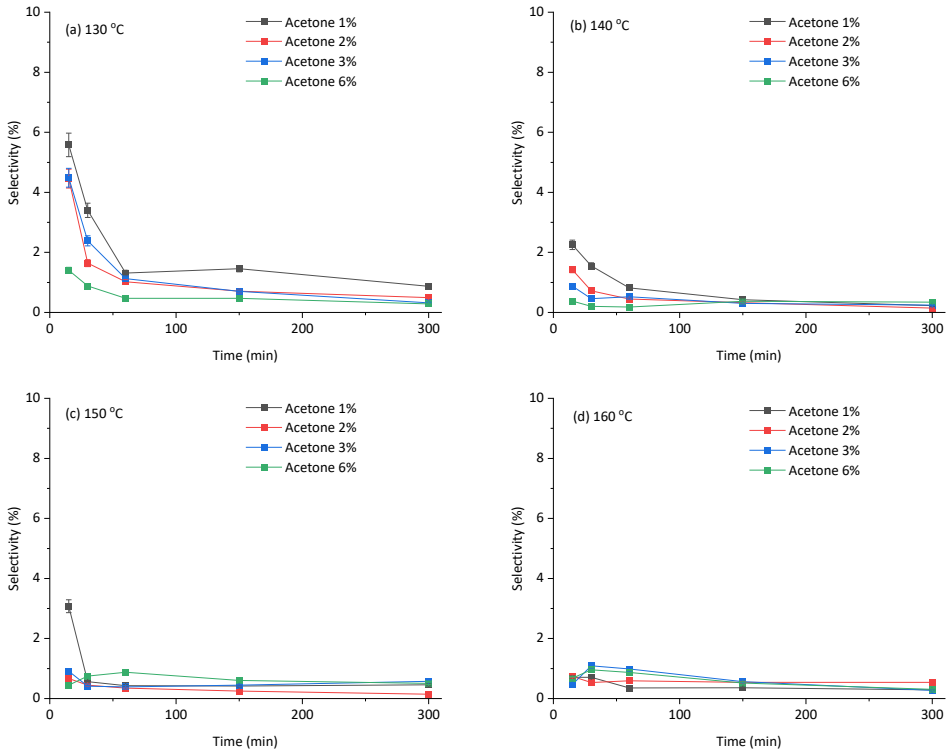

Figure 4-11: Selectivity of acetone with various catalyst concentration for (a) 130 °C (b) 140 °C (c) 150 °C (d) 160 °C.

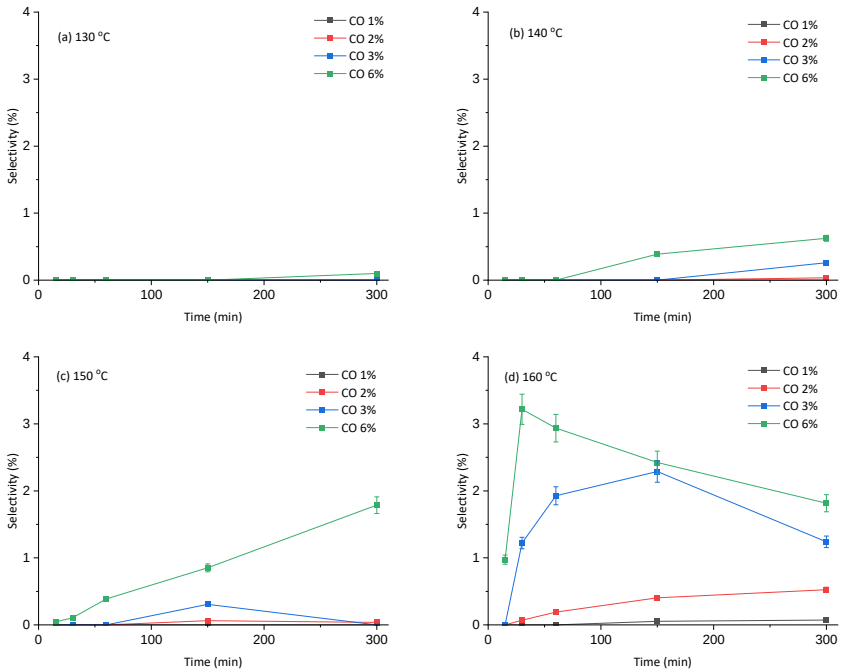

Figure 4-12: Selectivity of CO with various catalyst concentration for (a) 130 °C (b) 140 °C (c) 150 °C (d) 160 °C.

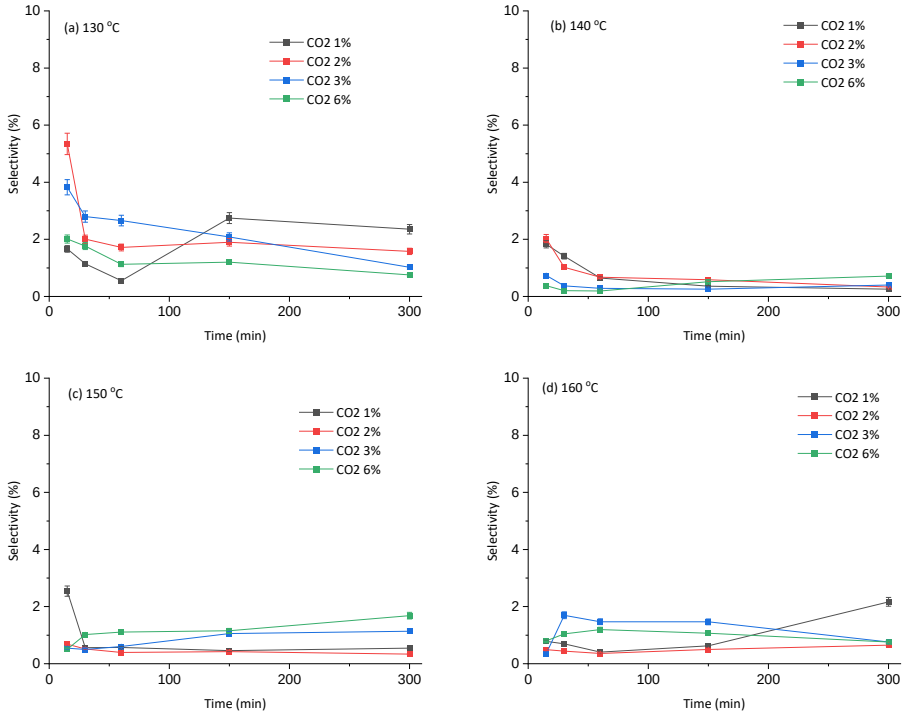

Figure 4-13: Selectivity of CO_2 with various catalyst concentration for (a) 130 °C (b) 140 °C (c) 150 °C (d) 160 °C.

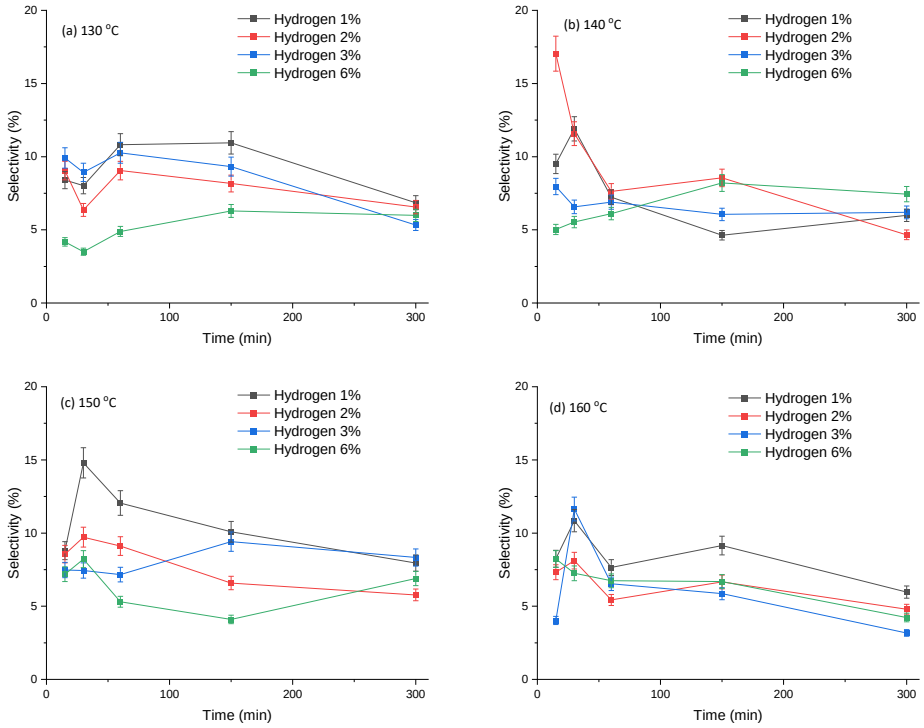

Figure 4-14: Selectivity of hydrogen with various catalyst concentration for (a) 130 °C (b) 140 °C (c) 150 °C (d) 160 °C.

Acrolein accounted for about 2% selectivity (*Figure* ***4-10***), acetone 0.5% (*Figure* ***4-11***), and carbon oxides approximately 1.5% (see *Figure* ***4-12*** and *Figure* ***4-13***). Hydrogen was the abundant by-product with approximately 8% selectivity (see *Figure* ***4-14***). Clearly, the selectivity's were both catalyst and temperature-dependant, especially the higher oligomers production.

4.1.4.2 Time

Reaction time is another important variable in glycerol etherification. Generally, glycerol oligomerisation has been reported to be "slow" due to high viscosity of glycerol (Galy et al., 2017). Hence, reaction times of up to 24h have been used in previous studies (Clacens et al., 2002, Richter et al., 2008). Here, the total glycerol conversion and the total polyglycerol yield increased monotonically with time, as would be expected. However, the diglycerol selectivity was observed to peak, due to its conversion to higher oligomers. This agrees with previous research in this area (Krisnandi et al., 2008, Richter et al., 2008, Ayoub and Abdullah, 2013a). All the previous authors reported a monotonical increase with time as expected. Salehpour and Dubé (2011) used up to 7h

with H_2SO_4. The authors achieved the highest conversion of 72% after 4h with 4.8 wt% catalyst concentration. However, method used by Salehpour and Dubé (2011) removed water produced as the reaction proceeds using Dean-Stark apparatus.

*Figure **4-8*** shows the selectivity of diglycerol using a temperature range of 130 °C to 160 °C at catalyst concentration 1, 2, 3, and 6 wt% and time up to 300 min. The highest selectivity achieved was approximately 90% at 130 °C at various catalyst concentration (1, 2, 3, and 6 wt%). The lowest selectivity of the diglycerol was 68% at 160 °C after 300 min. The selectivity decreases with an increase in time and temperature. This is due to an increase in production of both the higher oligomers and other by-products.

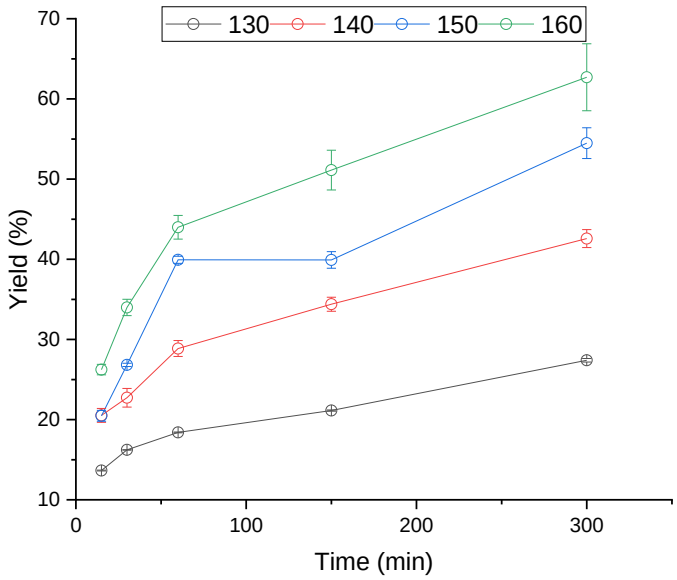

Figure 4-15: Yield of polyglycerol produced at various temperature and reaction time.

*Figure **4-15*** shows the effect of time at 6 wt% catalyst concentration and temperature of 130 – 160 °C. The reaction time considered was from 150 to 300 min. As expected, the yield of polyglycerol produced increases from 150 to 300 min. The highest yield obtained was 62% at 160 °C after 300 min. Lowest yield (26%) was achieved using 130 °C after 300 min. The low yield is associated with the high viscosity of the feedstock.

Anuar et al. (2013) reported that long reaction time with heterogeneous catalysts was due to glycerol viscous nature, diffusing into the pores of the catalyst. Anuar et al. (2013) used hydrotalcite heterogeneous catalysts to achieve 77% conversion after 960 min with 240 °C reaction temperature to reduce the reaction time and energy requirement.

Ayoub and Abdullah (2013a) reported about 80% glycerol conversion after 120 min and 100% after 240 min with LiOH. In contrast, 720 min was used with an acid-treated heterogeneous catalyst (lithium-intercalated montmorillonite (clay Li/MK-10)) for complete conversion. They also reported that the micropores in zeolite-based catalysts shorten the reaction time due to their high activity. Generally, homogeneous acid catalyst converts glycerol faster due to their higher activity than the alkaline. While with heterogeneous catalysts, the low diffusion of glycerol into the catalyst pores makes the reaction slow.

4.1.4.3 Temperature

Reaction temperature above 200 ^{o}C has been reported for glycerol step-growth polycondensation with an alkaline catalyst. Salehpour and Dubé (2011) reported results at 140 ^{o}C with a different catalyst ($Ca(OH)_2$, $CaCO_3$, H_2SO_4, and p-Toluenesulfonic acid) but with lower conversion (7 – 72%) and reaction time (4 – 9h). In this research, the influence of the reaction temperature was observed from 130 – 160 ^{o}C. As expected, a high polyglycerol yield (62%) was produced at 160 ^{o}C (see *Figure **4**-**15***).

A similar trend was reported by Ardila-Suárez et al. (2015) with sulfuric acid as catalyst and temperature at 130 to 170 ^{o}C. Although the authors did not calculate conversion or yield, they determined the hydroxyl number of the product. The authors suggest that a lower hydroxyl number refers to higher polyglycerol production. As expected, 170 ^{o}C produced the lowest hydroxyl number. However, Ardila-Suárez et al. (2015) used glasswares and removed water using Dean-Stark, which differs from this research methodology. Galy et al. (2017) used 230 – 270 ^{o}C with potassium carbonate as a catalyst. The authors reported increased in the high degree polyglycerols as the temperature increased to 270 ^{o}C.

Generally, the sample becomes more viscous as the temperature increases (see *Table **4**-**1***). This is due to the step growth-polycondensation reported by previous authors (Galy et al., 2017, Nguyen et al., 2017, Salehpour and Dubé, 2011). However, as the viscosity increased with an increase in temperature, so was the darkness of the polyglycerol sample produced for this research. This is due to the acid catalyst used, which can easily trigger oxidation reaction with the glycerol feed to produce by-products such as acrolein (Garti et al., 1981, Salehpour and Dubé, 2011).

4.1.5 FTIR of the Polyglycerol Samples

Pure glycerol and commercial polyglycerols were analysed using FTIR spectroscopy as standard for this work (*Figure **4-16***). All experimental products analysed with the FTIR were compared with the standard.

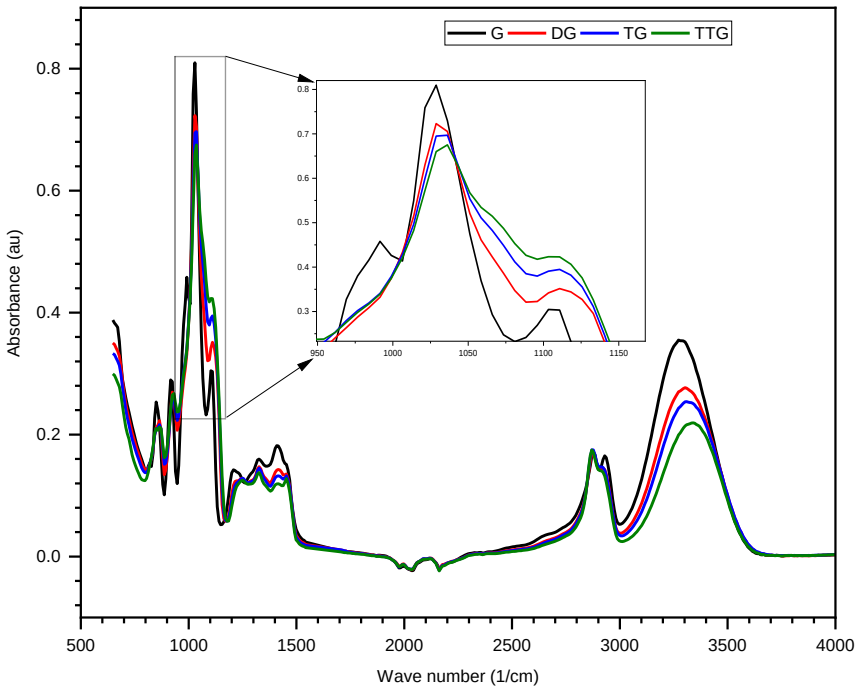

Figure 4-16: FTIR spectra of pure glycerol and commercial polyglycerols.

Clearly, FTIR spectra for the standards exhibit a decrease in the hydroxyl group (O – H bond) stretch in the range 3000 – 3400 cm^{-1} with an increasing degree of polymerisation, from glycerol to tetraglycerols. There are fewer hydroxyl groups per carbon atom, with an increasing polymerisation degree, leading to a reduced hydroxyl peak. This was in agreement with Ardila-Suárez et al. (2015) report that the hydroxyl number of glycerol is higher than that of the polymerised sample.

In previous research, the water produced during etherification is removed with the aid of a Dean-Stark apparatus and measured to determine the rate of conversion of the glycerol. Here, the water formed was not removed. The spectra peak becomes broad around 3000 to 3400 cm^{-1} with nearly flat surface when a high amount of water is present and the introduction of the H – O – H water scissors around 1630 cm^{-1} (as shown in *Figure **4-17***).

Mixtures of glycerol and water (% v/v) were produced and analysed using FTIR, to determine whether the –OH signal from each could be differentiated (*Figure **4-17***):

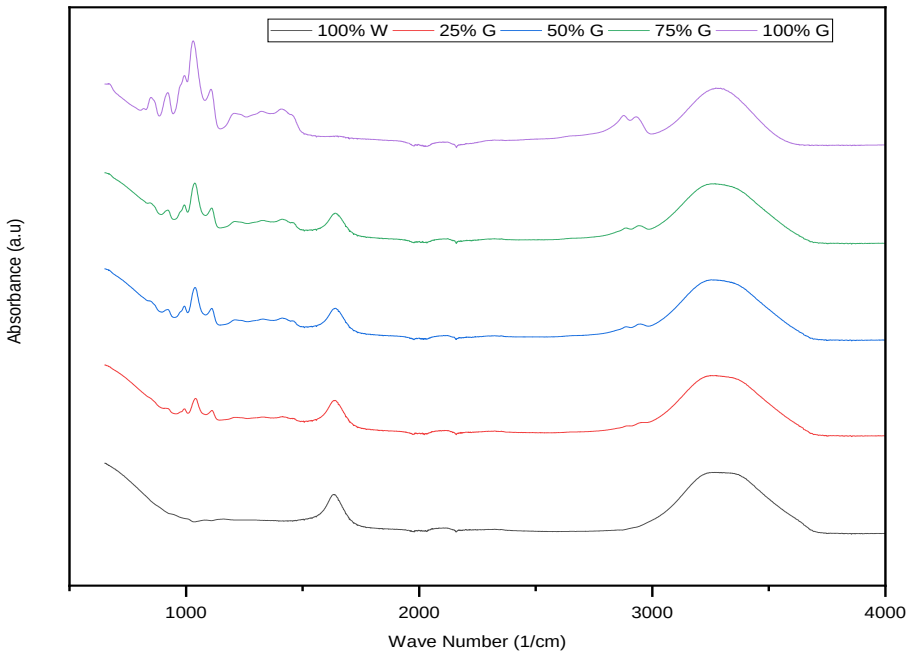

Figure 4-17: FTIR spectra of glycerol and water mixture.

A clear difference between the spectra of glycerol and water at 3000 – 3400 cm^{-1} was observed. At 100% water, the hydroxyl peak at 3000 – 3400 cm^{-1} was broad and flat at the top. The flat surface disappears as the percentage volume of glycerol increases in the mixture. The C – H stretch around 2850 – 3000 cm^{-1} was absent from the water spectrum (as expected), and as the glycerol in the mixture increased, the C – H stretch also increased. However, the water scissors around 1630 cm^{-1} were observed to reduce as the percentage of glycerol increases (*Figure **4-17***).

The polyglycerol produced from the etherification reactions were analysed using FTIR. *Figure **4-18*** below is the reaction at various catalyst concentrations, temperatures, and reaction time.

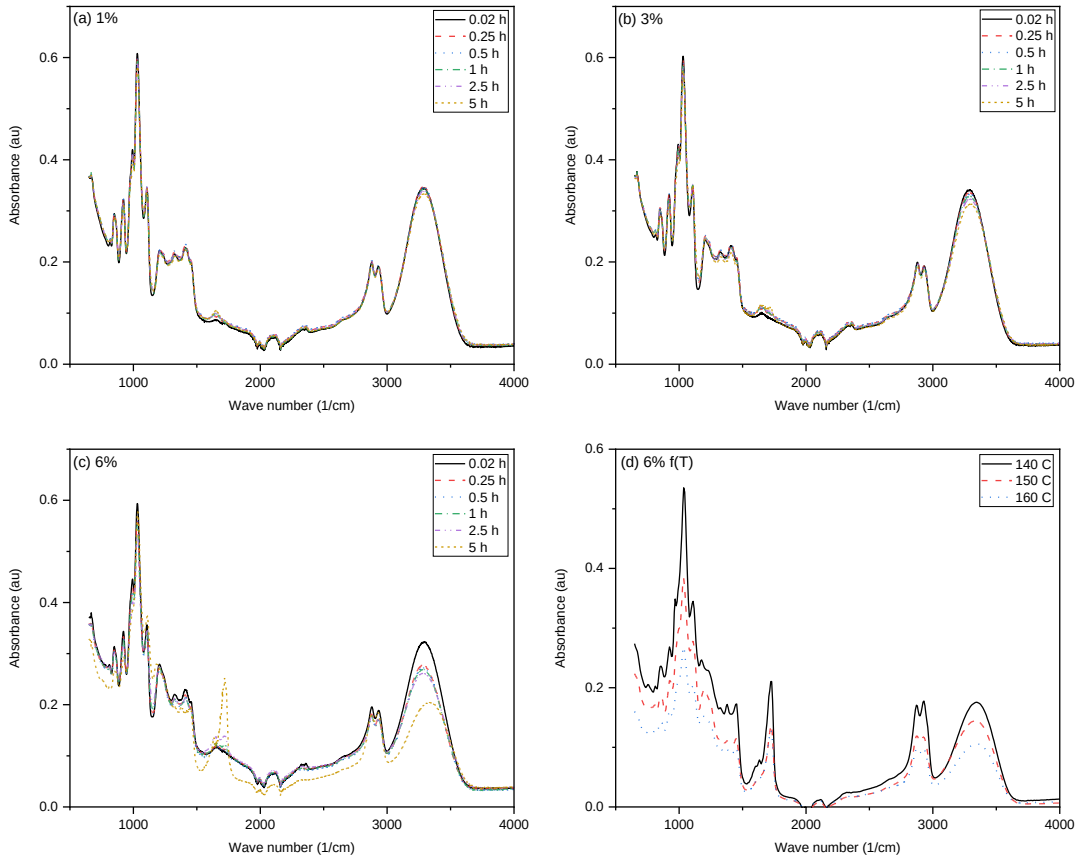

Figure 4-18: FTIR spectra of glycerol conversion with (a) 1% (b) 3% (c) 6% catalyst concentration and (d) solid residue at various temperature in nitrogen environment.

As the polyglycerols produced increased, all spectra exhibited a decrease in the hydroxyl group in the range of 3000 – 3400 cm^{-1} wavenumber (*Figure **4-18***). The decrease was also observed with increased catalyst concentration and temperature. This further confirmed the interaction between the variables in this reaction. The ether group with C – O – C stretch appears around wave number 1100 cm^{-1} increases from glycerol to polyglycerol (as shown in *Figure **4-16*** and *Figure **4-18***). The increase in ether group peak is accompanied by the hydroxyl group's disappearance (O – H) and the C – O stretch at wave number 1000 cm^{-1}.

Also, the appearance of the H – O – H scissor at 1630 cm^{-1} and aldehyde group (C = O) at 1715 cm^{-1} indicates the presence of water and acrolein, respectively. Though the peaks areas are small, it was observed to increase as temperature and catalyst concentration was increased. The aldehyde bond was more pronounced at a catalyst concentration of 3 and 6%.

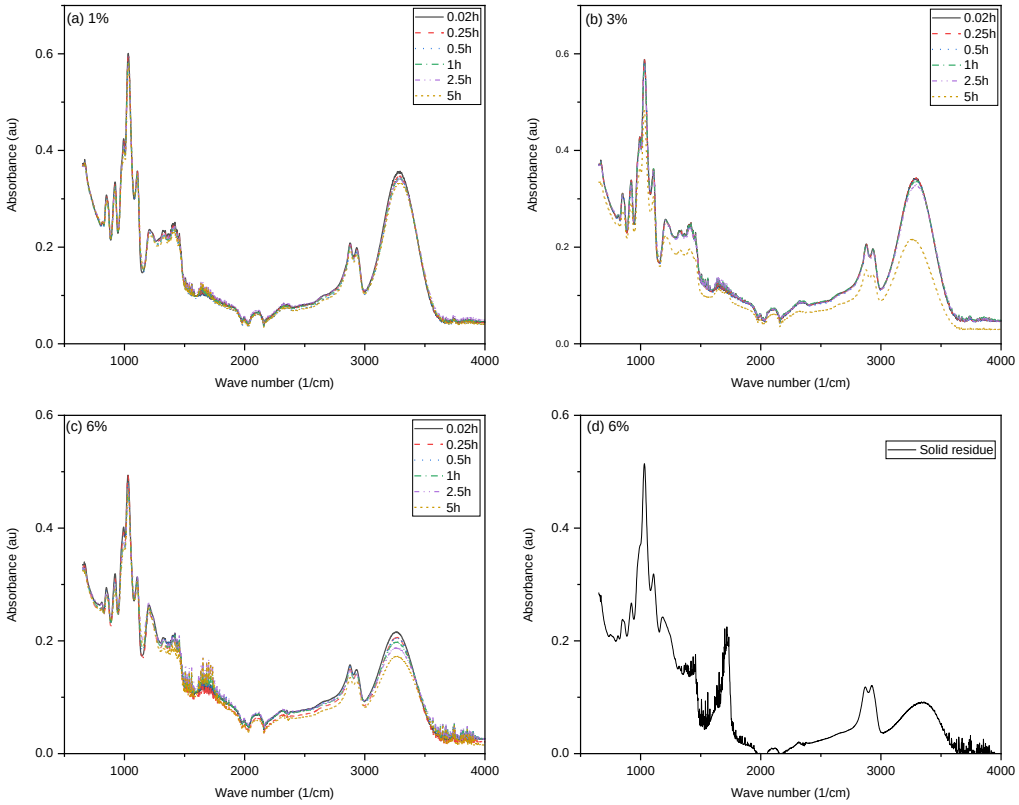

Figure 4-19: FTIR spectra of glycerol conversion with (a) 1% (b) 3% (c) 6% catalyst concentration and (d) solid residue in air.

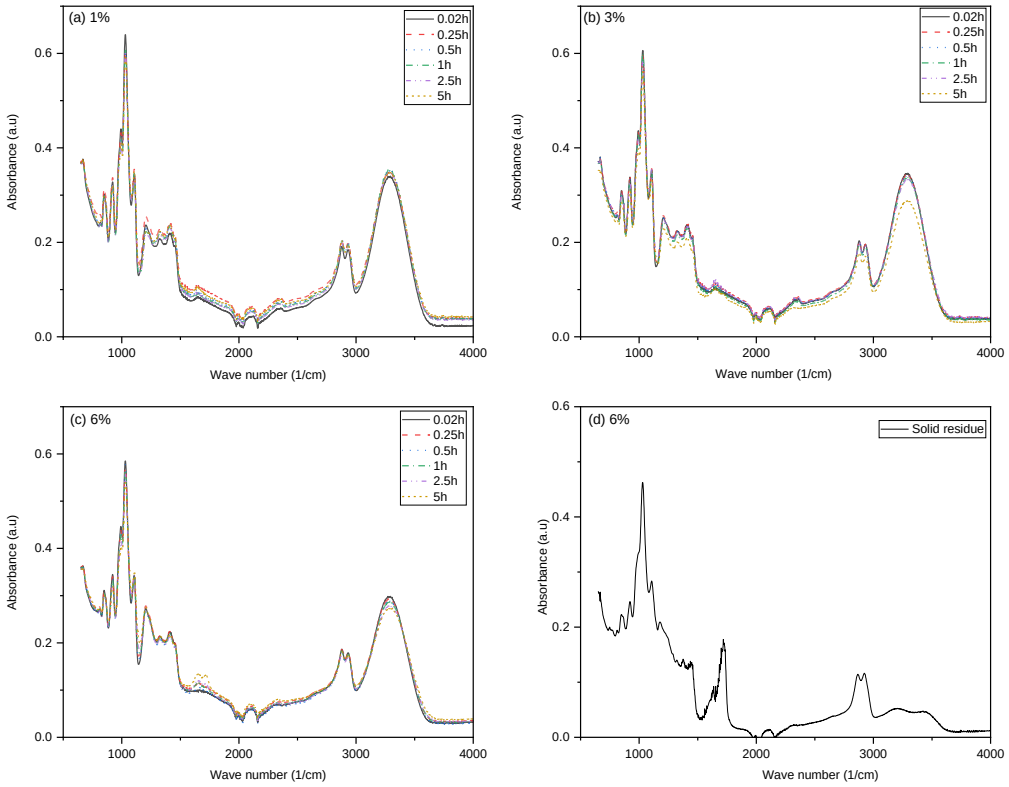

Figure 4-20: FTIR spectra of glycerol conversion with (a) 1% (b) 3% (c) 6% catalyst concentration and (d) solid residue in helium environment.

The reaction was also performed in air and helium environment (*Figure **4-19*** and *Figure **4-20***). Though a higher reduction of the C – O – C was observed in the helium environment than nitrogen, the gas cost is high. And when the air was used, the conversion to the desired product (polyglycerol) was low. This is due to the production of unwanted side products such as acrolein. The peak area at 1715 cm^{-1} (C = O) increases due to the oxidation of glycerol. This is in concomitance to the report of Garti et al. (1981) that reported the reaction to favour the production of acrolein when performed in an oxygen environment.

4.1.6 The Composition of the Solid Residue

*Figure **4-21*** below is the SEM images of the residual solid after the 5h glycerol etherification. The images are at various temperature (140, 150 and 160 ^{o}C) and 6 wt% catalyst concentration.

The solid residue is often produced after 2.5h and at higher (6%) catalyst concentration. The residue increases as the temperature of the reaction increase. There was no residue formed at 130 ^{o}C, though the polyglycerol yield was low as observed in the previous section. High catalyst concentration and temperature increase the residual solid, which is due to the pyrolysis of unreacted glycerol.

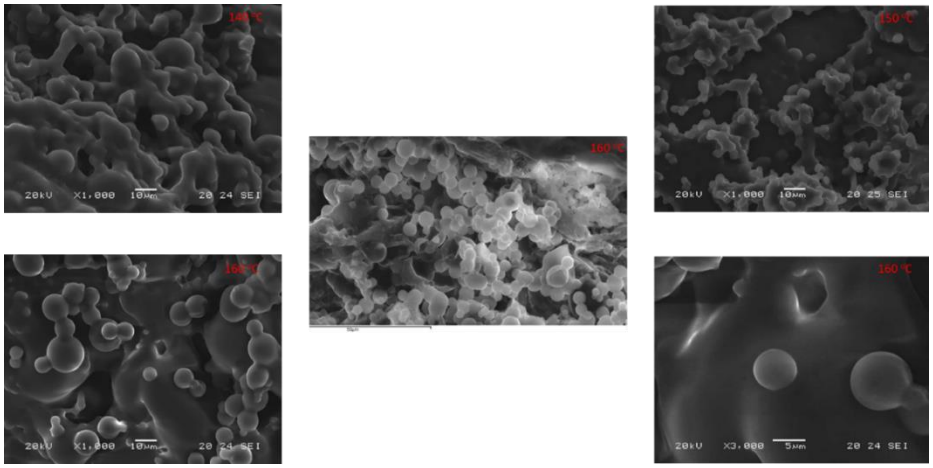

Figure 4-21: SEM image of the solid residue with 6% catalyst concentration.

The image of the carbonaceous material shows a spherical shape, which is probably carbon black (see also *Figure **4-22*** and *Figure **4-23***). Similar images were presented by Devi et al. (2014) when they hydrothermally produced the carbon sphere from glucose and water in a pressurised vessel. It was connected in chain form as reported by Zappielo et al. (2016) on carbon black SEM. Uniform spherical shapes were observed in the images (*Figure **4-21***). The spherical shape changes in its uniformity as the temperature increase to 160 ^{o}C.

The residue composition as the temperature increased is shown in *Figure **4-22*** and *Figure **4-23*** for EDX and CHON analysis, respectively. The composition might be different because the EDX determines the composition on the surface, while CHON analysed the internal part.

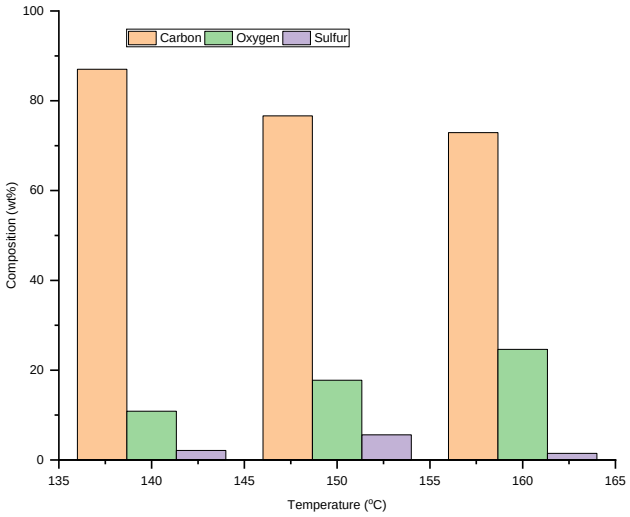

Figure 4-22: EDX analysis of the solid residue.

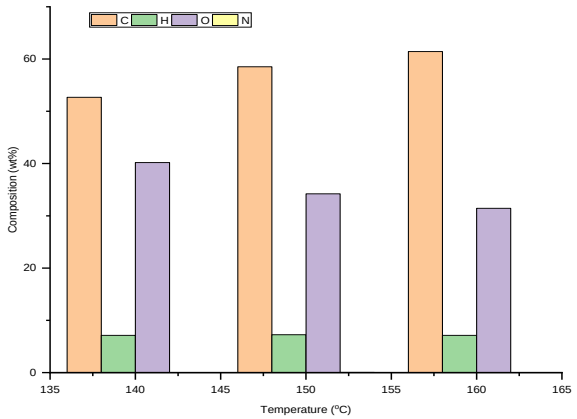

Figure 4-23: CHON analysis of the solid residue.

The residue shows a high percentage composition of carbon and is followed closely by oxygen. The EDX shows the residual solid contains 87 wt% carbon at 140 °C. The carbon composition decreases to 77 wt% at 150 °C and 73 wt% at 160 °C (*Figure **4-22***). The oxygen content increases (11, 18, and 25 wt%) with an increase in temperature (140, 150, and 160 °C). The composition indicates the presence of sulfur at 140 °C (2 wt%), 150 °C (6 wt%), and 160 °C (2 wt%). The presence of sulfur might be due to the catalyst (H_2SO_4) used for the reaction. Other metals (Al, Cr, Fe, and Ni) are obtained in trace amounts (less than 1%) from the reactor.

The result using CHON analyser differs from the EDX. The highest carbon content was 61 wt% obtained at 160 °C. A decrease in the carbon composition decreases to 59 wt%

at 150 °C and 53 wt% at 140 °C. Only traces of nitrogen were obtained for all the products, while the hydrogen was 7 wt% for all the temperatures.

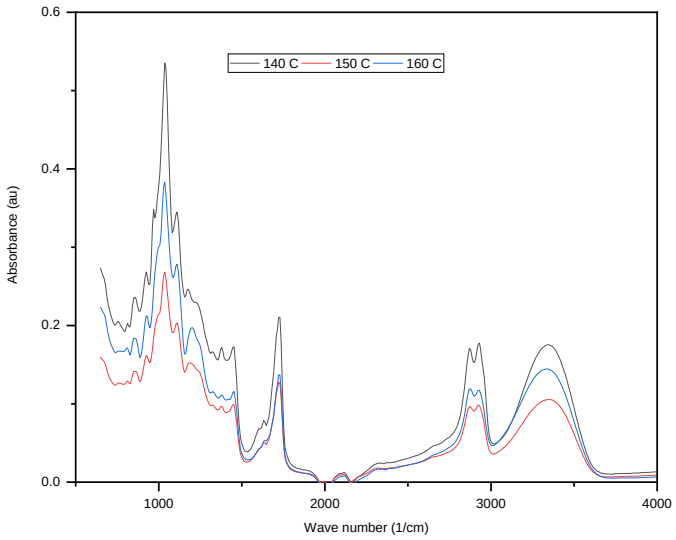

Figure 4-24: FTIR spectra of the solid residue.

FTIR of the solid residue was performed, as shown in *Figure **4**-**24*** above. The residues were formed at 140 – 160 °C and 6 wt% catalyst concentration. The SEM/EDX and CHON result corroborate to the FTIR spectra (*Figure **4**-**24***), which identify a decrease in the aldehyde (C=O) peak at wave number 1715 cm^{-1} as the temperature increase to 160 °C. The spectra are similar to polyglycerols but with a high content of the aldehyde group which might be due to the increase in the yield of acrolein in the final products (see *Figure **4**-**3*** to *Figure **4**-**6***).

4.1.7 Kinetics of Glycerol Valorisation

The rate of glycerol consumption using experimental data was determined. The kinetic equation was developed using the initial rate of 1h from the experimental data. The data fitted to the second-order rate law (see Appendix B *Figure B- **1***). This might be because the reaction was selective to the production of diglycerol. The plot of the natural logarithm of k_{obs} against the natural logarithm of catalyst concentration to determine the catalyst concentration order is shown in *Figure **4**-**25***(a) below. Also, the plot of the natural logarithm of k against the inverse of temperature in kelvin to determine activation energy (E_a) and pre-exponential value (A) from the Arrhenius equation is

shown in *Figure* ***4-25***(b) below. *Table* ***4-2*** below shows the rate constant, the catalyst order, and R^2 obtained from *Figure* ***4-25***(a) at 130, 140, 150, and 160 °C.

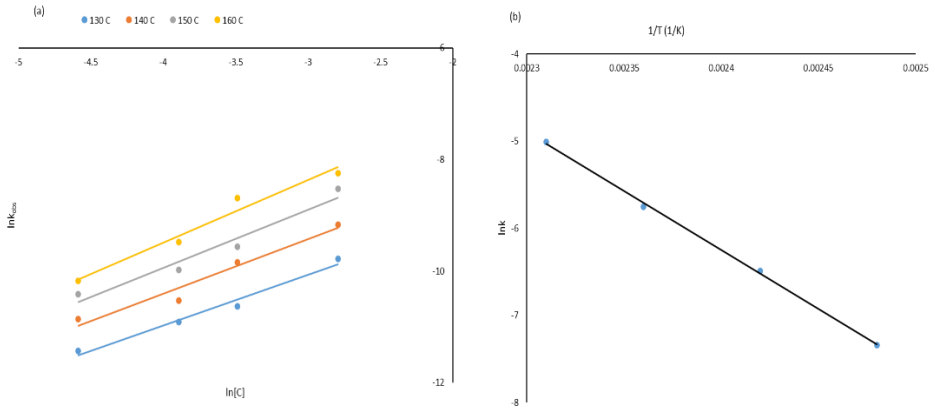

Figure 4-25: Determination of (a) order of catalyst (b) Arrhenius equation.

The intercept in *Figure 4-25*(a) for each temperature gives the natural logarithm of the rate constant (k) for the overall glycerol consumption. The plot at all the temperature used (130, 140, 150, and 160 °C) gives an approximate order of 1 for the catalyst concentration and R^2 of ≥ 0.95 (see *Table* ***4-2***). Where r is the reaction rate, k is rate constant, C_{GL} is the concentration of glycerol, C_C is the catalyst concentration, n is the order of the reaction to glycerol and m is the order of reaction to the catalyst. The activation energy (E_a) is 112.01 kJ·mol^{-1} and pre-exponential factor (A) of 2.18×10^{11} L·mol^{-1}·s^{-1}.

Table 4-2: Reaction rate constant and order of catalyst concentration at different temperature.

Temperature (°C)	**Rate Constant (L·mol^{-1}·s^{-1})**	**Catalyst order**	**R^2**
130	6.5×10^{-4}	0.94	0.98
140	1.5×10^{-3}	1.03	0.96
150	3.2×10^{-3}	1.01	0.95
160	6.7×10^{-3}	1.15	0.97

Hence, the rate equation can be simplified as:

$$r = 2.18 \times 10^{11} \times e^{\left(-\frac{112014.5}{8.314 \times T}\right)} \times {C_{GL}}^2 \times C_C \qquad 4.1$$

The equation was used with MATLAB R2020a for the simulation and the result compared to the experimental data. *Figure **4-26*** is the fitness of the model equation with the experimental data at various temperature (130, 140, 150, and 160 °C).

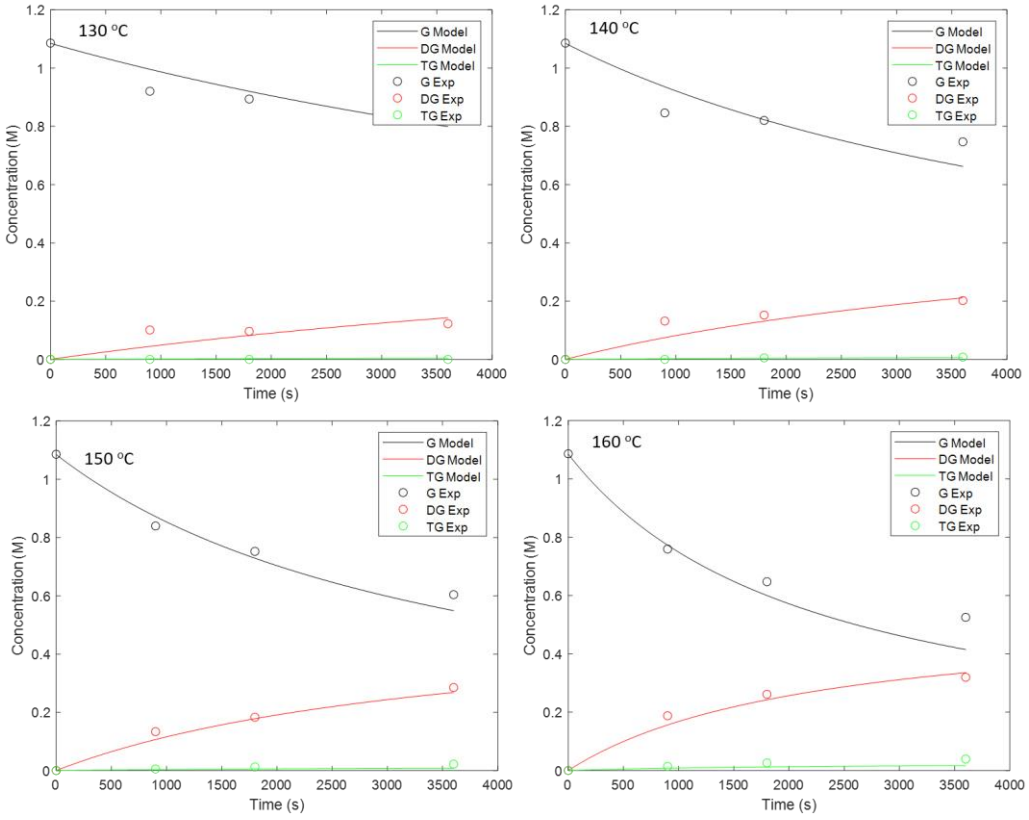

Figure 4-26: MATLAB simulation of the Arrhenius equation showing the consumption of glycerol and production of polyglycerol, comparing the model (line) and the experimental data (dot).

Where G Model is glycerol model, DG Model is diglycerol model, TG Model is triglycerol model, G Exp is glycerol (experimental data), DG Exp is diglycerol (experimental data), and TG Exp is triglycerol (experimental data). The equation correlates with the experimental values at 150 and 160 °C, as shown in *Table **4-3***. However, the model and experimental data lack good fitness at 130 and 140 °C. This might be due to low conversion with these temperatures and experimental data obtained. Although the reaction is fast with acid catalyst, the temperature of the reaction contribute immensely to the conversion of the feed to the desired products. Reactions were performed to

check the reversibility by reacting polyglycerol with water using the same conditions used for the reaction. The result did not produce any glycerol, rather increase the degree of polyglycerol. The correlation for triglycerol at 130 ^{o}C is undetermined. This is because no triglycerol was produced in the first hour of the reaction.

Table 4-3: Correlation of determination for the simulation of the kinetics of glycerol valorisation.

Temperature ^{o}C	**Correlation of determination (R^2)**		
	Glycerol	**Diglycerol**	**Triglycerol**
130	0.61	0.57	-
140	0.76	0.84	0.81
150	0.96	0.98	0.95
160	0.93	0.97	0.98

The equation developed will be used later in this research, together with the kinetic model for biodiesel production in the reactive coupling for the simultaneous production of biodiesel and glycerol valorisation.

The enthalpy (ΔH), entropy (ΔS), and Gibbs free energy (ΔG) can be determined in the glycerol etherification. From the Eyring-Polanyi equation, the rate of reaction was related to Gibbs free energy as shown in *Figure **4-27*** below.

$$k = \frac{K \times k_b \times T}{h} e^{\left(-\frac{\Delta G}{RT}\right)} \qquad 4.2$$

Where k = rate constant, K = transmission coefficient (≈1), k_b = Boltzmann constant (1.38 × 10^{-23} J·K^{-1}), h = Planck constant (6.63 × 10^{-34} J·s), T = absolute temperature (K) and R = gas constant (8.314 J·mol^{-1}·K^{-1}). Also, Gibbs free energy can be derived from:

$$\Delta G = \Delta H - T\Delta S \qquad 4.3$$

Substituting ΔG and rearranging (4.2),

$$\ln\left(\frac{k}{T}\right) = \ln K + \ln\left(\frac{k_b}{h}\right) - \frac{\Delta H}{RT} + \frac{\Delta S}{R} \qquad 4.4$$

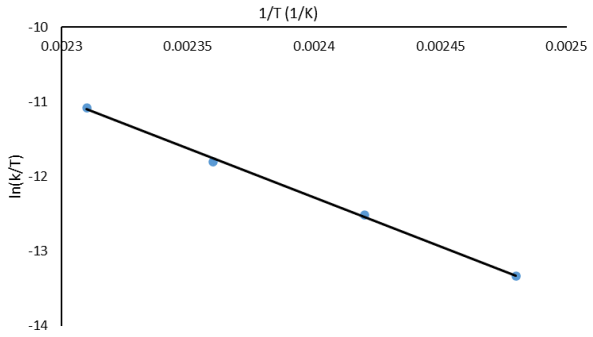

Figure 4-27: Determining the thermodynamic parameters using Eyring-Polanyi equation.

The plot of ln(k/T) against 1/T (*Figure **4-27***) produce an enthalpy of 109 kJ.mol^{-1} from the slope (– ΔH/R) and entropy of – 38.1 J·mol^{-1}·K^{-1} from the intercept (lnK + ln(k_b/h) + ΔS/R). The Gibbs free energy was determined from (4.4) as 124.3 kJ·mol^{-1} at 130 ^{o}C and 125.5 kJ·mol^{-1} at 160 ^{o}C.

The positive value of the enthalpy of activation means the reaction is endothermic. Clearly, this was expected as the reaction proceeds with an increase in temperature. The negative value of the entropy means the final product is less disordered than the reactant. This is also true when considering the increase in viscosity from glycerol to polyglycerol (see *Table **4-1***). The positive value of the Gibbs free energy indicates that the reaction is an endergonic (non-spontaneous) reaction, hence requires energy from the surroundings.

4.1.8 Summary of Glycerol Valorisation

The total glycerol conversion of 68% was achieved at 160 ^{o}C and 6 wt% catalyst concentration after 300 min. The conversion to polyglycerol increases with an increase in catalyst concentration and temperature. A temperature of 130 – 160 ^{o}C was sufficient for the polyglycerol production, although long reaction time is required for complete conversion due to high viscosity. The kinetics were fitted using second-order kinetics with an activation energy of 112.0 kJ·mol^{-1} and a pre-exponential factor of 2.2×10^{11} L·mol^{-1}·s^{-1}. Over 95% correlation was achieved at 150 and 160 ^{o}C. The thermodynamic properties show the reaction was endothermic with enthalpy

109 kJ·mol^{-1}, less disordered with an entropy of – 38.1 J·mol^{-1}·K^{-1}, and non-spontaneous with Gibbs free energy of 125 kJ·mol^{-1}.

4.2 Reactive Coupling

This section discusses the result of the simultaneous production of biodiesel and glycerol valorisation. First, some properties of the triglyceride and biodiesel produced were determined. The result for the conversion of triglyceride and the effect of process variables during reactive coupling. Finally, the kinetics of the reaction were fitted to the experimental value.

4.2.1 Properties of the Triglyceride Feed

Before and after the reaction, triglyceride physical properties include FFA, acid number, viscosity, density, and refractive index were determined. The results were compared with standards and previous literature, as shown in *Table **4-4*** below:

Table 4-4: Physical properties of triglyceride and biodiesel.

	FFA (%)	Acid number (mg·KOH·g^{-1} sample)	Density (g·cm^{-3})	Refractive index	Viscosity (Pa·s)
Triglyceride	0.2250	0.4500	0.9105	1.4729	0.0744
Biodiesel at 130 °C	0.0670	0.1340	0.8801	1.4585	0.0046
Biodiesel at 140 °C	0.0440	0.0880	0.8772	1.4587	0.0042
Biodiesel at 150 °C	0.0270	0.0540	0.8768	1.4586	0.0040
Biodiesel at 160 °C	0.0120	0.0240	0.8751	1.4589	0.0037
ASTM		0.80 max	-		0.0016 – 0.0054 [a]
EN			0.86 – 0.9		0.00301 – 0.0045 [a]
Geacai et al. (2012)			0.8840 0.8806 0.8823	1.4548 1.4545 1.4540	0.0041 [a] 0.0044 [a] 0.0041 [a]
Tesfa et al. (2010)			0.8793		0.0048[a]

[a] the literature value was converted from kinematic viscosity ($mm^2 \cdot s^{-1}$) to dynamic viscosity (Pa·s) using the density.

The FFA and the acid value of the triglyceride obtained from this research were 0.225% and 0.450 $mg \cdot KOH \cdot g^{-1}$ respectively. The FFA obtained from rapeseed oil used for this research was low compared to 0.65% reported by Konuskan et al. (2019) from virgin rapeseed oil. The low FFA might be due to possible purification of the triglyceride since it was purchased from a local store. High FFA effect includes high alcohol use during transesterification, soap production when an alkaline catalyst is used, and difficult separation (Berchmans and Hirata, 2008). After the reactive coupling, the acid number was between 0.13 to 0.02 $mg \cdot KOH \cdot g^{-1}$ which is lower than the 0.8 maximum stipulated by ASTM. This result implies with proper storage, the FAME produced will stay long without deteriorating.

Triglyceride has an adverse effect when used directly in the diesel engine due to its high viscosity. This causes poor atomisation and incomplete combustion in the engine (Gürü et al., 2010, Tesfa et al., 2010). To reduce the viscosity of triglyceride, various methods have been used (among which is transesterification). The transesterification of triglyceride removes the glycerol backbone, thereby decreasing the viscosity. *Table **4**-**4*** shows that the triglyceride (0.0744 Pa·s) is slightly lower to 0.0788 Pa·s reported by Noureddini et al. (1992b). However, the viscosity was reduced to 0.0048 – 0.0041 after transesterification. As expected, the low viscosity is due to the removal of glycerol from the triglyceride. The result was also in concomitance to the report by Tesfa et al. (2010) and Geacai et al. (2012) (see *Table **4**-**4***). The low viscosity of biodiesel improves the atomisation and combustion of the fuel in the diesel engine.

The refractive index can be used to determine the extent of transesterification. It also has a good relationship with both density and viscosity. The result shows a decrease in the refractive index from a triglyceride to biodiesel from 1.47 to 1.45, respectively. The reduction might be due to the reduction in both viscosity and density, as shown in *Table **4**-**4***. The refractive value of the FAME from this research is similar to the FAME reported by Geacai et al. (2012). The authors also used the refractive index to predict the density and viscosity of biodiesel.

The density is another essential property for both the triglyceride and biodiesel. It is used to determine the volume of fuel required during combustion (Verduzco, 2013). Noureddini et al. (1992a) and Sahasrabudhe et al. (2017) relate density to the mass transfer rate. Tesfa et al. (2010) reported that high density and viscosity of triglyceride leads to the clogging of the diesel engine through incomplete atomisation unless the engine is modified. The triglyceride density was 0.9105 $g{\cdot}cm^{-3}$, which is slightly higher than 0.9073 $g{\cdot}cm^{-3}$ reported by Noureddini et al. (1992a). After reactive coupling, the biodiesels densities decreased to 0.87 – 0.88 $g{\cdot}cm^{-3}$, which is in accordance with the report of Geacai et al. (2012) and Tesfa et al. (2010). The result was also within the 0.86 – 0.9 $g{\cdot}cm^{-3}$ EN standard.

*Figure **4-28*** below is the FTIR of the rapeseed oil used, FAME produced from the reactive coupling at 130 ^{o}C and various catalyst concentration (1, 2, and 3 wt%), and methanol before and after the reaction.

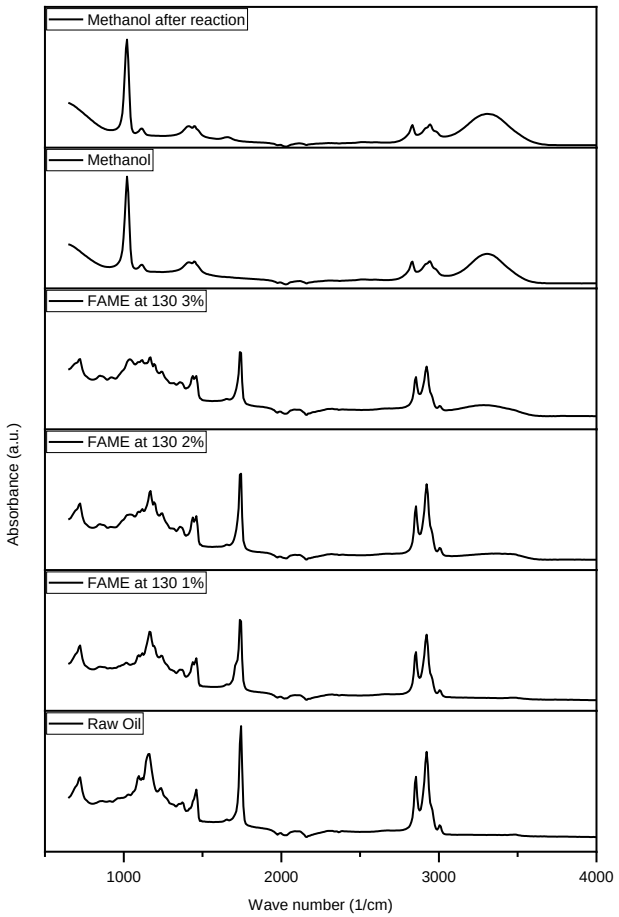

Figure 4-28: FTIR spectra of raw rapeseed oil, FAME from reactive coupling at 130 oC and methanol before and after the reaction.

Figure ***2-30*** shows rapeseed oil spectra, FAME produced with various catalyst concentration, methanol before and after the reaction. The spectra for both the rapeseed oil and FAME indicates an asymmetric and symmetric stretching vibration of -CH_2 and -CH_3 group at wave number 2914 and 2847 cm^{-1}, respectively. At 2 and 3 wt% catalyst concentration, a stretching and bending vibration of the hydroxyl group (-OH) was observed between 3056 – 3615 cm^{-1}. This might be due to the glycerol etherification that produced water in the process. Carbonyl group (C = O) with a strong peak at 1744 cm^{-1} appears in both rapeseed oil and biodiesel due to carbonyl group of vegetable oil. These were the same as the spectra reported by Nisar et al. (2017) for jatropha oil and biodiesel from jatropha oil.

The spectrum of the rapeseed oil is like that of FAME, with few differences. Peaks that appears in the rapeseed oil at 1103 cm^{-1} and 961 cm^{-1} disappears in the biodiesel spectra. Rabelo et al. (2015) reported the peak within 1103 cm^{-1} to be associated with the asymmetric axial stretching of O – CH_2, which is present in the oil. The appearance of -CH_3 group peaks at 1200 and 1430 cm^{-1} in the biodiesel confirmed the transesterification reaction of the triglyceride.

The reactive coupling can be observed with the appearance of the water molecules in the spectrum. The H – O – H water scissors were detected around 1640 cm^{-1} in the methanol after reaction but absent in the methanol before the reaction. This is due to the glycerol etherification reaction taking place simultaneously with the biodiesel production. This can also be confirmed with the appearance of a slight peak of the hydroxyl group between 3056 – 3615 cm^{-1} in the FAME spectra.

4.2.2 Total Triglyceride Conversion

Triglyceride was converted to biodiesel by varying reaction temperature (130, 140, 150, and 160 ^oC), catalyst concentration (1, 2, 3, 5 wt%), reaction time (up to 1h), and alcohol to oil mole ratio (4:1, 5:1, 6:1, and 8:1). H_2SO_4 was used for this research as catalyst. This is because the acid catalyst is fast in glycerol etherification, according to the study of Bookong et al. (2015) that reported homogeneous catalysts to have a higher conversion of glycerol though with low selectivity. However, Salehpour and Dubé (2011) specified acid catalysts to convert the glycerol among the homogeneous catalysts.

*Figure **4-29*** shows the chromatogram of biodiesel produced at various reaction times. While *Figure **4-30*** is FAME collected at an interval after separating the glycerol rich phase.

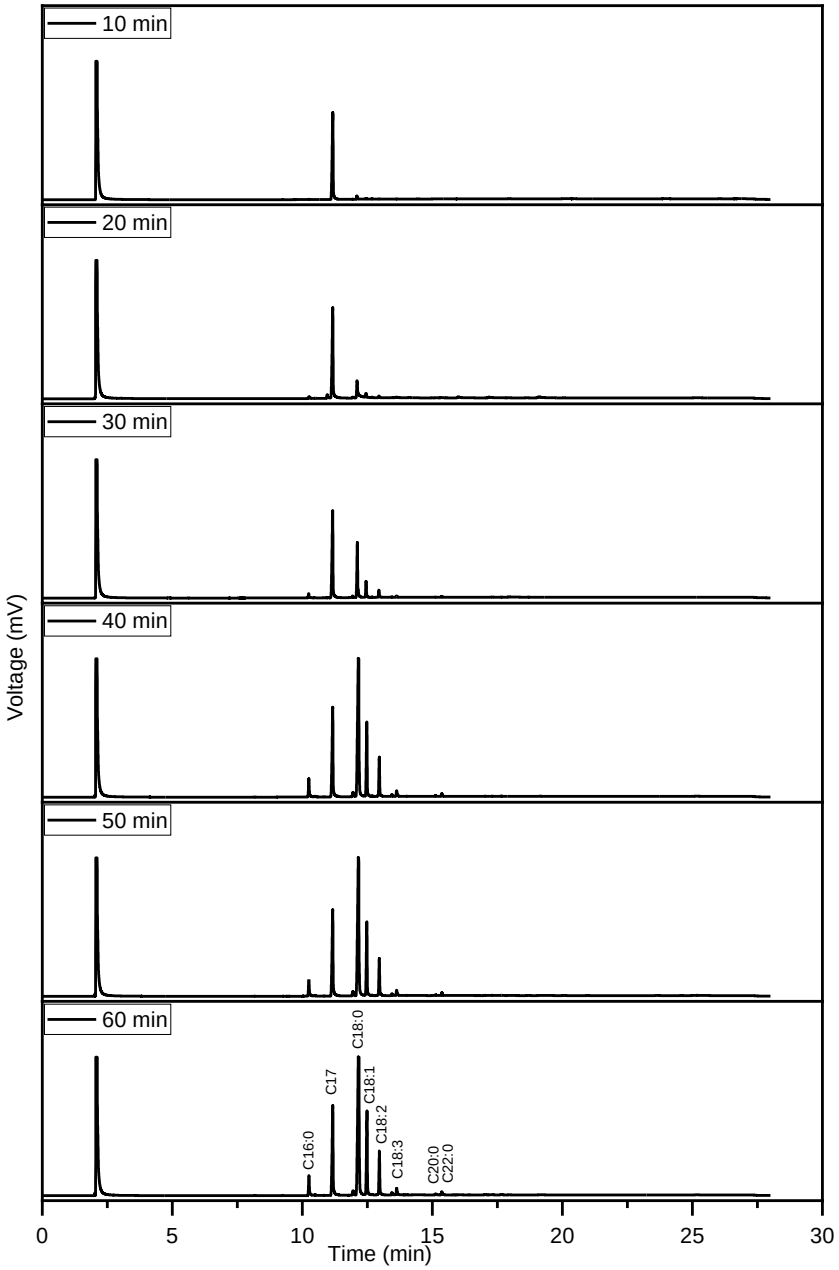

Figure 4-29: GC peaks of biodiesel produced during reactive coupling.

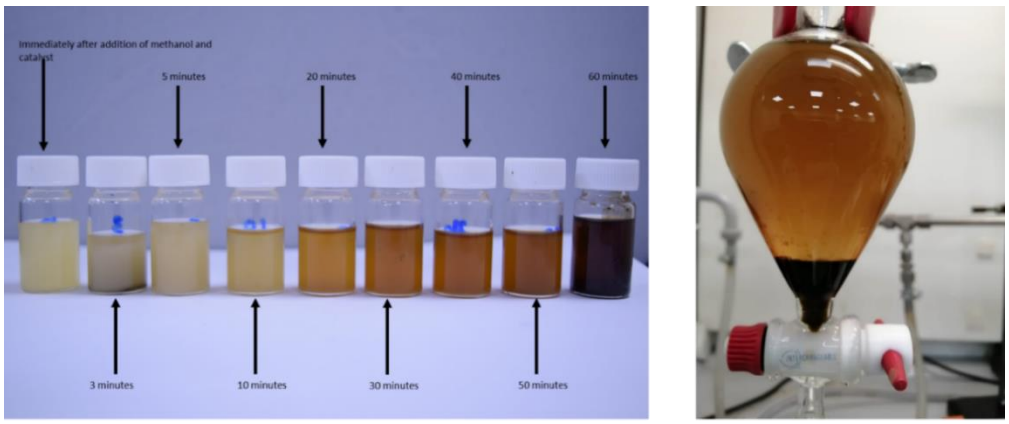

Figure 4-30: Image of (a) biodiesel samples at the interval and (b) biodiesel separation during reactive coupling.

More peaks were observed as the reaction proceeds from 10 to 60 min (*Figure **4**-**29***). C17 was used as standard, and it appears around 11 min. The fatty acids that appear in the chromatogram include C16:0 (palmitic acid), C18:0 (stearic acid), C18:1 (oleic acid), C18:2 (linoleic acid), C18:3 (linolenic acid), C20:0 (arachidic acid), and C22:0 (behenic acid). C16 appears around 10 min while C18s were within 12 to 13 min. C20 and C22 are less appeared peaks around 15 min, respectively. Oleic fatty acid (C18:1) has the largest peak in the chromatogram. One advantage from this research was the fast separation into phases. Once the mixture is poured into a separating funnel at the end of the reaction, the etherified phase settles immediately at the bottom (*Figure **4**-**30***). This might be due to the high density of the etherified phase. It was observed that decantation is possible to separate the two phases.

The triglyceride conversion shown below (*Figure **4**-**31*** to *Figure **4**-**34***) are at 130, 140, 150, and 160 ^{o}C, catalyst concentration 1, 2,3, and 5 wt%, and mole ratio of methanol to oil 4:1, 5:1, 6:1, and 8:1. The reactive coupling was performed for up to 1h.

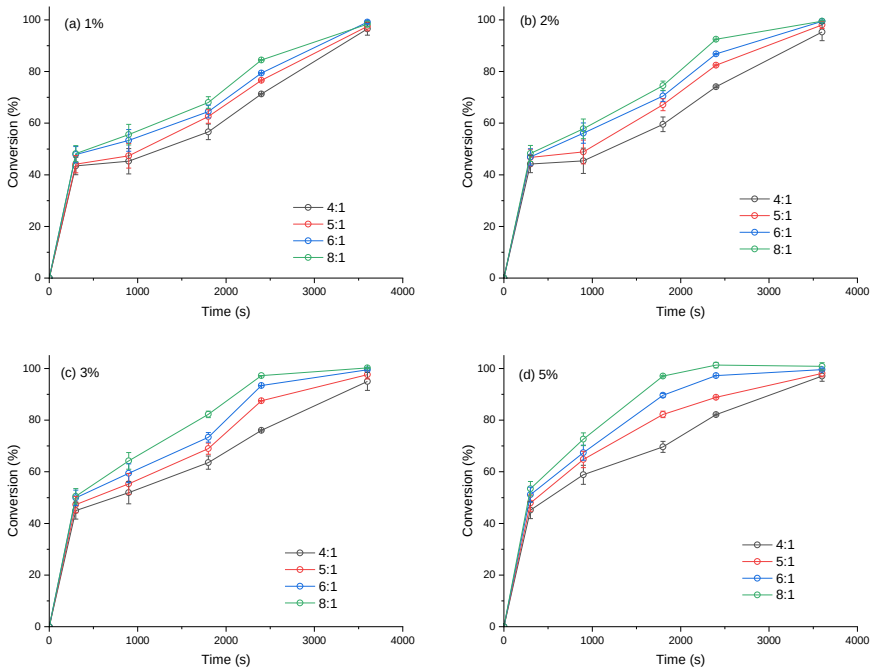

Figure 4-31: Triglyceride conversion during reactive coupling at 130 ^{o}C with (a) 1 wt% (b) 2 wt% (c) 3 wt% (d) 5 wt% catalyst concentration and various molar ratio (4:1, 5:1, 6:1, and 8:1).

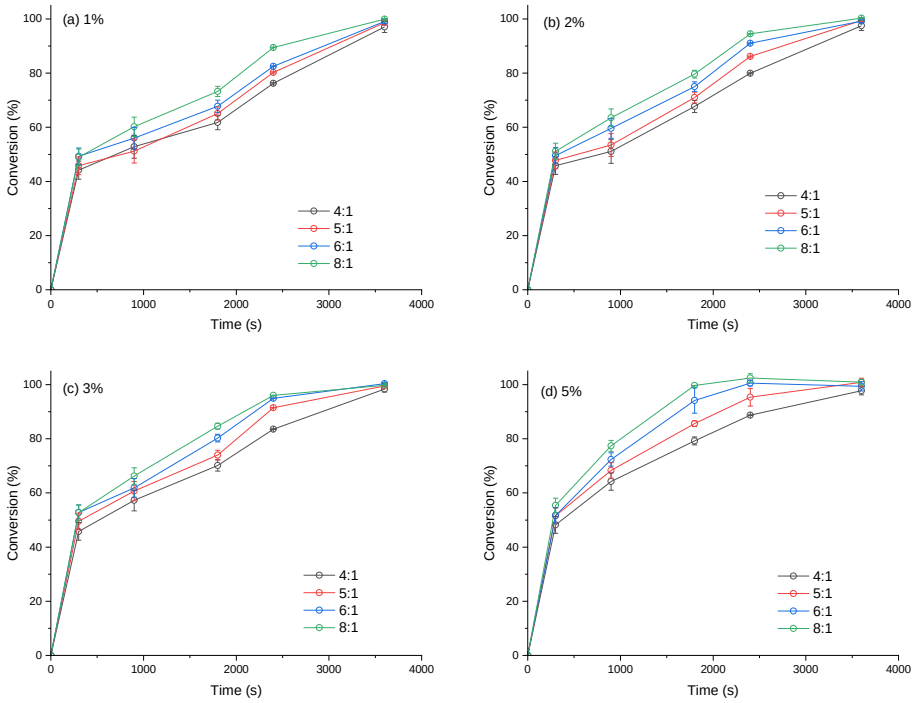

Figure 4-32: Triglyceride conversion during reactive coupling at 140 oC with (a) 1 wt% (b) 2 wt% (c) 3 wt% (d) 5 wt% catalyst concentration and various molar ratio (4:1, 5:1, 6:1, and 8:1).

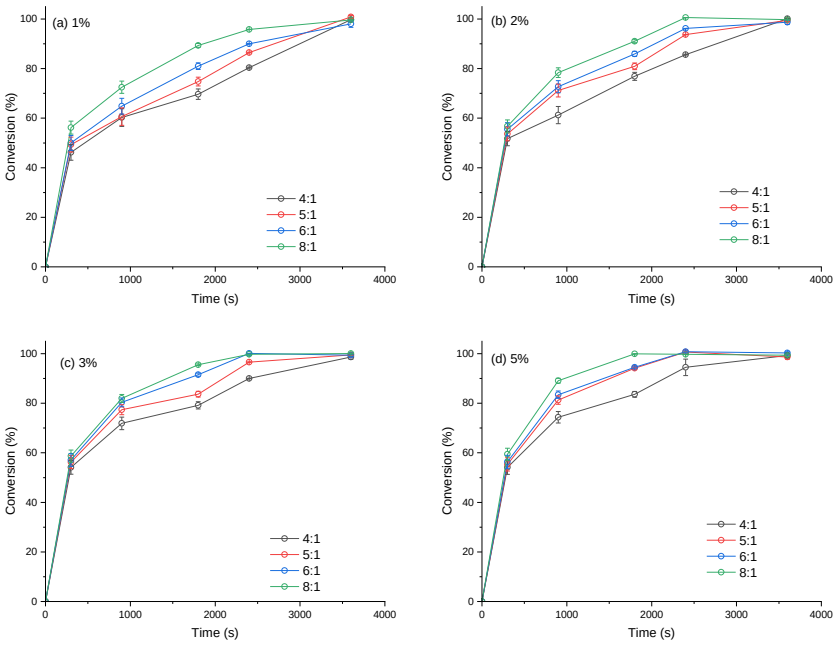

Figure 4-33: Triglyceride conversion during reactive coupling at 150 °C with (a) 1 wt% (b) 2 wt% (c) 3 wt% (d) 5 wt% catalyst concentration and various molar ratio (4:1, 5:1, 6:1, and 8:1).

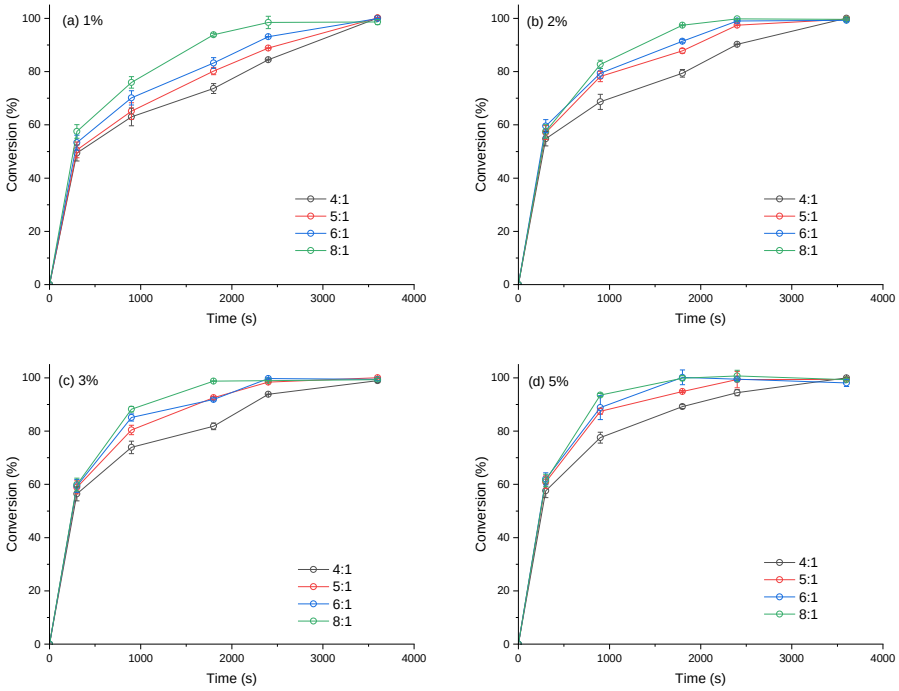

Figure 4-34: Triglyceride conversion during reactive coupling at 160 °C with (a) 1 wt% (b) 2 wt% (c) 3 wt% (d) 5 wt% catalyst concentration and various molar ratio (4:1, 5:1, 6:1, and 8:1).

From the result of the conversion, high catalyst concentration and molar ratio of methanol to oil were observed to respond to completion faster. The result also shows

1h is efficient for complete conversion of the triglyceride to FAME. Generally, a high concentration of homogenous base catalyst produces more soap during transesterification when used in a feedstock with high FFA content. This will hinder the production of biodiesel. The record has shown its excellent performance in a feedstock with less FFA and used at commercial level. The concentration of catalyst during transesterification depends on either its homogeneous or heterogeneous reaction. Higher catalyst concentration is mostly reported with a heterogeneous catalyst which is due to mass transfer limitation.

The acid catalyst has been associated with the slow reaction compared to the base catalyst in biodiesel production (Ma and Hanna, 1999). Using reactive coupling technique, the reaction was observed to be faster in converting triglyceride. This might be due to alteration of the equilibrium of the system, with continued removal (conversion) of the glycerol by-product. As shown in *Figure **4**-**34***, the total conversion of the triglyceride was achieved within 60 min.

As expected, an increase in catalyst concentration and molar ratio increased the conversion of the triglyceride. At 160 ^{o}C, 2400s, and 5% catalyst concentration, complete conversion was achieved, except for the reaction with a molar ratio of 4:1 that achieved approximately 90% conversion. When compared to the reaction with 1% catalyst concentration, only 8:1 achieved total conversion at 2400s. This agreed with Lotero et al. (2005) that an increase in catalyst concentration increased the triglyceride conversion.

The yield of biodiesel production has a similar pattern to the conversion. As shown in *Figure **4**-**35*** to *Figure **4**-**38*** below, the yield is at 1, 2, 3, and 5 wt% catalyst concentration, 130 – 160 ^{o}C reaction temperature, and 4:1 – 8:1 molar ratio of methanol to oil.

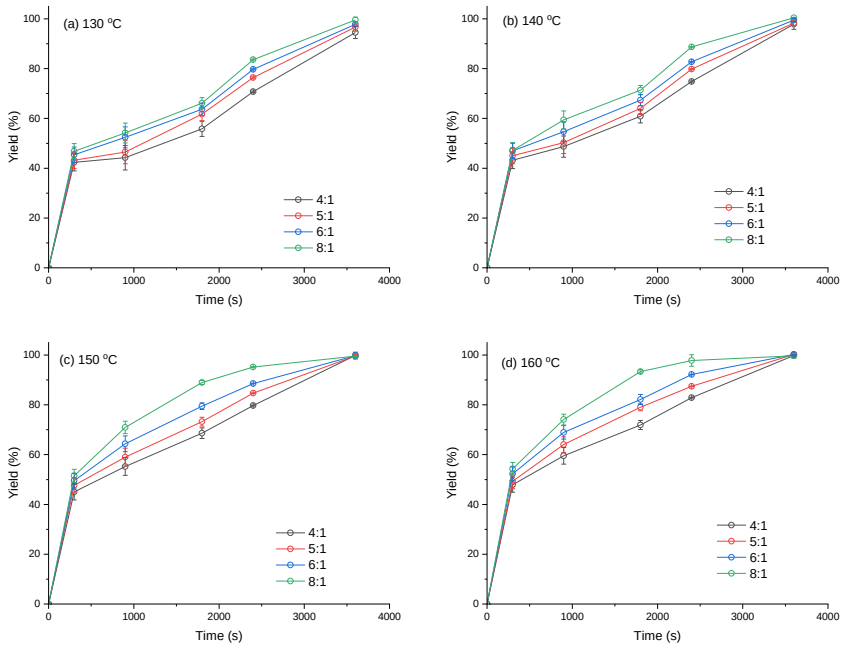

Figure 4-35: Biodiesel yield at 1 wt% with (a) 130 °C (b) 140 °C (c) 150 °C (d) 160 °C and various molar ratio (4:1, 5:1, 6:1, and 8:1).

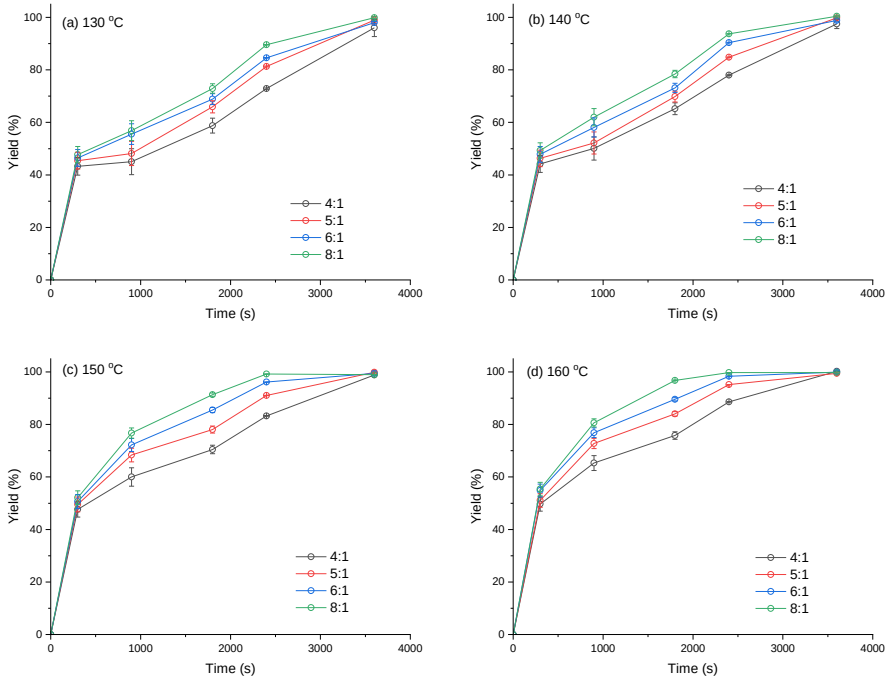

Figure 4-36: Biodiesel yield at 2 wt% with (a) 130 °C (b) 140 °C (c) 150 °C (d) 160 °C and various molar ratio (4:1, 5:1, 6:1, and 8:1).

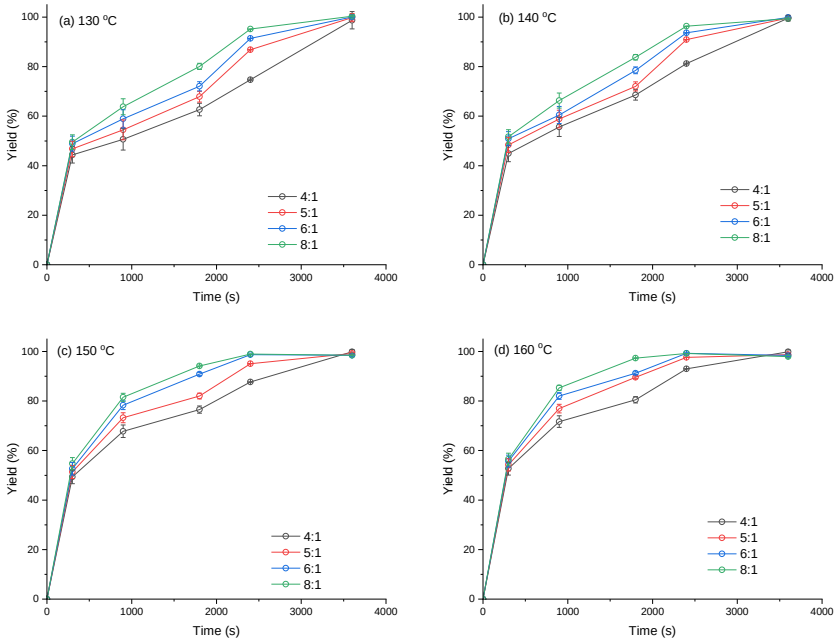

Figure 4-37: Biodiesel yield at 3 wt% with (a) 130 °C (b) 140 °C (c) 150 °C (d) 160 °C and various molar ratio (4:1, 5:1, 6:1, and 8:1).

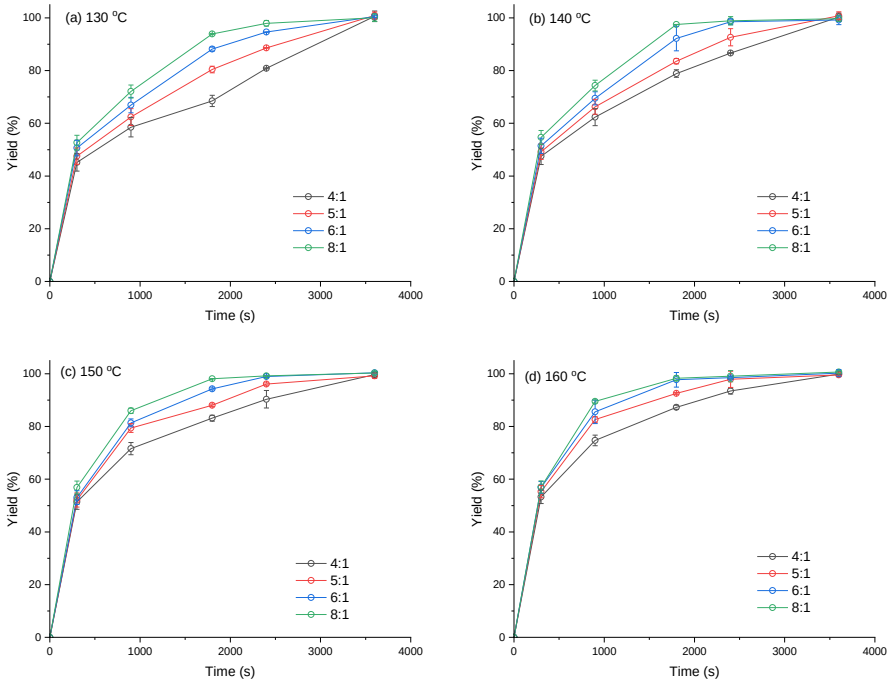

Figure 4-38: Biodiesel yield at 5 wt% with (a) 130 °C (b) 140 °C (c) 150 °C (d) 160 °C and various molar ratio (4:1, 5:1, 6:1, and 8:1).

The yield of 100% was achieved at 60 min with the various catalyst concentration and temperatures used for this research (*Figure **4-35*** to *Figure **4-38***). As expected, higher

molar ratio attained complete conversion faster and obtained higher yield. At 160 ^{o}C, a yield of approximately 90% was achieved after 900s (15 min) with 8:1 molar ratio. At the same condition but with molar ratio 4:1, the yield obtained was 75%. This shows a yield of about 90% can be achieved within the first 15 minutes of the reaction using reactive coupling with sulphuric acid as catalyst and higher temperature than 60 ^{o}C used in the conventional method.

The role of the reaction temperature in biodiesel production can never be overemphasised as it influences the rate of reaction. High yield of biodiesel is obtained close to the boiling point of the short-chain alcohol used. In the conventional biodiesel production method, the loss of alcohol through evaporation is avoided by keeping the reaction temperature below the boiling point of alcohol (Demirbas, 2009). This research used a pressure vessel to enable high temperatures above the boiling point of the alcohol. The advantage of using high temperature includes short reaction time and good miscibility of the reactant.

This research shows 150, and 160 ^{o}C achieved the highest conversion much faster. Using 8:1 molar ratio and 2 – 5 wt% catalyst concentration, the complete conversion was achieved at 160 ^{o}C after 1800s (*Figure **4**-**38***). The lowest conversion was approximately 96% at 130 ^{o}C, 4:1 molar ratio, and 1 wt% catalyst concentration after 1h. Freedman et al. (1984) reported complete conversion at 1% catalyst concentration (H_2SO_4), 3h, 117 ^{o}C, and 30:1 molar ratio of butanol to oil. The authors also reported 69h for complete conversion using 30:1 methanol to oil molar ratio and 65 ^{o}C. Lotero et al. (2005) reported that increasing temperature of the transesterification reaction with acid catalyst takes the conversion near completion.

Since the transesterification reaction is reversible, to shift the reaction to the product requires excess alcohol. This is following Le-Chatelier's principle. As high as 100:1 molar ratio of alcohol to oil has been reported. Though the alcohol can be recovered, it increases the reaction cost due to the purchase of an additional unit to recover the excess alcohol and the energy cost of recovering the excess alcohol. It was also reported that excess alcohol contributes to the difficulty in separation in downstream processing (Demirbas, 2009, Lotero et al., 2005). Reactive coupling was used to convert the co-product of biodiesel (glycerol) to an added-value product to reduce the use of excess

methanol in transesterification. This also is in accordance with the principle of Le-Chatelier's. To continuously remove (or convert) one of the products, the reaction favours the product.

The result shows high triglyceride conversion and biodiesel yield with 8:1 and 6:1 after 1h. The conversion was reduced to approximately 96% when 4:1 molar ratio was used. Complete conversion after 0.5h was observed at 160 ^{o}C with 5% catalyst concentration using 8:1 and 6:1 molar ratio. Approximately 91% conversion was achieved with 5:1 molar ratio and even lower (82%) when 4:1 molar ratio was used. 98% conversion was reported by Canakci and Van Gerpen (1999) at 60 ^{o}C with a molar ratio of 30:1. At the same time, Zheng et al. (2006) achieved 98% conversion with 50:1 molar ratio at 80 ^{o}C after 4 h. The molar ratio of the acid transesterification was reduced to 4:1 – 8:1 from this work with reactive coupling.

Reaction time is valuable in biodiesel production as it determines the rate at which the feed (vegetable oil) is consumed, or product (biodiesel) is produced. Alkaline catalysts have been reported to achieve high conversion within short reaction time, while the longer reaction time is recorded with an acid catalyst (Saifuddin et al., 2015, Lotero et al., 2005).

The complete conversion was achieved after 0.5h at 160 ^{o}C. This is faster than 24h reported by Bhatti et al. (2008) at 60 ^{o}C and 4h reported by Zheng et al. (2006) at 80 ^{o}C. The lowest conversion after 1h from this research was 96% at 130 ^{o}C. Other reactions achieved approximately complete conversion within 0.5 – 1h. The fast conversion achieved might be due to the high reaction temperature and simultaneous conversion of glycerol to value-added products.

4.2.3 Total Glycerol Conversion

Converting glycerol simultaneously during biodiesel production to an added-value product has been done with some reaction techniques. The addition of acetone during transesterification coupled glycerol to produces solketal. While the addition of dimethyl carbonate simultaneously produces biodiesel and glycerol carbonate. Both methods mentioned have recorded high conversion of the glycerol (82% glycerol conversion for solketal production (Al-Saadi et al., 2019) and 90% glycerol conversion for glycerol

carbonate (Al-Saadi et al., 2018)), though with the addition of extra solvent. The advantage of this research is, no additional solvent is required. However, the glycerol conversion was low compared to the previous research mentioned above. The chromatogram of some of the glycerol rich phase is shown in *Figure **4**-**39*** below.

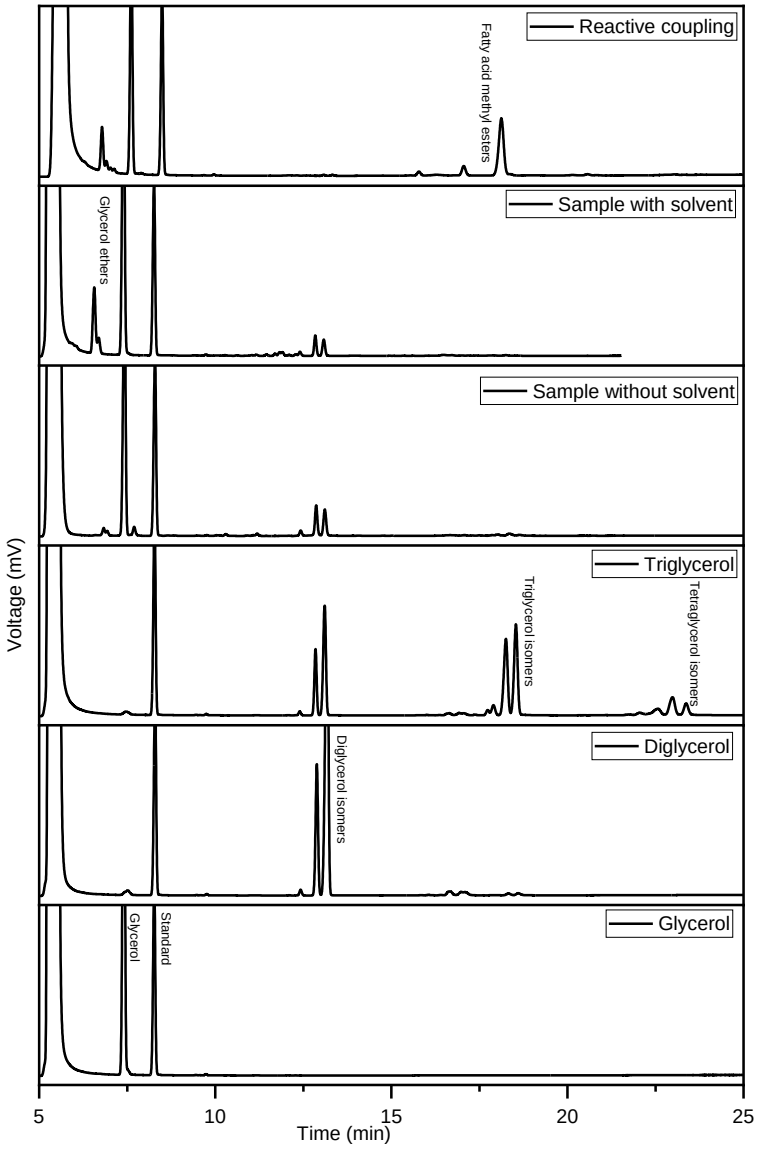

Figure 4-39: GC peaks of glycerol valorisation.

Immediately after 5 min of retention time, the solvent (methanol) appears due to its high volatility. The peaks of the glycerol ethers appear around 6 min while glycerol appears about 7 min. The early appearance of the glycerol ethers might be due to the fewer OH group than glycerol. Butan 1,2,4 triol was used as standard, and its peaks appear around 8 min. The peaks of diglycerol isomers appear from 12 to 14 min, while

the isomers of triglycerols and tetraglycerols appear from 16 to 18 min and 21 to 23 min, respectively. However, if the cyclic isomers of the oligomers are produced, the retention time is much earlier.

The gas chromatography and mass spectroscopy (GCMS) of glycerol, diglycerol, and etherified samples were also performed at Drummund building in Newcastle University. *Figure **4-40*** is the spectrum for pure glycerol after silylation with N,O-Bis (trimethylsilyl) trifluoroacetamide (BSTFA). Each of the hydroxyl groups in glycerol is attacked, and a trimethylsilyl group is attached, as shown in section 3.3.3.2. The spectrum obtained was matched with the trimethylsilyl ether of glycerol in the library.

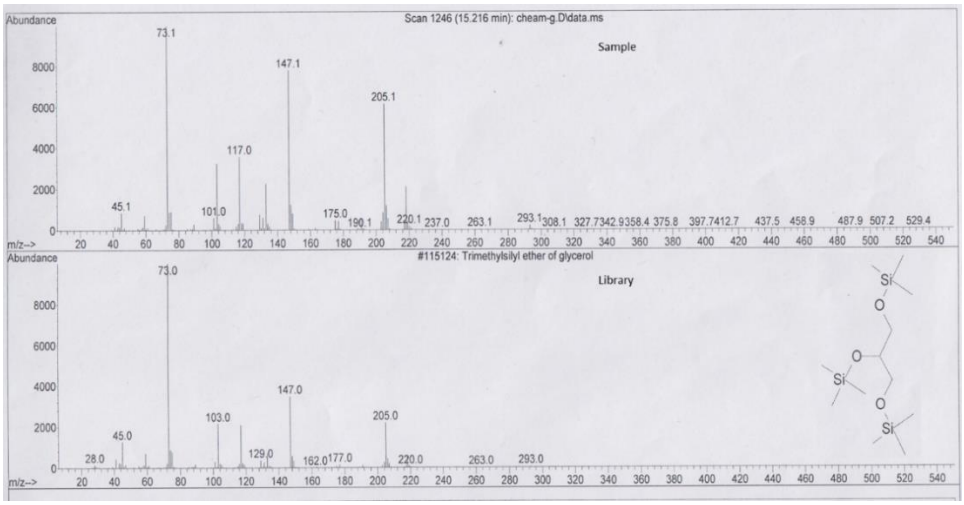

Figure 4-40: GC-MS of glycerol and the library match.

The molecular ion after the silylation of the glycerol is 308. The fragmentation of one of the methyl groups attached to the trimethylsilyl ether gives a mass to charge ratio (m/z) of 293, as seen in *Figure **4-40***. The heterolytic cleavage of O – $SiMe_3$ produced m/z of 220. An alpha cleavage (homolytic cleavage) to the oxygen in the middle, the fragmentation of C – O – $SiMe_3$ occurs to give m/z of 205. For m/z of 147, a combined heterolytic cleavage of O – $SiMe_3$ and fragmentation of $SiMe_3$ occurs. When the molecular ion undergoes both homolytic cleavages to fragment C – O – $SiMe_3$ and heterolytic cleavage of O – $SiMe_3$, the m/z is 117 as indicated in the spectrum. The m/z of 73 is the fragmentation of one of the trimethylsilyl. Similar fragmentation occurs with the diglycerol, and the Samples analysed. Figures of the fragmentation are shown in Appendix C.

The glycerol by-product produced during transesterification was converted to value-added products simultaneously. The unreacted glycerol at 160 °C with various catalyst concentration (1, 2, 3, and 5 wt%) and molar ratio (4:1, 5:1, 6:1, and 8:1) is shown in *Figure **4-41*** below.

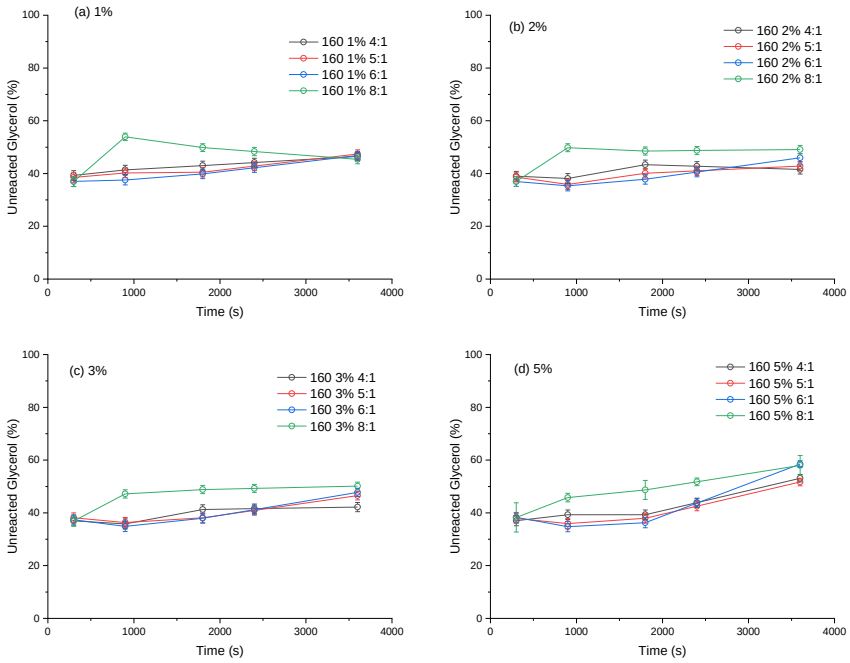

Figure 4-41: Unreacted glycerol for reactive coupling at 160 °C (a) 1 (b) 2 (c) 3 (d) 5 wt% catalyst concentration with various molar ratio.

The unreacted glycerol at 150 and 160 °C was approximately 40% with a slight increase after 0.5h, at 5 wt% catalyst concentration. About 30% unreacted glycerol was observed at 140 °C, and approximately 20% when the temperature decreases to 130 °C (see *Figure B- **2*** to *Figure B- **4***). The high conversion at 130 and 140 °C might be due to less triglyceride conversion. This is because there is less crude glycerol to compete in parallel reaction to produce glycerol ethers and polyglycerol. This might be because glycerol conversion is faster with a low concentration of feeds in the reaction.

4.2.4 Effect of Process Variables on Reactive Coupling

The effect of reaction temperature, molar ratio, catalyst concentration, and time was examined. Sulfuric acid was used as the catalyst for this research with concentrations of 1, 2, 3, and 5 wt%. The molar ratio of alcohol to oil used was 4:1, 5:1, 6:1, and 8:1, which is very low compared to the higher molar ratios used in the conventional method. The

temperatures 130, 140, 150, and 160 °C for up to 1h were used as the maximum reaction time because long reaction time will increase biodiesel production cost.

4.2.4.1 Catalyst Concentration

The effect of the catalyst was considered with the production of diglycerol and glycerol ethers. *Figure **4-42*** to *Figure **4-45*** are diglycerol yield at various temperature (130 – 160 °C, catalyst concentration (1, 2, 3, and 5 wt%), and molar ratio (4:1, 5:1, 6:1, and 8:1) after 1h.

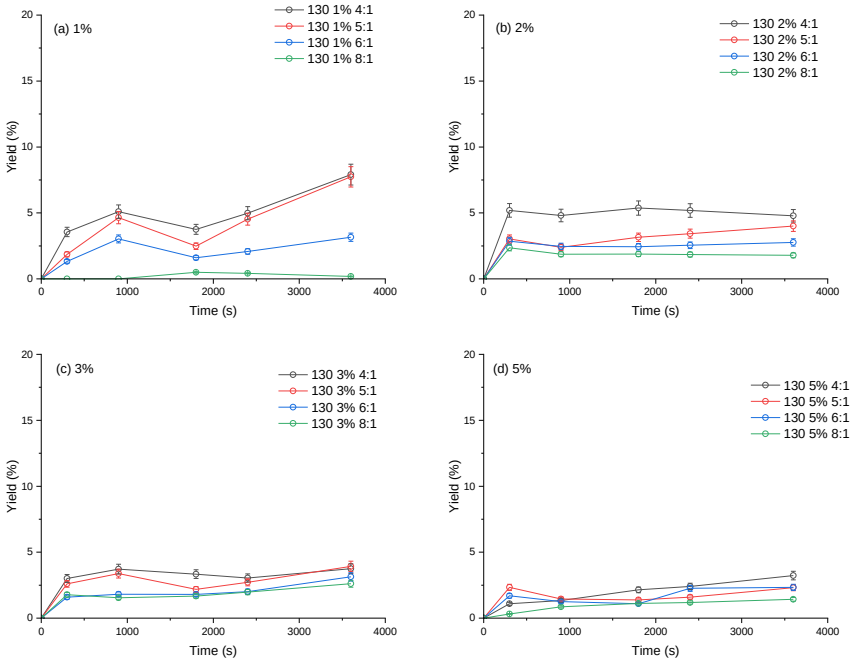

Figure 4-42: Diglycerol yield at 130 °C at (a) 1%, (b) 2%, (c) 3%, and (d) 5% with various molar ratio.

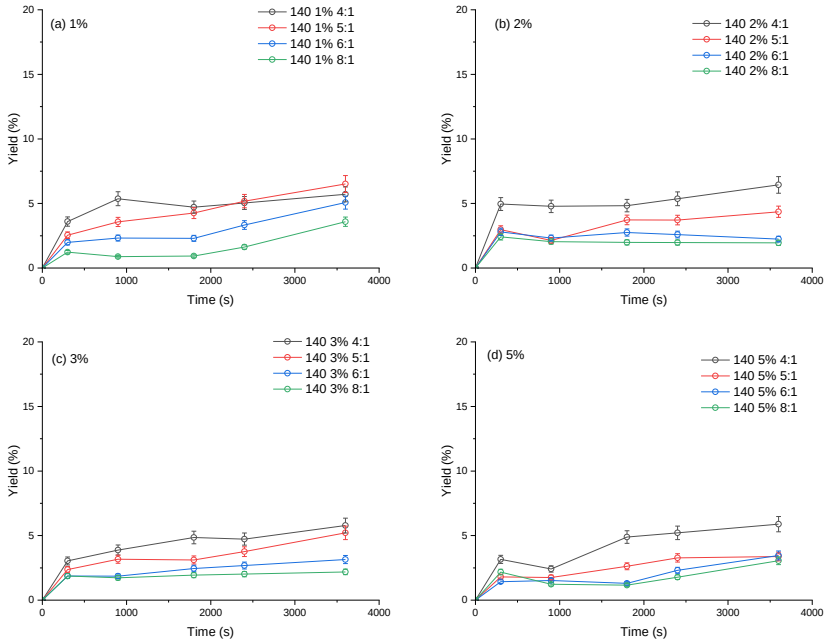

Figure 4-43: Diglycerol yield at 140 °C at (a) 1%, (b) 2%, (c) 3%, and (d) 5% with various molar ratio.

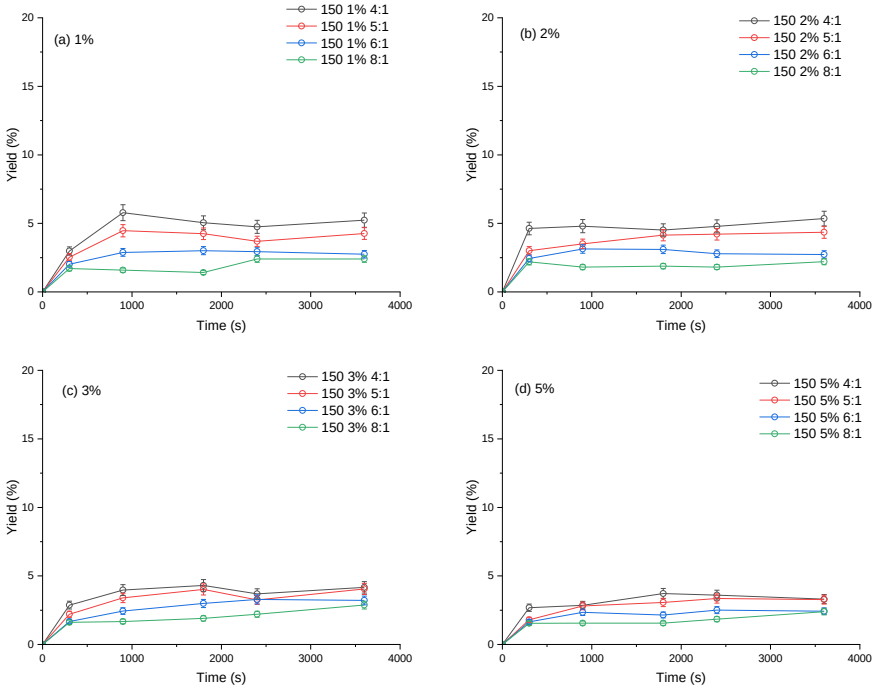

Figure 4-44: Diglycerol yield at 150 °C at (a) 1%, (b) 2%, (c) 3%, and (d) 5% with various molar ratio.

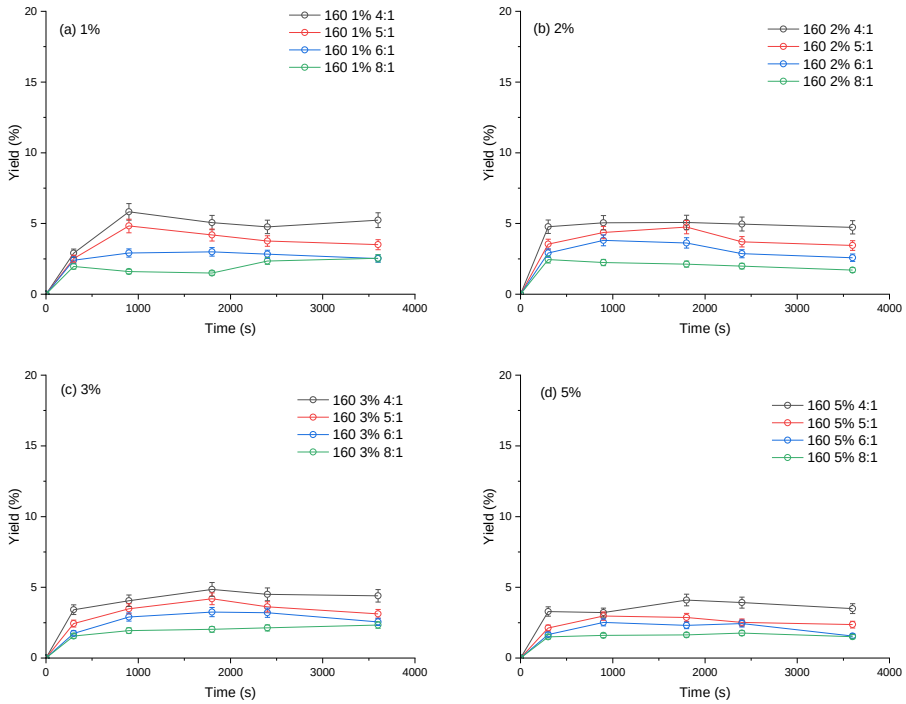

Figure 4-45: Diglycerol yield at 160 °C at (a) 1%, (b) 2%, (c) 3%, and (d) 5% with various molar ratio.

In glycerol etherification, the yield is expected to increase with the increase in catalyst concentration. However, a decrease was observed in diglycerol yield as the catalyst concentration increase. In contrast, the yield of glycerol ethers increases with an increase in catalyst concentration until 5 wt% when a decrease was observed (see *Figure **4-46*** to *Figure **4-49***). This implies the best catalyst concentration required for the glycerol etherification is about 3 wt%.

Etherification is a secondary reaction in the reactive coupling, and the same catalyst was used for both reactions (transesterification and etherification). The etherification reaction between methanol and glycerol is faster than glycerol self-etherification. This might be due to the complete solubility of methanol in glycerol. The presence of the three polar groups in glycerol makes it more soluble in the solvent. From the result obtained, sulfuric acid has low selectivity towards diglycerol production.

The highest yield of diglycerol was approximately 8% at 1 wt% catalyst concentration and 130 °C. The yield decreased to about 3% as the catalyst concentration increased to 5 wt%. However, the highest yield of glycerol ether production was about 80% then slightly decrease as the reaction proceeds to 1h. With the low catalyst concentration, the reaction was able to produce biodiesel and glycerol ethers. Supercritical method of

biodiesel production was reported to also simultaneously produce biodiesel and glycerol ethers (Sakdasri et al., 2015, Aimaretti et al., 2009). In supercritical, a catalyst is not required. This is one of the advantages of the supercritical method. No cost for purchase of catalyst nor purification after production. However, the supercritical method is not economically viable for biodiesel production.

4.2.4.2 Molar Ratio

The molar ratio in reactive coupling is considered an important variable for biodiesel and glycerol ethers simultaneous production. *Figure **4-46*** to *Figure **4-49*** below are glycerol ether yield at 130 – 160 °C, 1 – 5 wt% catalyst concentration, and 4:1 – 8:1 molar ratio.

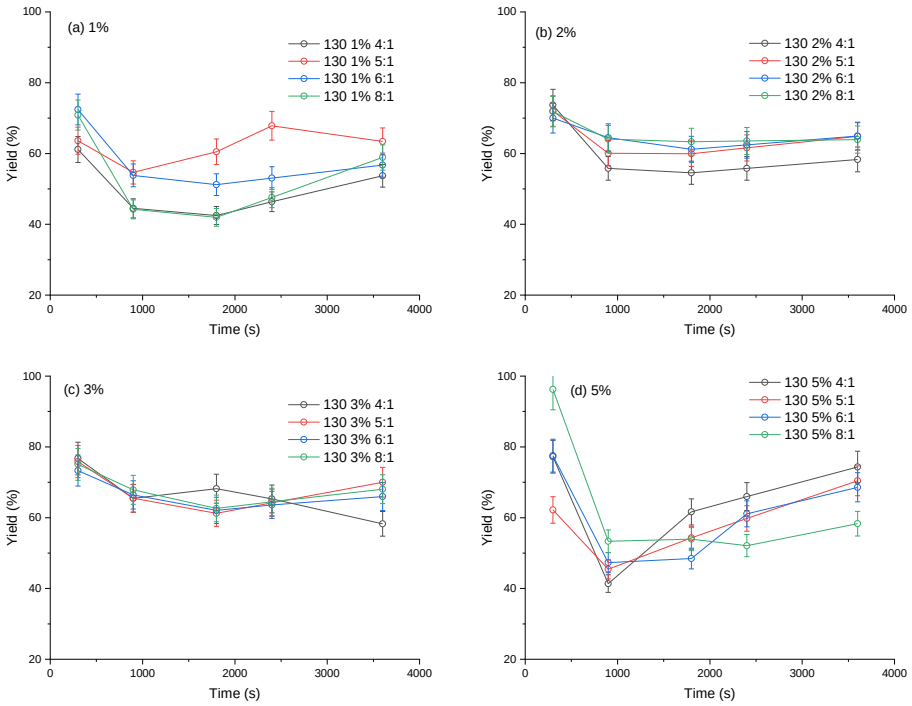

Figure 4-46: Glycerol ether yield at 130 °C at (a) 1%, (b) 2%, (c) 3%, and (d) 5% with various molar ratio.

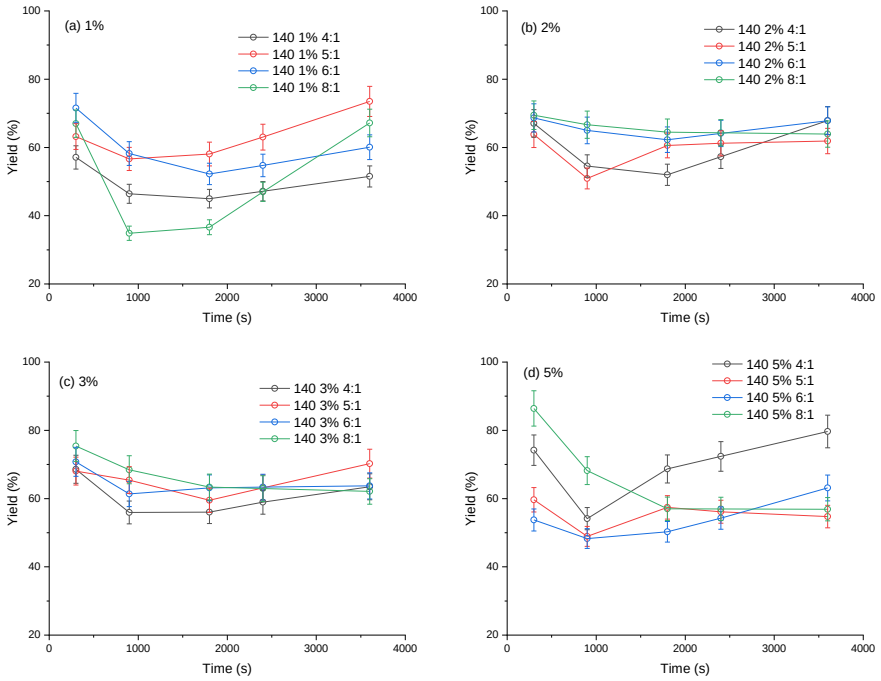

Figure 4-47: Glycerol ether yield at 140 °C at (a) 1%, (b) 2%, (c) 3%, and (d) 5% with various molar ratio.

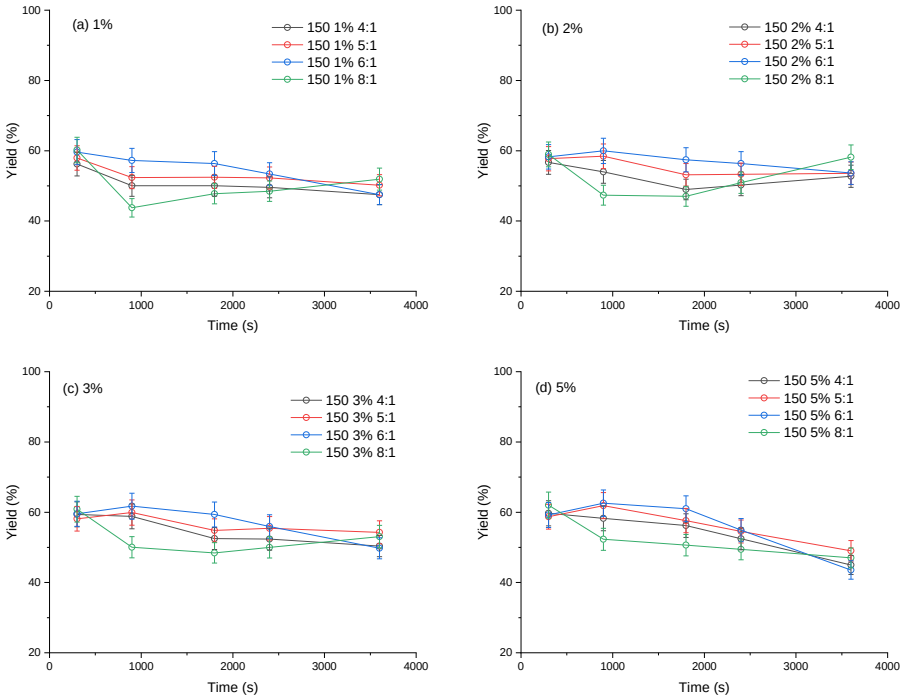

Figure 4-48: Glycerol ether yield at 150 °C at (a) 1%, (b) 2%, (c) 3%, and (d) 5% with various molar ratio.

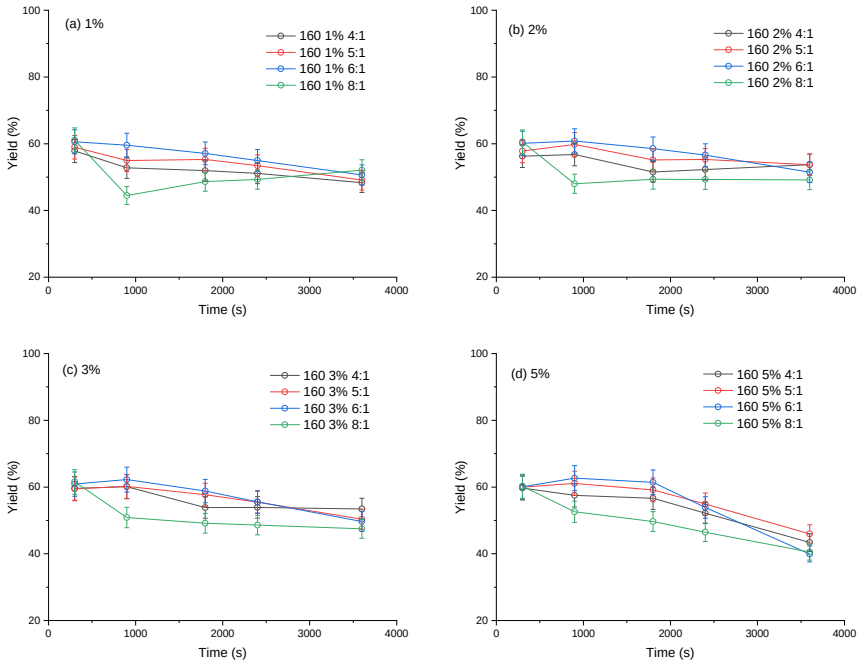

Figure 4-49: Glycerol ether yield at 160 °C at (a) 1%, (b) 2%, (c) 3%, and (d) 5% with various molar ratio.

The excess use of alcohol during biodiesel production has been a problem for commercial production through increased production cost. An additional unit is required to purify excess alcohol. In this research, this excess alcohol is utilised to produce glycerol added-value product, thereby reducing the purification unit requirement.

The result of this research shows a decrease in the yield of diglycerol as the molar ratio decreases. At the same time, the yield of glycerol ether increases with an increase in the molar ratio. This is in concomitance to Aimaretti et al. (2009) report that more methanol is consumed during glycerol methanolysis. The increase in the yield of glycerol ethers was observed before the complete conversion of triglyceride. However, it becomes approximately equal when the triglyceride conversion was completed. This shows that excess methanol presence influenced the production of polyglycerol negatively and increases the production of glycerol ethers. Previous work on reactive coupling used extra solvent to react with glycerol (acetone for solketal, dimethyl carbonate for glycerol carbonate, and methyl acetate for triacetins). No solvent is required for polyglycerol production, while glycerol ethers utilise the excess alcohol in transesterification. This is another advantage over the previous work on coupling methods.

The highest polyglycerol yield achieved was approximately 8% using a molar ratio of 4:1. The yield decreases as the molar ratio increase to 8:1. This might be because the glycerol ether production is faster than glycerol self-etherification. The highest yield of glycerol ether produced was approximately 80% at 8:1. Hence, reactive coupling favours polyglycerol production when low alcohol was used and glycerol ether when alcohol was high.

In related work, the effect of the molar ratio was observed with supercritical biodiesel production. Sakdasri et al. (2015) reported an increase in the fuel yield by about 7% due to the production of glycerol ether, at molar ratio 12:1. Also, Aimaretti et al. (2009) reported the highest yield at 20:1 with no glycerol by-product. Marulanda et al. (2010a) reported the production of both diglycerol glycerol ethers from the supercritical biodiesel production. The authors reported their best yield at 9:1, with approximately 80% biodiesel yield. Both Sakdasri et al. (2015) and Marulanda et al. (2010a) agreed that glycerol ether would increase biodiesel value as an oxygenated compound.

4.2.4.3 Temperature

This research shows that increasing the temperature leads to a slight decrease in glycerol conversion and yield value-added products. The highest polyglycerol yield was 8%, produced at 130 ^{o}C. This slightly reduces to about 5% when the temperature was increased to 160 ^{o}C. Similarly, glycerol ethers yield decreases from approximately 60% at 130 ^{o}C to about 50% at 160 ^{o}C. The decrease in yield might be due to competing reactions. At higher temperatures, triglyceride conversion is achieved faster and higher FAME yield, which produced more glycerol by-product to compete for conversion with the same catalyst and methanol for triglyceride conversion. As shown in section 4.2.2, the triglyceride conversion at 130 ^{o}C was slow compared to the conversion at 160 ^{o}C. The lower the glycerol by-product, the faster the conversion since the condition is favourable.

The temperature used here is less than 270 – 400 ^{o}C used in the supercritical biodiesel production method. It also required high pressure of between 100 – 400 bar. The supercritical biodiesel method was compared because the method simultaneously produced biodiesel, diglycerol, and glycerol ethers. Marulanda et al. (2010a) reported 80% yield of biodiesel with glycerol conversion to diglycerol and glycerol ethers at 400

^{o}C. Lee et al. (2012) reported glycerol conversion during supercritical biodiesel production to 3-methoxyl 1,2, propanediol, and other oxygenated compounds to reduce soot formation diesel engine. The authors achieved 102% yield of biodiesel at 270 ^{o}C with a 2:1 molar ratio of methanol to oil for 45 minutes. The high temperature and pressure of supercritical make it more expensive compared to other methods.

4.2.4.4 Time

Reaction time plays a vital role in every reaction. For conventional glycerol self-etherification, a reaction time of up to 24h was used. The high viscosity of glycerol causes the reaction to be slow (Galy et al., 2017). The high solubility of glycerol in methanol reduced the viscosity, hence makes the reaction faster. Approximately 60% of glycerol conversion was achieved at 160 ^{o}C after 1h with reactive coupling. The result is slightly lower than 68% glycerol conversion reported at 160 ^{o}C after 5h as reported in section 4.1.2 for polyglycerol production. The highest glycerol conversion of approximately 80% was achieved in 1 h using the reactive coupling at 130 ^{o}C. However, the biodiesel yield at this condition is less.

The reaction time was less with the supercritical methods due to the high reaction temperature and pressure. Marulanda et al. (2010a) achieved 80% biodiesel yield and added value products within 3 – 10 min. In a similar work, the same authors (Marulanda et al., 2010b) reported 2 – 6 min. Aimaretti et al. (2009) reported above 90% biodiesel yield with complete glycerol conversion after 1h at 280 ^{o}C. Lee et al. (2012) reported 45 min to produce 102% biodiesel yield. The complete conversion of glycerol was not achieved in this research after 1h. However, lower temperature, pressure, molar ratio of methanol to oil, catalyst concentration, and reaction time were used, compared to supercritical biodiesel production.

4.2.5 Kinetics of Reactive Coupling

The kinetics model for the reactive coupling was fitted to the experimental values. Marchetti et al. (2010) model for biodiesel production using H_2SO_4 as catalyst was adopted. The equation developed for polyglycerol production in this study (*see* section 4.1.7) was used for diglycerols, while trial and error method was used to determine the equation for glycerol ether. The equations were combined in fitting the data obtained

from the reactive coupling. The model fitting was affected by both variables (temperature, catalyst concentration, time, and mole ratio) used for the experiment. The models fitted to the experimental data at 130, 140, 150, and 160 °C are shown in *Figure **4-50***, *Figure **4-51***, *Figure **4-52***, and *Figure **4-53***.

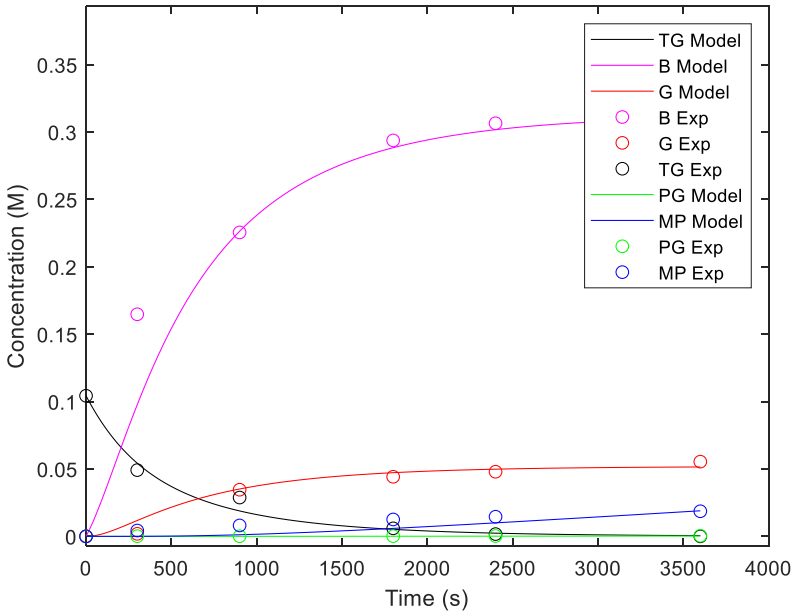

Figure 4-50: Experimental values compared to the model at 130 °C.

(Where TG is model triglyceride, TGE is experimental triglyceride, B is model biodiesel, BE is experimental biodiesel, G is model glycerol, GE is experimental glycerol, PG is model polyglycerol, PGE is the experimental polyglycerol, MP is the model glycerol ether, and MPE is the experimental glycerol ether).

*Figure **4-50*** is the model fitted to the experimental values at 130°C with 5 wt% catalyst concentration and 8:1 molar ratio. The R^2 shows 96% (R^2 = 0.96) correlation of the biodiesel model to the experimental data. The triglyceride conversion achieved 97% (R^2 = 0.97) fitting of the model, while approximately 92% of the experimental data was fitted for the production and conversion of glycerol. A lower polyglycerol fitting (R^2 = 0.84) and glycerol ethers (R^2 = 0.60) was obtained at 130 °C.

This means the biodiesel model adopted from Marchetti et al. (2010) has a good fitting even at a higher temperature (130 °C) than the temperature used to develop the model.

Generally, an increase was observed in the correlation as the molar ratio increased from 4:1 to 8:1 for the biodiesel production and triglyceride conversion. Also, about 90% of fitness was achieved for the glycerol ethers at 130 ^{o}C, 1 wt% catalyst concentration, and 8:1 molar ratio. In comparison, 60% was recorded when the catalyst concentration was increased to 5 wt%. Further work should be done to improve the fitness of the glycerol ethers in the reactive coupling.

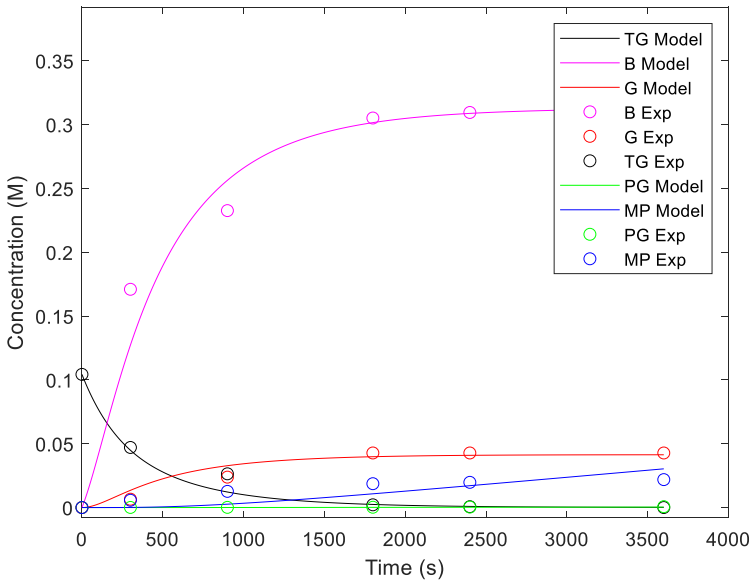

Figure 4-51: Experimental values compared to the model at 140 ^{o}C.

Increasing the temperature to 140 ^{o}C, the correlation between the model and experimental data for a biodiesel production increase to *Figure* ***4-51***). In contrast, a slight decrease in the triglyceride conversion correlation to R2 of 0.96 was obtained.

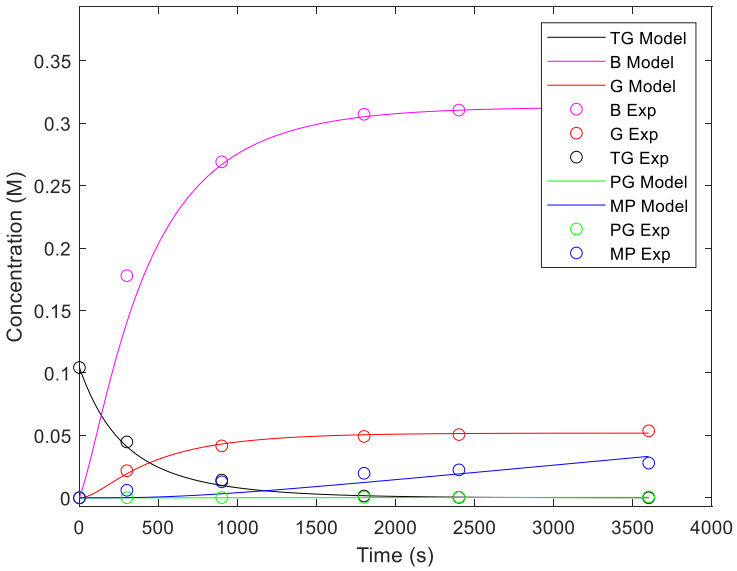

Figure 4-52:Experimental values compared to the model at 150 °C.

The polyglycerol model in *Figure **4-51*** was able to explain over 95% of the experimental result. This indicates that the developed polyglycerol model using glycerol conversion can predict the production in reactive coupling. However, the model was not always favourable for the glycerol ethers.

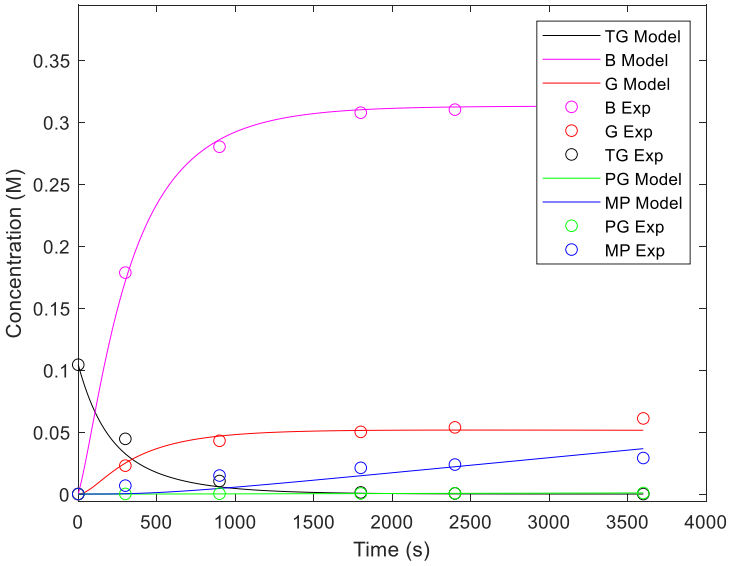

Figure 4-53: Experimental values compared to the model at 160 °C.

The biodiesel model in both *Figure **4**-**52*** and *Figure **4**-**53*** correlates to the experimental data with over 99% fitness (R^2 = 0.99 at 150 ^oC and 160 ^oC). The model fitness was similar to Marchetti et al. (2010) report, however with a much faster conversion of the triglycerides. The fast conversion is due to the high temperature of the reaction and simultaneous conversion of the glycerol to added value product, which reduces the effect of a reversible reaction. The fitness for the triglyceride conversion in both figures was 98%. The glycerol production and conversion achieved an approximately 96% fitness and 90% fitness for the polyglycerol production.

Generally, the experimental result for the reactive coupling fit a combined model of biodiesel production from acid and the developed glycerol valorisation models. The model for biodiesel was multiparametric and non-linear. The glycerol valorisation was fitted to second-order kinetics with a pre-exponential factor of 2.2×10^{11} $Lmol^{-1}s^{-1}$ and activation energy (E_a) of 112.0 kJ/mol.

4.2.6 Summary of Reactive Coupling

A proof-of-concept for the reactive coupling for biodiesel and glycerol valorisation was established. This study has also shown that acid catalyst can be used for total triglyceride conversion within 1 h with a low molar ratio (4:1). Another important observation from this research is the fast separation of the phases. With reactive coupling, decantation from the reactor is possible. For the glycerol valorisation, the excess alcohol reacted faster with the hydroxyl group of the glycerol than glycerol self-etherification. The reactive coupling model successfully explained over 99% of the biodiesel experimental data and 98% on the triglyceride conversion. The glycerol coupling was able to achieve over 96% and 95% polyglycerol production. A single model equation for the reactive coupling reaction will be interesting and might explain the result better. However, the use of multiple equations achieved good fitting.

4.3 Extraction and Reactive Extraction

This study combined the extraction from the seed with reactive coupling to further reduce the units involved in biodiesel and glycerol valorisation. This will combine reactive extraction and reactive coupling in a single reaction pot. The properties of the seed, extraction using Soxhlet, and reactive extraction were studied to achieve this.

Soxhlet extraction method was used to determine the yield of oil in the seed. Reactive extraction techniques was also used to produce biodiesel and determined the yield that can be produced with 200:1 – 480:1.

4.3.1 Properties of the Seed

The presence of water in triglyceride slows down the conversion to biodiesel when using an alkaline catalyst. The iodine value of biodiesel can be affected if water is present in the final fuel by making it rancid in a short time and causes poor combustion. However, acid-catalysed biodiesel production is not affected by the presence of water. This is because the reaction between triglyceride and water produced free fatty acid, which can be converted to biodiesel.

The water content in the seed used for this study was determined, as shown in section 3.4.5.1. Approximately 15.9 ±0.61 wt% of water content was obtained. This is higher than 6.7±0.5 wt% reported by Zakaria (2010). The water content difference might be due to the improvement in species or time in storage after collection from the farm. For this work, the water content was determined two weeks after collection from the farm.

The FTIR of the seed after grinding indicates water molecules presence with a peak of the hydroxyl group (-OH) between 3034 – 3660 cm^{-1} and a water scissor (H – O – H) at 1640 cm^{-1} as shown in *Figure **4-54*** below.

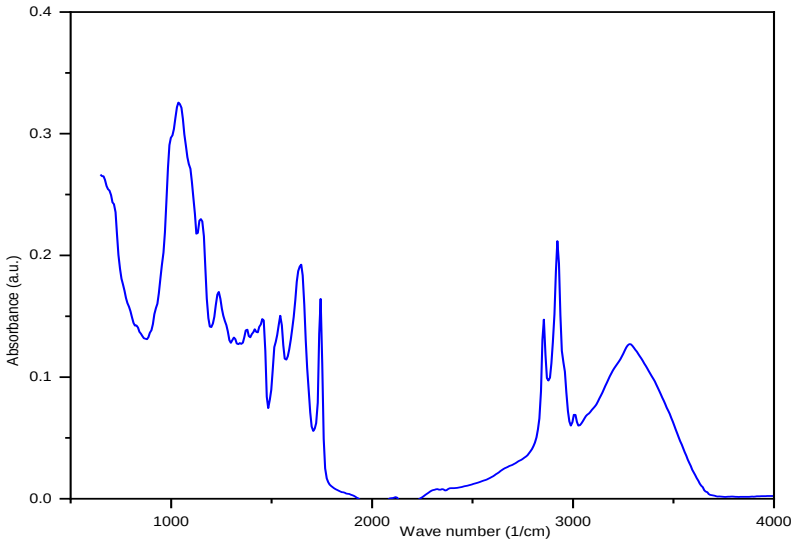

Figure 4-54: FTIR spectra of rapeseed before extraction.

The spectrum also shows an asymmetric and symmetric stretching vibration of -CH_2 and -CH_3 group around wave number 2922 and 2847 cm^{-1}. The appearance of a strong peak around 1744 cm^{-1} indicates the carbonyl groups presence (C = O) which is found in vegetable oil. The spectrum is the same as that of rapeseed oil shown in *Figure **4-28***, except for the presence of the water in the seed. This, as expected, confirmed the presence of the triglyceride in the seed.

The SEM image in *Figure **4-55*** below shows the sample covered with lipid. The image is similar to the reported by Ren et al. (2010) on rapeseed. The slight difference might be due to the particle size characterised. For this work, the sample was crushed into flakes with the seed coat. Also, the high moisture content contributed to the agglomeration of the sample. Although the sample was dried to remove the moisture before analysis, it might still affect the sample morphology.

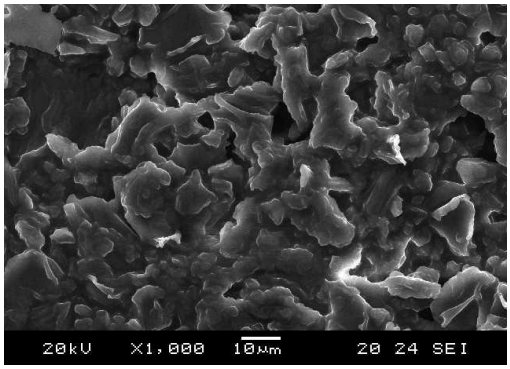

Figure 4-55: SEM of rapeseed before extraction

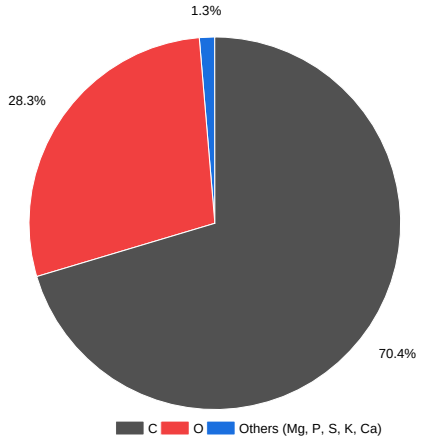

Figure 4-56: EDX of the rapeseed before extraction

The EDX shows must of the composition on the surface of the sample are carbon. This is true considering the presence of the seed coat in the sample. Also, triglycerides consist of carbon, hydrogen, and oxygen. However, the hydrogen is not detected because EDX detects elements in the K shell and not valences like hydrogen. Other elements included magnesium, phosphorus, sulphur, potassium, and calcium were detected only in a trace amount. Most of which might come from the seed coat.

4.3.2 Yield of Extraction using Hexane and Methanol

The percentage yield of the oil was determined by extracting using hexane and methanol. The experiment was performed, as explained in section 3.4.1. The result for both solvents is shown in *Figure **4-57*** below.

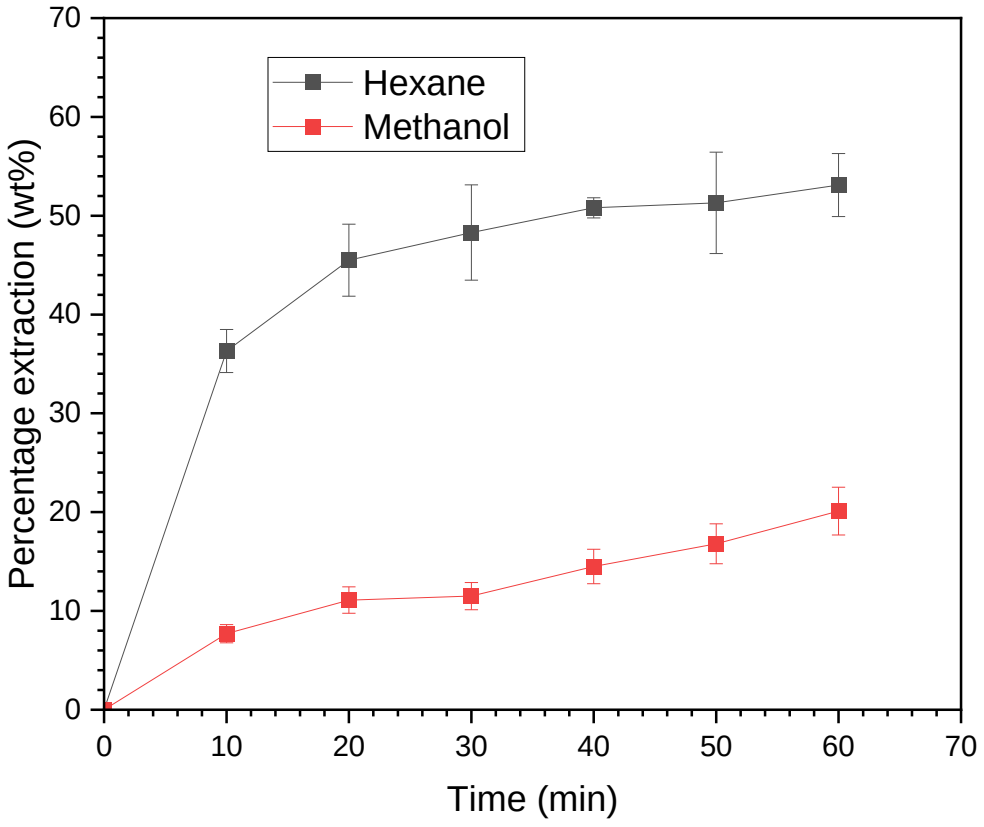

Figure 4-57: Soxhlet extraction of rapeseed using hexane and methanol with 500:1 molar ratio.

The extraction with hexane was mainly the triglyceride. No other non-triglyceride substance was observed. Hence, the percentage extraction for hexane is the same as the percentage of oil content. The result obtained with hexane is higher than 44 – 45 wt% reported by Li et al. (2014) and 45.9 wt% reported by Zakaria (2010). The difference

reported from this study might be due to the higher temperature used. However, the oil content using methanol was low. The highest achieved was 20 wt%. Szydłowska-Czerniak et al. (2010) extracted 40.5 – 46.5% using methanol and water from seven different rapeseed species. Methanol as solvent extract mixture of phospholipids, sterols, phenols, and vitamins from the oil seed (Szydłowska-Czerniak et al., 2010, Zakaria, 2010). This was because all these compounds which are found in the seed oil are soluble in methanol. The low oil content extracted might be due to short extraction time (60 minutes) compared 6 hours reported by Zakaria (2010). The high oil content obtained by Szydłowska-Czerniak et al. (2010) might be due to the mixture of methanol to water. The authors also mix the oil seed into the solvent compared to the thimble used for this study.

4.3.3 Properties of the Extracted Oil

The oil extracted was characterised for free fatty acid, acid number, density, refractive index, and viscosity. The result is shown in *Table **4-5*** below.

Table 4-5: Characterisation of extracted oil using hexane and methanol.

	Triglyceride	Hexane 60 min	Hexane 20 min	Methanol 60 min	Methanol 20 min
FFA (%)	0.225	1.8±0.4	1.5±0.7	2.1±0.3	1.8±0.6
Acid number (mgKOH/g sample)	0.45	3.6	3.0	4.2	3.6
Density (g/cm^3)	0.911	0.911	0.911	0.914	0.914
Refractive index	1.473	1.471	1.470	1.405	1.356
Viscosity (Pa.s)	0.074	0.078	0.077	0.073	0.072

Both free fatty acid and acid number are important in biodiesel production to choose catalysts to avoid soap formation. Knothe et al. (2005) reported that the presence of free fatty acid, unreacted triglyceride, excess alcohol, glycerol by-product, and catalyst in the biodiesel might deteriorate the fuel or cause a performance problem. The importance of all the properties is, as mentioned in section 4.2.1.

The free fatty acid from the commercial triglyceride was lower than the extracted oil. Pre-treatment might be necessary if alkaline transesterification is to be used, to reduce

soap formation and increase yield, though not necessary with an acid catalyst. The FFA reported for this work is lower than 3.35% reported by Zakaria (2010), though higher than 0.65% reported by Konuskan et al. (2019). The difference might be due to the rapeseed species, a period after harvest, and handling and extraction method.

The density for all the samples was similar. However, oil extracted using methanol were slightly higher. This might be due to the non-triglyceride compound present. The result also corresponds to 0.907 g/cm^3 reported by Noureddini et al. (1992a). Similarly, the viscosity of all the extracted oils was within the range of the commercial triglyceride. Again, triglycerides extracted with methanol were slightly lower. This might also be due to the non-triglyceride since they are soluble in the solvent. All the values were within the range (0.0788 Pa.s) reported by Noureddini et al. (1992b).

The FTIR spectra of the triglycerides extracted is shown in *Figure **4-58*** below.

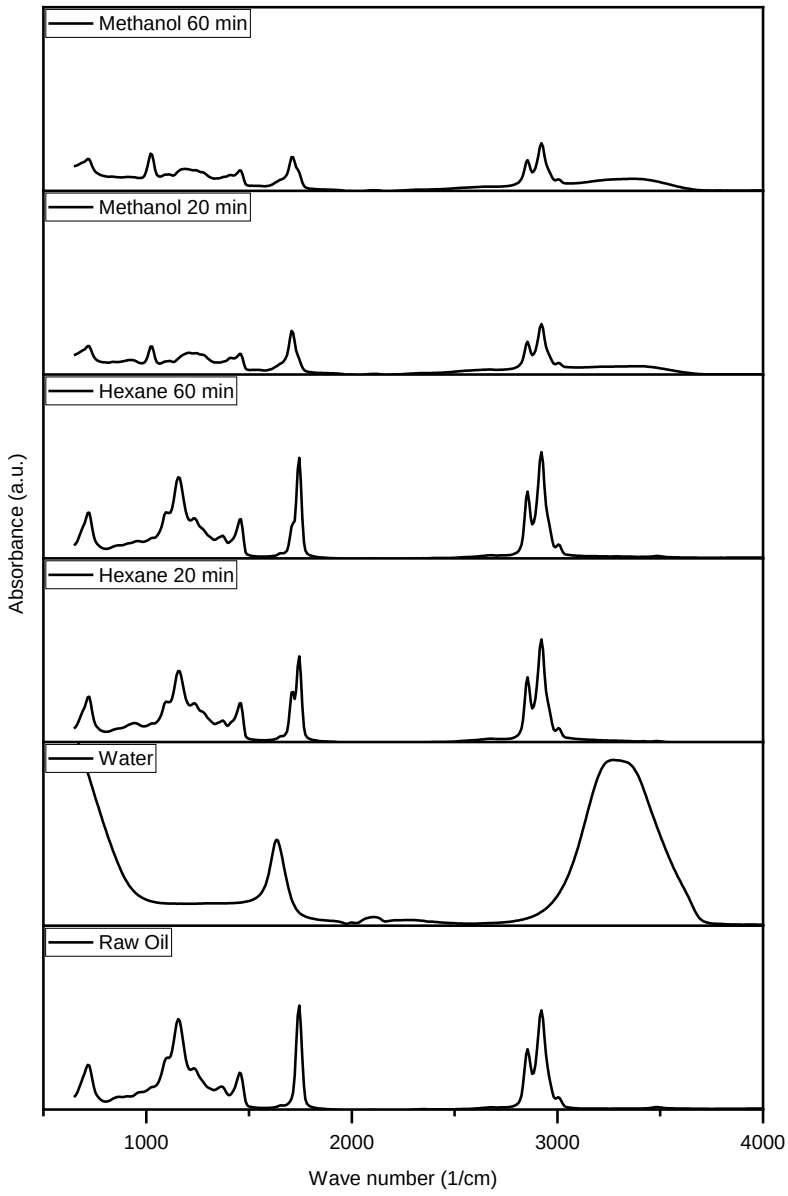

Figure 4-58: FTIR spectrum of extracted oil.

The commercial triglyceride and triglyceride extracted with hexane after 1 h have similar spectra. Both have a strong peak of the Carbonyl group (C = O) at 1744 cm^{-1} and C – O group at 1157 cm^{-1}. They also do not have the hydroxy stretch at 3000 – 3600 cm^{-1} which shows the triglycerides were clear from any hydroxyl containing compounds such as methanol or water. The triglyceride extracted with hexane for 20 min also has an asymmetric and symmetric stretching vibration of $-CH_2$ and $-CH_3$ group around wave number 2914 and 2847 cm^{-1}. The spectrum is the same as the commercial triglyceride, though with a lower signal. The signal was less with the methanol extracted triglyceride.

This might be due to the impurities in the triglyceride. Slight hydroxyl vibration at 3000 – 3600 cm^{-1} appears in these spectra, which might be due to the extraction with methanol.

Fewer lipids can be seen covering the seeds surface after extraction (as shown in *Figure **4-59*** below) compared to the feed before extraction.

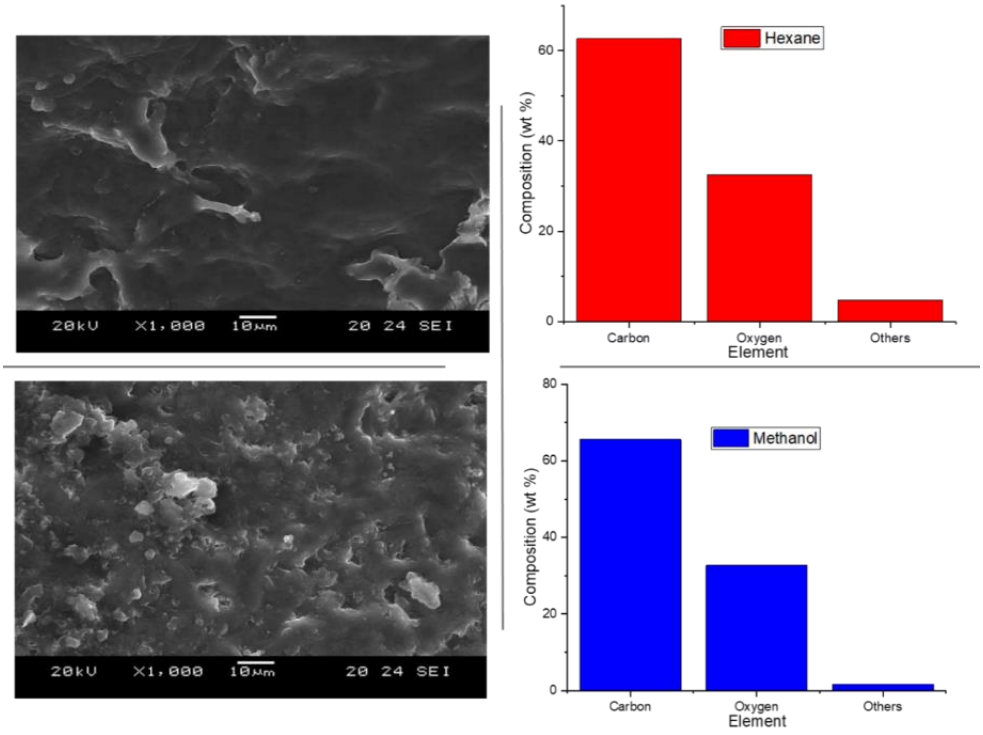

Figure 4-59: SEM and EDX of the residue after extraction.

Hexane as a solvent interacts better with the lipids, hence the pores after extraction are more visible. However, the extraction might be better if the seeds were soaked to the solvent rather than packed in a thimble.

The composition on the surface of the residues for both solvent recorded higher carbon content (above 60 wt%). The values are slightly lower than 70 wt% recorded for the feed before extraction. This might be due to the high carbon content in triglyceride before extraction. More triglyceride was extracted with hexane as a solvent than methanol. After extraction with methanol (~ 66 wt%), the carbon content is slightly higher than when hexane (~ 63 wt%) was used. This also shows that both rapeseed cake and seed coats are mainly carbon compounds, as expected. The residues oxygen content for both

extractions is equal (~ 33 wt%), though higher than 28 wt% found in the feed before extraction. The other elements of magnesium, phosphorus, sulphur, potassium, and calcium make up less than 5 wt% of the composition. Methanol recorded less of the other elements than the extraction with hexane. This might be because the non-triglyceride compounds are soluble in methanol and extracted together with the oil.

4.3.4 Reactive Extraction

The reactive extraction method is to extract and transesterified triglyceride. Much research is available on reactive extraction, and a few have been reported by this group (Kasim and Harvey, 2011, Salam et al., 2016, Zakaria and Harvey, 2012). Reactive extraction can either be conventional in which the seed is poured directly into alcohol. Reactive extraction can also be done with the seed poured in a thimble and placed in the extractor of the Soxhlet extractor. For this study, this method was referred to as "reactive extraction in Soxhlet extractor". In this method, the residual seed cake filtration after the reaction is not required since the feeds are in a thimble. The result for both methods is shown in *Figure **4-60*** and *Figure **4-61*** below.

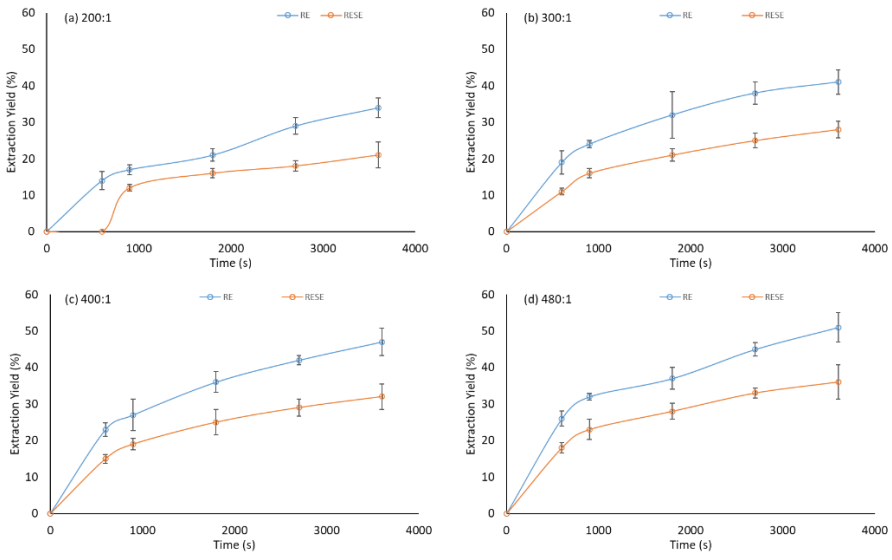

Figure 4-60: Extraction yield for reactive extraction at (a) 200:1, (b) 300:1, (c) 400:1, and (d) 480:1 using H_2SO_4 as catalyst.

The yield of both extraction and FAME in reactive extraction (RE) is greater than the yield of reactive extraction in Soxhlet extractor (RESE). The yield was determined in relation

to the amount of triglyceride extracted using hexane. Approximately 50 wt% yield of the extraction was the highest achieved with RE. The method has the advantage of close contact to the bulk solvent and continuous stirring to increase the diffusion through the pores. In contrast, 36 wt% was the highest yield of extraction in terms of RESE. This might be due to mass transfer limitations. RESE used the same principle as Soxhlet extraction, with the triglyceride conversion after extraction in the bulk solvent. The solvent must diffuse through the thimble and into the pores of the seed. This will be time-consuming when compared to RE. The yield extracted for RESE was slightly lower than 45 wt% reported for Soxhlet extraction using methanol. Shuit et al. (2009) reported 54% oil content in Jatropha curcas seed. The authors reported a 91% efficiency of the extraction after 24 h. The addition of n-hexane as a co-solvent increases the solubility of the oil in the mixture.

The poor solubility of methanol during Soxhlet extraction contributed to the low extraction yield. Zeng et al. (2009) reported 9% oil extraction from sunflower using methanol as the lowest compared to the other solvent used. The authors relate the low yield to the extraction of sugars and proteins from the seed. Özgül and Türkay (1993) reported that methanol extracts more of the free fatty acid and leaves behind the rice bran triglyceride. Zakaria (2010) also confirmed a low yield with methanol. The author relates the low yield to the non-triglyceride that was extracted from the seed. This was the reason for introducing a co-solvent, to increase the triglycerides solubility during extraction while methanol takes part in the transesterification.

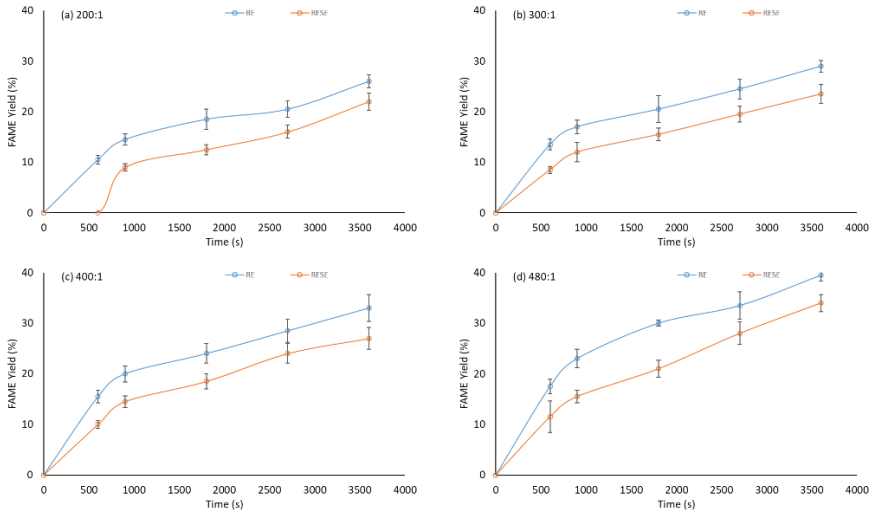

Figure 4-61: FAME yield for reactive extraction at (a) 200:1, (b) 300:1, (c) 400:1, and (d) 480:1 using H_2SO_4 as catalyst.

The highest FAME yield achieved from this study (*Figure **4-61***) was approximately 40%, in RE with 480:1 molar ratio. RESE achieved 34% as the highest FAME yield. Zakaria (2010) achieved 90% FAME yield with 475:1 molar ratio using an alkaline catalyst. Shuit et al. (2009) reported 99.8% FAME yield with an acid catalyst, though in the presence of a co-solvent and after 24h. Zeng et al. (2009) achieved about 98% FAME with 100:1 molar ratio of methanol to oil and diethoxymethane as a co-solvent. The low FAME yield from this study might be due to acid catalyst used and methanol as solvent.

RESE was observed to be slow at the beginning of the reaction due to the extraction technique. However, the conversion becomes faster as the triglyceride mixed to the bulk solvent and catalyst. Also, since the extraction is in a cycle, each batch extracted has a good time to achieve reasonable conversion before the next cycle. The conversion decreases as the bulk solvent are saturated with the triglyceride extracted.

Shuit et al. (2009) reported the triglycerides conversion to occur in the pores of the seed in reactive extraction. The authors affirmed that the rate of FAME production is the same as the rate of extraction. This conclusion might not be true in all cases, especially when methanol is used as the only solvent. This is because non-triglyceride is accompanied during the extraction. Shuit et al. (2009) also reported that the feeds particle size does not affect both extraction and transesterification in the first eight (8) hours of the process. This was because the extraction can be improved with a large

surface area of the seed. Since the process was monitored for this study for one hour, no significant difference will be recorded with different particle sizes.

*Figure **4-62*** below is the SEM and EDX of the residual cake after reactive extraction at 480:1 and 1h.

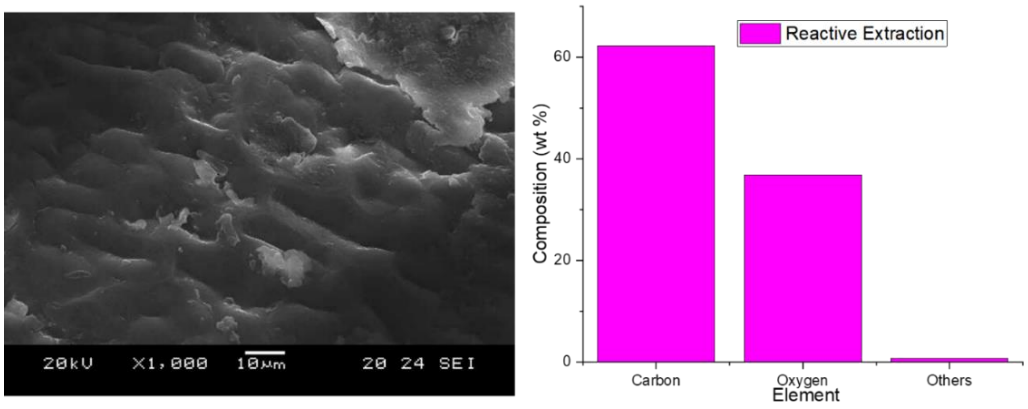

Figure 4-62: SEM and EDX of a sample after reactive extraction.

The SEM image (*Figure **4-62***) shows pores after extraction with fewer lipids covering the seeds surface. A clear image of the pores was achieved due to the high diffusion of the solvent. The empty pores trapping the lipids are seen after reactive extraction than when Soxhlet extraction was performed or the feeds image before extraction. The EDX has a similar result to the extraction with Soxhlet. About 62% of carbon content was recorded compared to 70% from the feed. The less carbon compared to the feed indicates the triglycerides extraction, which majorly consists of carbon and hydrogen.

4.3.5 Combined Reactive Extraction and Reactive Coupling

In this section, reactive extraction and reactive coupling were combined. The effect of molar ratio (150:1 – 450:1), temperature (130 – 160 ^{o}C), and catalyst concentration (0.5 – 5 wt%) was studied. *Figure **4-63*** below shows the effect of molar ratio in combined reactive extraction and reactive coupling.

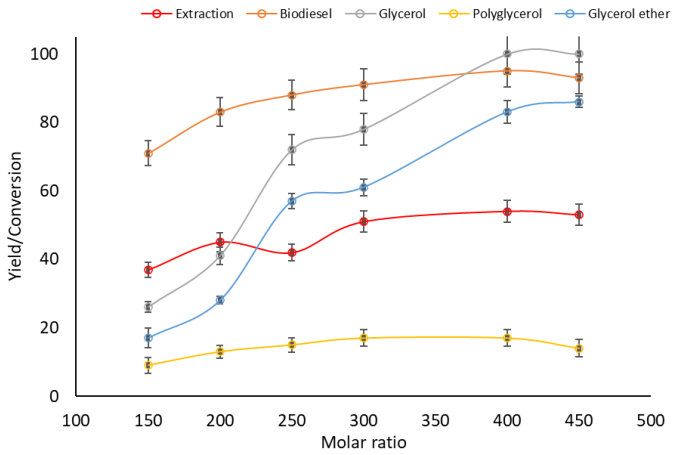

Figure 4-63: Effect of molar ratio on the combined reactive extraction and reactive coupling.

Among the important variables in reactive extraction is the molar ratio. This is because it determined the extent of the extraction. The extraction is fast in the beginning. The extraction becomes slow when the bulk solvent becomes concentrated with the extract.

The extraction yield increased from 37% at 150:1 to 53% as the molar ratio increased to 450:1. This is because more of the bulk solvent could interact with the exposed inner part of the seed. It was also noted that the extract consists of the non-triglyceride due to the solvent used. This also contributed to the difficulty in the separation.

The FAME yield increase with an increase in the molar ratio. The yield increased from 71% at 150:1 to 95% at 400:1 molar ratio. This might be due to more solvent, increasing the rate of triglyceride extraction. It can also be because the triglycerides conversion to biodiesel occurs inside the pores of the seed during reactive extraction (Shuit et al., 2009, Zakaria, 2010). A slight decrease to 93% was observed when the molar ratio was increased to 450:1. The decrease might be due to difficulty in separation due to the excess alcohol or competing reaction to convert glycerol by-product.

The experiment observed the peaks disappearance related to the glycerol as the molar ratio increased to 400:1. At this stage, the glycerol is assumed to be converted completely. The glycerol was observed to increase in conversion from 26% (at 150:1) to 78% (at 300:1) and then totally converted as the molar ratio increase 400:1. This is because glycerol etherification is fast and favoured with excess methanol for glycerol ethers. The highest yield of 86% was achieved with 450:1 molar ratio. However, the

lowest yield of 17% was recorded with 150:1 molar ratio. The highest polyglycerol was achieved at 300:1 and 400:1 with 17% each. The lower polyglycerol yield at 150:1 (9%) might be due to the low extraction of the triglyceride and FAME production. A slight decrease was observed at 450:1.

The effect of temperature for the combined reactive extraction and reactive coupling was considered, as shown in *Figure **4-64*** below. The temperature used was 130, 140, 150, and 160 °C for 1h. The temperature chosen was the same as used in glycerol valorisation and reactive coupling. According to Le-Chatelier's principle, temperature change alters the equilibrium of a reaction. This makes temperature vital in must reactions.

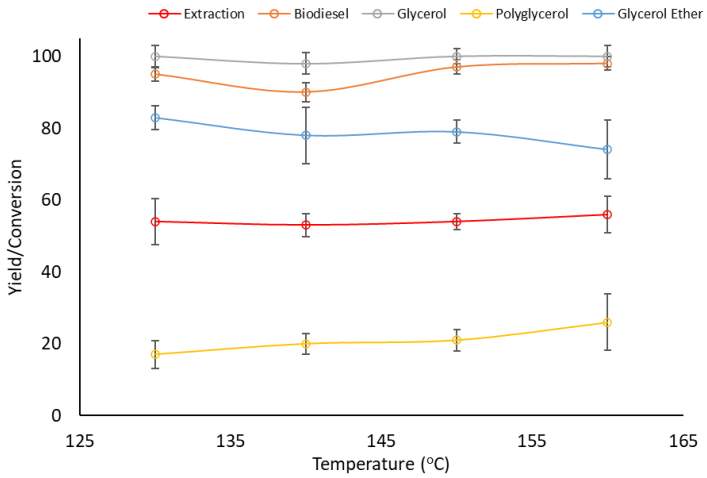

Figure 4-64: Effect of temperature on the combined reactive extraction and reactive coupling.

The extraction was observed to be relatively constant. This might be because the bulk solvent (400:1) is concentrated, though the extraction rate was faster. Approximately 53% of extraction was achieved as the temperature increased from 130 to 160 °C in 1 h. Such high temperatures might not be necessary for such extraction, rather increase the cost. However, the high temperature was not purposely for the extraction but for the other reactions that were coupled.

The yield of biodiesel was observed to be relatively constant also as the temperature increased from 130 to 160 °C with the highest yield of 98% achieved. As expected, by using high temperatures, higher triglyceride conversion is achieved. This is because

higher temperature contributes to higher miscibility and fast reaction. However, since transesterification in reactive extraction takes place in the pores of the seeds before extraction, the extraction is proportional to biodiesel produce at a constant molar ratio and catalyst concentration.

An increase in the percentage yield of the polyglycerol production was observed from 17 to 26% as the temperature increased from 130 to 160 ^{o}C. However, glycerol ethers slightly decrease from approximately 83 to 74%. In section 4.2.4.3 of this study, it was observed that an increase in temperature during reactive coupling slightly decreased the yield of polyglycerol and glycerol ethers. This might be due to a competing reaction between the triglyceride conversion and glycerol valorisation. In this section, an increase in polyglycerol was observed. This is due to the solubility of alcohol to the non-triglyceride, reducing the available excess methanol that will take part in the glycerol etherification. This will then favoured the polyglycerol production as reported in section 4.2.4.2.

*Figure **4-65*** below shows the effect of catalyst concentration (0.5, 1, 2, 3, and 5 wt%) for the combined reactive extraction and reactive coupling. The reaction was performed for 1h at 400:1 and 130 ^{o}C.

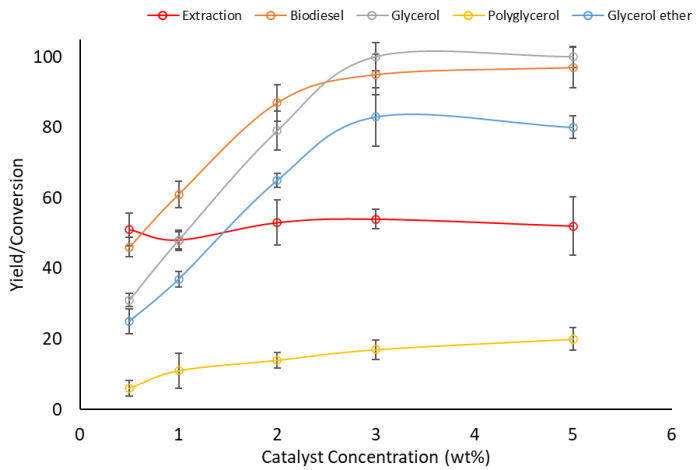

Figure 4-65: Effect of catalyst concentration on the combined reactive extraction and reactive coupling

Another important variable mentioned by Le-Chatelier catalyst concentration. An acid catalyst for this study is to favour the reactions due to the high moisture content in the

seed. The high moisture leads to the high free fatty acid, which produces soap during transesterification with an alkaline catalyst.

The constant yield of extraction from the result shows catalyst does not affect extraction. However, the effect was observed as expected with triglyceride conversion. The biodiesel yield increased from 46 to 97% as catalyst concentration increase from 0.5 to 5 wt%, respectively. High acid catalyst concentration is required for higher triglyceride conversion (Lotero et al., 2005).

A similar trend was observed with glycerol conversion and glycerol ethers yield. This shows both transesterification and glycerol etherification are catalytic driven. The glycerol conversion increase from 31 to 100% as catalyst concentration increase from 0.5 to 5 wt%, respectively. In comparison, 25 to 80% yield of glycerol ethers was achieved with 0.5 to 5 wt% respectively. Also, the yield of polyglycerol produced was observed to increase from 6 to 20%. The low yield of the polyglycerol compared to the glycerol ethers is due to the excess alcohol used and the faster reaction rate.

4.3.6 Summary of Combined Reactive Extraction and Reactive Coupling

This section majorly shows the proof-of-concept for the combined reactive extraction and reactive coupling. The high moisture content of the seed leads to high free fatty acid in the triglyceride, hence using the acid catalyst for the process. Combined reactive extraction and reactive coupling achieved high extraction and conversion within an hour with a higher molar ratio of methanol to oil (400:1). The excess molar ratio contributes to the higher conversion of glycerol to glycerol ethers.

Chapter 5. CONCLUSIONS AND FURTHER WORK

This research aimed to intensify biodiesel production, whilst reducing/valorising waste glycerol, via reactive coupling. If this can be done in situ, without adverse effects on other steps of the process, biodiesel production economics could be substantially improved. "Reactive coupling" is a technique in which the by-product of one reaction is simultaneously converted to an added-value product in a second, in a "single pot"/single step. Here, the glycerol by-product was simultaneously converted to polyglycerol (mainly diglycerol, triglycerol, and tetraglycerol used in the pharmaceutical, food, and cosmetics industries) and glycerol ethers (used as oxygenated compounds to improve biofuel combustion in a diesel engine) in the second reaction. This is an attractive approach to the production of biodiesel. The technique has the advantages of (i) reducing the production of glycerol by-product by converting it to an added-value product, (ii) reducing the methanol usage during transesterification, (iii) faster conversion of triglyceride to biodiesel using an acid catalyst, and (iv) easier downstream phase separation. The process may be further enhanced if it is allied to reactive extraction, i.e., the extraction of oil from the seed and its conversion to biodiesel in one step. In a reactive extraction/coupling process the oil in the seed would be converted to biodiesel, glycerol ether, and polyglycerol in one step, thereby greatly reducing the number of process steps, and the methanol requirement (and therefore cost).

The process was studied in three steps:

(i) A parametric study of the polymerisation (etherification) of glycerol was performed, to allow its kinetics to be determined and validated. The reaction was performed at 130 – 160 ^{o}C and 1 – 6 wt% catalyst concentration (using H_2SO_4) for up to 5h. A kinetic model for this reaction was developed and implemented in MATLAB, and the results compared with experimental data.

(ii) The parametric study of simultaneous biodiesel production and conversion of glycerol by-product to added value product was conducted. The reactive coupling was performed at molar ratio 4:1 – 8:1, temperature 130 – 160 ^{o}C, and concentration of H_2SO_4 as catalyst (1 – 5 wt%) for up to 1h. The kinetics of the reactive coupling was simulated to fit the experimental result using MATLAB. The kinetics model for biodiesel using H_2SO_4 was adopted from literature, while

the developed model for glycerol etherification were both used for the kinetics of reactive coupling.

(iii) Finally, the proof-of-concept for combined reactive extraction/reactive coupling was demonstrated. The effect of molar ratio (150:1 – 450:1), temperature (130 – 160 ^{o}C), and catalyst concentration (0.5 – 5 wt%) were studied.

Glycerol valorisation was performed in the range 130 – 160 ^{o}C at catalyst (sulfuric acid) concentrations of 1 – 6 wt%. The highest conversion achieved was 68% at 160 ^{o}C and 6 wt% after 5h. Due to the low reaction rate, high temperatures and catalyst concentrations are required to achieve higher conversion. For complete conversion to be achieved, the reaction will take over 5h. The highest polyglycerol yield achieved was approximately 63%, comprising 47% diglycerol, 9% triglycerol, and 6% tetraglycerol. Use of an acid catalyst here led to the formation of unwanted by-products at the higher temperatures and catalyst concentrations. The principal by-products were acrolein, formed through dehydration and hydrogen, by decomposition of glycerol. The highest yield of hydrogen was 4.3% at 150 ^{o}C, 6 wt%, and 5h, while the highest yield of acrolein was 1.6% at 160 ^{o}C, 6 wt%, and 5h. The by-products and residual carbon production can be reduced/avoided with low catalyst concentration and low temperature.

A kinetic reaction model fitted the experimental data with R^2 of over 0.95. The model was second order in glycerol consumption, with an activation energy of 112 kJ/mol and a pre-exponential factor of 2.18×10^{11} $Lmol^{-1}s^{-1}$. The thermodynamic properties show the reaction was endothermic with enthalpy 109 $kJ.mol^{-1}$, less disordered with an entropy of – 38.1 $Jmol^{-1}K^{-1}$, and endergonic with Gibbs free energy of about 125 $kJ.mol^{-1}$.

It was shown that reactive coupling could be used to achieve 100% conversion of triglyceride after 1h using sulfuric acid at a molar ratio of 4:1. The relatively low molar ratio (conventional processes use 6:1 at least) is advantageous for the process economics. It reduces the amount of methanol that has to be recycled, representing a significant energy saving. This is possible because the crude glycerol takes part in a second reaction, favouring the forward reaction in transesterification and reducing the requirement of methanol.

Reactive coupling technique achieved up to 100% FAME yield. Both triglyceride conversion and yield of FAME increased with increase in the reaction parameters

(temperature (130 – 160^{o}C), molar ratio (4:1 – 8:1), catalyst concentration (1 – 5 wt%) and time (up to 1h). The separation into phases was immediate with reactive coupling than the conventional methods that required up to 24h to settle.

The reactive coupling converts the glycerol by-product into glycerol ethers and polyglycerols via an etherification reaction. Approximately 60% glycerol conversion was achieved after 1h with about 90% selectivity towards glycerol ethers. Increasing the molar ratio of methanol to oil from 4:1 to 8:1, increased glycerol ethers production whilst reducing polyglycerol production. The methanol remaining after biodiesel production reacted more quickly with the hydroxyl groups of the glycerol than glycerol self-etherification. An unexpected decrease in polyglycerol and glycerol ethers was observed as the temperature increased. However, 100% conversion of the triglyceride was achieved. Catalyst concentration was expected to cause an increase in glycerol etherification. The increase was observed, but due to the slow reaction rate, the yield slightly increased as the concentration was increased. Reaction time in reactive coupling has a positive effect as all the products increased with time.

The reactive coupling model fitted the FAME and triglyceride data well (R^2 of 0.99 and 0.98, respectively). The experimental data for glycerol conversion was able to fit the model with an R^2 of 0.96. Similarly, the experimental data for polyglycerol production fit the model with an R^2 of 0.95.

The oil content of the rapeseed used for combined reactive extraction/reactive coupling was ~50%. The moisture content (~16%) and free fatty acid level (2.1%) were relatively high, which suggested using an acid catalyst rather than the base, which fitted well with the subsequent oligomerisation of the glycerol.

A proof-of-concept was established for combined reactive extraction/reactive coupling. 50% extraction yield was achieved within an hour with a molar ratio of 300:1 to 480:1 and reduced as expected to 37% at 150:1. High FAME yield of up to 98% was achieved at 130 to 160 ^{o}C due to fast reaction and improved miscibility. The excess methanol increased the conversion of glycerol from 26% at 150:1 to 100% at 400:1. This was

because of the fast reaction of glycerol to methanol etherification than glycerol self-etherification.

Overall, it demonstrates proof-of-concept for reactive coupling and combined reactive extraction/reactive coupling. This technique could intensify biodiesel production by reducing the excess alcohol requirement, thereby removing the process alcohol purification and recycling units. It will also reduce the production of crude glycerol by directly converting it to a value-added product. Fast conversion of triglyceride is achieved with the technique and easy downstream phase separation.

5.1 Further Work

Reactive coupling is a new technique; hence, more work should be done to take it to the commercial level.

(i) In line with industry 4.0, online analysis for reactive coupling will add value to the study and give a more accurate result since the FTIR spectra can show the increase in the ether group and a decrease in the hydroxyl group for the glycerol conversion. It can also detect the methyl groups appearance during transesterification; then it will be a viable option for online analysis. Also, a set refractive index can be used online for all the expected products. However, there will be a need for the re-structuring of the reactor.

(ii) One of the challenges faced during this study was the low conversion of glycerol to added-value products. This was because the reaction rate was low, which requires a longer reaction time to achieve complete conversion. The use of microreactors and the oscillatory baffled reactor will reduce the mass transfer limitation, hence might be a good option. However, using a microreactor or OBR might require good insulation to avoid heat loss to the surrounding.

(iii) A single kinetics model showing biodiesel production, triglyceride conversion, glycerol production and conversion, and glycerol added value products should be developed for the future. This will be more realistic and useful, explaining how the variables affect the reactants/products than the separate models.

(iv) Much research has been reported on reactive extraction, but more work can be done on Soxhlet extractor reactive extraction to enable fast reaction and possible reactive coupling. The optimisation study should be done by varying temperature, molar ratio, the particle size of the seeds, and stirring rate. Also, the use of various catalysts such as alkaline and heterogeneous catalysts might see an increase in the conversion of the triglyceride. Again, the use of co-solvent such as hexane and petroleum ether can increase the extraction with less of the non-triglycerides.

(v) More work should be done on the combined reactive extraction/reactive coupling to optimise the process parameters and study more parameters, such as stirring and particle size. Studying the kinetics of the process will also add value to knowledge, especially since transesterification was reported to occur in the pores during reactive extraction. In the future, various catalyst should be tried, such as alkaline due to cheapness, availability, and commercial importance. The use of co-solvent to reduce the extraction of non-triglyceride and increase the extraction of lipids could improve this studys result. This will enhance the miscibility and increase the yield of extraction. It is also essential to study the process engineering for reactive coupling and combined reactive extraction/reactive coupling. This is to improve the design, control, and industrial optimisation of the biodiesel with reactive coupling technique.

(vi) The model developed should be used to determine the optimal reaction conditions of the process. The operation conditions should also be used to determine the experimental values. Techno-economic analysis of the technique should also be perform. This will show if the technique is economically viable compared to the conventional method used in large scale production.

REFERENCES

ABDALLA, B. K. & OSHAIK, F. O. A. 2013. Base-transesterification process for biodiesel fuel production from spent frying oils. *Agricultural Sciences,* 4**,** 85 - 88.

ABOELAZAYEM, O., GADALLA, M. & SAHA, B. 2018a. Biodiesel production from waste cooking oil via supercritical methanol: Optimisation and reactor simulation. *Renewable Energy,* 124**,** 144-154.

ABOELAZAYEM, O., GADALLA, M. & SAHA, B. 2018b. Valorisation of high acid value waste cooking oil into biodiesel using supercritical methanolysis: Experimental assessment and statistical optimisation on typical Egyptian feedstock. *Energy,* 162**,** 408-420.

ADHIKARI, S., FERNANDO, S., GWALTNEY, S. R., FILIP TO, S. D., MARK BRICKA, R., STEELE, P. H. & HARYANTO, A. 2007. A thermodynamic analysis of hydrogen production by steam reforming of glycerol. *International Journal of Hydrogen Energy,* 32**,** 2875-2880.

AHMAD, K. A., ABDULLAH, M. E., HASSAN, N. A., AMBAK, K. B., MUSBAH, A., USMAN, N. & BAKAR, S. K. B. A. 2016. Extraction techniques and industrial applications of jatropha curcas. *Jurnal Teknologi,* 78**,** 53-60.

AIMARETTI, N., MANUALE, D. L., MAZZIERI, V., VERA, C. R. & YORI, J. C. 2009. Batch study of glycerol decomposition in one-stage supercritical production of biodiesel. *Energy & Fuels,* 23**,** 1076-1080.

AL-SAADI, L. S., EZE, V. C. & HARVEY, A. P. 2018. Experimental determination of optimal conditions for reactive coupling of biodiesel production with in situ glycerol carbonate formation in a triglyceride transesterification process. *Frontiers in chemistry,* 6**,** 1 - 11.

AL-SAADI, L. S., EZE, V. C. & HARVEY, A. P. 2019. A reactive coupling process for co-production of solketal and biodiesel. *Green Processing and Synthesis,* 8**,** 516-524.

AL-ZUHAIR, S., HUSSEIN, A., AL-MARZOUQI, A. H. & HASHIM, I. 2012. Continuous production of biodiesel from fat extracted from lamb meat in supercritical CO2 media. *Biochemical Engineering Journal,* 60**,** 106-110.

ALGOUFI, Y. T., KABIR, G. & HAMEED, B. H. 2017. Synthesis of glycerol carbonate from biodiesel by-product glycerol over calcined dolomite. *Journal of the Taiwan Institute of Chemical Engineers,* 70**,** 179-187.

ALHANASH, A., KOZHEVNIKOVA, E. F. & KOZHEVNIKOV, I. V. 2010. Gas-phase dehydration of glycerol to acrolein catalysed by caesium heteropoly salt. *Applied Catalysis A: General,* 378**,** 11-18.

ALMAS, Q., SIEVERS, C. & JONES, C. W. 2019. Role of the mesopore generation method in structure, activity and stability of MFI catalysts in glycerol acetylation. *Applied Catalysis A: General,* 571**,** 107-117.

ALPTEKIN, E. & CANAKCI, M. 2011. Optimization of transesterification for methyl ester production from chicken fat. *Fuel,* 90**,** 2630-2638.

AMMAJI, S., RAO, G. S. & CHARY, K. V. 2018. Acetalization of glycerol with acetone over various metal-modified SBA-15 catalysts. *Applied Petrochemical Research,* 8**,** 107-118.

ANASTOPOULOS, G., ZANNIKOU, Y., STOURNAS, S. & KALLIGEROS, S. 2009. Transesterification of vegetable oils with ethanol and characterization of the key fuel properties of ethyl esters. *Energies,* 2**,** 362-376.

ANITHA, M., KAMARUDIN, S. K. & KOFLI, N. T. 2016. The potential of glycerol as a value-added commodity. *Chemical Engineering Journal,* 295**,** 119-130.
ANUAR, M. R., ABDULLAH, A. Z. & OTHMAN, M. R. 2013. Etherification of glycerol to polyglycerols over hydrotalcite catalyst prepared using a combustion method. *Catalysis Communications,* 32**,** 67-70.
ARDILA-SUÁREZ, C., ROJAS-AVELLANEDA, D. & RAMIREZ-CABALLERO, G. E. 2015. Effect of Temperature and Catalyst Concentration on Polyglycerol during Synthesis. *International Journal of Polymer Science,* 2015**,** 1 - 8.
ASHBY, R., SOLAIMAN, D. Y. & FOGLIA, T. 2004. Bacterial Poly(Hydroxyalkanoate) Polymer Production from the Biodiesel Co-product Stream. *Journal of Polymers and the Environment,* 12**,** 105-112.
ATADASHI, I., AROUA, M. K., AZIZ, A. A. & SULAIMAN, N. 2011. Membrane biodiesel production and refining technology: A critical review. *Renewable and Sustainable Energy Reviews,* 15**,** 5051-5062.
ATADASHI, I. M., AROUA, M. K., AZIZ, A. R. A. & SULAIMAN, N. M. N. 2013. The effects of catalysts in biodiesel production: A review. *Journal of industrial and engineering chemistry,* 19**,** 14-26.
ATTAPHONG, C., DO, L. & SABATINI, D. A. 2012. Vegetable oil-based microemulsions using carboxylate-based extended surfactants and their potential as an alternative renewable biofuel. *Fuel,* 94**,** 606-613.
ATTAPHONG, C. & SABATINI, D. A. 2013. Phase behaviors of vegetable oil-based microemulsion fuels: the effects of temperatures, surfactants, oils, and water in ethanol. *Energy & fuels,* 27**,** 6773-6780.
AYOUB, M. & ABDULLAH, A. Z. 2013a. Diglycerol synthesis via solvent-free selective glycerol etherification process over lithium-modified clay catalyst. *Chemical engineering journal,* 225**,** 784-789.
AYOUB, M. & ABDULLAH, A. Z. 2013b. LiOH-modified montmorillonite K-10 as catalyst for selective glycerol etherification to diglycerol. *Catalysis Communications,* 34**,** 22-25.
AYOUB, M., ABDULLAH, A. Z., AHMAD, M. & SULTANA, S. 2014. Performance of lithium modified zeolite Y catalyst in solvent-free conversion of glycerol to polyglycerols. *Journal of Taibah University for Science,* 8**,** 231-235.
AZAM, N. A. M., UEMURA, Y., KUSAKABE, K. & BUSTAM, M. A. 2016. Biodiesel production from palm oil using micro tube reactors: effects of catalyst concentration and residence time. *Procedia engineering,* 148**,** 354-360.
BAMBASE, M. E., NAKAMURA, N., TANAKA, J. & MATSUMURA, M. 2007. Kinetics of hydroxide-catalyzed methanolysis of crude sunflower oil for the production of fuel-grade methyl esters. *Journal of Chemical Technology & Biotechnology: International Research in Process, Environmental & Clean Technology,* 82**,** 273-280.
BANU, I., BUMBAC, G., BOMBOS, D., VELEA, S., GĂLAN, A.-M. & BOZGA, G. 2020. Glycerol acetylation with acetic acid over Purolite CT-275. Product yields and process kinetics. *Renewable Energy,* 148**,** 548-557.
BAROUTIAN, S., AROUA, M. K., RAMAN, A. A. A. & SULAIMAN, N. M. 2011. A packed bed membrane reactor for production of biodiesel using activated carbon supported catalyst. *Bioresource technology,* 102**,** 1095-1102.
BARROS, F. J. S., MORENO-TOST, R., CECILIA, J. A., LEDESMA-MUÑOZ, A. L., DE OLIVEIRA, L. C. C., LUNA, F. M. T. & VIEIRA, R. S. 2017. Glycerol oligomers

production by etherification using calcined eggshell as catalyst. *Molecular Catalysis,* 433**,** 282-290.
BASHIRI, H. & POURBEIRAM, N. 2016. Biodiesel production through transesterification of soybean oil: A kinetic Monte Carlo study. *Journal of Molecular Liquids,* 223**,** 10-15.
BEDOGNI, G. A., PADRÓ, C. L. & OKULIK, N. B. 2014. A combined experimental and computational study of the esterification reaction of glycerol with acetic acid. *Journal of molecular modeling,* 20**,** 2167.
BERCHMANS, H. J. & HIRATA, S. 2008. Biodiesel production from crude Jatropha curcas L. seed oil with a high content of free fatty acids. *Bioresource technology,* 99**,** 1716-1721.
BERRIOS, M., SILES, J., MARTIN, M. A. & MARTIN, A. 2007. A kinetic study of the esterification of free fatty acids (FFA) in sunflower oil. *Fuel,* 86**,** 2383-2388.
BHATTI, H. N., HANIF, M. A. & QASIM, M. 2008. Biodiesel production from waste tallow. *Fuel,* 87**,** 2961-2966.
BHUIYA, M. M. K., RASUL, M. G., KHAN, M. M. K. & ASHWATH, N. Comparison of oil refining and biodiesel production process between screw press and n-hexane techniques from beauty leaf feedstock. *In:* MORSHED, A. K. M. M., ALI, M. & AKANDA, M. A. S., eds. International Conference on Mechanical Engineering, 2016 2016. American Institute of Physics Inc., 1 - 6.
BIANCHI, P., WILLIAMS, J. D. & KAPPE, C. O. 2020. Oscillatory flow reactors for synthetic chemistry applications. *Journal of Flow Chemistry***,** 1-16.
BOOKONG, P., RUCHIRAWAT, S. & BOONYARATTANAKALIN, S. 2015. Optimization of microwave-assisted etherification of glycerol to polyglycerols by sodium carbonate as catalyst. *Chemical Engineering Journal,* 275**,** 253-261.
BORA, P., BORO, J., KONWAR, L. J. & DEKA, D. 2016. Formulation of microemulsion based hybrid biofuel from waste cooking oil–A comparative study with biodiesel. *Journal of the Energy Institute,* 89**,** 560-568.
BOZKURT, Ö. D., YILMAZ, F., BAĞLAR, N., ÇELEBI, S. & UZUN, A. 2019. Compatibility of di-and tri-tert-butyl glycerol ethers with gasoline. *Fuel,* 255**,** 1 - 10.
BRUNIAUX, S., VARMA, R. S. & LEN, C. 2019. A novel strategy for selective O-methylation of glycerol in subcritical methanol. *Frontiers in chemistry,* 7**,** 1 - 7.
BYRD, A. J., PANT, K. K. & GUPTA, R. B. 2008. Hydrogen production from glycerol by reforming in supercritical water over Ru/Al2O3 catalyst. *Fuel,* 87**,** 2956-2960.
CANAKCI, M. & VAN GERPEN, J. 1999. Biodiesel production via acid catalysis. *Transactions of the ASAE,* 42**,** 1203 - 1210.
CAO, P., DUBÉ, M. A. & TREMBLAY, A. Y. 2008a. High-purity fatty acid methyl ester production from canola, soybean, palm, and yellow grease lipids by means of a membrane reactor. *Biomass and Bioenergy,* 32**,** 1028-1036.
CAO, P., DUBÉ, M. A. & TREMBLAY, A. Y. 2008b. Methanol recycling in the production of biodiesel in a membrane reactor. *Fuel,* 87**,** 825-833.
CAO, P., TREMBLAY, A. Y., DUBE, M. A. & MORSE, K. 2007. Effect of membrane pore size on the performance of a membrane reactor for biodiesel production. *Industrial & engineering chemistry research,* 46**,** 52-58.
CARMONA-CABELLO, M., SÁEZ-BASTANTE, J., PINZI, S. & DORADO, M. 2019. Optimization of solid food waste oil biodiesel by ultrasound-assisted transesterification. *Fuel,* 255**,** 115817.

CASAS, A., RAMOS, M. J. & PEREZ, A. 2011. New trends in biodiesel production: Chemical interesterification of sunflower oil with methyl acetate. *Biomass and bioenergy,* 35**,** 1702-1709.

CASAS, A., RAMOS, M. J. & PÉREZ, Á. 2013. Methanol-enhanced chemical interesterification of sunflower oil with methyl acetate. *Fuel,* 106**,** 869-872.

CECILIA, J. A., GARCÍA-SANCHO, C., MÉRIDA-ROBLES, J. M., GONZÁLEZ, J. S., MORENO-TOST, R. & MAIRELES-TORRES, P. 2016. WO3 supported on Zr doped mesoporous SBA-15 silica for glycerol dehydration to acrolein. *Applied Catalysis A: General,* 516**,** 30-40.

CHAI, F., CAO, F., ZHAI, F., CHEN, Y., WANG, X. & SU, Z. 2007. Transesterification of vegetable oil to biodiesel using a heteropolyacid solid catalyst. *Advanced Synthesis & Catalysis,* 349**,** 1057-1065.

CHAI, S.-H., WANG, H.-P., LIANG, Y. & XU, B.-Q. 2009. Sustainable production of acrolein: preparation and characterization of zirconia-supported 12-tungstophosphoric acid catalyst for gas-phase dehydration of glycerol. *Applied Catalysis A: General,* 353**,** 213-222.

CHANG, J.-S., LEE, Y.-D., CHOU, L. C.-S., LING, T.-R. & CHOU, T.-C. 2012. Methylation of glycerol with dimethyl sulfate to produce a new oxygenate additive for diesels. *Industrial & engineering chemistry research,* 51**,** 655-661.

CHEE LOONG, T. & IDRIS, A. 2017. One step transesterification of biodiesel production using simultaneous cooling and microwave heating. *Journal of Cleaner Production,* 146**,** 57-62.

CHEN, C.-L., HUANG, C.-C., TRAN, D.-T. & CHANG, J.-S. 2012. Biodiesel synthesis via heterogeneous catalysis using modified strontium oxides as the catalysts. *Bioresource technology,* 113**,** 8-13.

CHEN, L., NOHAIR, B. & KALIAGUINE, S. 2016. Glycerol acetalization with formaldehyde using water-tolerant solid acids. *Applied Catalysis A: General,* 509**,** 143-152.

CHEN, L., NOHAIR, B., ZHAO, D. & KALIAGUINE, S. 2018. Glycerol acetalization with formaldehyde using heteropolyacid salts supported on mesostructured silica. *Applied Catalysis A: General,* 549**,** 207-215.

CHENG, L.-H., YEN, S.-Y., SU, L.-S. & CHEN, J. 2010. Study on membrane reactors for biodiesel production by phase behaviors of canola oil methanolysis in batch reactors. *Bioresource technology,* 101**,** 6663-6668.

CIRIMINNA, R., PINA, C. D., ROSSI, M. & PAGLIARO, M. 2014. Understanding the glycerol market. *European Journal of Lipid Science and Technology,* 116**,** 1432-1439.

CLACENS, J. M., POUILLOUX, Y. & BARRAULT, J. 2002. Selective etherification of glycerol to polyglycerols over impregnated basic MCM-41 type mesoporous catalysts. *Applied Catalysis A: General,* 227**,** 181-190.

CORMA, A., HUBER, G. W., SAUVANAUD, L. & O'CONNOR, P. 2008. Biomass to chemicals: catalytic conversion of glycerol/water mixtures into acrolein, reaction network. *Journal of Catalysis,* 257**,** 163-171.

CUCCINIELLO, R., RICCIARDI, M., VITIELLO, R., DI SERIO, M., PROTO, A. & CAPACCHIONE, C. 2016. Synthesis of monoalkyl glyceryl ethers by ring opening of glycidol with alcohols in the presence of lewis acids. *ChemSusChem,* 9**,** 3272-3275.

DA SILVA, D. S., ALTINO, F. M., BORTOLUZZI, J. H. & MENEGHETTI, S. M. 2020. Investigation of Sn (IV) catalysts in glycerol acetylation. *Molecular Catalysis,* 494**,** 111130.

DA SILVA, G. P., MACK, M. & CONTIERO, J. 2009. Glycerol: A promising and abundant carbon source for industrial microbiology. *Biotechnology Advances,* 27**,** 30-39.
DA SILVA, M. J., JULIO, A. A., FERREIRA, S. O., DA SILVA, R. C. & CHAVES, D. M. 2019. Tin (II) phosphotungstate heteropoly salt: An efficient solid catalyst to synthesize bioadditives ethers from glycerol. *Fuel,* 254**,** 1 - 11.
DA SILVA, M. J., LIBERTO, N. A., LELES, L. C. D. A. & PEREIRA, U. A. 2016. Fe4 (SiW12O40) 3-catalyzed glycerol acetylation: Synthesis of bioadditives by using highly active Lewis acid catalyst. *Journal of Molecular Catalysis A: Chemical,* 422**,** 69-83.
DALIL, M., EDAKE, M., SUDEAU, C., DUBOIS, J.-L. & PATIENCE, G. S. 2016. Coke promoters improve acrolein selectivity in the gas-phase dehydration of glycerol to acrolein. *Applied Catalysis A: General,* 522**,** 80-89.
DALLA COSTA, B. O., DECOLATTI, H. P., LEGNOVERDE, M. S. & QUERINI, C. A. 2017. Influence of acidic properties of different solid acid catalysts for glycerol acetylation. *Catalysis Today,* 289**,** 222-230.
DARNOKO, D. & CHERYAN, M. 2000. Kinetics of palm oil transesterification in a batch reactor. *Journal of the American Oil Chemists' Society,* 77**,** 1263-1267.
DAUENHAUER, P. J., SALGE, J. R. & SCHMIDT, L. D. 2006. Renewable hydrogen by autothermal steam reforming of volatile carbohydrates. *Journal of Catalysis,* 244**,** 238-247.
DAWODU, F. A., AYODELE, O. O., XIN, J. & ZHANG, S. 2014. Dimethyl carbonate mediated production of biodiesel at different reaction temperatures. *Renewable Energy,* 68**,** 581-587.
DECOLATTI, H. P., DALLA COSTA, B. O. & QUERINI, C. A. 2015. Dehydration of glycerol to acrolein using H-ZSM5 zeolite modified by alkali treatment with NaOH. *Microporous and Mesoporous Materials,* 204**,** 180-189.
DELEPLANQUE, J., DUBOIS, J. L., DEVAUX, J. F. & UEDA, W. 2010. Production of acrolein and acrylic acid through dehydration and oxydehydration of glycerol with mixed oxide catalysts. *Catalysis Today,* 157**,** 351-358.
DEMIRBAS, A. 2005. Biodiesel production from vegetable oils via catalytic and non-catalytic supercritical methanol transesterification methods. *Progress in energy and combustion science,* 31**,** 466-487.
DEMIRBAS, A. 2008. *Biodiesel: A realistic Fuel Alternative for Diesel Engines,* London, Springer- Verlag London Limited.
DEMIRBAS, A. 2009. Progress and recent trends in biodiesel fuels. *Energy Conversion and Management,* 50**,** 14-34.
DEMIRBAS, A. 2011. Competitive liquid biofuels from biomass. *Applied Energy,* 88**,** 17-28.
DESHMANE, V. G., GOGATE, P. R. & PANDIT, A. B. 2009. Ultrasound assisted synthesis of isopropyl esters from palm fatty acid distillate. *Ultrasonics sonochemistry,* 16**,** 345-350.
DEVI, S., DEVASENA, T., SARATHA, S., THARMARAJ, P. & PANDIAN, K. 2014. Dithiocarbamate Post Functionalized Polypyrrole Modified Carbon Sphere for the Selective and Sensitive Detection of Mercury by Voltammetry Method. *Int. J. Electrochem. Sci,* 9**,** 670-683.
DHAWAN, M. S. & YADAV, G. D. 2018. Insight into a catalytic process for simultaneous production of biodiesel and glycerol carbonate from triglycerides. *Catalysis today,* 309**,** 161-171.

DHAWANE, S. H., BORA, A. P., KUMAR, T. & HALDER, G. 2017. Parametric optimization of biodiesel synthesis from rubber seed oil using iron doped carbon catalyst by Taguchi approach. *Renewable Energy,* 105**,** 616-624.

DIALLO, M. M., MIJOIN, J., LAFORGE, S. & POUILLOUX, Y. 2016. Preparation of Fe-BEA zeolites by isomorphous substitution for oxidehydration of glycerol to acrylic acid. *Catalysis Communications,* 79**,** 58-62.

DIN, N., IDRIS, Z., KIAN, Y. S. & HASSAN, H. A. 2013. Preparation of polyglycerol from palm-biodiesel crude glycerin. *Journal of Oil Palm Research,* 25**,** 289-297.

DIZGE, N., KESKINLER, B. & TANRISEVEN, A. 2009. Biodiesel production from canola oil by using lipase immobilized onto hydrophobic microporous styrene–divinylbenzene copolymer. *Biochemical Engineering Journal,* 44**,** 220-225.

DO, L. D., SINGH, V., CHEN, L., KIBBEY, T. C., GOLLAHALLI, S. R. & SABATINI, D. A. 2011. Algae, canola, or palm oils—diesel microemulsion fuels: phase behaviors, viscosity, and combustion properties. *International Journal of Green Energy,* 8**,** 748-767.

DOS SANTOS, M. B., ANDRADE, H. M. C. & MASCARENHAS, A. J. S. 2019. Oxidative dehydration of glycerol over alternative H, Fe-MCM-22 catalysts: Sustainable production of acrylic acid. *Microporous and Mesoporous Materials,* 278**,** 366-377.

DOSUNA-RODRÍGUEZ, I., ADRIANY, C. & GAIGNEAUX, E. M. 2011. Glycerol acetylation on sulphated zirconia in mild conditions. *Catalysis today,* 167**,** 56-63.

DOU, B., JIANG, B., SONG, Y., ZHANG, C., WANG, C., CHEN, H., DU, B. & XU, Y. 2016. Enhanced hydrogen production by sorption-enhanced steam reforming from glycerol with in-situ CO2 removal in a fixed-bed reactor. *Fuel,* 166**,** 340-346.

DOU, B., WANG, C., SONG, Y., CHEN, H. & XU, Y. 2014. Activity of Ni-Cu-Al based catalyst for renewable hydrogen production from steam reforming of glycerol. *Energy Conversion and Management,* 78**,** 253-259.

DU, W., XU, Y. & LIU, D. 2003. Lipase-catalysed transesterification of soya bean oil for biodiesel production during continuous batch operation. *Biotechnology and Applied Biochemistry,* 38**,** 103-106.

DUBÉ, M., TREMBLAY, A. & LIU, J. 2007. Biodiesel production using a membrane reactor. *Bioresource technology,* 98**,** 639-647.

ENDALEW, A. K., KIROS, Y. & ZANZI, R. 2011. Inorganic heterogeneous catalysts for biodiesel production from vegetable oils. *Biomass and bioenergy,* 35**,** 3787-3809.

ESTEBAN, J., DOMÍNGUEZ, E., LADERO, M. & GARCIA-OCHOA, F. 2015. Kinetics of the production of glycerol carbonate by transesterification of glycerol with dimethyl and ethylene carbonate using potassium methoxide, a highly active catalyst. *Fuel Processing Technology,* 138**,** 243-251.

ESTEVEZ, R., LÓPEZ, M., JIMÉNEZ-SANCHIDRIÁN, C., LUNA, D., ROMERO-SALGUERO, F. & BAUTISTA, F. 2016. Etherification of glycerol with tert-butyl alcohol over sulfonated hybrid silicas. *Applied Catalysis A: General,* 526**,** 155-163.

EZE, V. C. & HARVEY, A. P. 2018. Continuous reactive coupling of glycerol and acetone–A strategy for triglyceride transesterification and in-situ valorisation of glycerol by-product. *Chemical Engineering Journal,* 347**,** 41-51.

EZE, V. C., PHAN, A. N. & HARVEY, A. P. 2018. Intensified one-step biodiesel production from high water and free fatty acid waste cooking oils. *Fuel,* 220**,** 567-574.

EZE, V. C., PHAN, A. N., PIREZ, C., HARVEY, A. P., LEE, A. F. & WILSON, K. 2013. Heterogeneous catalysis in an oscillatory baffled flow reactor. *Catalysis Science & Technology,* 3**,** 2373-2379.

FADHIL, A. B., AHMED, K. M. & DHEYAB, M. M. 2017. Silybum marianum L. seed oil: A novel feedstock for biodiesel production. *Arabian Journal of Chemistry,* 10**,** S683-S690.

FALAHATI, H. & TREMBLAY, A. 2012. The effect of flux and residence time in the production of biodiesel from various feedstocks using a membrane reactor. *Fuel,* 91**,** 126-133.

FAN, P., WANG, J., XING, S., YANG, L., YANG, G., FU, J., MIAO, C. & LV, P. 2017. Synthesis of Glycerol-Free Biodiesel with Dimethyl Carbonate over Sulfonated Imidazolium Ionic Liquid. *Energy & Fuels,* 31**,** 4090-4095.

FAN, X., WANG, X. & CHEN, F. 2011. Biodiesel production from crude cottonseed oil: an optimization process using response surface methodology. *The Open Fuels & Energy Science Journal,* 4**,** 1 - 8.

FAROBIE, O., YANAGIDA, T. & MATSUMURA, Y. 2014. New approach of catalyst-free biodiesel production from canola oil in supercritical tert-butyl methyl ether (MTBE). *Fuel,* 135**,** 172-181.

FATONI, R., RAHMAN, M. & ELKAMEL, A. Optimization of biodiesel production by various plant sources and micro-reactor simulation. IOP Conference Series: Materials Science and Engineering, 2018. IOP Publishing, 012011.

FELICZAK-GUZIK, A. & NOWAK, I. 2019. Application of glycerol to synthesis of solvo-surfactants by using mesoporous materials containing niobium. *Microporous and Mesoporous Materials,* 277**,** 301-308.

FENG, X., YAO, Y., SU, Q., ZHAO, L., JIANG, W., JI, W. & AU, C.-T. 2015. Vanadium pyrophosphate oxides: The role of preparation chemistry in determining renewable acrolein production from glycerol dehydration. *Applied Catalysis B: Environmental,* 164**,** 31-39.

FERREIRA, P., FONSECA, I., RAMOS, A., VITAL, J. & CASTANHEIRO, J. 2009. Glycerol acetylation over dodecatungstophosphoric acid immobilized into a silica matrix as catalyst. *Applied Catalysis B: Environmental,* 91**,** 416-422.

FEYZI, M. & SHAHBAZI, Z. 2017. Preparation, kinetic and thermodynamic studies of Al–Sr nanocatalysts for biodiesel production. *Journal of the Taiwan Institute of Chemical Engineers,* 71**,** 145-155.

FREEDMAN, B., BUTTERFIELD, R. O. & PRYDE, E. H. 1986. Transesterification kinetics of soybean oil 1. *Journal of the American oil chemists' society,* 63**,** 1375-1380.

FREEDMAN, B., PRYDE, E. & MOUNTS, T. 1984. Variables affecting the yields of fatty esters from transesterified vegetable oils. *Journal of the American Oil Chemists Society,* 61**,** 1638-1643.

FRUSTERI, F., ARENA, F., BONURA, G., CANNILLA, C., SPADARO, L. & DI BLASI, O. 2009. Catalytic etherification of glycerol by tert-butyl alcohol to produce oxygenated additives for diesel fuel. *Applied Catalysis A: General,* 367**,** 77-83.

FURUTA, S., MATSUHASHI, H. & ARATA, K. 2004. Biodiesel fuel production with solid superacid catalysis in fixed bed reactor under atmospheric pressure. *Catalysis communications,* 5**,** 721-723.

GALADIMA, A. & MURAZA, O. 2016. A review on glycerol valorization to acrolein over solid acid catalysts. *Journal of the Taiwan Institute of Chemical Engineers,* 67**,** 29-44.

GALY, N., NGUYEN, R., BLACH, P., SAMBOU, S., LUART, D. & LEN, C. 2017. Glycerol oligomerization in continuous flow reactor. *Journal of Industrial and Engineering Chemistry,* 51**,** 312-318.

GARCÍA-MARTÍN, J. F., BARRIOS, C. C., ALÉS-ÁLVAREZ, F.-J., DOMINGUEZ-SÁEZ, A. & ALVAREZ-MATEOS, P. 2018. Biodiesel production from waste cooking oil in an oscillatory flow reactor. Performance as a fuel on a TDI diesel engine. *Renewable Energy,* 125**,** 546-556.

GARCÍA-SANCHO, C., MORENO-TOST, R., MÉRIDA-ROBLES, J. M., SANTAMARÍA-GONZÁLEZ, J., JIMÉNEZ-LÓPEZ, A. & TORRES, P. M. 2011. Etherification of glycerol to polyglycerols over MgAl mixed oxides. *Catalysis Today,* 167**,** 84-90.

GARTI, N., ASERIN, A. & ZAIDMAN, B. 1981. Polyglycerol esters: Optimization and techno-economic evaluation. *Journal of the American Oil Chemists' Society,* 58**,** 878-883.

GEACAI, S., NITA, I., IULIAN, O. & GEACAI, E. 2012. Refractive indices for biodiesel mixtures. *UPB Sci. Bull. Series B,* 74**,** 149-160.

GEORGOGIANNI, K., KONTOMINAS, M., POMONIS, P., AVLONITIS, D. & GERGIS, V. 2008. Conventional and in situ transesterification of sunflower seed oil for the production of biodiesel. *Fuel processing technology,* 89**,** 503-509.

GHOLAMI, Z., ABDULLAH, A. Z. & LEE, K.-T. 2013a. Glycerol etherification to polyglycerols using Ca 1+ x Al 1− x La x O 3 composite catalysts in a solventless medium. *Journal of the Taiwan Institute of Chemical Engineers,* 44**,** 117-122.

GHOLAMI, Z., ABDULLAH, A. Z. & LEE, K.-T. 2014. Dealing with the surplus of glycerol production from biodiesel industry through catalytic upgrading to polyglycerols and other value-added products. *Renewable and Sustainable Energy Reviews,* 39**,** 327-341.

GHOLAMI, Z., ABDULLAH, A. Z. & LEE, K. T. 2013b. Selective etherification of glycerol over heterogeneous mixed oxide catalyst: optimization of reaction parameters. *Chemical Engineering and Science,* 1**,** 79-86.

GINJUPALLI, S. R., MUGAWAR, S., BALLA, P. K. & KOMANDUR, V. R. C. 2014. Vapour phase dehydration of glycerol to acrolein over tungstated zirconia catalysts. *Applied Surface Science,* 309**,** 153-159.

GOEMBIRA, F., MATSUURA, K. & SAKA, S. 2012. Biodiesel production from rapeseed oil by various supercritical carboxylate esters. *Fuel,* 97**,** 373-378.

GRANADOS, M. L., POVES, M. Z., ALONSO, D. M., MARISCAL, R., GALISTEO, F. C., MORENO-TOST, R., SANTAMARÍA, J. & FIERRO, J. 2007. Biodiesel from sunflower oil by using activated calcium oxide. *Applied Catalysis B: Environmental,* 73**,** 317-326.

GU, Y., AZZOUZI, A., POUILLOUX, Y., JÉRÔME, F. & BARRAULT, J. 2008. Heterogeneously catalyzed etherification of glycerol: new pathways for transformation of glycerol to more valuable chemicals. *Green Chemistry,* 10**,** 164-167.

GU, Y., LIU, S., LI, C. & CUI, Q. 2013. Selective conversion of glycerol to acrolein over supported nickel sulfate catalysts. *Journal of catalysis,* 301**,** 93-102.

GUERRERO-URBANEJA, P., GARCÍA-SANCHO, C., MORENO-TOST, R., MÉRIDA-ROBLES, J., SANTAMARÍA-GONZÁLEZ, J., JIMÉNEZ-LÓPEZ, A. & MAIRELES-TORRES, P. 2014. Glycerol valorization by etherification to polyglycerols by using metal oxides derived from MgFe hydrotalcites. *Applied Catalysis A: General,* 470**,** 199-207.

GÜRÜ, M., KOCA, A., CAN, Ö., ÇıNAR, C. & ŞAHIN, F. 2010. Biodiesel production from waste chicken fat based sources and evaluation with Mg based additive in a diesel engine. *Renewable Energy,* 35**,** 637-643.

HARVEY, A. P., MACKLEY, M. R. & SELIGER, T. 2003. Process intensification of biodiesel production using a continuous oscillatory flow reactor. *Journal of Chemical Technology & Biotechnology: International Research in Process, Environmental & Clean Technology,* 78**,** 338-341.

HASENHUETTL, G. L. 2019. Synthesis and commercial preparation of food emulsifiers. *In:* HASENHUETTL, G. L. & HARTEL, R. W. (eds.) *Food emulsifiers and their applications.* Third Edition ed. Switzerland: Springer.

HE, Q. S., MCNUTT, J. & YANG, J. 2017. Utilization of the residual glycerol from biodiesel production for renewable energy generation. *Renewable and Sustainable Energy Reviews,* 71**,** 63-76.

HILL, J., NELSON, E., TILMAN, D., POLASKY, S. & TIFFANY, D. 2006. Environmental, economic, and energetic costs and benefits of biodiesel and ethanol biofuels. *Proceedings of the National Academy of sciences,* 103**,** 11206-11210.

IEA. 2019. *World Energy Outlook 2019* [Online]. IEA, Paris. Available: https://world-energy-outlook-2019 [Accessed 15/06 2019].

IRIONDO, A., BARRIO, V. L., CAMBRA, J. F., ARIAS, P. L., GUEMEZ, M. B., SANCHEZ-SANCHEZ, M. C., NAVARRO, R. M. & FIERRO, J. L. G. 2010. Glycerol steam reforming over Ni catalysts supported on ceria and ceria-promoted alumina. *International Journal of Hydrogen Energy,* 35**,** 11622-11633.

ISHAK, Z. I., SAIRI, N. A., ALIAS, Y., AROUA, M. K. T. & YUSOFF, R. 2016. Production of glycerol carbonate from glycerol with aid of ionic liquid as catalyst. *Chemical Engineering Journal,* 297**,** 128-138.

ISLAM, M. N., SABUR, A., AHMMED, R. & HOQUE, M. E. 2015. Oil Extraction from Pine Seed (Polyalthia longifolia) by Solvent Extraction Method and its Property Analysis. *Procedia Engineering,* 105**,** 613-618.

JAIRUROB, P., PHALAKORNKULE, C., NA-UDOM, A. & PETIRAKSAKUL, A. 2013. Reactive extraction of after-stripping sterilized palm fruit to biodiesel. *Fuel,* 107**,** 282-289.

JALILIANNOSRATI, H., AMIN, N. A. S., TALEBIAN-KIAKALAIEH, A. & NOSHADI, I. 2013. Microwave assisted biodiesel production from Jatropha curcas L. seed by two-step in situ process: optimization using response surface methodology. *Bioresource technology,* 136**,** 565-573.

JAZIE, A. A., NUHMA, M. J., ABBAS, H. A. & ALIAS, H. Micro-Reactor Device For Dbsa-catalyzed Biodiesel Synthesis from Microalgae Chlorella Sp. E3S Web of Conferences, 2020. EDP Sciences, 01005.

JIMMY, C. A. 2015. Microwave assisted to biodiesel production from palm oil in time and material feeding frequency. *International Journal of ChemTech Research,* 8**,** 1695-1700.

JITPUTTI, J., KITIYANAN, B., RANGSUNVIGIT, P., BUNYAKIAT, K., ATTANATHO, L. & JENVANITPANJAKUL, P. 2006. Transesterification of crude palm kernel oil and crude coconut oil by different solid catalysts. *Chemical Engineering Journal,* 116**,** 61-66.

KALE, S., ARMBRUSTER, U., UMBARKAR, S., DONGARE, M. & MARTIN, A. Esterification of glycerol with acetic acid for improved production of triacetin using toluene as an entrainer. 10th Green Chemistry Conference, 2013 Barcelona, Spain. 1 - 2.

KALE, S., UMBARKAR, S., DONGARE, M., ECKELT, R., ARMBRUSTER, U. & MARTIN, A. 2015. Selective formation of triacetin by glycerol acetylation using acidic ion-exchange resins as catalyst and toluene as an entrainer. *Applied Catalysis A: General,* 490**,** 10-16.

KALU, E. E., CHEN, K. S. & GEDRIS, T. 2011. Continuous-flow biodiesel production using slit-channel reactors. *Bioresource technology,* 102**,** 4456-4461.

KARMAKAR, A., KARMAKAR, S. & MUKHERJEE, S. 2012. Biodiesel production from neem towards feedstock diversification: Indian perspective. *Renewable and Sustainable Energy Reviews,* 16**,** 1050-1060.

KARTHIKEYAN, S., ELANGO, A. & PRATHIMA, A. 2014. An environmental effect of GSO methyl ester with ZnO additive fuelled marine engine. *Indian Journal of Geo-Marine Sciences,* 43**,** 564-570.

KASIM, F. H. & HARVEY, A. P. 2011. Influence of various parameters on reactive extraction of Jatropha curcas L. for biodiesel production. *Chemical Engineering Journal,* 171**,** 1373-1378.

KHAYOON, M. & HAMEED, B. 2011. Acetylation of glycerol to biofuel additives over sulfated activated carbon catalyst. *Bioresource technology,* 102**,** 9229-9235.

KHEDRI, B., MOSTAFAEI, M. & SAFIEDDIN ARDEBILI, S. M. 2019. A review on microwave-assisted biodiesel production. *Energy Sources, Part A: Recovery, Utilization, and Environmental Effects,* 41**,** 2377-2395.

KHEMTHONG, P., LUADTHONG, C., NUALPAENG, W., CHANGSUWAN, P., TONGPREM, P., VIRIYA-EMPIKUL, N. & FAUNGNAWAKIJ, K. 2012. Industrial eggshell wastes as the heterogeneous catalysts for microwave-assisted biodiesel production. *Catalysis Today,* 190**,** 112-116.

KIM, I., KIM, J. & LEE, D. 2014. A comparative study on catalytic properties of solid acid catalysts for glycerol acetylation at low temperatures. *Applied Catalysis B: Environmental,* 148**,** 295-303.

KIM, M. & LEE, H. 2017. Highly selective production of acrylic acid from glycerol via two steps using Au/CeO2 catalysts. *ACS Sustainable Chemistry & Engineering,* 5**,** 11371-11376.

KISS, A. A. 2014. *Process intensification technologies for biodiesel production: reactive separation processes*, Springer Science & Business Media.

KLEMEŠ, J. J. & VARBANOV, P. S. 2013. Process intensification and integration: an assessment. *Clean Technologies and Environmental Policy,* 15**,** 417-422.

KNAPP, D. R. 1979. *Handbook of analytical derivatization reactions*, John Wiley & Sons.

KNOTHE, G., KRAHL, J. & VAN GERPEN, J. 2005. *The biodiesel handbook,* New York, USA, AOCS.

KOMINTARACHAT, C., SAWANGKEAW, R. & NGAMPRASERTSITH, S. 2015. Continuous production of palm biofuel under supercritical ethyl acetate. *Energy Conversion and Management,* 93**,** 332-338.

KONUSKAN, D. B., ARSLAN, M. & OKSUZ, A. 2019. Physicochemical properties of cold pressed sunflower, peanut, rapeseed, mustard and olive oils grown in the Eastern Mediterranean region. *Saudi Journal of Biological Sciences,* 26**,** 340-344.

KONWAR, L. J., MÄKI-ARVELA, P., BEGUM, P., KUMAR, N., THAKUR, A. J., MIKKOLA, J.-P., DEKA, R. C. & DEKA, D. 2015. Shape selectivity and acidity effects in glycerol acetylation with acetic anhydride: Selective synthesis of triacetin over Y-zeolite and sulfonated mesoporous carbons. *Journal of catalysis,* 329**,** 237-247.

KORKUT, I. & BAYRAMOGLU, M. 2016. Ultrasound assisted biodiesel production in presence of dolomite catalyst. *Fuel,* 180**,** 624-629.
KORKUT, I. & BAYRAMOGLU, M. 2018. Selection of catalyst and reaction conditions for ultrasound assisted biodiesel production from canola oil. *Renewable energy,* 116**,** 543-551.
KOUTSOUKI, A., TEGOU, E., BADEKA, A., KONTAKOS, S., POMONIS, P. & KONTOMINAS, M. 2016. In situ and conventional transesterification of rapeseeds for biodiesel production: The effect of direct sonication. *Industrial Crops and Products,* 84**,** 399-407.
KRAHL, J., KNOTHE, G. & VAN GERPEN, J. H. 2010. *Biodiesel Handbook,* USA, AOCS Press Urbana, IL, USA.
KRISNANDI, Y. K., ECKELT, R., SCHNEIDER, M., MARTIN, A. & RICHTER, M. 2008. Glycerol Upgrading over Zeolites by Batch-Reactor Liquid-Phase Oligomerization: Heterogeneous versus Homogeneous Reaction. *ChemSusChem,* 1**,** 835-844.
KUMAR, T. N., SASTRY, Y. S. R. & LAKSHMINARAYANA, G. 1984. Analysis of polyglycerols by high-performance liquid chromatography. *Journal of Chromatography A,* 298**,** 360-365.
LEE, S., POSARAC, D. & ELLIS, N. 2012. An experimental investigation of biodiesel synthesis from waste canola oil using supercritical methanol. *Fuel,* 91**,** 229-237.
LEE, Y., LEE, J. H., YANG, H. J., JANG, M., KIM, J. R., BYUN, E.-H., LEE, J., NA, J.-G., KIM, S. W. & PARK, C. 2017. Efficient simultaneous production of biodiesel and glycerol carbonate via statistical optimization. *Journal of Industrial and Engineering Chemistry,* 51**,** 49-53.
LEMOS, C. O., RADE, L. L., BARROZO, M. A. D. S., CARDOZO-FILHO, L. & HORI, C. E. 2018. Study of glycerol etherification with ethanol in fixed bed reactor under high pressure. *Fuel processing technology,* 178**,** 1-6.
LEONETI , A. B., VALQUIRIA ARAGÃO-LEONETI & OLIVEIRA, S. V. W. B. D. 2012. Glycerol as a by-product of biodiesel production in Brazil: Alternatives for the use of unrefined glycerol. *Renewable Energy* 45**,** 138-145.
LERTSATHAPORNSUK, V., RUANGYING, P., PAIRINTRA, R. & KRISNANGKURA, K. Continuous transethylation of vegetable oils by microwave irradiation. Proceedings of the 1st conference on energy network, 2005.
LI, Y., FINE, F., FABIANO-TIXIER, A.-S., ABERT-VIAN, M., CARRE, P., PAGES, X. & CHEMAT, F. 2014. Evaluation of alternative solvents for improvement of oil extraction from rapeseeds. *Comptes Rendus Chimie,* 17**,** 242-251.
LIM, S., HOONG, S. S., TEONG, L. K. & BHATIA, S. 2010. Supercritical fluid reactive extraction of Jatropha curcas L. seeds with methanol: a novel biodiesel production method. *Bioresource technology,* 101**,** 7169-7172.
LIM, S. & LEE, K. T. 2013. Process intensification for biodiesel production from Jatropha curcas L. seeds: Supercritical reactive extraction process parameters study. *Applied Energy,* 103**,** 712-720.
LIM, S. & LEE, K. T. 2014. Investigation of impurity tolerance and thermal stability for biodiesel production from Jatropha curcas L. seeds using supercritical reactive extraction. *Energy,* 68**,** 71-79.
LIU, F., VIGIER, K. D. O., PERA-TITUS, M., POUILLOUX, Y., CLACENS, J.-M., DECAMPO, F. & JÉRÔME, F. 2013. Catalytic etherification of glycerol with short chain alkyl alcohols in the presence of Lewis acids. *Green Chemistry,* 15**,** 901-909.

LIU, J., CAO, X., CHU, Y., ZHAO, Y., WU, P. & XUE, S. 2018. Novel approach for the direct transesterification of fresh microalgal cells via micro-reactor. *Algal research,* 32**,** 38-43.

LIU, L., WANG, B., DU, Y., ZHONG, Z. & BORGNA, A. 2015. Bifunctional Mo3VOx/H4SiW12O40/Al2O3 catalysts for one-step conversion of glycerol to acrylic acid: Catalyst structural evolution and reaction pathways. *Applied Catalysis B: Environmental,* 174**,** 1-12.

LIU, R., LYU, S. & WANG, T. 2016a. Sustainable production of acrolein from biodiesel-derived crude glycerol over H3PW12O40 supported on Cs-modified SBA-15. *Journal of Industrial and Engineering Chemistry,* 37**,** 354-360.

LIU, X., MA, H., WU, Y., WANG, C., YANG, M., YAN, P. & WELZ-BIERMANN, U. 2011. Esterification of glycerol with acetic acid using double SO 3 H-functionalized ionic liquids as recoverable catalysts. *Green Chemistry,* 13**,** 697-701.

LIU, Y., LU, H., AMPONG-NYARKO, K., MACDONALD, T., TAVLARIDES, L. L., LIU, S. & LIANG, B. 2016b. Kinetic studies on biodiesel production using a trace acid catalyst. *Catalysis today,* 264**,** 55-62.

LIU, Y., TU, Q., KNOTHE, G. & LU, M. 2017. Direct transesterification of spent coffee grounds for biodiesel production. *Fuel,* 199**,** 157-161.

LÓPEZ-GUAJARDO, E. A., TREVIÑO, F. E., ORTIZ, E. & MONTESINOS-CASTELLANOS, A. 2011. Intensificación del proceso de producción de biodiesel utilizando un micro-reactor tubular. *Tecnología, ciencia, educación,* 26**,** 45-50.

LOPEZ-PEDRAJAS, S., ESTEVEZ, R., SCHNEE, J., GAIGNEAUX, E. M., LUNA, D. & BAUTISTA, F. 2018. Study of the gas-phase glycerol oxidehydration on systems based on transition metals (Co, Fe, V) and aluminium phosphate. *Molecular Catalysis,* 455**,** 68-77.

LOTERO, E., GOODWIN JR, J. G., BRUCE, D. A., SUWANNAKARN, K., LIU, Y. & LOPEZ, D. E. 2006. The catalysis of biodiesel synthesis. *Ind. Eng. Chem. Res., ACS,* 44**,** 5353 - 5363.

LOTERO, E., LIU, Y., LOPEZ, D. E., SUWANNAKARN, K., BRUCE, D. A. & GOODWIN JR, J. G. 2005. Synthesis of biodiesel via acid catalysis. *carbon (wt%),* 87**,** 77.

LUO, N., FU, X., CAO, F., XIAO, T. & EDWARDS, P. P. 2008. Glycerol aqueous phase reforming for hydrogen generation over Pt catalyst - Effect of catalyst composition and reaction conditions. *Fuel,* 87**,** 3483-3489.

LUU, P. D., TAKENAKA, N., VAN LUU, B., PHAM, L. N., IMAMURA, K. & MAEDA, Y. 2014. Co-solvent Method Produce Biodiesel form Waste Cooking Oil with Small Pilot Plant. *Energy Procedia,* 61**,** 2822-2832.

MA, F. & HANNA, M. A. 1999. Biodiesel production: A review. *Bioresource Technology,* 70**,** 1-15.

MA, Y., WANG, Q., SUN, X., WU, C. & GAO, Z. 2017. Kinetics studies of biodiesel production from waste cooking oil using FeCl3-modified resin as heterogeneous catalyst. *Renewable Energy,* 107**,** 522-530.

MALANI, R. S., UMRIWAD, S. B., KUMAR, K., GOYAL, A. & MOHOLKAR, V. S. 2019. Ultrasound–assisted enzymatic biodiesel production using blended feedstock of non–edible oils: Kinetic analysis. *Energy Conversion and Management,* 188**,** 142-150.

MANIQUE, M. C., LACERDA, L. V., ALVES, A. K. & BERGMANN, C. P. 2017. Biodiesel production using coal fly ash-derived sodalite as a heterogeneous catalyst. *Fuel,* 190**,** 268-273.

MARCHETTI, J., PEDERNERA, M. & SCHBIB, N. 2010. Production of biodiesel from acid oil using sulfuric acid as catalyst: kinetics study. *International Journal of Low-Carbon Technologies,* 6**,** 38 - 43.

MARTINEZ ARIAS, E. L., FAZZIO MARTINS, P., JARDINI MUNHOZ, A. L., GUTIERREZ-RIVERA, L. & MACIEL FILHO, R. 2012. Continuous synthesis and in situ monitoring of biodiesel production in different microfluidic devices. *Industrial & Engineering Chemistry Research,* 51**,** 10755-10767.

MARTINUZZI, I., AZIZI, Y., ZAHRAA, O. & LECLERC, J.-P. 2015. Deactivation study of a heteropolyacid catalyst for glycerol dehydration to form acrolein. *Chemical Engineering Science,* 134**,** 663-670.

MARULANDA, V. F., ANITESCU, G. & TAVLARIDES, L. L. 2010a. Biodiesel fuels through a continuous flow process of chicken fat supercritical transesterification. *Energy & Fuels,* 24**,** 253-260.

MARULANDA, V. F., ANITESCU, G. & TAVLARIDES, L. L. 2010b. Investigations on supercritical transesterification of chicken fat for biodiesel production from low-cost lipid feedstocks. *The Journal of Supercritical Fluids,* 54**,** 53-60.

MAZUBERT, A., AUBIN, J., ELGUE, S. & POUX, M. 2014. Intensification of waste cooking oil transformation by transesterification and esterification reactions in oscillatory baffled and microstructured reactors for biodiesel production. *Green Processing and Synthesis,* 3**,** 419-429.

MAZZOCCHIA, C., MODICA, G., KADDOURI, A. & NANNICINI, R. 2004. Fatty acid methyl esters synthesis from triglycerides over heterogeneous catalysts in the presence of microwaves. *Comptes Rendus Chimie,* 7**,** 601-605.

MEDEIROS, A. M., SANTOS, Ê. R., AZEVEDO, S. H., JESUS, A. A., OLIVEIRA, H. N. & SOUSA, E. M. 2018. CHEMICAL INTERESTERIFICATION OF COTTON OIL WITH METHYL ACETATE ASSISTED BY ULTRASOUND FOR BIODIESEL PRODUCTION. *Brazilian Journal of Chemical Engineering,* 35**,** 1005-1018.

MEDEIROS, M. A., ARAUJO, M. H., AUGUSTI, R., DE OLIVEIRA, L. C. A. & LAGO, R. M. 2009. Acid-catalyzed oligomerization of glycerol investigated by electrospray ionization mass spectrometry. *Journal of the Brazilian Chemical Society,* 20**,** 1667-1673.

MELERO, J. A., VICENTE, G., PANIAGUA, M., MORALES, G. & MUÑOZ, P. 2012. Etherification of biodiesel-derived glycerol with ethanol for fuel formulation over sulfonic modified catalysts. *Bioresource technology,* 103**,** 142-151.

MICHELIN, S., PENHA, F. M., SYCHOSKI, M. M., SCHERER, R. P., TREICHEL, H., VALÉRIO, A., DI LUCCIO, M., DE OLIVEIRA, D. & OLIVEIRA, J. V. 2015. Kinetics of ultrasound-assisted enzymatic biodiesel production from Macauba coconut oil. *Renewable Energy,* 76**,** 388-393.

MIRANDA, C., RAMÍREZ, A., SACHSE, A., POUILLOUX, Y., URRESTA, J. & PINARD, L. 2019. Sulfonated graphenes: Efficient solid acid catalyst for the glycerol valorization. *Applied Catalysis A: General,* 580**,** 167-177.

MIRANDA, C., URRESTA, J., CRUCHADE, H., TRAN, A., BENGHALEM, M., ASTAFAN, A., GAUDIN, P., DAOU, T., RAMÍREZ, A. & POUILLOUX, Y. 2018. Exploring the impact of zeolite porous voids in liquid phase reactions: The case of glycerol etherification by tert-butyl alcohol. *Journal of catalysis,* 365**,** 249-260.

MOHAMMED, I. A., LEE, J. G. M. & HARVEY, A. P. 2019. Simultaneous transesterification and reactive coupling for biodiesel and polyglycerol production. *In:* XIAOXIN ZHOU, V. V., HONGBIN SUN, QINGHUA WU, GUANGFU

TANG, LIANGZHONG YAO, JINLIANG HE (ed.) *International Conference on Applied Energy (ICAE 2019).* Vasteras, Sweden.
MOLDOVEANU, S. C. & DAVID, V. 2019. Derivatization Methods in GC and GC/MS. *In:* KUSCH, P. (ed.) *Gas Chromatography-Derivatization, Sample Preparation, Application.* London: IntechOpen.
MOTA, C. J. A., DA SILVA, C. X. A., ROSENBACH, N., COSTA, J. & DA SILVA, F. 2010. Glycerin Derivatives as Fuel Additives: The Addition of Glycerol/Acetone Ketal (Solketal) in Gasolines. *Energy & Fuels,* 24**,** 2733-2736.
MOTASEMI, F. & ANI, F. 2012. A review on microwave-assisted production of biodiesel. *Renewable and Sustainable Energy Reviews,* 16**,** 4719-4733.
MRAVEC, D., TURAN, A., FILKOVÁ, A., MIKESKOVÁ, N., VOLKOVICSOVÁ, E., ONYESTYÁK, G., HARNOS, S., LÓNYI, F., VALYON, J. & KASZONYI, A. 2017. Catalytic etherification of bioglycerol with bioethanol over H-Beta, HY and H-MOR zeolites. *Fuel Processing Technology,* 159**,** 111-117.
MU, Y., TENG, H., ZHANG, D.-J., WANG, W. & XIU, Z.-L. 2006. Microbial production of 1,3-propanediol by Klebsiella pneumoniae using crude glycerol from biodiesel preparations. *Biotechnology Letters,* 28**,** 1755-1759.
MUSA, I. A. 2016. The effects of alcohol to oil molar ratios and the type of alcohol on biodiesel production using transesterification process. *Egyptian Journal of Petroleum,* 25**,** 21-31.
MUTHUKUMARAN, C., PRANIESH, R., NAVAMANI, P., SWATHI, R., SHARMILA, G. & KUMAR, N. M. 2017a. Process optimization and kinetic modeling of biodiesel production using non-edible Madhuca indica oil. *Fuel,* 195**,** 217-225.
MUTHUKUMARAN, C., PRANIESH, R., NAVAMANI, P., SWATHI, R., SHARMILA, G. & MANOJ KUMAR, N. 2017b. Process optimization and kinetic modeling of biodiesel production using non-edible Madhuca indica oil. *Fuel,* 195**,** 217-225.
NANDA, M. R., YUAN, Z., QIN, W., GHAZIASKAR, H. S., POIRIER, M.-A. & XU, C. 2014. Catalytic conversion of glycerol to oxygenated fuel additive in a continuous flow reactor: Process optimization. *Fuel,* 128**,** 113-119.
NARKHEDE, N. & PATEL, A. 2014. Room temperature acetalization of glycerol to cyclic acetals over anchored silicotungstates under solvent free conditions. *RSC Advances,* 4**,** 19294-19301.
NAYAK, M. G. & VYAS, A. P. 2019. Optimization of microwave-assisted biodiesel production from Papaya oil using response surface methodology. *Renewable Energy,* 138**,** 18-28.
NAYLOR, R. L. & HIGGINS, M. M. 2018. The rise in global biodiesel production: implications for food security. *Global food security,* 16**,** 75-84.
NDA-UMAR, U. I., RAMLI, I., MUHAMAD, E. N., TAUFIQ-YAP, Y. H. & AZRI, N. 2020. Synthesis and characterization of sulfonated carbon catalysts derived from biomass waste and its evaluation in glycerol acetylation. *Biomass Conversion and Biorefinery***,** 1-16.
NEGM, N. A., SAYED, G. H., YEHIA, F. Z., HABIB, O. I. & MOHAMED, E. A. 2017. Biodiesel production from one-step heterogeneous catalyzed process of Castor oil and Jatropha oil using novel sulphonated phenyl silane montmorillonite catalyst. *Journal of Molecular Liquids,* 234**,** 157-163.
NGAMCHARUSSRIVICHAI, C., WIWATNIMIT, W. & WANGNOI, S. 2007. Modified dolomites as catalysts for palm kernel oil transesterification. *Journal of Molecular Catalysis A: Chemical,* 276**,** 24-33.

NGUYEN, R., GALY, N., SINGH, A. K., PAULUS, F., STÖBENER, D., SCHLESENER, C., SHARMA, S. K., HAAG, R. & LEN, C. 2017. A simple and efficient process for large scale glycerol oligomerization by microwave irradiation. *Catalysts,* 7**,** 1 - 12.

NGUYEN, T., DO, L. & SABATINI, D. A. 2010. Biodiesel production via peanut oil extraction using diesel-based reverse-micellar microemulsions. *Fuel,* 89**,** 2285-2291.

NIGAM, P. S. & SINGH, A. 2011. Production of liquid biofuels from renewable resources. *Progress in energy and combustion science,* 37**,** 52-68.

NISAR, J., RAZAQ, R., FAROOQ, M., IQBAL, M., KHAN, R. A., SAYED, M., SHAH, A. & UR RAHMAN, I. 2017. Enhanced biodiesel production from Jatropha oil using calcined waste animal bones as catalyst. *Renewable Energy,* 101**,** 111-119.

NIZA, N. M., TAN, K. T., LEE, K. T. & AHMAD, Z. 2013. Biodiesel production by non-catalytic supercritical methyl acetate: Thermal stability study. *Applied energy,* 101**,** 198-202.

NOSAL, H., NOWICKI, J., WARZAŁA, M., NOWAKOWSKA-BOGDAN, E. & ZARĘBSKA, M. 2015. Synthesis and characterization of alkyd resins based on Camelina sativa oil and polyglycerol. *Progress in Organic Coatings,* 86**,** 59-70.

NOUREDDINI, H., GAO, X. & PHILKANA, R. 2005. Immobilized Pseudomonas cepacia lipase for biodiesel fuel production from soybean oil. *Bioresource technology,* 96**,** 769-777.

NOUREDDINI, H., TEOH, B. & DAVIS CLEMENTS, L. 1992a. Densities of vegetable oils and fatty acids. *Journal of the American Oil Chemists' Society,* 69**,** 1184-1188.

NOUREDDINI, H., TEOH, B. & DAVIS CLEMENTS, L. 1992b. Viscosities of vegetable oils and fatty acids. *Journal of the American Oil Chemists' Society,* 69**,** 1189-1191.

NOUREDDINI, H. & ZHU, D. 1997. Kinetics of transesterification of soybean oil. *Journal of the American Oil Chemists' Society,* 74**,** 1457-1463.

NYE, M. J., WILLIAMSON, T. W., DESHPANDE, W., SCHRADER, J. H., SNIVELY, W. H., YURKEWICH, T. P. & FRENCH, C. L. 1983. Conversion of used frying oil to diesel fuel by transesterification: preliminary tests. *Journal of the American Oil Chemists' Society,* 60**,** 1598-1601.

OMATA, K., MATSUMOTO, K., MURAYAMA, T. & UEDA, W. 2016. Direct oxidative transformation of glycerol to acrylic acid over Nb-based complex metal oxide catalysts. *Catalysis Today,* 259**,** 205-212.

ONG, H. C., SILITONGA, A. S., MASJUKI, H. H., MAHLIA, T. M. I., CHONG, W. T. & BOOSROH, M. H. 2013a. Production and comparative fuel properties of biodiesel from non-edible oils: Jatropha curcas, Sterculia foetida and Ceiba pentandra. *Energy Conversion and Management,* 73**,** 245-255.

ONG, L., KURNIAWAN, A., SUWANDI, A., LIN, C., ZHAO, X. & ISMADJI, S. 2013b. Transesterification of leather tanning waste to biodiesel at supercritical condition: Kinetics and thermodynamics studies. *The Journal of Supercritical Fluids,* 75**,** 11-20.

ÖZGÜL, S. & TÜRKAY, S. 1993. In situ esterification of rice bran oil with methanol and ethanol. *Journal of the American Oil Chemists' Society,* 70**,** 145-147.

PAHL, G. 2008. *Biodiesel: growing a new energy economy*, Chelsea Green Publishing.

PANADARE, D. & RATHOD, V. 2016. Microwave assisted enzymatic synthesis of biodiesel with waste cooking oil and dimethyl carbonate. *Journal of Molecular Catalysis B: Enzymatic,* 133**,** S518-S524.

PAPANIKOLAOU, S., MUNIGLIA, L., CHEVALOT, I., AGGELIS, G. & MARC, I. 2002. Yarrowia lipolytica as a potential producer of citric acid from raw glycerol. *Journal of Applied Microbiology,* 92**,** 737-744.

PARIENTE, S., TANCHOUX, N. & FAJULA, F. 2009. Etherification of glycerol with ethanol over solid acid catalysts. *Green Chemistry,* 11**,** 1256-1261.

PAULA, A. S., POSSATO, L. G., RATERO, D. R., CONTRO, J., KEINAN-ADAMSKY, K., SOARES, R. R., GOOBES, G., MARTINS, L. & NERY, J. G. 2016. One-step oxidehydration of glycerol to acrylic acid using ETS-10-like vanadosilicates. *Microporous and Mesoporous Materials,* 232**,** 151-160.

PÉREZ-BARRADO, E., PUJOL, M. C., AGUILÓ, M., LLORCA, J., CESTEROS, Y., DÍAZ, F., PALLARÈS, J., MARSAL, L. F. & SALAGRE, P. 2015. Influence of acid–base properties of calcined MgAl and CaAl layered double hydroxides on the catalytic glycerol etherification to short-chain polyglycerols. *Chemical Engineering Journal,* 264**,** 547-556.

PHAN, A. N., HARVEY, A. P. & EZE, V. 2012. Rapid production of biodiesel in mesoscale oscillatory baffled reactors. *Chemical Engineering & Technology,* 35**,** 1214-1220.

PHAN, A. N., HARVEY, A. P. & RAWCLIFFE, M. 2011. Continuous screening of base-catalysed biodiesel production using new designs of mesoscale oscillatory baffled reactors. *Fuel Processing Technology,* 92**,** 1560-1567.

PINTO, B. P., DE LYRA, J. T., NASCIMENTO, J. A. & MOTA, C. J. 2016. Ethers of glycerol and ethanol as bioadditives for biodiesel. *Fuel,* 168**,** 76-80.

PONTES, P. C., NAVEIRA-COTTA, C. P. & QUARESMA, J. N. 2017. Three-dimensional reaction-convection-diffusion analysis with temperature influence for biodiesel synthesis in micro-reactors. *International Journal of Thermal Sciences,* 118**,** 104-122.

POSSATO, L. G., CASSINELLI, W. H., GARETTO, T., PULCINELLI, S. H., SANTILLI, C. V. & MARTINS, L. 2015. One-step glycerol oxidehydration to acrylic acid on multifunctional zeolite catalysts. *Applied Catalysis A: General,* 492**,** 243-251.

POSSATO, L. G., CHAVES, T. F., CASSINELLI, W. H., PULCINELLI, S. H., SANTILLI, C. V. & MARTINS, L. 2017. The multiple benefits of glycerol conversion to acrolein and acrylic acid catalyzed by vanadium oxides supported on micro-mesoporous MFI zeolites. *Catalysis Today,* 289**,** 20-28.

QING, S., JIXIAN, G., YUHUI, L. & JINFU, W. 2011. Reaction kinetics of biodiesel synthesis from waste oil using a carbon-based solid acid catalyst. *Chinese Journal of Chemical Engineering,* 19**,** 163-168.

QIU, Z., ZHAO, L. & WEATHERLEY, L. 2010. Process intensification technologies in continuous biodiesel production. *Chemical Engineering and Processing: Process Intensification,* 49**,** 323-330.

QUISPE , C. A. G., CORONADO, C. J. R. & CARVALHO JR, J. A. 2013. Glycerol: Production, consumption, prices, characterization and new trends in combustion. *Renewable and Sustainable Energy Reviews,* 27**,** 475-493.

RABELO, S. N., FERRAZ, V. P., OLIVEIRA, L. S. & FRANCA, A. S. 2015. FTIR analysis for quantification of fatty acid methyl esters in biodiesel produced by microwave-assisted transesterification. *International Journal of Environmental Science and Development,* 6**,** 964 - 969.

RASHID, U., ANWAR, F., MOSER, B. R. & ASHRAF, S. 2008. Production of sunflower oil methyl esters by optimized alkali-catalyzed methanolysis. *Biomass and bioenergy,* 32**,** 1202-1205.

RASTEIRO, L. F., VIEIRA, L. H., POSSATO, L. G., PULCINELLI, S. H., SANTILLI, C. V. & MARTINS, L. 2017. Hydrothermal synthesis of Mo-V mixed oxides possessing several crystalline phases and their performance in the catalytic oxydehydration of glycerol to acrylic acid. *Catalysis Today,* 296**,** 10-18.

RATHORE, V., TYAGI, S., NEWALKAR, B. & BADONI, R. P. 2014. Glycerin-Free Synthesis of Jatropha and Pongamia Biodiesel in Supercritical Dimethyl and Diethyl Carbonate. *Industrial & Engineering Chemistry Research,* 53**,** 10525-10533.

REAY, D., RAMSHAW, C. & HARVEY, A. 2013. *Process Intensification: Engineering for efficiency, sustainability and flexibility*, Butterworth-Heinemann.

REMÓN, J., GIMÉNEZ, J. R., VALIENTE, A., GARCÍA, L. & ARAUZO, J. 2016. Production of gaseous and liquid chemicals by aqueous phase reforming of crude glycerol: Influence of operating conditions on the process. *Energy Conversion and Management,* 110**,** 90-112.

REN, Y., HARVEY, A. & ZAKARIA, R. 2010. Biorefining based on biodiesel production: chemical and physical characterisation of reactively extracted rapeseed. *Journal of Biobased Materials and Bioenergy,* 4**,** 79-86.

REYERO, I., ARZAMENDI, G., ZABALA, S. & GANDÍA, L. M. 2015. Kinetics of the NaOH-catalyzed transesterification of sunflower oil with ethanol to produce biodiesel. *Fuel Processing Technology,* 129**,** 147-155.

RIBEIRO, J. S., CELANTE, D., BRONDANI, L. N., TROJAHN, D. O., DA SILVA, C. & DE CASTILHOS, F. 2018. Synthesis of methyl esters and triacetin from macaw oil (Acrocomia aculeata) and methyl acetate over γ-alumina. *Industrial crops and products,* 124**,** 84-90.

RICCIARDI, M., PASSARINI, F., CAPACCHIONE, C., PROTO, A., BARRAULT, J., CUCCINIELLO, R. & CESPI, D. 2018. First Attempt of Glycidol-to-Monoalkyl Glyceryl Ethers Conversion by Acid Heterogeneous Catalysis: Synthesis and Simplified Sustainability Assessment. *ChemSusChem,* 11**,** 1829-1837.

RICHTER, M., KRISNANDI, Y. K., ECKELT, R. & MARTIN, A. 2008. Homogeneously catalyzed batch reactor glycerol etherification by CsHCO3. *Catalysis Communications,* 9**,** 2112-2116.

ROYON, D., DAZ, M., ELLENRIEDER, G. & LOCATELLI, S. 2007. Enzymatic production of biodiesel from cotton seed oil using t-butanol as a solvent. *Bioresource technology,* 98**,** 648-653.

RUPPERT, A. M., MEELDIJK, J. D., KUIPERS, B. W. M., ERNÉ, B. H. & WECKHUYSEN, B. M. 2008. Glycerol Etherification over Highly Active CaO-Based Materials: New Mechanistic Aspects and Related Colloidal Particle Formation. *Chemistry-A European Journal,* 14**,** 2016-2024.

SAHANI, S. & SHARMA, Y. C. 2018. Economically viable production of biodiesel using a novel heterogeneous catalyst: Kinetic and thermodynamic investigations. *Energy Conversion and Management,* 171**,** 969-983.

SAHASRABUDHE, S. N., RODRIGUEZ-MARTINEZ, V., O'MEARA, M. & FARKAS, B. E. 2017. Density, viscosity, and surface tension of five vegetable oils at elevated temperatures: Measurement and modeling. *International journal of food properties,* 20**,** 1965-1981.

SAIFUDDIN, N., SAMIUDDIN, A. & KUMARAN, P. 2015. A review on processing technology for biodiesel production. *Trends in Applied Sciences Research,* 10**,** 1 - 37.

SAKDASRI, W., SAWANGKEAW, R. & NGAMPRASERTSITH, S. 2015. Continuous production of biofuel from refined and used palm olein oil with supercritical

methanol at a low molar ratio. *Energy conversion and management,* 103**,** 934-942.
SALAM, K. A., VELASQUEZ-ORTA, S. B. & HARVEY, A. P. 2016. A sustainable integrated in situ transesterification of microalgae for biodiesel production and associated co-product-a review. *Renewable and Sustainable Energy Reviews,* 65**,** 1179-1198.
SALEHPOUR, S. & DUBÉ, M. A. 2011. Towards the sustainable production of higher-molecular-weight polyglycerol. *Macromolecular Chemistry and Physics,* 212**,** 1284-1293.
SALEHPOUR, S. & DUBÉ, M. A. 2012. Reaction Monitoring of Glycerol Step-Growth Polymerization Using ATR-FTIR Spectroscopy. *Macromolecular Reaction Engineering,* 6**,** 85-92.
SALIMON, J., MOHD NOOR, D. A., NAZRIZAWATI, A. T., MOHD FIRDAUS, M. Y. & NORAISHAH, A. 2010. Fatty acid composition and physicochemical properties of Malaysian castor bean ricinus communis L. seed oil. *Sains Malaysiana,* 39**,** 761-764.
SANKUMGON, A., ASSAWADITHALERD, M., PHASUKARRATCHAI, N., CHOLLACOOP, N. & TONGCUMPOU, C. 2018. Properties and performance of microemulsion fuel: blending of jatropha oil, diesel, and ethanol-surfactant. *Renewable Energy Focus,* 24**,** 28-32.
SANLI, H. & CANAKCI, M. 2008. Effects of different alcohol and catalyst usage on biodiesel production from different vegetable oils. *Energy and Fuels,* 22**,** 2713-2719.
SANTIBÁÑEZ, C., VARNERO, M. T. & BUSTAMANTE, M. 2011. Residual glycerol from biodiesel Manufacturing, waste or potential source of Bioenergy: A review. *Chilean Journal of Agricultural Research,* 71**,** 469-475.
SANTIKUNAPORN, M., TECHOPITTAYAKUL, T., ECHAROJ, S., CHAVADEJ, S., CHEN, Y.-H., YUAN, M.-H. & ASAVATESANUPAP, C. 2020. Optimization of biodiesel production from waste cooking oil in a continuous mesoscale oscillatory baffled reactor. *Engineering Journal,* 24**,** 19-28.
SANTOS, F. F., MALVEIRA, J. Q., CRUZ, M. G. & FERNANDES, F. A. 2010. Production of biodiesel by ultrasound assisted esterification of Oreochromis niloticus oil. *Fuel,* 89**,** 275-279.
SAYOUD, N., VIGIER, K. D. O., CUCU, T., DE MEULENAER, B., FAN, Z., LAI, J., CLACENS, J.-M., LIEBENS, A. & JÉRÔME, F. 2015. Homogeneously-acid catalyzed oligomerization of glycerol. *Green Chemistry,* 17**,** 4307-4314.
SEMWAL, S., ARORA, A. K., BADONI, R. P. & TULI, D. K. 2011. Biodiesel production using heterogeneous catalysts. *Bioresource technology,* 102**,** 2151-2161.
SEONG, P.-J., JEON, B. W., LEE, M., CHO, D. H., KIM, D.-K., JUNG, K. S., KIM, S. W., HAN, S. O., KIM, Y. H. & PARK, C. 2011. Enzymatic coproduction of biodiesel and glycerol carbonate from soybean oil and dimethyl carbonate. *Enzyme and microbial technology,* 48**,** 505-509.
SHAH, P., CHIU, F. S. & LAN, J. C. W. 2014. Aerobic utilization of crude glycerol by recombinant Escherichia coli for simultaneous production of poly 3-hydroxybutyrate and bioethanol. *Journal of Bioscience and Bioengineering,* 117**,** 343-350.
SHAH, S. & GUPTA, M. N. 2007. Lipase catalyzed preparation of biodiesel from Jatropha oil in a solvent free system. *Process Biochemistry,* 42**,** 409-414.

SHAH, S., SHARMA, S. & GUPTA, M. 2004. Biodiesel preparation by lipase-catalyzed transesterification of Jatropha oil. *Energy & Fuels,* 18**,** 154-159.

SHARMA, A., KODGIRE, P. & KACHHWAHA, S. S. 2019. Biodiesel production from waste cotton-seed cooking oil using microwave-assisted transesterification: Optimization and kinetic modeling. *Renewable and Sustainable Energy Reviews,* 116**,** 109394.

SHARMA, M., KHAN, A. A., PURI, S. & TULI, D. 2012. Wood ash as a potential heterogeneous catalyst for biodiesel synthesis. *Biomass and bioenergy,* 41**,** 94-106.

SHEN, L., YIN, H., WANG, A., LU, X. & ZHANG, C. 2014a. Gas phase oxidehydration of glycerol to acrylic acid over Mo/V and W/V oxide catalysts. *Chemical Engineering Journal,* 244**,** 168-177.

SHEN, L., YIN, H., WANG, A., LU, X., ZHANG, C., CHEN, F., WANG, Y. & CHEN, H. 2014b. Liquid phase catalytic dehydration of glycerol to acrolein over Brønsted acidic ionic liquid catalysts. *Journal of Industrial and Engineering Chemistry,* 20**,** 759-766.

SHIKHALIEV, K. S., STOLPOVSKAYA, N. V., KRYSIN, M. Y., ZORINA, A. V., LYAPUN, D. V., ZUBKOV, F. I. & YANKINA, K. Y. 2016. Production and Emulsifying Effect of Polyglycerol and Fatty Acid Esters with Varying Degrees of Esterification. *JAOCS, Journal of the American Oil Chemists' Society,* 93**,** 1429-1440.

SHU, Q., ZOU, W., HE, J., LESMANA, H., ZHANG, C., ZOU, L. & WANG, Y. 2019. Preparation of the F−-SO42-/MWCNTs catalyst and kinetic studies of the biodiesel production via esterification reaction of oleic acid and methanol. *Renewable Energy,* 135**,** 836-845.

SHUIT, S. H., LEE, K. T., KAMARUDDIN, A. H. & YUSUP, S. 2009. Reactive extraction and in situ esterification of Jatropha curcas L. seeds for the production of biodiesel. *Fuel,* 89**,** 527-530.

SHUIT, S. H., LEE, K. T., KAMARUDDIN, A. H. & YUSUP, S. 2010. Reactive extraction of Jatropha curcas L. seed for production of biodiesel: process optimization study. *Environmental science & technology,* 44**,** 4361-4367.

SHUIT, S. H., ONG, Y. T., LEE, K. T., SUBHASH, B. & TAN, S. H. 2012. Membrane technology as a promising alternative in biodiesel production: A review. *Biotechnology Advances,* 30**,** 1364-1380.

SILVA, L. N., GONÇALVES, V. L. & MOTA, C. J. 2010. Catalytic acetylation of glycerol with acetic anhydride. *Catalysis Communications,* 11**,** 1036-1039.

SIMONE, N., CARVALHO, W. A., MANDELLI, D. & RYOO, R. 2016. Nanostructured MFI-type zeolites as catalysts in glycerol etherification with tert-butyl alcohol. *Journal of Molecular Catalysis A: Chemical,* 422**,** 115-121.

SIVAIAH, M. V., ROBLES-MANUEL, S., VALANGE, S. & BARRAULT, J. 2012. Recent developments in acid and base-catalyzed etherification of glycerol to polyglycerols. *Catalysis Today,* 198**,** 305-313.

SMIRNOV, A., SELISHCHEVA, S. & YAKOVLEV, V. 2018. Acetalization Catalysts for Synthesis of Valuable Oxygenated Fuel Additives from Glycerol. *Catalysts,* 8**,** 595.

SOI, H. S., BAKAR, Z. A., DIN, N. S. M. N. M., IDRIS, Z., KIAN, Y. S., HASSAN, H. A. & AHMAD, S. 2014. Process of producing polyglycerol from crude glycerol. Google Patents.

SOUFI, M. D., GHOBADIAN, B., NAJAFI, G., MOUSAVI, S. M. & AUBIN, J. 2017. Optimization of methyl ester production from waste cooking oil in a batch tri-orifice oscillatory baffled reactor. *Fuel Processing Technology,* 167**,** 641-647.

STAVARACHE, C., VINATORU, M., NISHIMURA, R. & MAEDA, Y. 2003. Conversion of vegetable oil to biodiesel using ultrasonic irradiation. *Chemistry letters,* 32**,** 716-717.

STOŠIĆ, D., BENNICI, S., SIROTIN, S., CALAIS, C., COUTURIER, J.-L., DUBOIS, J.-L., TRAVERT, A. & AUROUX, A. 2012. Glycerol dehydration over calcium phosphate catalysts: Effect of acidic–basic features on catalytic performance. *Applied Catalysis A: General,* 447**,** 124-134.

SU, E., YOU, P. & WEI, D. 2009. In situ lipase-catalyzed reactive extraction of oilseeds with short-chained dialkyl carbonates for biodiesel production. *Bioresource Technology,* 100**,** 5813-5817.

SUBROTO, E., MANURUNG, R., HEERES, H. J. & BROEKHUIS, A. A. 2015. Mechanical extraction of oil from Jatropha curcas L. kernel: Effect of processing parameters. *Industrial Crops and Products,* 63**,** 303-310.

SULAIMAN, S., AZIZ, A. A. & AROUA, M. K. 2013. Reactive extraction of solid coconut waste to produce biodiesel. *Journal of the Taiwan Institute of Chemical Engineers,* 44**,** 233-238.

SUN, D., YAMADA, Y., SATO, S. & UEDA, W. 2017. Glycerol as a potential renewable raw material for acrylic acid production. *Green Chemistry,* 19**,** 3186-3213.

SUN, J., JU, J., JI, L., ZHANG, L. & XU, N. 2008. Synthesis of biodiesel in capillary microreactors. *Industrial & Engineering Chemistry Research,* 47**,** 1398-1403.

SUPRAJA, K. V., BEHERA, B. & PARAMASIVAN, B. 2020. Optimization of process variables on two-step microwave-assisted transesterification of waste cooking oil. *Environmental Science and Pollution Research,* 27**,** 27244-27255.

SZYDŁOWSKA-CZERNIAK, A., TROKOWSKI, K., KARLOVITS, G. R. & SZŁYK, E. 2010. Determination of antioxidant capacity, phenolic acids, and fatty acid composition of rapeseed varieties. *Journal of Agricultural and Food Chemistry,* 58**,** 7502-7509.

TALEBIAN-KIAKALAIEH, A. & AMIN, N. A. S. 2015. Supported silicotungstic acid on zirconia catalyst for gas phase dehydration of glycerol to acrolein. *Catalysis Today,* 256**,** 315-324.

TALEBIAN-KIAKALAIEH, A., AMIN, N. A. S. & ZAKARIA, Z. Y. 2016. Gas phase selective conversion of glycerol to acrolein over supported silicotungstic acid catalyst. *Journal of Industrial and Engineering Chemistry,* 34**,** 300-312.

TAN, H. W., ABDUL AZIZ, A. R. & AROUA, M. K. 2013. Glycerol production and its applications as a raw material: A review. *Renewable and Sustainable Energy Reviews,* 27**,** 118-127.

TAN, J. C. X., CHUAH, C. H. & CHENG, S. F. 2017. A combined microwave pretreatment/solvent extraction process for the production of oil from palm fruit: optimisation, oil quality and effect of prolonged exposure. *Journal of the Science of Food and Agriculture,* 97**,** 1784-1789.

TAN, K. T., LEE, K. T. & MOHAMED, A. R. 2011. Prospects of non-catalytic supercritical methyl acetate process in biodiesel production. *Fuel processing technology,* 92**,** 1905-1909.

TAN, S. X., LIM, S., ONG, H. C. & PANG, Y. L. 2019. State of the art review on development of ultrasound-assisted catalytic transesterification process for biodiesel production. *Fuel,* 235**,** 886-907.

TAN, Z., ZHANG, X., KUANG, Y., DU, H., SONG, L., HAN, X. & LIANG, X. 2014. Optimized microemulsion production of biodiesel over lipase-catalyzed transesterification of soybean oil by response surface methodology. *Green Processing and Synthesis,* 3**,** 471-478.

TESFA, B., MISHRA, R., GU, F. & POWLES, N. 2010. Prediction models for density and viscosity of biodiesel and their effects on fuel supply system in CI engines. *Renewable energy,* 35**,** 2752-2760.

TESSER, R., CASALE, L., VERDE, D., DI SERIO, M. & SANTACESARIA, E. 2010. Kinetics and modeling of fatty acids esterification on acid exchange resins. *Chemical Engineering Journal,* 157**,** 539-550.

THANASILP, S., SCHWANK, J. W., MEEYOO, V., PENGPANICH, S. & HUNSOM, M. 2013. Preparation of supported POM catalysts for liquid phase oxydehydration of glycerol to acrylic acid. *Journal of Molecular Catalysis A: Chemical,* 380**,** 49-56.

TIAN, Y., XIANG, J., VERNI, C. C. & SOH, L. 2018. Fatty acid methyl ester production via ferric sulfate catalyzed interesterification. *Biomass and bioenergy,* 115**,** 82-87.

TREJDA, M., STAWICKA, K., DUBINSKA, A. & ZIOLEK, M. 2012. Development of niobium containing acidic catalysts for glycerol esterification. *Catalysis today,* 187**,** 129-134.

TREMBLAY, A. Y., CAO, P. & DUBÉ, M. A. 2008. Biodiesel production using ultralow catalyst concentrations. *Energy and Fuels,* 22**,** 2748-2755.

UMBARKAR, S. B., KOTBAGI, T. V., BIRADAR, A. V., PASRICHA, R., CHANALE, J., DONGARE, M. K., MAMEDE, A.-S., LANCELOT, C. & PAYEN, E. 2009. Acetalization of glycerol using mesoporous MoO3/SiO2 solid acid catalyst. *Journal of Molecular Catalysis A: Chemical,* 310**,** 150-158.

VAN GERPEN, J. 2005. Biodiesel processing and production. *Fuel processing technology,* 86**,** 1097-1107.

VEIGA, P. M., GOMES, A. C., VELOSO, C. O. & HENRIQUES, C. A. 2017. Acid zeolites for glycerol etherification with ethyl alcohol: Catalytic activity and catalyst properties. *Applied Catalysis A: General,* 548**,** 2-15.

VELEZ, A., SOTO, G., HEGEL, P., MABE, G. & PEREDA, S. 2012. Continuous production of fatty acid ethyl esters from sunflower oil using supercritical ethanol. *Fuel,* 97**,** 703-709.

VELJKOVIĆ, V. B., AVRAMOVIĆ, J. M. & STAMENKOVIĆ, O. S. 2012. Biodiesel production by ultrasound-assisted transesterification: State of the art and the perspectives. *Renewable and Sustainable Energy Reviews,* 16**,** 1193-1209.

VELUTURLA, S., NARULA, A. & SHETTY, S. P. 2017. Kinetic study of synthesis of bio-fuel additives from glycerol using a hetropolyacid. *Resource-Efficient Technologies,* 3**,** 337-341.

VERDUZCO, L. F. R. 2013. Density and viscosity of biodiesel as a function of temperature: empirical models. *Renewable and Sustainable Energy Reviews,* 19**,** 652-665.

VICENTE, G., MARTıNEZ, M. & ARACIL, J. 2004. Integrated biodiesel production: a comparison of different homogeneous catalysts systems. *Bioresource technology,* 92**,** 297-305.

VIOLA, E., BLASI, A., VALERIO, V., GUIDI, I., ZIMBARDI, F., BRACCIO, G. & GIORDANO, G. 2012. Biodiesel from fried vegetable oils via transesterification by heterogeneous catalysis. *Catalysis Today,* 179**,** 185-190.

WAGGONER, D. C. & HATCHER, P. G. 2016. Thermally assisted methylation of glycerol by tetramethylammonium hydroxide thermochemolysis. *Journal of Analytical and Applied Pyrolysis,* 122**,** 289-293.
WAHIDIN, S., IDRIS, A., YUSOF, N. M., KAMIS, N. H. H. & SHALEH, S. R. M. 2018. Optimization of the ionic liquid-microwave assisted one-step biodiesel production process from wet microalgal biomass. *Energy Conversion and Management,* 171**,** 1397-1404.
WAN, F. L., TENG, Y. L., WANG, Y., LI, A. J. & ZHANG, N. 2015. Optimization of oligoglycerol fatty acid esters preparation catalyzed by Lipozyme 435. *Grasas y Aceites,* 66**,** 088.
WANG, P. S., TAT, M. E. & VAN GERPEN, J. 2005. The production of fatty acid isopropyl esters and their use as a diesel engine fuel. *Journal of the American Oil Chemists' Society,* 82**,** 845-849.
WANG, Z.-M., LEE, J.-S., PARK, J.-Y., WU, C.-Z. & YUAN, Z.-H. 2008. Optimization of biodiesel production from trap grease via acid catalysis. *Korean Journal of Chemical Engineering,* 25**,** 670-674.
WEN, Z., YU, X., TU, S.-T., YAN, J. & DAHLQUIST, E. 2009. Intensification of biodiesel synthesis using zigzag micro-channel reactors. *Bioresource technology,* 100**,** 3054-3060.
WITSUTHAMMAKUL, A. & SOOKNOI, T. 2012. Direct conversion of glycerol to acrylic acid via integrated dehydration–oxidation bed system. *Applied Catalysis A: General,* 413**,** 109-116.
WU, H., LIU, Y., ZHANG, J. & LI, G. 2014. In situ reactive extraction of cottonseeds with methyl acetate for biodiesel production using magnetic solid acid catalysts. *Bioresource technology,* 174**,** 182-189.
WU, H., ZHANG, J., WEI, Q., ZHENG, J. & ZHANG, J. 2013. Transesterification of soybean oil to biodiesel using zeolite supported CaO as strong base catalysts. *Fuel processing technology,* 109**,** 13-18.
WU, W., ZHU, M. & ZHANG, D. 2017. An experimental and kinetic study of canola oil transesterification catalyzed by mesoporous alumina supported potassium. *Applied Catalysis A: General,* 530**,** 166-173.
YADAV, V. P., MAITY, S. K. & SHEE, D. 2017. Etherification of glycerol with ethanol over solid acid catalysts: kinetic study using cation exchange resin. *Indian Chemical Engineer,* 59**,** 117-135.
YANG, F., HANNA, M. A. & SUN, R. 2012. Value-added uses for crude glycerol - A byproduct of biodiesel production. *Biotechnology for Biofuels,* 5**,** 1 - 10.
YINGYING, L., HOUFANG, L., JIANG, W., DONGSHENG, L., SHIJIE, L. & LIANG, B. 2012. Biodiesel production from crude Jatropha curcas L. oil with trace acid catalyst. *Chinese Journal of Chemical Engineering,* 20**,** 740-746.
YUAN, H., LI, X. & YANG, B. 2013. Kinetics for the Synthesis of Biodiesel Based on the Calculation of Hot Spot Temperatures in the Catalyst. *Industrial & Engineering Chemistry Research,* 52**,** 15549-15559.
YÜCEL, Y. 2011. Biodiesel production from pomace oil by using lipase immobilized onto olive pomace. *Bioresource technology,* 102**,** 3977-3980.
YURDAKUL, M., AYAS, N., BIZKARRA, K., EL DOUKKALI, M. & CAMBRA, J. F. 2016. Preparation of Ni-based catalysts to produce hydrogen from glycerol by steam reforming process. *International Journal of Hydrogen Energy,* 41**,** 8084-8091.
ZAKARIA, R. 2010. *Reactive Extraction of Rapeseed for Biodiesel Production* PhD, Newcastle University.

ZAKARIA, R. & HARVEY, A. P. 2012. Direct production of biodiesel from rapeseed by reactive extraction/in situ transesterification. *Fuel Processing Technology,* 102**,** 53-60.

ZAPPIELO, C. D., NANICUACUA, D. M., DOS SANTOS, W. N. L., DA SILVA, D. L. F., DALL'ANTÔNIA, L. H., OLIVEIRA, F. M. D., CLAUSEN, D. N. & TARLEY, C. R. T. 2016. Solid Phase Extraction to On-Line Preconcentrate Trace Cadmium Using Chemically Modified Nano-Carbon Black with 3-Mercaptopropyltrimethoxysilane. *Journal of the Brazilian Chemical Society,* 27**,** 1715-1726.

ZENG, D., YANG, L. & FANG, T. 2017. Process optimization, kinetic and thermodynamic studies on biodiesel production by supercritical methanol transesterification with CH3ONa catalyst. *Fuel,* 203**,** 739-748.

ZENG, J., WANG, X., ZHAO, B., SUN, J. & WANG, Y. 2009. Rapid in situ transesterification of sunflower oil. *Industrial & Engineering Chemistry Research,* 48**,** 850-856.

ZHANG, B., TANG, X., LI, Y., XU, Y. & SHEN, W. 2007. Hydrogen production from steam reforming of ethanol and glycerol over ceria-supported metal catalysts. *International Journal of Hydrogen Energy,* 32**,** 2367-2373.

ZHANG, L., SHENG, B., XIN, Z., LIU, Q. & SUN, S. 2010. Kinetics of transesterification of palm oil and dimethyl carbonate for biodiesel production at the catalysis of heterogeneous base catalyst. *Bioresource Technology,* 101**,** 8144-8150.

ZHANG, Y., DUBE, M., MCLEAN, D. & KATES, M. 2003. Biodiesel production from waste cooking oil: 1. Process design and technological assessment. *Bioresource technology,* 89**,** 1-16.

ZHAO, H., ZHOU, C. H., WU, L. M., LOU, J. Y., LI, N., YANG, H. M., TONG, D. S. & YU, W. H. 2013. Catalytic dehydration of glycerol to acrolein over sulfuric acid-activated montmorillonite catalysts. *Applied Clay Science,* 74**,** 154-162.

ZHENG, M., SKELTON, R. & MACKLEY, M. 2007. Biodiesel reaction screening using oscillatory flow meso reactors. *Process Safety and Environmental Protection,* 85**,** 365-371.

ZHENG, S., KATES, M., DUBÉ, M. & MCLEAN, D. 2006. Acid-catalyzed production of biodiesel from waste frying oil. *Biomass and bioenergy,* 30**,** 267-272.

ZHOU, L., NGUYEN, T.-H. & ADESINA, A. A. 2012. The acetylation of glycerol over amberlyst-15: Kinetic and product distribution. *Fuel processing technology,* 104**,** 310-318.

ZHU, M., HE, B., SHI, W., FENG, Y., DING, J., LI, J. & ZENG, F. 2010. Preparation and characterization of PSSA/PVA catalytic membrane for biodiesel production. *Fuel,* 89**,** 2299-2304.

ZUBIR, M. & CHIN, S. 2010. Kinetics of modified zirconia-catalyzed heterogeneous esterification reaction for biodiesel production. *Journal of Applied Sciences,* 10**,** 2584-2589.

APPENDIX A: Calibrations

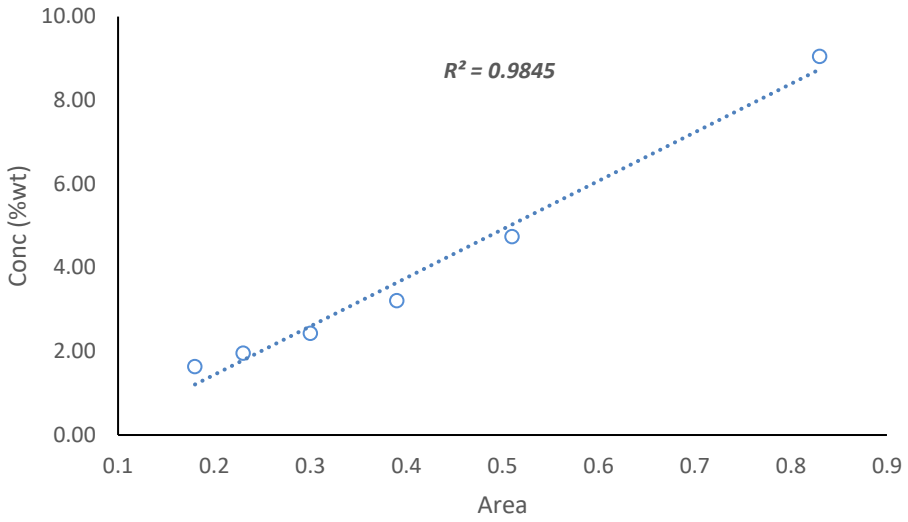

Figure A- 1: Calibration of glycerol standard using HPLC.

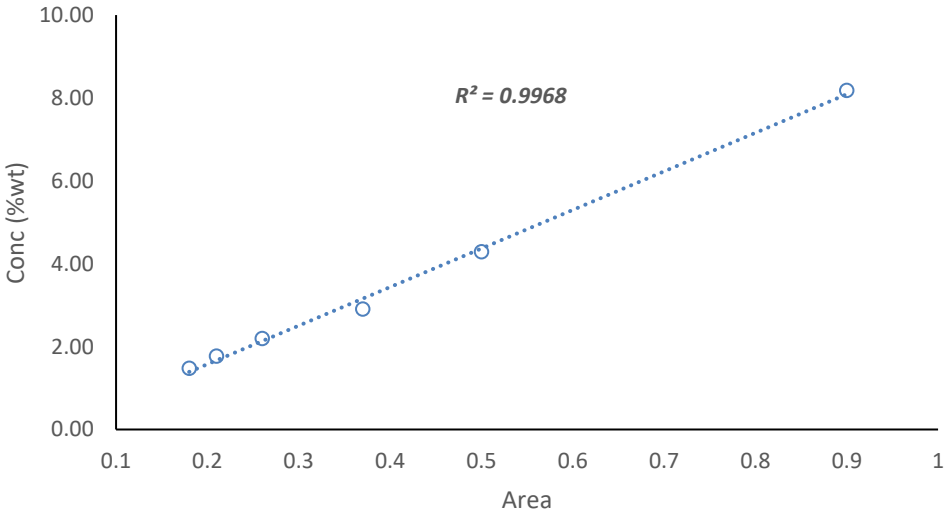

Figure A- 2: Calibration of diglycerol standard using HPLC.

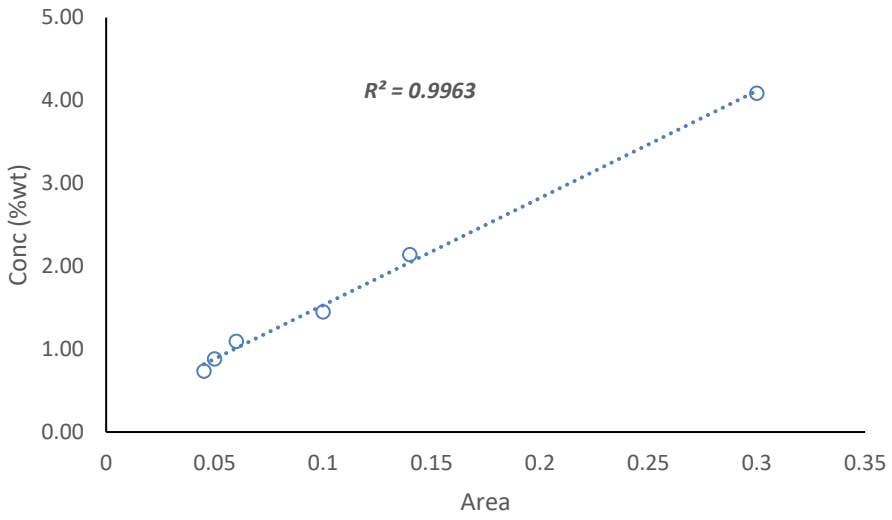

Figure A- 3: Calibration of triglycerol standard using HPLC.

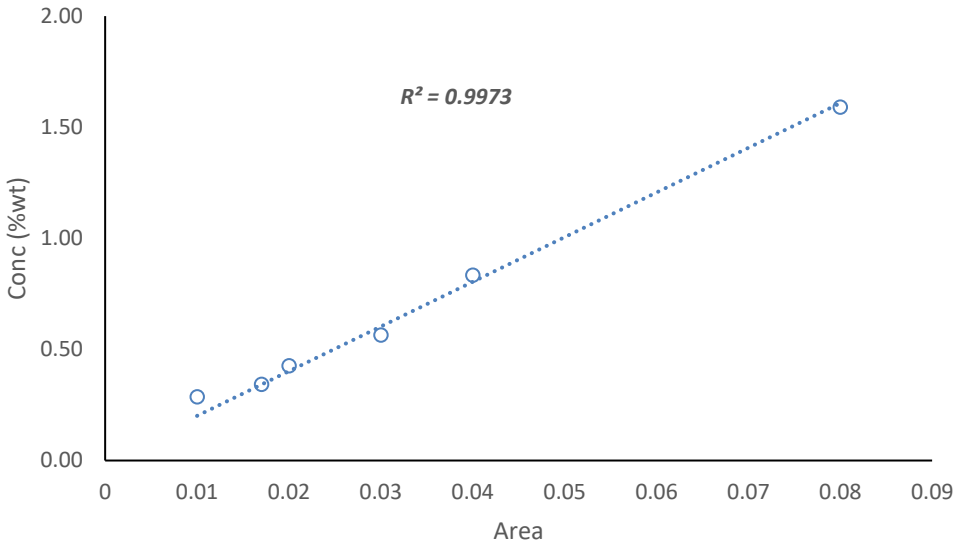

Figure A- 4: Calibration of tetraglycerol standard using HPLC.

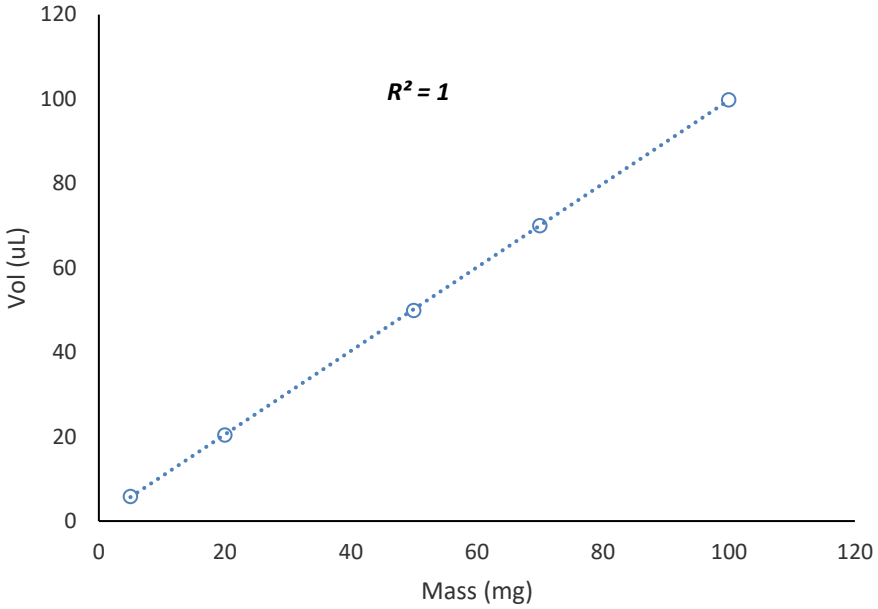

Figure A- 5: Checking the calibration of 20 – 200 µL pipette used for the study.

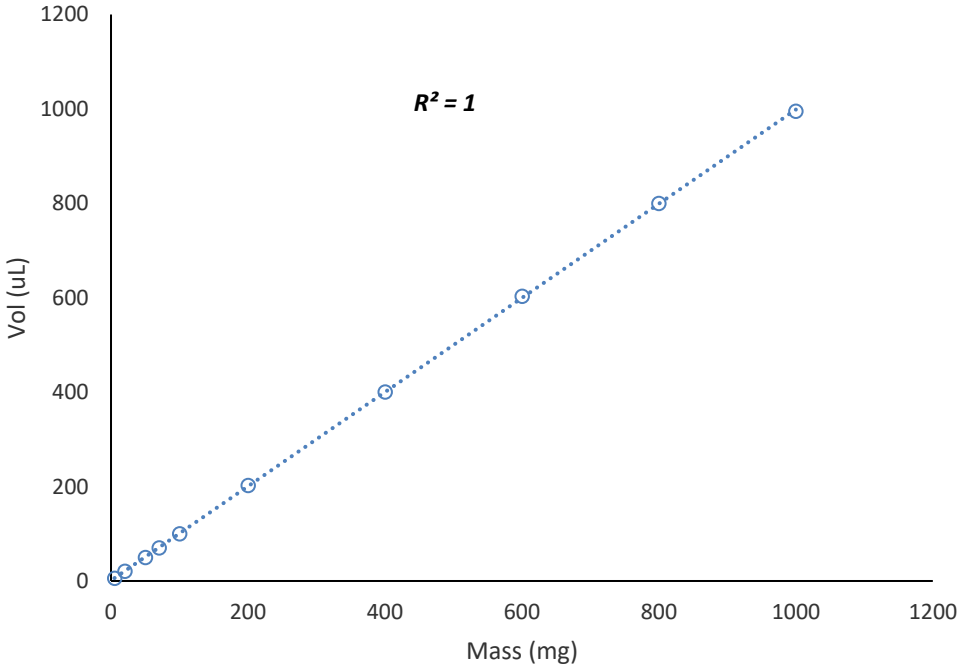

Figure A- 6: Checking the calibration of 100 – 1000 µL pipette used for the study.

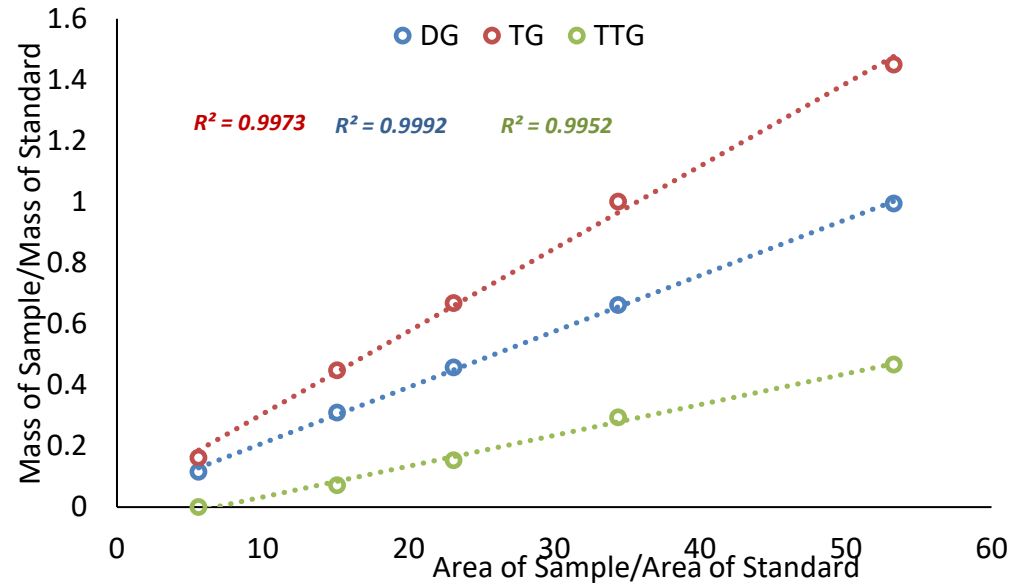

Figure A- 7: GC calibration of polyglycerol standards.

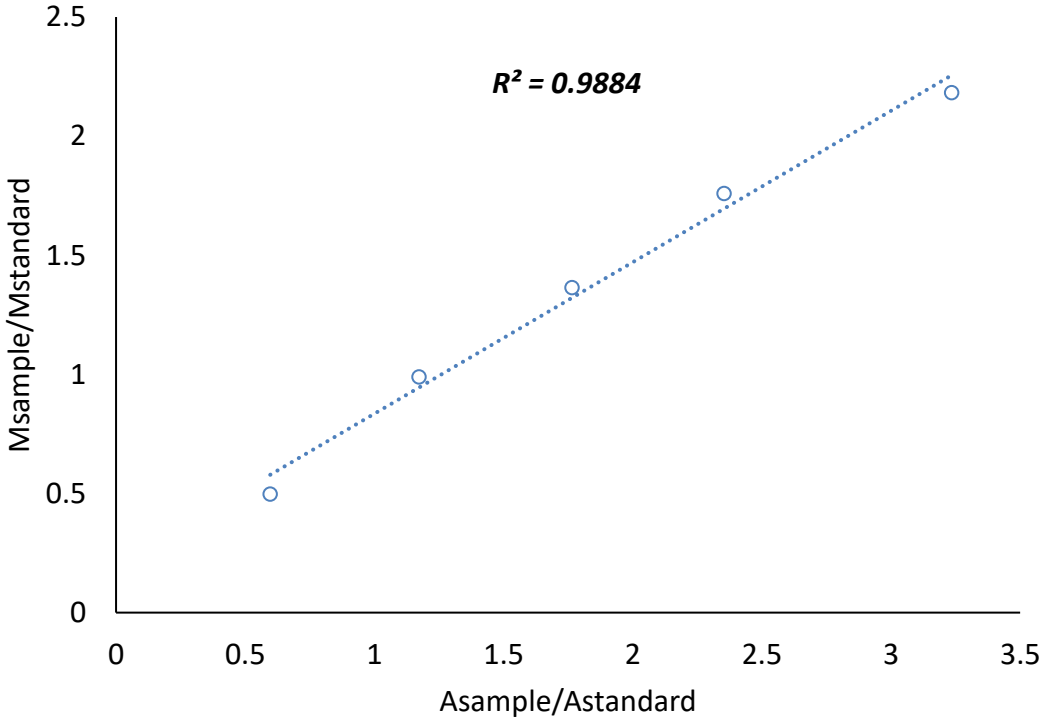

Figure A- 8: GC calibration for glycerol ether standard.

APPENDIX B: Plots

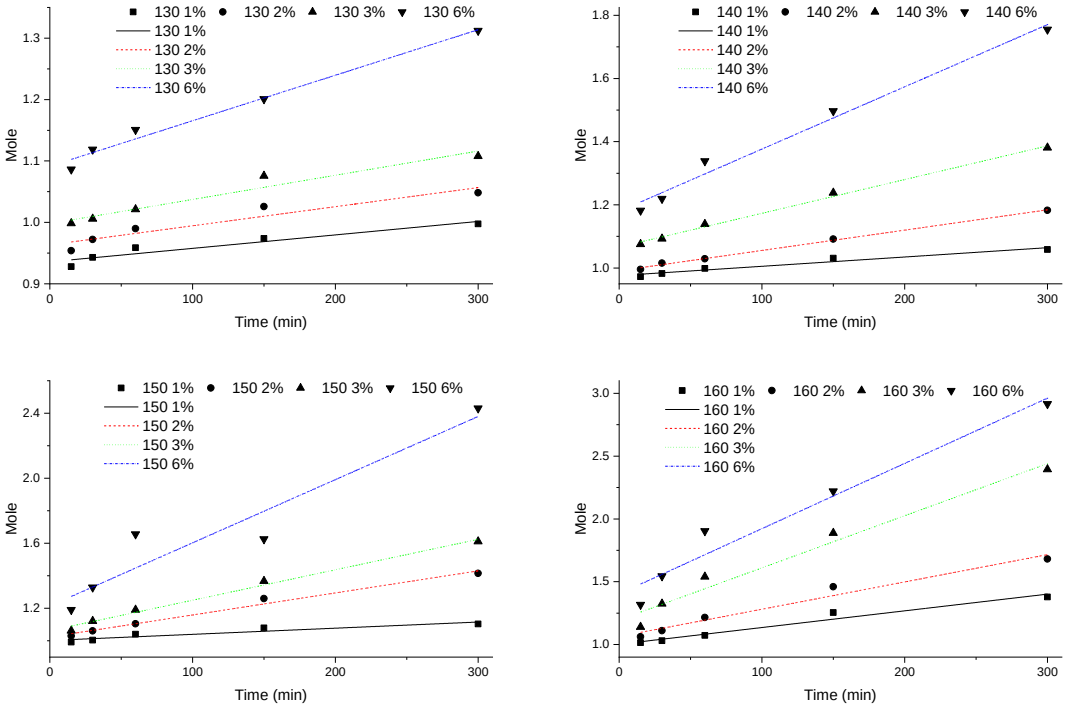

Equation	y = a + b*x															
Plot	130 1%	130 2%	130 3%	130 6%	140 1%	140 2%	140 3%	140 6%	150 1%	150 2%	150 3%	150 6%	160 1%	160 2%	160 3%	160 6%
Weight	No Weighting															
Intercept	0.93579 ±	0.96347 ±	0.99806 ±	1.09149 ±	0.976 ± 0.	0.99141 ±	1.0667 ±	1.17973	1.00221 ±	1.02374	1.06302	1.21483	1.00245	1.06406	1.19645	1.40361
Slope	2.19318E-	3.10848E-	3.94015E-	7.41291E-	2.9466E-	6.43285E-	0.00107	0.00197	3.78381E-	0.00136	0.00187	0.00389	0.00133	0.00217	0.00415	0.0052 ±
Residual	2.63061E-	5.80748E-	4.66235E-	5.21072E-	2.51662E	7.21608E-	3.14994E	0.00352	0.00112	0.00148	0.00186	0.08229	0.00357	0.00799	0.03001	0.06652
Pearson's	0.95419	0.94999	0.97405	0.99158	0.97492	0.99844	0.99753	0.99195	0.93654	0.99283	0.99528	0.95436	0.98233	0.98513	0.9847	0.97856
R-Square	0.91047	0.90248	0.94877	0.98324	0.95047	0.99687	0.99506	0.98397	0.87711	0.98571	0.99058	0.91081	0.96498	0.97048	0.96962	0.95758
Adj. R-Sq	0.88063	0.86997	0.9317	0.97765	0.93396	0.99583	0.99341	0.97863	0.83615	0.98095	0.98743	0.88107	0.95331	0.96064	0.9595	0.94344

Figure B- 1: Kinetic fitting to the second rate law.

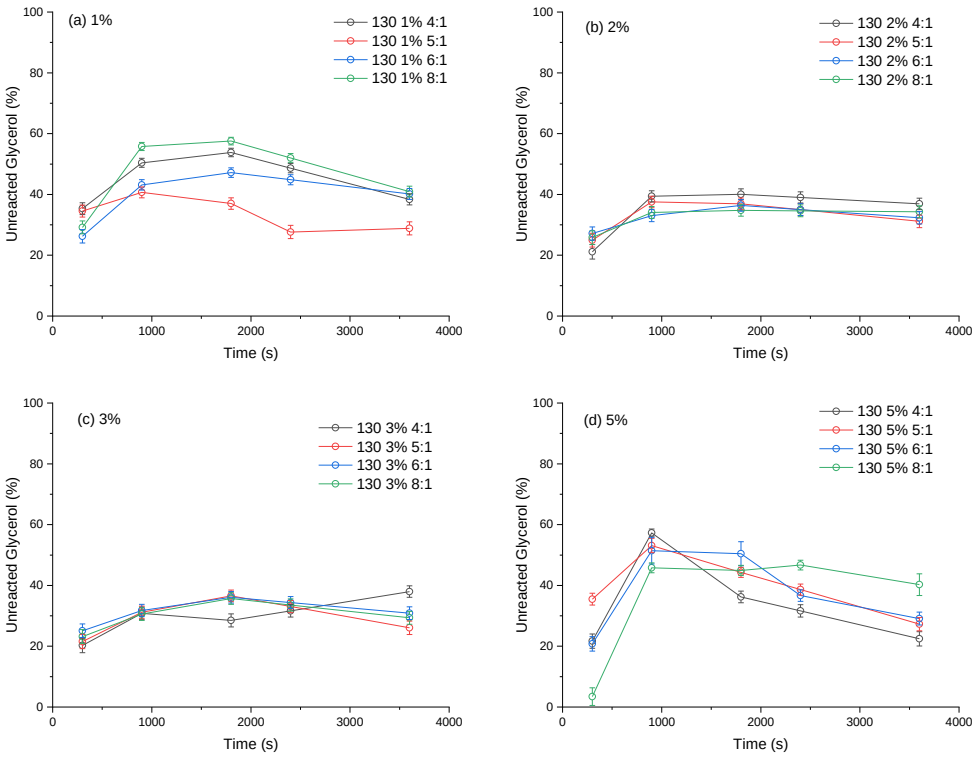

Figure B- 2: Unreacted glycerol for reactive coupling at 130 °C (a) 1 (b) 2 (c) 3 (d) 5 wt% catalyst concentration with various molar ratio.

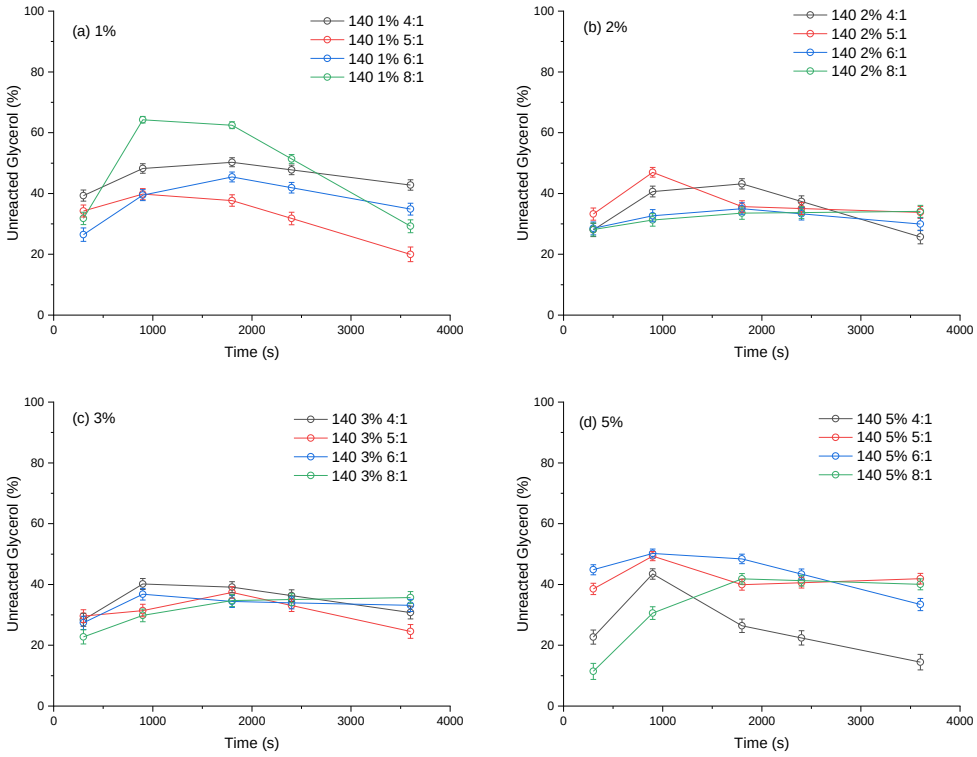

Figure B- 3: Unreacted glycerol for reactive coupling at 140 °C (a) 1 (b) 2 (c) 3 (d) 5 wt% catalyst concentration with various molar ratio.

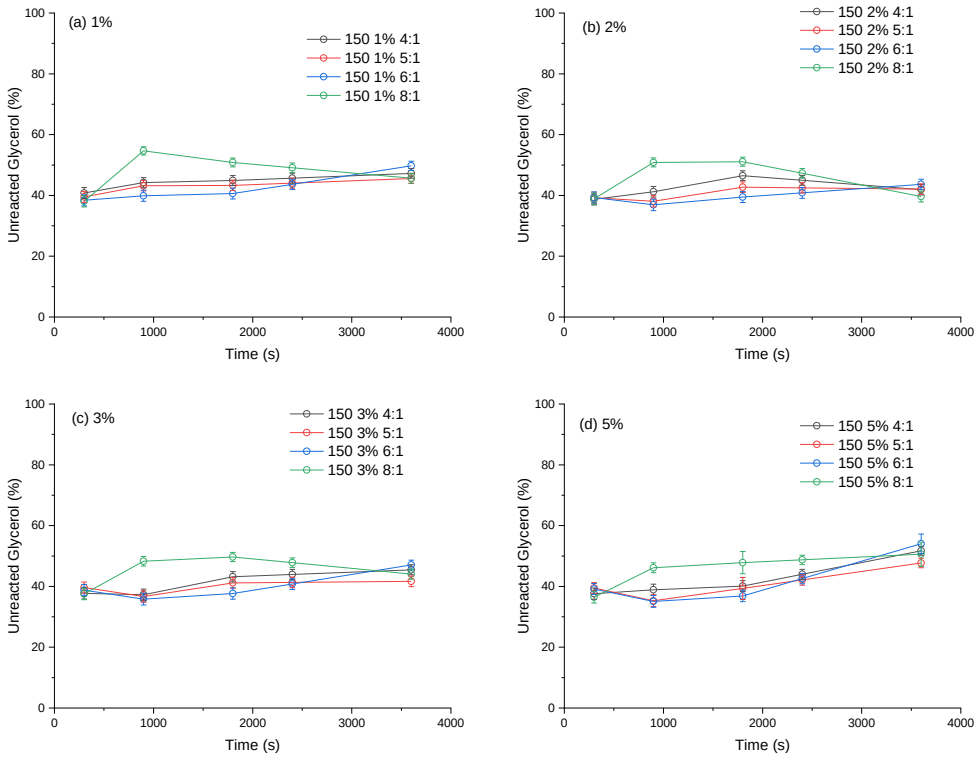

Figure B- 4: Unreacted glycerol for reactive coupling at 150 °C (a) 1 (b) 2 (c) 3 (d) 5 wt% catalyst concentration with various molar ratio.

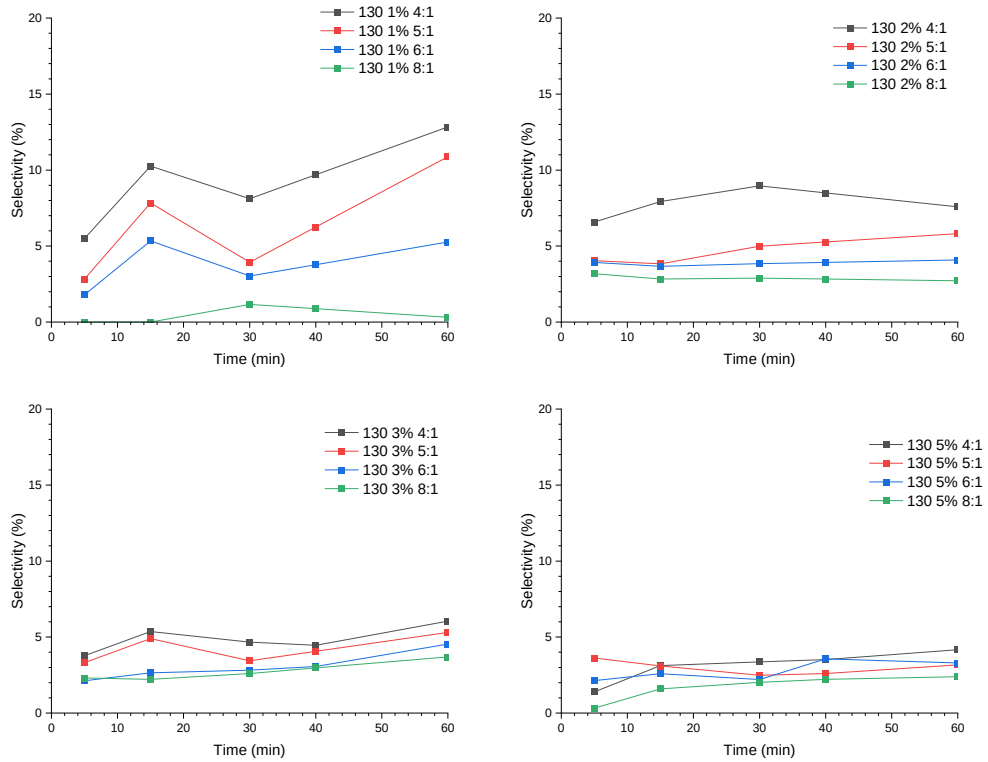

Figure B- 5: Diglycerol selectivity during reactive coupling at 130 °C.

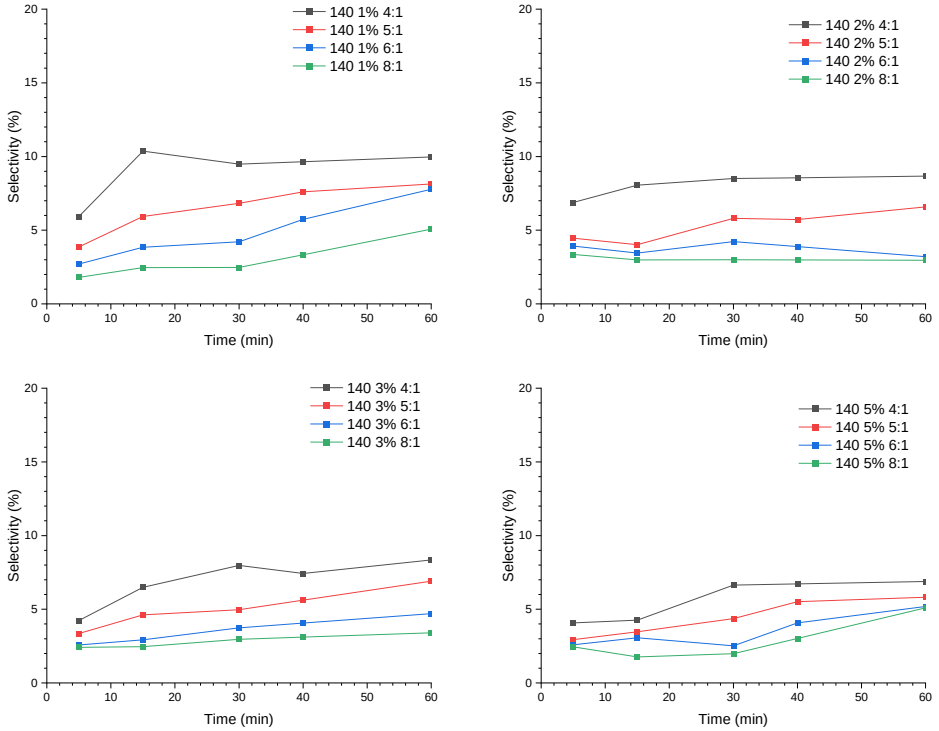

Figure B- 6: Diglycerol selectivity during reactive coupling at 140 °C.

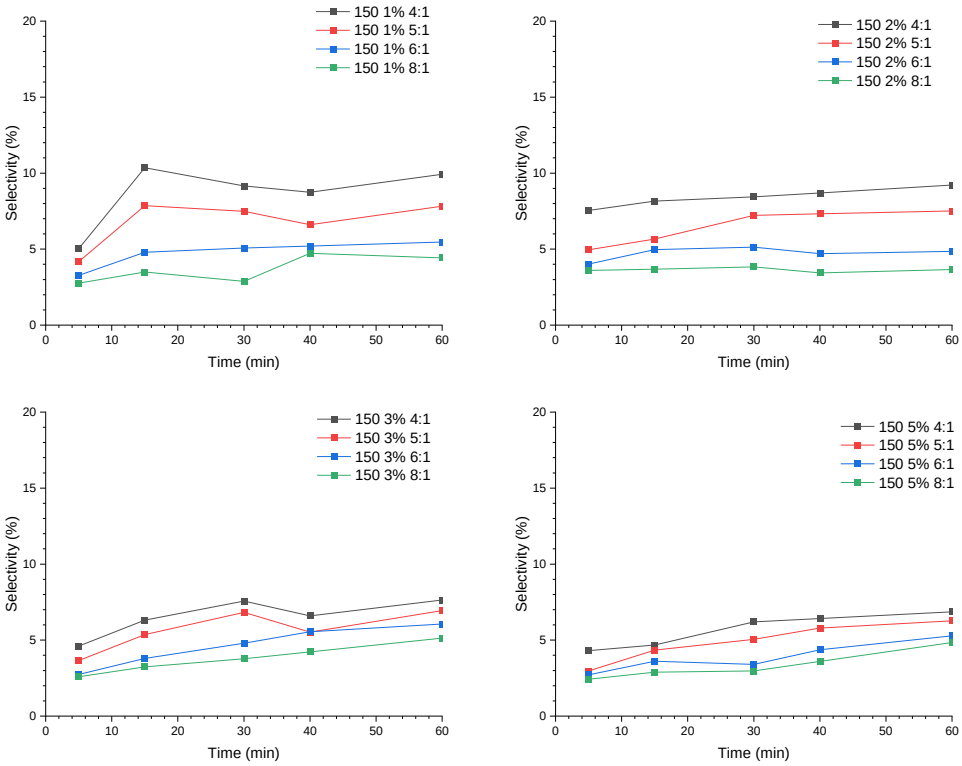

Figure B- 7: Diglycerol selectivity during reactive coupling at 150 °C.

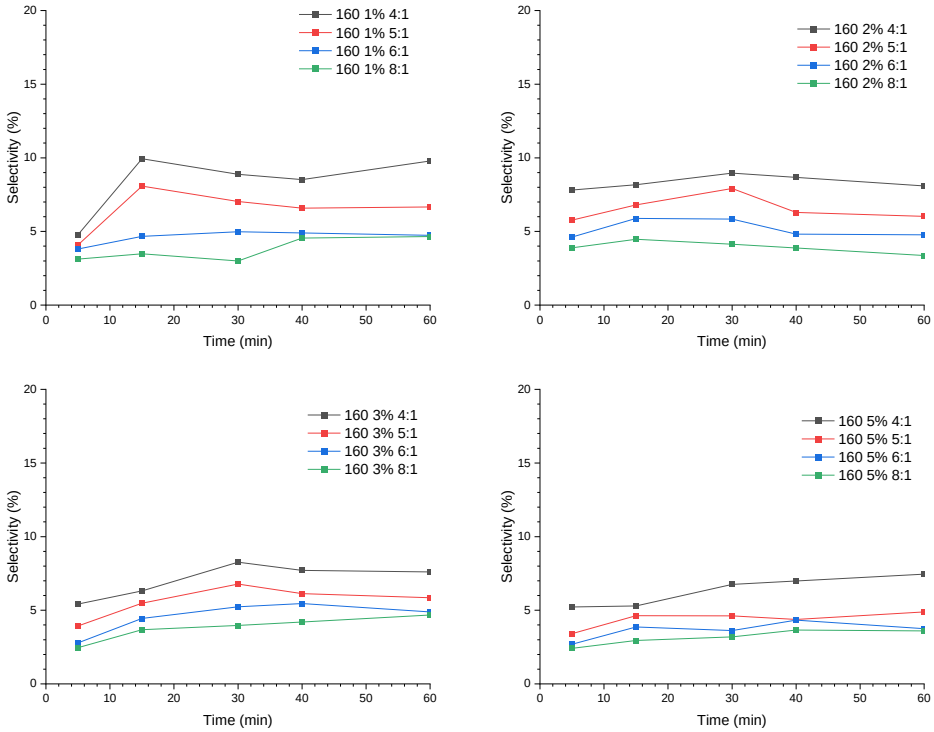

Figure B- 8: Diglycerol selectivity during reactive coupling at 160 °C.

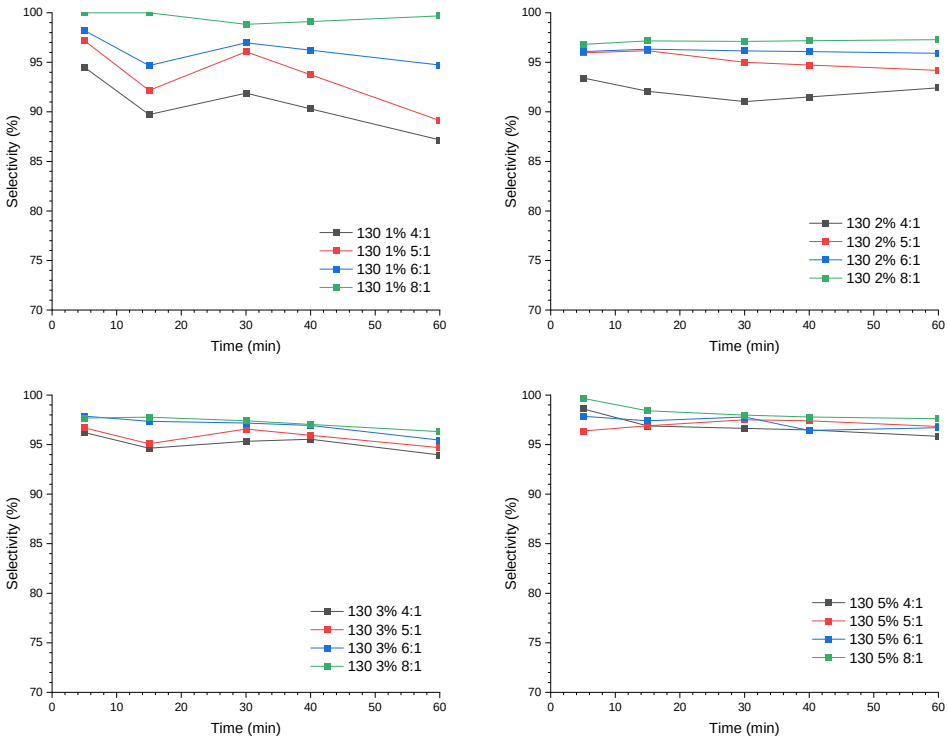

Figure B- 9: Methoxyl propanediol selectivity during reactive coupling at 130 °C.

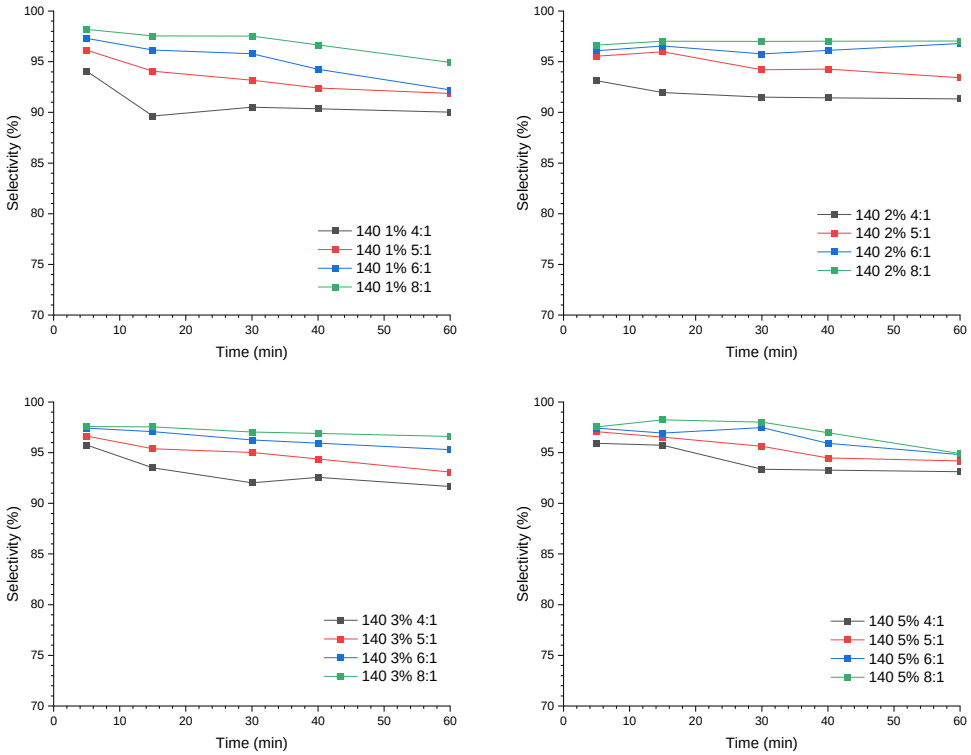

Figure B- 10: Methoxyl propanediol selectivity during reactive coupling at 140 °C

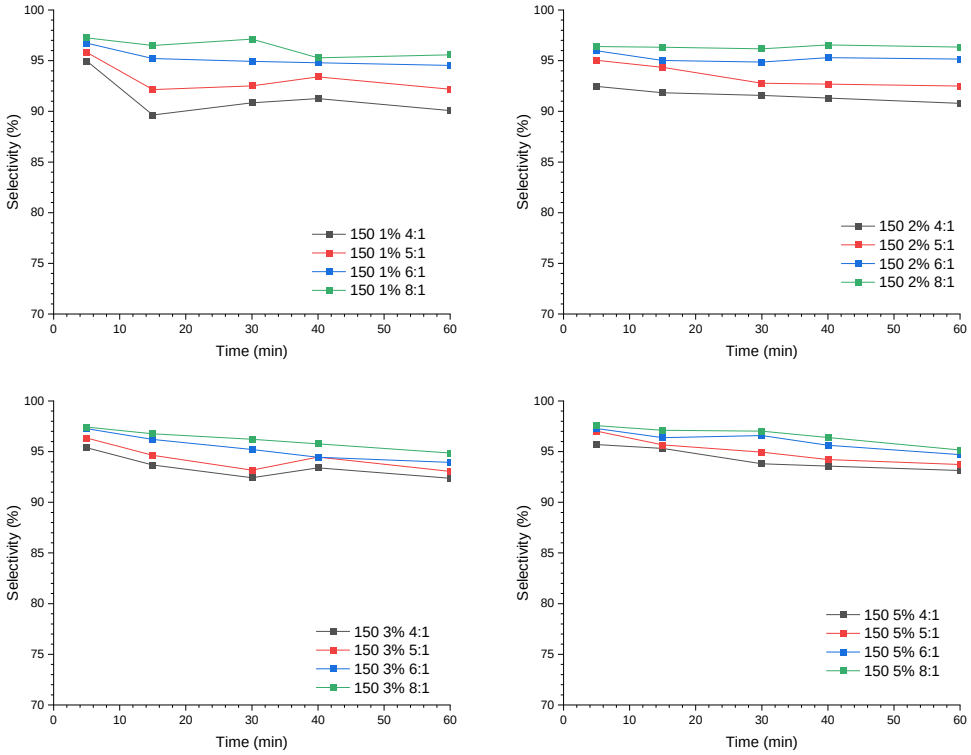

Figure B- 11: Methoxyl propanediol selectivity during reactive coupling at 150 °C

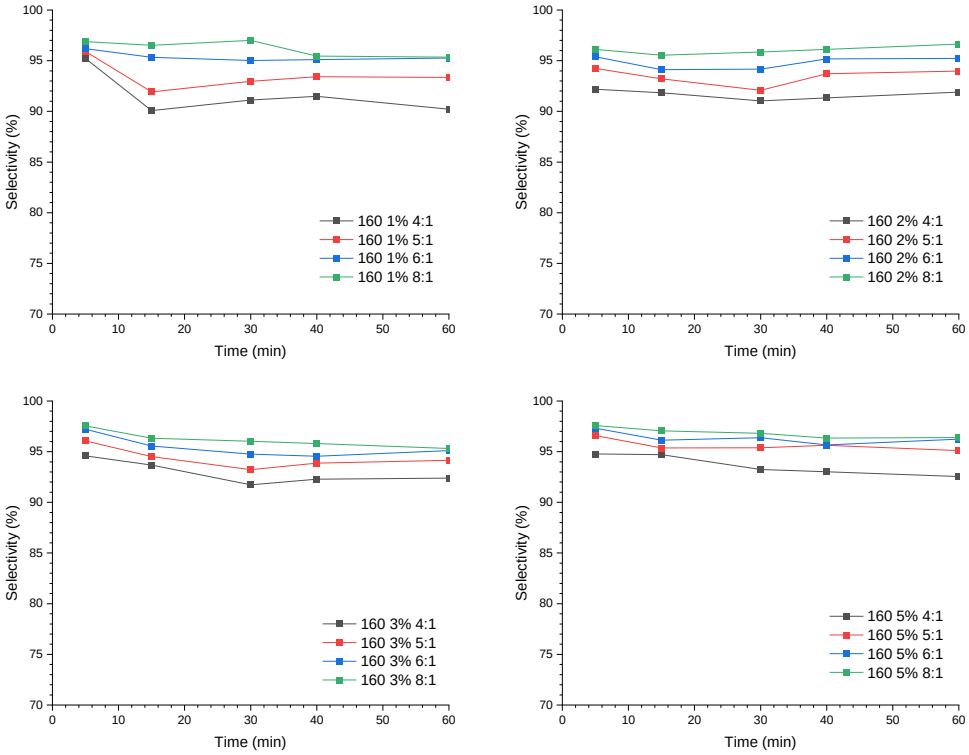

Figure B- 12: Methoxyl propanediol selectivity during reactive coupling at 160 °C

APPENDIX C: MS Fragmentation

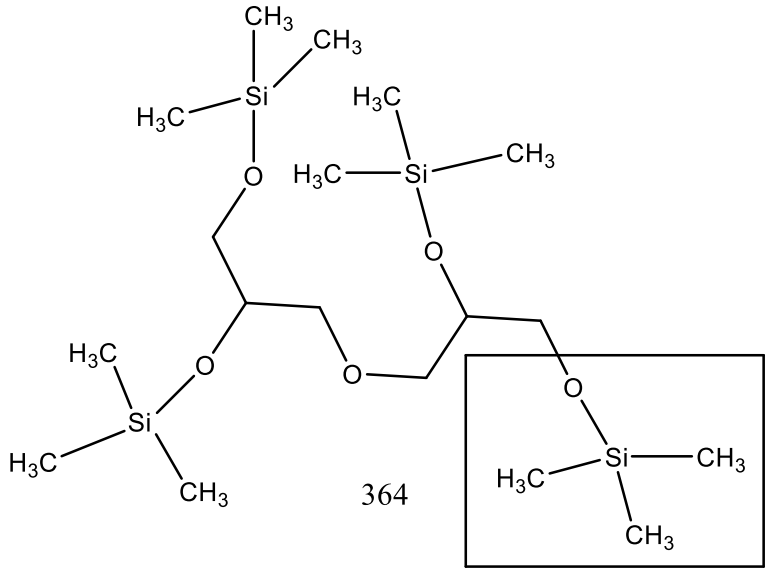

1,2,4 trimethylsilyl ether diglycerol

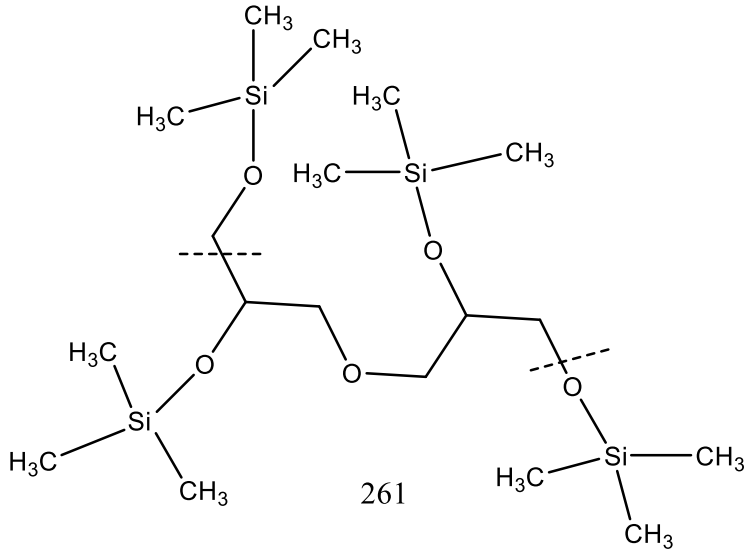

1,3 trimethylsilyl ether of diglycerol

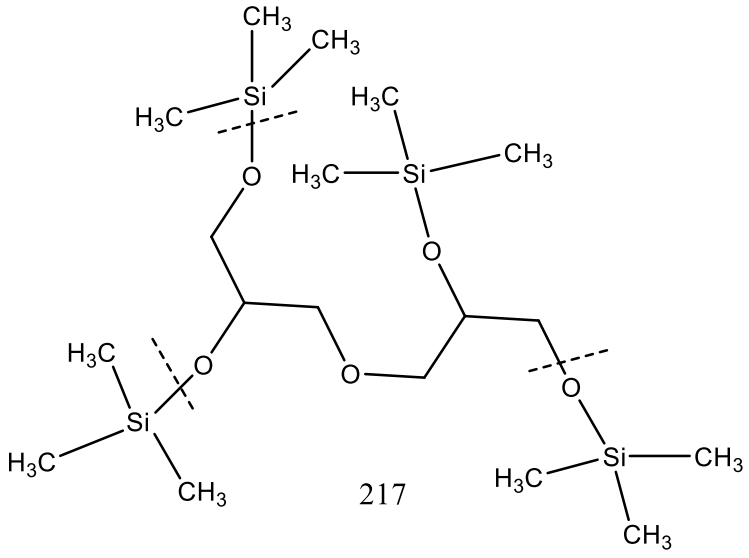

Trimethylsilyl ether diglycerol

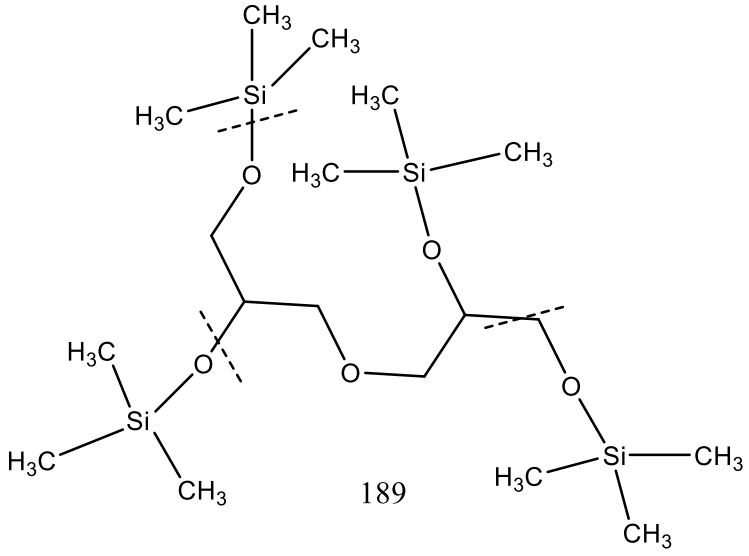

Trimethylsilyl ether of diglycerol

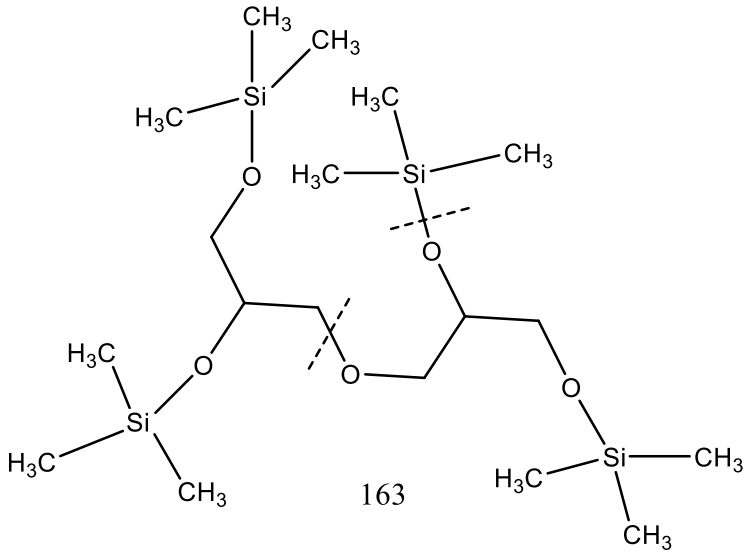

Trimethylsilyl ether glycerol

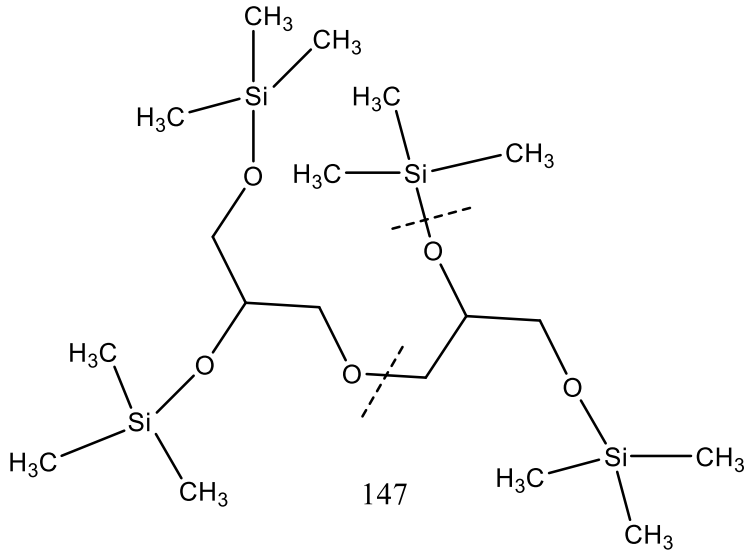

147

Trimethylsilyl ether of glycerol

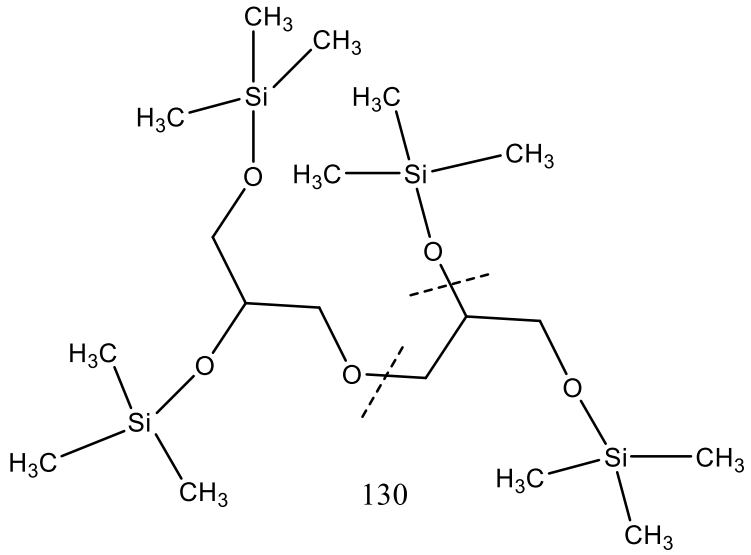

130

Trimethylsilyl propane

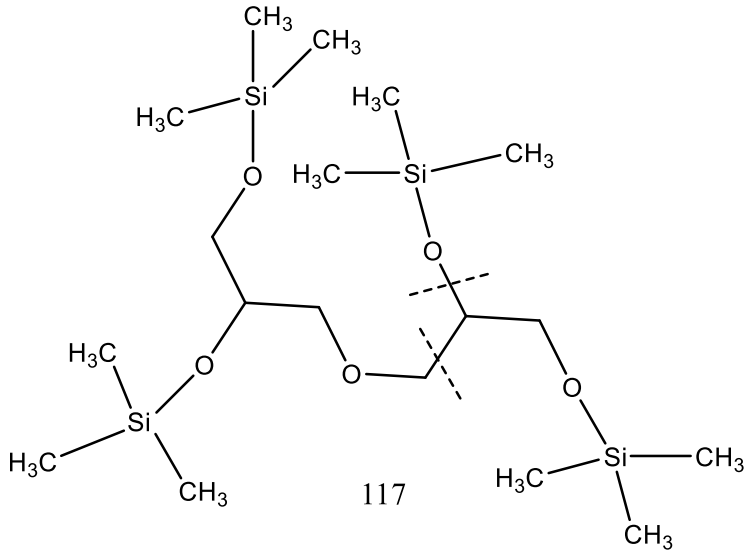

Ethyl trimethylsilyl

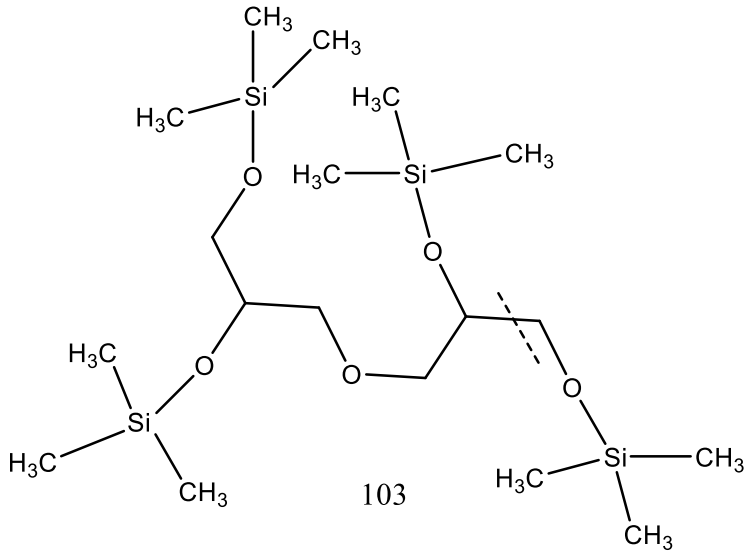

Methyl trimethylsilyl

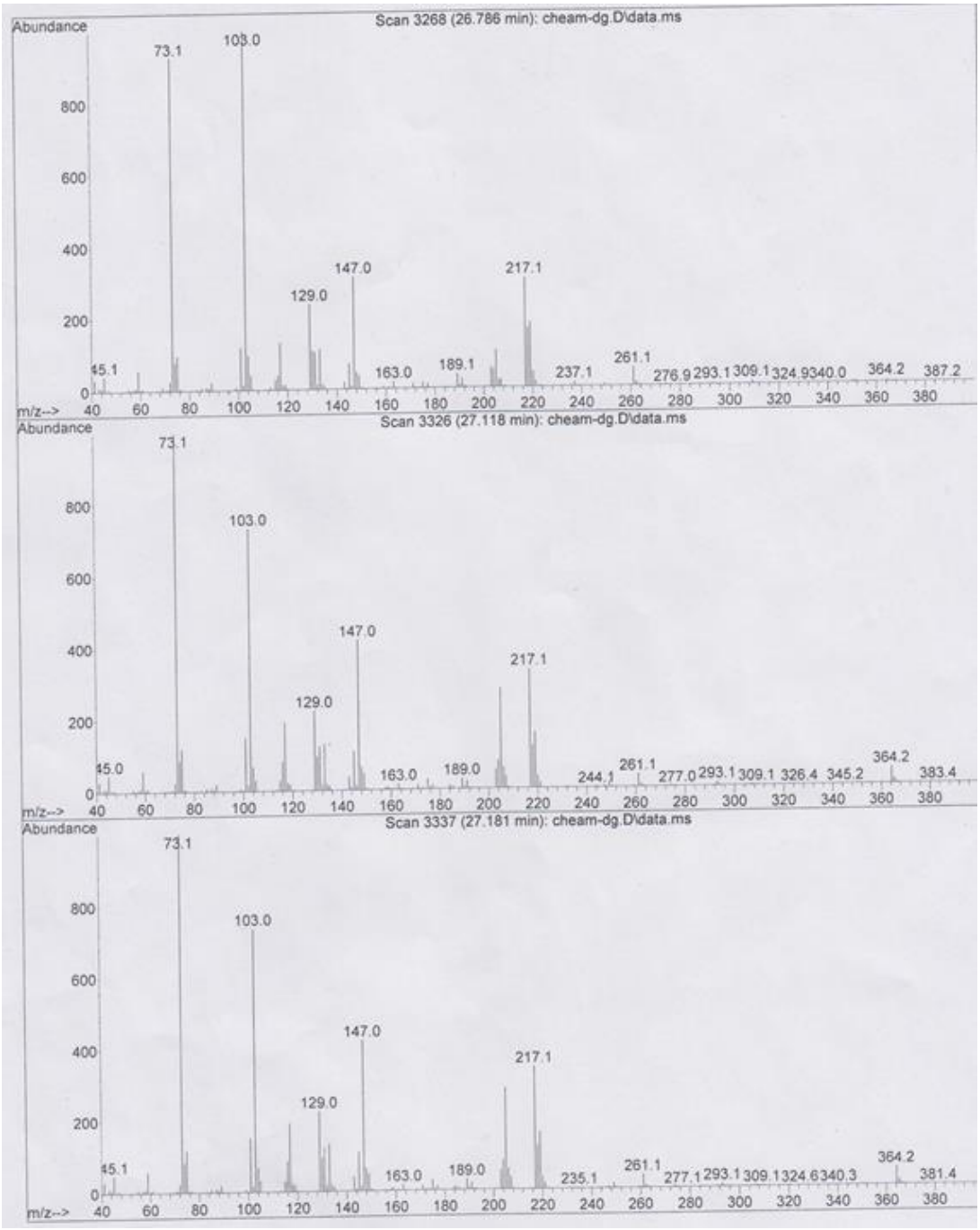

GC-MS of the isomers of Diglycerol

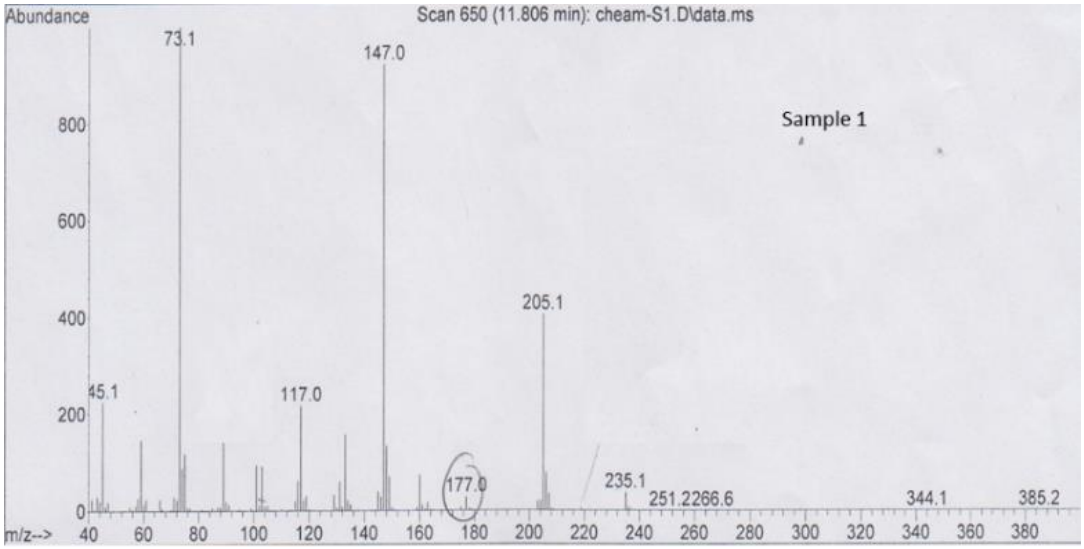

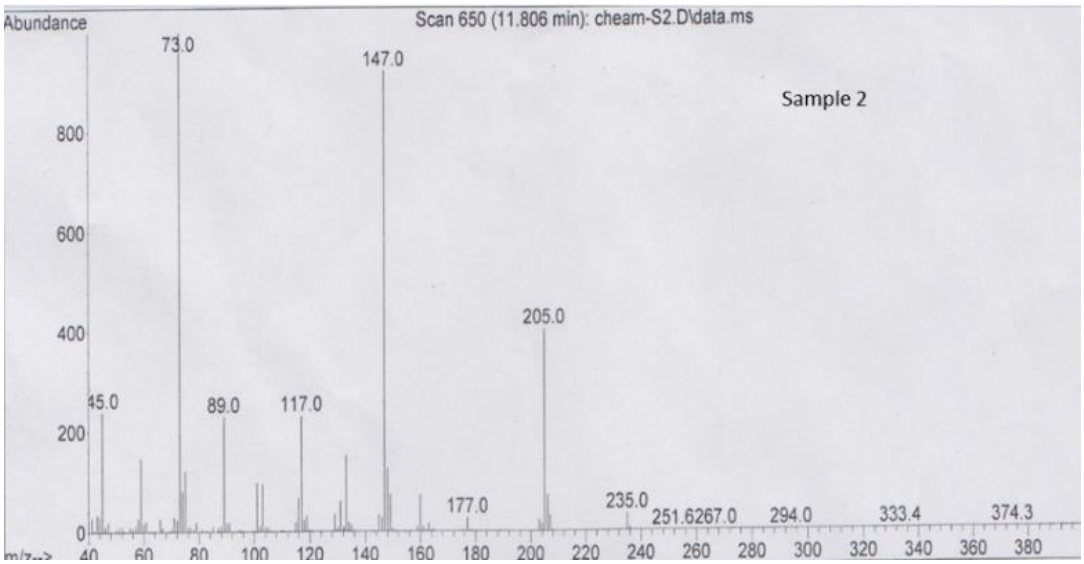

GC-MS of glycerol ether

APPENDIX D: MATLAB Coding

Glycerol valorisation (kinetics coding)

```
function dC = GG(t, C)

%{      The function file biodiesel.m contains the mass balances for
the
%       reaction network:
%
%       2G -> DG + W
%       DG + G -> TG + W
%       TG + G -> TTG + W
%       G  -> 3CO + 4H2
%       CO + W  -> CO2 + H2
%       2CO  ->  CO2 + C
%       G  -> ACR + 2W
%       ACR + H2 -> ACC

%       Define terms
CG = C(1); CDG = C(2); CTG = C(3); %CTTG = C(4); CCO = C(5); CH2 =
C(6); CCO2 = C(7); CACR = C(8); CACC = C(9); CW = C(10);

%       Rate constant
T = 130 + 273; % Temperature of the reaction in kelvin from 130 to 160
oC (403, 413, 423 and 433)
R = 8.314; % gas constant
k1 = (2.28E+11*exp(-111014.5/(R*T)));        %2nd order with zero
a = 0.95; % Order of catalyst for glycerol
m = 0.06; % cat conc. 0.010196, 0.020392, 0.030588, 0.061175

% Reaction rates:
r1 = (k1*CG^2)*m^a;

% Mass balance
dCG = -2*r1;
dCDG = r1;
dCTG = 0.03*dCDG;
%Assign output variables

dC(1,:) = dCG;
dC(2,:) = dCDG;
dC(3,:) = dCTG;



Rate = readtable('poly1.xlsx')
% Initial concentrations:
C0 = [1.085, 0, 0]; % C0 for methanol 4:1-8:1 (0.4202, 0.5191, 0.6180,
0.8157)


% Time range for the model (seconds)
t = 0:3600;

% Call the ode15s solver
[t,C] = ode45(@GG,t,C0);
```

```
% Plot the data
figure

 plot(t,C(:,1),'-k',...
     t,C(:,2),'-r',...
     t,C(:,3),'-g',...
     Rate.Time,Rate.G1306, 'ko',...
     Rate.Time,Rate.DG1306, 'ro',...
     Rate.Time,Rate.TG1306,'go')%,..

legend('G M','DG M', 'TG M', 'G E', 'DG E', 'TG E')
xlabel('Time (sec)')
ylabel('Concentration (M)')


num1 = xlsread ('poly1.xlsx', 1, 'D7:D10');   % Time
num2 = xlsread ('poly1.xlsx', 1, 'H7:H10'); % Glycerol
num3 = xlsread ('poly1.xlsx', 1, 'Y7:Y10'); % Diglycerol
num4 = xlsread ('poly1.xlsx', 1, 'AP7:AP10'); % Triglycerol

x1 = num1;
y11 = num2;
y12 = num3;
y13 = num4;

z1 = [x1 y11 y12 y13];

y21 = C(:,1);
y22 = C(:,2);
y23 = C(:,3);

z2 = zeros (4,4);
z2 (1,1) = t (1);
z2 (1,2) = y21 (1);
z2 (1,3) = y22 (1);
z2 (1,4) = y23 (1);
z2 (2,1) = t (901);
z2 (2,2) = y21 (901);
z2 (2,3) = y22 (901);
z2 (2,4) = y23 (901);
z2 (3,1) = t (1801);
z2 (3,2) = y21 (1801);
z2 (3,3) = y22 (1801);
z2 (3,4) = y23 (1801);
z2 (4,1) = t (3601);
z2 (4,2) = y21 (3601);
z2 (4,3) = y22 (3601);
z2 (4,4) = y23 (3601);

z3 = [x1 z1(:,2) z2(:,2)];
z4 = [x1 z1(:,3) z2(:,3)];
z5 = [x1 z1(:,4) z2(:,4)];

Mn1=mean(z3(:,2));
Mn2=mean(z4(:,2));
Mn3=mean(z5(:,2));

SST1 = sum((z3(:,2)-Mn1).^2);
SST2 = sum((z4(:,2)-Mn2).^2);
SST3 = sum((z5(:,2)-Mn3).^2);
```

```
SSR1=sum((z3(:,2)-z3(:,3)).^2);
SSR2=sum((z4(:,2)-z4(:,3)).^2);
SSR3=sum((z5(:,2)-z5(:,3)).^2);

Rsq_Glycerol =1-(SSR1/SST1);
Rsq_Diglycerol =1-(SSR2/SST2);
Rsq_Triglycerol =1-(SSR3/SST3);

Rsq = [Rsq_Glycerol Rsq_Diglycerol Rsq_Triglycerol]
```

Coding for the kinetics of reactive coupling

```
function dC = BioAcid(t, C)

%{      The function file biodiesel.m contains the mass balances for
the
%       reaction network:
%
%       TG + M -> DG + B
%       DG + M -> MG + B
%       MG + M -> G + B
%       FFA + M -> W + B
%       G  -> PG + W
%       G + M -> MP + W
%       Define terms
CTG = C(1); CDG = C(2); CMG = C(3); CFFA = C(4); CM = C(5); CB = C(6);
CG = C(7); CPG = C(8); CW = C(9); CMP = C(10);

%       Rate constant
T = 160 + 273; % Temperature of the reaction in kelvin from 130 to 160
oC (403, 413, 423 and 433)
R = 8.314; % gas constant (J/mol.K)
k1 = (1.59E+3*exp(-38700/(R*T)));        % Acid        (ref: Marchetti
et al. 2010)
k2 = (0.33E+3*exp(-38700/(R*T)));        % Acid
k3 = (3.194E+3*exp(-38700/(R*T)));       % Acid
k4 = (5.97E+3*exp(-38700/(R*T)));        % Acid
k5 = (1.01E+14*exp(-107110/(R*T)));    % Acid
k6 = (4.03E-1*exp(-38740/(R*T)));      % Acid
k7 = (9.50E+3*exp(-37990/(R*T)));        % Acid
k8 = (1.67E-2*exp(-12760/(R*T)));      % Acid
K1 = 1.17E+6;                              % Acid  (l^2/mol^2)
K2 = 1.10E+6;                              % Acid
K3 = 2.00E+3;                              % Acid
f = 0.60; % Order of catalyst for biodiesel
a = 1.33; % Order of Cat for polyglycerol
mc = 0.0469; % cat. conc. 1,2, 3 and 5% (0.0094, 0.0187, 0.0281 and
0.0469)
k9  = (2.18E+11*exp(-112014.5/(R*T)));

% Reaction rates:
r1 = (k1*CTG*CM - k2*CDG*CB)*mc^f;
r2 = (k3*CDG*CM - k4*CMG*CB)*mc^f;
r3 = (k5*CMG*CM - k6*CG*CB)*mc^f;
r4 = (mc/(1+K1*CB*CW+(K2*CB*CW/CM)+K3*CB))*(k7*CFFA-(k8*CB*CW/CM)); %
r4 = k7*(CFFA*CM)*mc^f;
r5 = k9*(CG^2)*mc^a;
r6 = r5;

% Mass balance
```

```
dCTG = -r1;
dCDG = r1-r2;
dCMG = r2-r3;
dCFFA = -r4;
dCB = r1+r2+r3+r4;
dCPG = 1.0*r5;
dCMP = 40*r6;
dCG = 0.50*r3-0.25*r5-0.5*r6;
dCM = -dCB-dCMP;
dCW = r4+r5+r6;
%Assign output variables

dC(1,:) = dCTG;
dC(2,:) = dCDG;
dC(3,:) = dCMG;
dC(4,:) = dCFFA;
dC(5,:) = dCM;
dC(6,:) = dCB;
dC(7,:) = dCG;
dC(8,:) = dCPG;
dC(9,:) = dCW;
dC(10,:) = dCMP;


Rate = readtable('updated.xlsx')
% Initial concentrations:
C0 = [0.1043, 0, 0, 2.6E-4, 0.8157, 0, 0, 0, 0, 0]; % C0 for methanol
4:1-8:1 (0.4202, 0.5191, 0.6180, 0.8157)



% Time range for the model (seconds)
t = 0:1:3600;

% Call the ode15s solver
[t,C] = ode45(@BioAcid,t,C0);

% Plot the data
figure
% yyaxis left

 plot(t,C(:,1),'-k',... %t,C(:,2),'-r',... %t,C(:,3),'-
g',...%t,C(:,4),'-b',...%t,C(:,5),'-c',...%t,C(:,9),'--y',...
     t,C(:,6),'-m',...
     t,C(:,7),'-r',...
     Rate.Time,Rate.B16058, 'mo',...
     Rate.Time,Rate.G16058, 'ro',...
     Rate.Time,Rate.T16058, 'ko',...
     t,C(:,8),'-g',...
     t,C(:,10),'-b',...
     Rate.Time,Rate.D16058, 'go',... % B biodiesel, 130 T, 5 cat conc,
4 mole ratio
     Rate.Time,Rate.M16058, 'bo')


legend('TG','B','G','BE','GE', 'TGE','PG', 'MP', 'PGE', 'MPE')
xlabel('Time (sec)')
ylabel('Concentration (M)')

num1 = xlsread ('updated.xlsx', 1, 'B6:B11');   % Time
num2 = xlsread ('updated.xlsx', 1, 'BN6:BN11'); % Glycerol
num3 = xlsread ('updated.xlsx', 1, 'EA6:EA11'); % Biodiesel
num4 = xlsread ('updated.xlsx', 1, 'GO6:GO11'); % Triglyceride
```

```
num5 = xlsread ('updated.xlsx', 1, 'JC6:JC11'); % Diglycerol
num6 = xlsread ('updated.xlsx', 1, 'LQ6:LQ11'); % MPD

x1 = num1;
y11 = num2;
y12 = num3;
y13 = num4;
y14 = num5;
y15 = num6;
z1 = [x1 y11 y12 y13 y14 y15];

y21 = C(:,7);
y22 = C(:,6);
y23 = C(:,1);
y24 = C(:,8);
y25 = C(:,10);

z2 = zeros (6,6);
z2 (1,1) = t (1);
z2 (1,2) = y21 (1);
z2 (1,3) = y22 (1);
z2 (1,4) = y23 (1);
z2 (1,5) = y24 (1);
z2 (1,6) = y25 (1);
z2 (2,1) = t (301);
z2 (2,2) = y21 (301);
z2 (2,3) = y22 (301);
z2 (2,4) = y23 (301);
z2 (2,5) = y24 (301);
z2 (2,6) = y25 (301);
z2 (3,1) = t (901);
z2 (3,2) = y21 (901);
z2 (3,3) = y22 (901);
z2 (3,4) = y23 (901);
z2 (3,5) = y24 (901);
z2 (3,6) = y25 (901);
z2 (4,1) = t (1801);
z2 (4,2) = y21 (1801);
z2 (4,3) = y22 (1801);
z2 (4,4) = y23 (1801);
z2 (4,5) = y24 (1801);
z2 (4,6) = y25 (1801);
z2 (5,1) = t (2401);
z2 (5,2) = y21 (2401);
z2 (5,3) = y22 (2401);
z2 (5,4) = y23 (2401);
z2 (5,5) = y24 (2401);
z2 (5,6) = y25 (2401);
z2 (6,1) = t (3601);
z2 (6,2) = y21 (3601);
z2 (6,3) = y22 (3601);
z2 (6,4) = y23 (3601);
z2 (6,5) = y24 (3601);
z2 (6,6) = y25 (3601);

z3 = [x1 z1(:,2) z2(:,2)];
z4 = [x1 z1(:,3) z2(:,3)];
z5 = [x1 z1(:,4) z2(:,4)];
z6 = [x1 z1(:,5) z2(:,5)];
z7 = [x1 z1(:,6) z2(:,6)];

Mn1=mean(z3(:,2));
Mn2=mean(z4(:,2));
```

```
Mn3=mean(z5(:,2));
Mn4=mean(z6(:,2));
Mn5=mean(z7(:,2));

SST1 = sum((z3(:,2)-Mn1).^2);
SST2 = sum((z4(:,2)-Mn2).^2);
SST3 = sum((z5(:,2)-Mn3).^2);
SST4 = sum((z6(:,2)-Mn4).^2);
SST5 = sum((z7(:,2)-Mn5).^2);

SSR1=sum((z3(:,2)-z3(:,3)).^2);
SSR2=sum((z4(:,2)-z4(:,3)).^2);
SSR3=sum((z5(:,2)-z5(:,3)).^2);
SSR4=sum((z6(:,2)-z6(:,3)).^2);
SSR5=sum((z7(:,2)-z7(:,3)).^2);

Rsq_Glycerol =1-(SSR1/SST1);
Rsq_Biodiesel =1-(SSR2/SST2);
Rsq_Triglyceride =1-(SSR3/SST3);
Rsq_Polyglycerol =1-(SSR4/SST4);
Rsq_Propanediol =1-(SSR5/SST5);

Rsq = [Rsq_Glycerol Rsq_Biodiesel Rsq_Triglyceride Rsq_Polyglycerol
Rsq_Propanediol]
```